Πανεπιστήμιο Ιωαννίνων
Σχολή Θετικών Επιστημών
Τμήμα Φυσικής

Φαινομενολογική Μελέτη Θεωριών Πέρα από το Καθιερωμένο Πρότυπο των Στοιχειωδών Σωματιδίων στο Μεγάλο Αδρονικό Επιταχυντή

Χρηστάκης Σούτζιος

ΔΙΔΑΚΤΟΡΙΚΗ ΔΙΑΤΡΙΒΗ

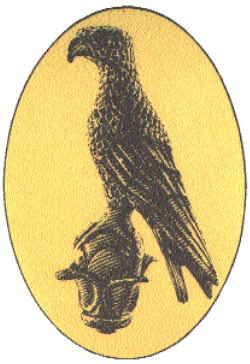

ΙΩΑΝΝΙΝΑ 2013

University of Ioannina
Physics Department

Phenomenological Study of Theories Beyond the Standard Model of Particle Physics in Large Hadron Collider

Kristaq Suxho

PhD Thesis

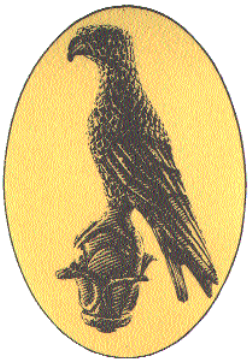

IOANNINA 2013

Three member advisory committee

- A. Dedes, Ass. Professor in the Department of Physics of the University of Ioannina (supervisor)
- K. Tamvakis, Professor in the Department of Physics of the University of Ioannina
- L. Perivolaropoulos, Professor in the Department of Physics of the University of Ioannina

Dissertation evaluation committee

- A. Dedes, Ass. Professor in the Department of Physics of the University of Ioannina (supervisor)
- K. Tamvakis, Professor, Department of Physics, University of Ioannina
- L. Perivolaropoulos, Professor, Department of Physics, University of Ioannina
- J.D.Vergados, Professor, Department of Physics, University of Ioannina
- C.E. Vayonakis, Professor, Department of Physics, University of Ioannina
- G.K. Leontaris, Professor, Department of Physics, University of Ioannina
- K. Fountas, Professor, Department of Physics, University of Ioannina

ΠΡΑΚΤΙΚΟ
ΔΗΜΟΣΙΑΣ ΠΑΡΟΥΣΙΑΣΗΣ, ΕΞΕΤΑΣΗΣ ΚΑΙ ΑΞΙΟΛΟΓΗΣΗΣ
ΔΙΔΑΚΤΟΡΙΚΗΣ ΔΙΑΤΡΙΒΗΣ

Σήμερα Τρίτη **25-6-2013**, ώρα **18.00μ.μ.** στην αίθουσα **Σεμιναρίων του Τμήματος Φυσικής, κτίριο Φ2,** του Πανεπιστημίου Ιωαννίνων, πραγματοποιήθηκε, σύμφωνα με το άρθρο 12, παρ. 5 του Ν.2083/92, η διαδικασία της δημόσιας παρουσίασης, εξέτασης και αξιολόγησης της εργασίας του υποψήφιου για την απόκτηση Διδακτορικής Διατριβής **κ. Χρηστάκη Σούτζιο.**

Την Επταμελή Εξεταστική Επιτροπή, που συγκροτήθηκε με απόφαση της Γενικής Συνέλευσης Ειδικής Σύνθεσης του Τμήματος Φυσικής (συν. 424/11-6-2013), αποτελούν τα ακόλουθα μέλη:

1) Αθανάσιος Δέδες, Αναπληρωτής Καθηγητής του Τμήματος Φυσικής του Παν/μίου Ιωαννίνων(Επιβλέπων)
2) Κυριάκος Ταμβάκης, Καθηγητής του Τμήματος Φυσικής του Παν/μίου Ιωαννίνων
3) Λέανδρος Περιβολαρόπουλος, Καθηγητής του Τμήματος Φυσικής του Παν/μίου Ιωαννίνων
4) Ιωάννης Βέργαδος, Ομότιμος Καθηγητής του Τμήματος Φυσικής του Παν/μίου Ιωαννίνων
5) Κωνσταντίνος Βαγιονάκης, Καθηγητής του Τμήματος Φυσικής του Παν/μίου Ιωαννίνων
6) Γεώργιος Λεοντάρης, Καθηγητής του Τμήματος Φυσικής του Παν/μίου Ιωαννίνων
7) Κωνσταντίνος Φουντάς, Καθηγητής του Τμήματος Φυσικής του Παν/μίου Ιωαννίνων

Παρόντα ήταν και τα 7 μέλη της εξεταστικής επιτροπής. Το θέμα της διδακτορικής διατριβής που εκπόνησε ο κ. Σούτζιος και που παρουσίασε σήμερα είναι **«Φαινομενολογική Μελέτη Θεωριών Πέρα από το Καθιερωμένο Πρότυπο των Στοιχειωδών Σωματιδίων στο Μεγάλο Αδρονικό Επιταχυντή».**

Ο υποψήφιος παρουσίασε και ανάπτυξε το θέμα και απάντησε σε σχετικές ερωτήσεις τόσο των μελών της εξεταστικής επιτροπής όσο και του ακροατηρίου. Στη συνέχεια αποσύρθηκε η εξεταστική επιτροπή και μετά από συζήτηση κατέληξε στα ακόλουθα:

α) Η συγγραφή της διατριβής έγινε με τρόπο που δείχνει ιδιαίτερη μεθοδικότητα και πλήρη ενημέρωση του υποψήφιου πάνω στη σχετική βιβλιογραφία.

β) Η ερευνητική εργασία καταλήγει σε σημαντικά αποτελέσματα τα οποία προάγουν την επιστήμη. Από την εργασία αυτή έχουν προκύψει τρείς εργασίες δημοσιευμένες σε έγκριτα επιστημονικά περιοδικά.

γ) Η παρουσίαση και ανάπτυξη του θέματος της εργασίας από τον υποψήφιο και οι εύστοχες απαντήσεις στις ερωτήσεις που του τέθηκαν έδειξαν πλήρη γνώση του θέματος και γενικότερων σχετικών θεμάτων Φυσικής Στοιχειωδών Σωματιδίων.

Με βάση τα ανωτέρω, τα μέλη της Επταμελούς Εξεταστικής Επιτροπής εγκρίνουν ομόφωνα την εργασία και εισηγούνται ανεπιφύλακτα την απονομή Διδακτορικού Διπλώματος στον κ. Χρηστάκη Σούτζιο με βαθμό Άριστα.

Τα μέλη της Εξεταστικής Επιτροπής

1.Αναπληρωτής Καθηγητής Α. Δέδες
(Επιβλέπων)

2.Καθηγητής Κ. Ταμβάκης

3. Καθηγητής Λ. Περιβολαρόπουλος

4. Ομότιμος Καθηγητής Ιωάννης Βέργαδος

5. Καθηγητής Κ. Βαγιονάκης

6. Καθηγητής Γ. Λεοντάρης

7. Καθηγητής Κ. Φουντάς

Η παρούσα διδακτορική διατριβή χρηματοδοτήθηκε πλήρως από το Ίδρυμα Κρατικών Υποτροφιών (ΙΚΥ).

ΙΚΥ

ΕΛΛΗΝΙΚΗ ΔΗΜΟΚΡΑΤΙΑ

ΙΔΡΥΜΑ ΚΡΑΤΙΚΩΝ ΥΠΟΤΡΟΦΙΩΝ

STATE SCHOLARSHIPS FOUNDATION

dedicated to: my family

ACKNOWLEDGEMENTS

I would like to express my deepest appreciation to all of them that helped me to finalize my thesis.
First of all I would like to thank my supervisor Ass. Prof. Athanasios Dedes, for his encouragement, inspiration and guidance during the period of supervising this thesis. The excellent cooperation and his valuable advices helped me to improve my expertise and will be reference points in my life. The endless hours of discussions about physics and the details of calculations were the most exiting and enjoyable moments of my study.

In addition I would like to thank my committee members Prof. Kyriakos Tamvakis and Prof. Leandros Perivolaropoulos for supporting and assisting me generously. Special thanks to Prof. John D.Vergados for useful discussions especially on dark matter issues.
Furthermore I would like to thank my family for endless understanding and support.
I am in particular indebted to PhD students Panagiota Giannaka, Konstantina Zerva, Nikolaos Pappas, Michael Paraskevas and Evangelos Paradas for their support and multilateral help.
This work was totally financed by a scholarship from the Greek State Scholarships Foundation (IKY), which I thank especially.

ABSTRACT

Nowadays there is an increasing amount of efforts in searching for answers to a plethora of questions about the world around us. It seems that in the Large Hadron Collider's (LHC) era, those efforts are coming to fruition, and at the same time new triggering questions appear. Among them, the most important are questions about the nature of dark energy, the particle nature of dark matter, the existence of extra dimensions, the verification of the mechanism that gives mass to the particle content of the Standard Model (SM) of particle physics, the existence of supersymmetric particles etc.

In this thesis, motivated by experimental results in direct connection with some of the questions above, we first examined scenarios of dark matter interaction with SM leptons, focusing to the study of low energy recoiling electrons and found promising results that can be verified in near future experiments. In order to extent these findings, the dark matter annihilation into photons brought us into the study of triple vertices with external photons or different gauge bosons in general. Within this framework we studied in detail the triple gauge boson one-loop vertex containing virtual heavy fermions and reproduced the most general, analytical expression for that vertex. From a calculational point of view we developed a new approach to the problem by exclusively performing calculations in four dimensions and by using physical arguments to handle infinities or anomalously behaved quantities. Analyzing further the triple gauge boson vertex we examined the decoupling effects that arise when the virtual fermions mass becomes very large. The interesting point here was the conclusion that in fact, these heavy fermions do not decouple completely from the theory. They leave remnants that are necessary to guarantee the self-consistency of the theory. Moreover, we worked out quite interesting applications of these results in the SM framework, as well as in theories beyond the SM.

Furthermore, by using the same techniques we clarified some computational issues about W-boson one-loop contribution to Higgs boson decay into two photons ($H \to \gamma\gamma$). Performing the calculation in the unitary gauge and strictly in four dimensions, we encountered divergent quantities that we managed to handle by inserting arbitrary four-vectors. The remaining ambiguites were removed by exploiting physical arguments. The results obtained by using the combination of these two techniques (introducing four-vectors to reduce divergencies and using physical considerations to determine unambiguously the result), verify previous similar results. The validity of those results has been also tested by the use of a new proposed method (Four Dimensional Regularization) FDR.

Certainly there are open problems that the techniques described above, could answer. These problems constitute the inspiration for further extension of this work.

Contents

0.1 Outline

It is widely accepted that the SM describes in high accuracy a considerable variety of phenomena. However there is evidence for the appearance of new phenomena that do not suit into the SM framework. There appear open questions, which suggest that the SM must be extended in order to encompass all these new phenomena.

In this thesis we try to shed light on some of them. In particular we are concerned about dark matter searches, the possible existence of heavy fermions or exotic heavy bosons and their impact on low energy effective theories such as the SM, as well as about mass generation mechanism and properties of the Higgs boson which is directly connected with this mechanism. The outline of this thesis is as follows:

In the first Chapter, we present the basic features of the (SM), emphasizing in its mathematical construction and the fundamental postulates that it is based on. We present a list of questions that remain open in the current SM framework. Some selected issues are presented in more detail since they constitute the necessary theoretical basis into which the following Chapters are developed.

The second Chapter is concentrated on the efforts to reveal the dark matter's corpuscular nature. After introducing a theory setup, where different models that describe the possible dark matter and ordinary matter connection are presented, it follows a study of conventional and non-conventional dark matter searches. We have studied the relevant cross sections and event rates of processes that contain recoiling nuclei or low energy electrons scattered in dark matter-nucleus collisions and dark matter-hydrogen like atoms collisions respectively. It follows a detailed calculation of time modulation effects on non-conventional searches for dark matter. Finally, an experimental proposal with promising abilities in the detection of dark matter, is presented.

The third Chapter deals with heavy fermions non-decoupling effects in triple gauge boson vertices containing one-loop diagrams where heavy fermions are circulating. The calculation is performed in exactly four dimensions and since the relevant integrals are divergent a special treatment has been used in order to remove the divergencies. The problem is treated by introducing arbitrary vectors that shift the integral variable. Requiring the final result to satisfy the Ward identities and be gauge invariant, we have found the more general triple gauge boson vertex with these properties. Next we consider the case where the internal fermions are extremely heavy and investigate if there are any remnants in the low energy limit. We find that, if at the beginning the whole fermionic spectrum (heavy and light fermions) constitutes an anomalous free model, after integrating out the heavy fermions a term survives and it is exactly the opposite of an anomalous term appearing in the light fermionic spectrum. This renders the low energy model anomalous free. These results are generalized further in SM extensions that contain exotic Z' gauge bosons or an extra fermion generation.

In Chapter 4 we extent the method of arbitrary shifting vectors that we used in the previous Chapter. The objective is to calculate the amplitude for the Higgs boson decay to two photons and to clarify some problems in this calculation appeared recently in the literature. Again the calculation is performed in four dimensions, in unitary gauge

and we find that the arbitrary vectors are capable to reduce high order ultraviolet divergencies to logarithmic ones. We demand the result to be gauge invariant and finite and by using the Goldstone Boson Equivalence Theorem we can finally obtain the desired result. As a cross check we perform the calculation using dimensional regularization and a recently proposed method useful in performing four-dimensional integral calculations, namely the Four Dimensional Regularization (FDR).

We conclude in a short Chapter 5, where we present future directions and possible extensions of our work.

A considerable supporting material is collected in several Appendices. In Appendix A are presented the basic properties of Dirac matrices and the main techniques of Dirac algebra. Also we append a collection of standard dimensional regularization integrals useful for checking several calculations especially those in Chapters 3 and 4.

Appendices B, C, D, E, F are related to calculations in Chapter 2. In Appendix B we describe in detail the calculation of the Feynman propagator related to the Lagrangian eq. (2.2) which describes the coupling of SM to an abelian dark sector with arbitrary kinetic or mass mixing. In Appendix C we analyze the general action related to the Lagrangian eq. (2.2) for different models. In Appendix D are presented the calculations about the time modulated effects in WIMP-nucleon or electron scattering. Subsequently in Appendix E we repeat the calculation of WIMP-electron scattering cross section using a non-relativistic approach since the WIMP's velocity is $\beta \approx 10^{-3}$. In the next Appendix F we carefully analyze the matrix element squared for WIMP-nucleon or electron scattering when the WIMP is a Dirac or Majorana particle. In the last case we show that this matrix element squared is suppressed by a factor of $\beta^2 \approx 10^{-6}$.

Appendices G-K deal with issues related to Chapter 3. In Appendix G we construct a simple toy model relevant to non-decoupling heavy fermion effects in triple gauge boson vertices. An analytic calculation of the general form of such a vertex, where all the internal, virtual fermions are considered of the same mass, is performed in Appendix H. This corresponds to a triple vertex containing neutral gauge bosons. The general case of charged gauge bosons, where the internal fermions have different masses is presented in Appendix I. In Appendix J we present some analytical expressions for the integral representations of form factors that determine the triple vertex and study their limit in various cases. In the following Appendix K we present necessary conditions for anomaly cancellation and non-decoupling heavy fermion effects in a model with three different U(1)'s corresponding to three distinct massive or massless gauge bosons X, Y, and Z.

In Appendices L and M we present calculations related to Chapter 4. In Appendix L, the analytical expressions for the coefficients of eq. (4.3), are presented. Appendix M contains an analytical derivation of the discontinuity of four-dimensional logarithmic divergent integrals due to surface terms appearing exactly in four dimensions.

Finally in the last Appendix N, some generalized Gordon identities are presented. These identities are useful during calculations especially in changing from the basis γ^μ, $\gamma^\mu\gamma^5$, k^μ, $k^\mu\gamma^5$ to the basis γ^μ, $\gamma^\mu\gamma^5$, $\sigma^{\mu\nu}k_\nu$, $\sigma^{\mu\nu}k_\nu\gamma^5$.

Chapter 1

The Standard Model of particle physics

In this introductory Chapter, we present the basic formulation of the SM, its mathematical structure, the fundamental particle content and the underlying symmetries which lead to laws that in many cases govern the behaviour of the world around us. Subsequently are presented the fundamental principles on which is based the construction of the SM as a self-consistent quantum field theory. This construction is realized in the framework of the Lagrangian formalism, and posses a variety of high energy physics features such as the spontaneous symmetry breaking, the renormalizability, the Higgs mechanism, the chiral anomalies. It follows a brief description of topics that are not included in the current status of the SM and therefore are basic ingredients of theories beyond the SM. Most of these topics are presented in more detail in the next Chapters. Naturally this first Chapter serves as a "building blocks" container that provides the necessary notions, techniques, notation and tools we will use throughout this thesis.

1.1 Introduction

The SM is a theory that describes the dynamics of subatomic particles and their interactions. It covers most of the study of fundamental interactions in Nature concentrating on electroweak and strong force. The other fundamental force in Nature, gravity, as it is described by the General Relativity (GR), is not included in the current frame of SM. The reason is that gravity is extremely weak and SM in the current form fails at energies that (graviton) is expected to exist. The SM has a dynamical nature in the sense that posses an interesting ability to supply for possible extensions to other theoretical models and at the same time to remain in the heart of them.

As a theory SM was developed during the 20th century and especially in 1960-1980 when its final formulation was almost completed [1–3]. Later developments and discoveries confirmed many of the predictions of the SM and enforced its role as a powerful theory in describing the fundamental interactions in Nature. The two main pillars that the SM is based on, are the Quantum Mechanics which deals with phenomena that take

place in microscopic scales, and the Special Relativity that describes the kinematics and dynamics of very fast moving objects. These two branches of modern physics cooperating with each other create the necessary theoretical framework where a field theory such as the SM can be developed and operate. Although its formulation is based on many assumptions, its predictability and the success in explaining various experimental results are impressive. But certainly the SM is not a theory that describes everything. There is a plethora of phenomena that do not suit into the SM formulation, since it does not provide any possible explanation. This fact constitutes an ideal opportunity to proceed to theories beyond the SM. Some of these topics, where extensions of the SM claim to provide a possible explanation, contain the corpuscular nature of dark matter whose existence has been supposed as a possible scenario to explain cosmological observations, the experimental verified neutrino oscillations that require that the neutrino is a massive particle (in contrast with the minimal SM construction where the neutrino is massless), the hierarchy problem (there is not any explanation in the SM framework why gravity is $\sim 10^{32}$ times weaker than the weak force), and as mentioned previously, the accession of gravity in the framework of a quantum field theoretical formalism.

1.2 Particle content of the SM

It is widely accepted that our world, at the low energy level of everyday life, is governed by four fundamental interactions: strong, electromagnetic, weak and gravitational. As the energy level where we study several phenomena increases, a unification of some of the above interactions (electromagnetic and weak) appears, and continuing further it is believed that a similar unification takes place again reducing the number of fundamental interactions. The SM is a theory that tends to describe our world in the relatively low energetic level. Among its basic postulates is the fact that all the matter content of our universe and the fundamental interactions can be described by the existence and interactions of a finite (relatively small) number of elementary particles. There are 61 elementary (based on the knowledge that we posses so far) particles in the SM, taking into account the number of families, the number of colors and the existence of antiparticles (Fig. 1.1). In this number is included the recently discovered Higgs boson [4, 5]. All elementary particles are divided into two big categories according to their spin: fermions that have a spin-1/2 and bosons that have an integer spin.

The first one of these categories is divided again in subcategories according to the way that fermions interact with each other or with other particles. According to the force that they are sensitive to, fermions are divided into leptons (electron, muon, tau, electron neutrino, muon neutrino, tau neutrino) which interact via the electroweak interaction (neutrinos are electrically neutral and therefore interact only through weak force) and quarks (up, down, charm, strange, top, bottom) which except from the electroweak are also sensitive to the strong interactions since they carry a quantity called color.

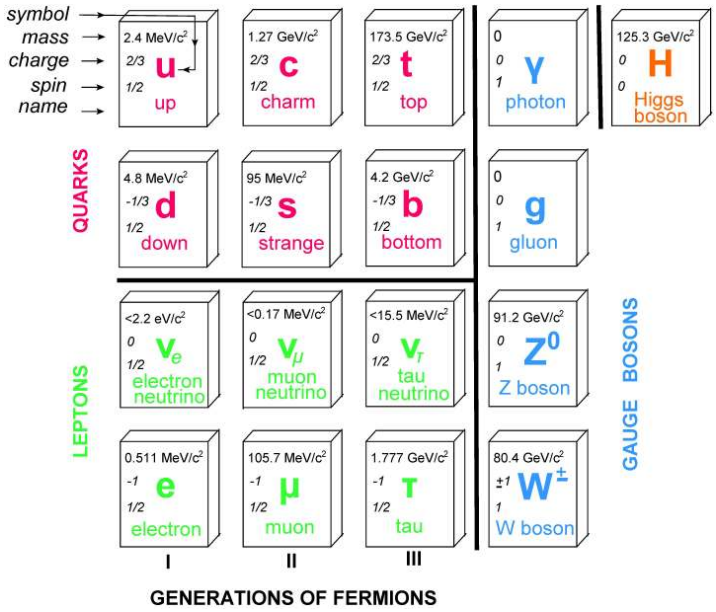

Figure 1.1: *The particle content of SM.*

The second category includes gauge bosons, particles that have spin 1 and are responsible for the mediation of different interactions. The electromagnetic interaction is mediated by the photon, a massless particle that does not carry any electric charge or color. The fact that the photon is massless characterizes the electromagnetic interaction as a long-range force. There are eight massless gluons that are the mediators of the strong nuclear force. As quarks, they are colored and this allows them to self-interact. Although they are massless, the strong interaction is not a long-range force. The reason for that is a phenomenon, called asymptotic freedom that enforces the quarks and gluons not to exist in a free form but to create colorless composite particles called hadrons (baryons and mesons). Finally the mediators of the weak interaction are the Z^0 and $W^{\pm}$ bosons. They are massive and therefore the weak interaction has a short range.

There is also one last boson that is contained into the SM set of particles. It is about the long-expected and possibly discovered Higgs boson [4–9]. It does not play the role of any interaction mediator, has spin 0, is massive and represents the quantum of the Higgs field that is responsible for giving mass to Z^0 and $W^{\pm}$ bosons and fermions as well. Since the Higgs boson is massive it possess self-interaction properties. It is unstable and can decay into other SM particles. Its detection was feasible by studying these decaying products.

1.3 The Lagrangian formulation

The SM is a quantum field theory. A basic concept of a field theory is the fact that the fundamental entity capable to represent essential qualities of a system is the concept of field, which is a continuous function of space-time $\phi(x^0, \vec{x})$, or short $\phi(x)$. Motivated by the Lagrangian formalism of classical mechanics, it is postulated that the dynamics of a system is described by the action:

$$S = \int d^4x \, \mathcal{L}[\phi_i(x), \partial_\mu \phi_i(x)], \tag{1.1}$$

where $\mathcal{L}[\phi_i(x), \partial_\mu \phi_i(x)]$ is the Lagrangian density, a function (usually polynomial) of the fields and their derivatives. Applying the fundamental principle of the stationary action under infinitesimal field variations and considering that these variations are equal to zero on the boundary of a closed region, one obtains the Euler-Lagrange equation, that is,

$$\begin{aligned} \delta S = 0 \Rightarrow \quad & \int d^4x \Big[\frac{\partial \mathcal{L}}{\partial \phi_i}\delta\phi_i + \frac{\partial \mathcal{L}}{\partial(\partial_\mu \phi_i)}\delta(\partial_\mu \phi_i)\Big] = \int d^4x \Big[\frac{\partial \mathcal{L}}{\partial \phi_i}\delta\phi_i + \frac{\partial \mathcal{L}}{\partial(\partial_\mu \phi_i)}\partial_\mu(\delta\phi_i)\Big] = \\ & \int d^4x \Big[\frac{\partial \mathcal{L}}{\partial \phi_i} - \partial_\mu\Big(\frac{\partial \mathcal{L}}{\partial(\partial_\mu \phi_i)}\Big)\Big]\delta(\phi_i) + \oint_{\mathcal{S}} d\mathcal{S}\Big(\frac{\partial \mathcal{L}}{\partial(\partial_\mu \phi_i)}\Big)\delta(\phi_i) = 0, \end{aligned} \tag{1.2}$$

where $\mathcal{S}$ is a surface that bounds a particular region and on this $\mathcal{S}$ the variation of the fields vanish, $\delta\phi_i = 0$. Therefore the surface integral above vanish. Since the variation $\delta\phi_i$ is arbitrary, in order the first integral in eq. (1.2) to vanish, the integrand should be zero, i.e.

$$\frac{\partial \mathcal{L}}{\partial \phi_i} - \partial_\mu\Big(\frac{\partial \mathcal{L}}{\partial(\partial_\mu \phi_i)}\Big) = 0. \tag{1.3}$$

This is the Euler-Lagrange equation for the field ϕ_i or its equation of motion. Using this formalism we can deduce Noether's theorem which relates symmetries of a system with conserved quantities. When we refer to a symmetry of a system we mean a set of transformations of fields under whom the Lagrangian of this system remains unchanged. Therefore if we assume that $\phi_i(x) \to \tilde{\phi}_i(x) = \phi_i(x) + \alpha\, \delta_\alpha \phi_i(x) + \mathcal{O}(\alpha^2)$, where α is a small parameter and require that $\mathcal{L}[\phi_i(x), \partial_\mu \phi_i(x)] = \mathcal{L}[\tilde{\phi}_i(x), \partial_\mu \tilde{\phi}_i(x)]$ we can find:

$$\begin{aligned} \delta_\alpha \mathcal{L} = 0 \;\Rightarrow\; & \sum_i \Big[\frac{\partial \mathcal{L}}{\partial \phi_i}\delta_\alpha\phi_i + \frac{\partial \mathcal{L}}{\partial(\partial_\mu \phi_i)}\delta_\alpha(\partial_\mu \phi_i)\Big] = 0 \Rightarrow \\ \Rightarrow\; & \sum_i \Big[\frac{\partial \mathcal{L}}{\partial \phi_i}\delta_\alpha\phi_i + \frac{\partial \mathcal{L}}{\partial(\partial_\mu \phi_i)}\partial_\mu(\delta_\alpha \phi_i)\Big] = 0 \Rightarrow \\ \Rightarrow\; & \sum_i \Big[\Big(\frac{\partial \mathcal{L}}{\partial \phi_i} - \partial_\mu(\frac{\partial \mathcal{L}}{\partial(\partial_\mu \phi_i)})\Big)\delta_\alpha\phi_i + \partial_\mu\Big(\frac{\partial \mathcal{L}}{\partial(\partial_\mu \phi_i)}\delta_\alpha\phi_i\Big)\Big] = 0. \end{aligned} \tag{1.4}$$

Taking into account the Euler-Lagrange equations, the first bracket is equal to zero. Therefore

$$\sum_i \Big[\partial_\mu \frac{\partial \mathcal{L}}{\partial(\partial_\mu \phi_i)}\delta_\alpha\phi_i\Big] = \partial_\mu \sum_i \Big[\frac{\partial \mathcal{L}}{\partial(\partial_\mu \phi_i)}\delta_\alpha\phi_i\Big] = \partial_\mu J^\mu = 0, \tag{1.5}$$

where $J^\mu \equiv \sum_i [\frac{\partial \mathcal{L}}{\partial(\partial_\mu \phi_i)} \delta_\alpha \phi_i]$ represents a conserved current. This fact constitutes the Noether's theorem which claims that for every continuous symmetry of a system, there is a conserved quantity (generalized charge). We can mention here the conservation of momentum, energy, angular momentum, electric charge etc., that corresponds to the invariance of the Lagrangian of this system under spatial translation, time translation, rotation invariance or other internal symmetries (gauge invariance) respectively.

1.4 Mathematical construction

The mathematical construction of SM is based on several postulates. First of all, the global Poincare symmetry is postulated. It contains space-time symmetries (invariance under translations and rotations), as well as internal symmetries e.g the local $SU(3)_C \otimes SU(2)_L \otimes U(1)_Y$ gauge symmetry that definitely characterizes the SM. A second basic postulate of SM is the fact that each particle is represented by a dynamical entity known as field. In fact the different fields, in addition to being represented by continuous functions of space-time, in many cases posses a quantum-mechanical character in the sense that are represented by non-commutative operators. A third postulate is that the operating framework of SM is constructed based on the Lagrangian formalism, whose fundamental quantity is the Lagrangian density, an entity invariant under Lorentz transformations, that describes the whole dynamics of a system. A last but not least postulate is that the SM Lagrangian remains unchanged under local gauge transformations. This fact has remarkable consequences in the whole theory and constitutes one of the basic foundations of the SM. We will return to this point later and will discuss the importance of gauge invariance in more detail.

Certainly all the above postulates are driven by undeniable experimental facts. The SM is a chiral theory i.e within the SM framework left-handed and right-handed fermions are treated differently. This is an experimentally verified occurrence. The name left-handed (right-handed) characterizes the way a particle transforms according to the left (right)-handed representation of Poincare group (the group of isometries of Minkowski spacetime).

1.4.1 Constructing the Quantum Electrodynamic (QED) gauge invariant Lagrangian

A free Dirac fermion is described in the coordinate space by the Dirac equation:

$$i\gamma^\mu \partial_\mu \Psi(x) = m\,\Psi(x), \tag{1.6}$$

where γ^μ are the Dirac matrices (for definition and properties see Appendix A) and Ψ represents the wave function of a Dirac spinor with mass m. This equation can be derived from the following Lagrangian:

$$\mathcal{L}_0 = i\overline{\Psi}(x)\gamma^\mu \partial_\mu \Psi(x) - m\,\overline{\Psi}(x)\Psi(x), \tag{1.7}$$

with $\overline{\Psi}(x) \equiv \Psi^{\dagger}(x)\gamma^0$. Obviously, this is invariant under the global transformation $\Psi'(x) = e^{i\,\alpha}\Psi(x)$, where α is a real parameter, but if we require that the Lagrangian above be invariant under a local transformation $\Psi'(x) = e^{i\,\alpha(x)}\Psi(x)$, where $\alpha(x)$ a real-valued function of space-time, then we should also add an extra field A_μ which has the following transformation property $A'_\mu(x) = A_\mu(x) - 1/q\,\partial_\mu\alpha(x)$, where q is the fermion's electric charge. In this way we can modify the eq. (1.7) in the following form:

$$\begin{aligned} \mathcal{L} &= i\overline{\Psi}(x)\gamma^\mu D_\mu\Psi(x) - m\overline{\Psi}(x)\Psi(x) = \\ &= \mathcal{L}_0 - q\,\overline{\Psi}(x)\gamma^\mu A_\mu\Psi(x), \end{aligned} \tag{1.8}$$

where $D_\mu \equiv \partial_\mu + i\,q\,A_\mu$ is the gauge covariant derivative. This expression is invariant under the above transformation which is called local gauge transformation. In the second form of eq. (1.8), it is clear that the requirement the Lagrangian remains invariant under the local gauge transformations, generates a term that represents an interaction between the fields $\Psi(x)$ and $A_\mu(x)$. On the other hand, requiring that the field A_μ is a propagating field, one should add the following gauge invariant kinetic term $-1/4F_{\mu\nu}F^{\mu\nu}$, where $F_{\mu\nu} \equiv \partial_\mu F_\nu - \partial_\nu F_\mu$ represents the electromagnetic field strength. Therefore eq. (1.8) now becomes:

$$\begin{aligned} \mathcal{L} &= -\frac{1}{4}F_{\mu\nu}F^{\mu\nu} + i\overline{\Psi}\not{D}\Psi - m\overline{\Psi}\Psi \\ &= -\frac{1}{4}F_{\mu\nu}F^{\mu\nu} + \overline{\Psi}(x)(i\not{\partial} - m)\Psi(x) - q\,\overline{\Psi}(x)\gamma^\mu\Psi(x)A_\mu(x) = \\ &= \mathcal{L}_{Maxwell} + \mathcal{L}_{Dirac} + \mathcal{L}_{int}, \end{aligned} \tag{1.9}$$

where $\not{D} \equiv \gamma^\mu D_\mu$, $\not{\partial} \equiv \gamma^\mu\partial_\mu$ and $\mathcal{L}_{int} \equiv -q\,\overline{\Psi}(x)\gamma^\mu\Psi(x)A_\mu(x)$ represents the interaction part of the Lagrangian above. The Euler-Lagrange equation for the field $A_\nu(x)$ is:

$$\partial_\mu F^{\mu\nu} = q\,\overline{\Psi}(x)\gamma^\nu\Psi(x) = q\,j^\nu, \tag{1.10}$$

with the current density given by $j^\nu = \overline{\Psi}(x)\gamma^\nu\Psi(x)$. A mass term for the field $A_\mu(x)$ of the form $1/2\,m_A^2 A_\mu(x)A^\mu(x)$ is forbidden because it clearly breaks the local gauge invariance. This leads to the fact that the field $A_\mu(x)$ represents a massless particle, the photon. The important fact of this subsection is that the requirement the Lagrangian of a system to be invariant under local gauge transformations, generates interactions between different fields in a natural way. This is a general fact not only applied in the case of QED theory.

1.4.2 Constructing the Quantum Chromodynamic (QCD) Lagrangian

There are experimental hints and theoretical requirements that hadrons (baryons and mesons) are composite particles and are constituted by other elementary particles, called quarks. Baryons contain 3 quarks and mesons contain a quark-antiquark pair. They carry a quantity called color which allows them to coexist in bound states although they are fermions (they obey the Fermi-Dirac statistic), and to interact via strong interactions. The experiment indicates that the number of colors is $N_C = 3$ (red, green, blue). In order to construct the QCD gauge invariant Lagrangian, as in the QED case, we start from the free quark Lagrangian:

$$\mathcal{L}_0 = \sum_f \overline{\Psi}_f (i\gamma^\mu \partial_\mu - m_f)\Psi_f, \tag{1.11}$$

where Ψ_f is the wavefunction of the quark with flavour f. Obviously this is invariant under the global gauge transformation $\Psi'_f = U\,\Psi_f$ where $U^\dagger U = U\,U^\dagger = I$, $det\,U = 1$ and $U = exp\{i\alpha^i t^i\}$. Here, t^i are the $SU(3)$ generators in the fundamental representation (3×3 hermitian matrices) with the commutation relation $[t^a, t^b] = i\,f^{abc}t^c$ where f^{abc} the $SU(3)$ structure constants (chosen totally antisymmetric) and α^i real constants. If we require, the Lagrangian remains unchanged under local gauge transformations, $\alpha^i \to \alpha^i(x)$, the partial derivative should be transformed into a covariant derivative and additional terms that contain extra fields should appear, among them terms that show the possible interactions. The covariant derivative related to the above local transformation is:

$$D_\mu = \partial_\mu - igA^a_\mu\, t^a, \tag{1.12}$$

where g is the strong coupling and for each generator t^a (eight in total in the $SU(3)$ case), corresponds the field A^a_μ. These fields represent the gauge bosons of strong interaction that are called gluons. Imposing the following infinitesimal transformations for Ψ_f and A_μ:

$$\begin{aligned} \Psi'_f &= U\,\Psi_f \approx (1 + i\alpha^a t^a)\,\Psi_f \\ A'^a_\mu &= A^a_\mu + \frac{1}{g}\partial_\mu\,\alpha^a + f^{abc}A^b_\mu\,\alpha^c, \end{aligned} \tag{1.13}$$

and adding the gauge invariant kinetic term for the A^a_μ field, the QCD Lagrangian takes the following form:

$$\begin{aligned} \mathcal{L}_{QCD} &= -\frac{1}{4}F^a_{\mu\nu}F^{\mu\nu}_a + \sum_f \overline{\Psi}_f(i\not{D} - m_f)\Psi_f = \\ &= -\frac{1}{4}(\partial_\mu A^a_\nu - \partial_\nu A^a_\mu)(\partial^\mu A^\nu_a - \partial^\nu A^\mu_a) + \sum_f \overline{\Psi}_f(i\not{\partial} - m_f)\Psi_f + \\ &\quad + g\,A^a_\mu \sum_f \overline{\Psi}_f\gamma^\mu\,t^a\,\Psi_f - g\,f^{abc}(\partial_\mu A^a_\nu)A^{\mu\,b}A^{\nu\,c} - \\ &\quad - \frac{1}{4}\,g^2\,f^{abc}\,f^{aed}A^b_\mu\,A^c_\nu\,A^{\mu\,e}A^{\nu\,d}, \end{aligned} \tag{1.14}$$

where $F^a_{\mu\nu} = \partial_\mu A^a_\nu - \partial_\nu A^a_\mu + g\, f^{abc} A^b_\mu A^c_\nu$ represents the strength tensor for the A^a_μ field. The second line of eq. (1.14) represents the kinetic term for the A^a_μ field and the kinetic and mass term for the quark field Ψ_f. The first term in the third line expresses the interaction between the fields A^a_μ and Ψ_f and involves the $SU(3)$ matrices t^a. The next two terms manifest the non-Abelian character of strong interactions corresponding to cubic and quartic gluon self-interactions respectively. There is not a similar gauge bosons self-interaction in QED Lagrangian. This new feature of strong interactions is responsible for two basic properties that they manifest themselves: the asymptotic freedom, where the interactions become weaker in short distances, and the confinement, where they become stronger as the distance increases. As in the case of QED, any mass term for the gauge bosons is forbidden, because it breaks the gauge invariance. Therefore the gauge bosons of the strong interaction, the gluons, remain massless.

1.4.3 Electroweak sector

Weak interactions constitute one of the fundamental interactions in nature and are responsible for flavour changing processes governing the fermionic sector of SM. There is a considerable amount of experimental facts (especially β-decay, $\pi^- \to \mu^- \overline{\nu}_\mu$) that have made clear that the left-handed and right-handed chiral fermions are treated differently by weak interactions. Data from neutrino scattering, as well as measures of neutrino emission from astrophysical sources show clearly that there are different neutrino flavours and also that neutrinos of one flavour can be transformed to another flavour, a phenomenon known as neutrino oscillation. The mediators of weak interactions are the massive $W^\pm$ and Z^0 gauge bosons which posses the following properties with respect to their interactions to fermions:

- $W^\pm$-bosons couple only to left-handed fermions and right-handed antifermions. This is a clear breaking of parity and charge conjugation. Also they interact with fermionic doublets that contain fermions which differ by one unit of electric charge. This kind of interactions has the same universal strength.

- Fermionic interactions with the Z^0 boson are characteristic for flavour conserving vertices. Interactions with neutrinos involve only left-handed chiralities.

Experimental facts suggest that d', s' and b' quarks flavours eigenstates, are a linear combination of their mass eigenstates and are related by the expression:

$$\begin{pmatrix} d' \\ s' \\ b' \end{pmatrix} = \mathbf{V} \begin{pmatrix} d \\ s \\ b \end{pmatrix}, \tag{1.15}$$

where $\mathbf{V}$ is a 3×3 unitary matrix $\mathbf{V}\mathbf{V}^\dagger = \mathbf{V}^\dagger\mathbf{V} = I$, called Cabibbo-Kobayashi-Maskawa (CKM) matrix and is present in flavour mixing processes. An analogous situation shows the neutrino sector, since as it is suggested by neutrino oscillation phenomena, neutrinos posses a tiny but non-zero mass and the neutrino flavour eigenstates

are a mixture of their mass eigenstates requiring an analogous to CKM matrix that relates the two eigenbases.

To construct the electroweak Lagrangian we should take into account left-handed chiral fermions that transform as doublets and right-handed chiral fermions as siglets under the weak interactions. Firstly, we define the fermionic doublets and singlets as follows:

$$E_L(x) = \begin{pmatrix} \nu_e \\ e^- \end{pmatrix}_L, \quad Q_L(x) = \begin{pmatrix} u \\ d \end{pmatrix}_L, \quad e_R(x), \quad u_R(x), \quad d_R(x), \tag{1.16}$$

where L refers to left-handed and R to right-handed fermions. In terms of the fields above the free Lagrangian takes the form:

$$\mathcal{L} = \overline{E}_L(i\partial\!\!\!/)E_L + \overline{e}_R(i\partial\!\!\!/)e_R + \overline{Q}_L(i\partial\!\!\!/)Q_L + \overline{u}_R(i\partial\!\!\!/)u_R + \overline{d}_R(i\partial\!\!\!/)d_R. \tag{1.17}$$

The Lagrangian in eq. (1.17) is obviously invariant under the global gauge transformations:

$$\begin{aligned} E'_L(x) &= \exp\{i\alpha\, y_{1L}\}\, U_L\, E_L(x), \quad Q'_L(x) = \exp\{i\alpha\, y_{2L}\}\, U_L\, Q_L(x), \\ e'_R(x) &= \exp\{i\alpha\, y_{1R}\}\, e_R(x) \quad u'_R(x) = \exp\{i\alpha\, y_{2R}\}\, u_R(x), \\ d'_R(x) &= \exp\{i\alpha\, y_{3R}\}\, d_R(x), \end{aligned} \tag{1.18}$$

where $U_L \equiv \exp\{i\frac{\sigma^i}{2}\alpha^i\}$ is the $SU(2)$ transformation acting on doublets E_L and Q_L and σ^i the Pauli matrices with $i = 1, 2, 3$. The parameters y_{1L}, y_{2L}, y_{1R}, y_{2R}, y_{3R} are called hypercharges and are analogous to phase transformation in QED. On the other hand U_L is non-Abelian as in the QCD case. Requiring the Lagrangian of eq. (1.17) to be invariant under local gauge transformations, the recipe is already known. The derivatives transform into covariant derivatives and new fields that represent gauge bosons are introduced as follows:

$$D_\mu \equiv \partial_\mu - i\, g A^a_\mu \tau^a - i\frac{1}{2}\, g' B_\mu, \tag{1.19}$$

where A^a_μ and B_μ represent the $SU(2)$ and $U(1)$ gauge bosons respectively, $\tau^a = \sigma^a/2$ and g and g' are the coupling constants of $SU(2)$ and $U(1)$ fields. As in the case of QED and QCD the fields B_μ and A^a_μ have the following transformation:

$$\begin{aligned} B'_\mu &= B_\mu + \frac{1}{g'}\partial_\mu \beta(x), \\ A'^a_\mu &= A^a_\mu + \frac{1}{g}\partial_\mu \alpha^a(x) + \epsilon^{a\,b\,c} A^b_\mu\, \alpha^c(x). \end{aligned} \tag{1.20}$$

Constructing the field strength tensors for B_μ and A^a_μ respectively,

$$\begin{aligned} B_{\mu\nu} &= \partial_\mu\, B_\nu - \partial_\nu B_\mu, \\ F^a_{\mu\nu} &= \partial_\mu\, A^a_\nu - \partial_\nu A^a_\mu + g\, \epsilon^{a\,b\,c} A^b_\mu A^c_\nu, \end{aligned} \tag{1.21}$$

we can see that they remain invariant under the transformations of eq. (1.20). Subsequently we can write down the properly transformed kinetic terms for A^a_μ and B_μ and the final Lagrangian reads:

$$\begin{aligned}\mathcal{L} &= -\frac{1}{4}F^{\mu\nu}_a F^a_{\mu\nu} - \frac{1}{4}B^{\mu\nu}B_{\mu\nu} + \overline{E}_L(i\not{D})E_L + \overline{e}_R(i\not{D})e_R + \\ &\quad + \overline{Q}_L(i\not{D})Q_L + \overline{u}_R(i\not{D})u_R + \overline{d}_R(i\not{D})d_R. \end{aligned} \tag{1.22}$$

The last term of $F^{\mu\nu}$, that constitutes its non-Abelian part, generates cubic and quartic self-interactions among gauge fields that have the same $SU(2)$ coupling g. The Lagrangian above describes a set of massless fermions. Any mass term for fermionic fields is forbidden by global gauge invariance. For example any term of the form $-m_e(\overline{e}_L\, e_R + \overline{e}_R\, e_L)$, is not allowed because the fields e_L and e_R belong to different $SU(2)$ representations and have different $U(1)$ couplings. Also any mass term for the gauge bosons is also forbidden since it violates the local gauge invariance. Therefore this Lagrangian describes a completely massless set of particles. However, this Lagrangian is far from reality. Since the weak force does not represent a long range interaction, the physical $W^\pm$ and Z^0 bosons should be massive. On the other hand, although it can describe the fermionic sector in high energies, where fermions can be considered massless, the description fails at low energies where fermions appear clearly massive. In order to generate masses we need to break the gauge symmetry somehow. For this, it is necessary to introduce a new mechanism that respects the gauge invariance of the Lagrangian, but generates stable minimal energy states that are transformed under gauge transformations in a specific way. Choosing one of these states, it is said that the symmetry is spontaneously broken.

1.4.4 Spontaneous Breaking of a global gauge Symmetry

Let consider first the notion of spontaneous breaking of a global gauge symmetry. For this we introduce a complex scalar field ϕ, with Lagrangian:

$$\mathcal{L} = \partial_\mu\phi^\dagger\partial^\mu\phi - V(\phi), \qquad V(\phi) = \mu^2\phi^\dagger\phi + \lambda(\phi^\dagger\phi)^2. \tag{1.23}$$

This Lagrangian is invariant under the global transformation $\phi' = \exp(i\,\alpha)\phi$. The parameter λ is chosen to be positive in order the potential posses a stable ground state. For the other parameter μ^2 there are two possibilities: $\mu^2 > 0$ where the only ground state corresponds to $\phi_0 = 0$ and is stable, and $\mu^2 < 0$ where an unstable state appears at $\phi_0 = 0$ and a stable minimum appears for field configurations satisfying the relation $\mid \phi_0 \mid = \sqrt{\frac{-\mu^2}{2\,\lambda}} \equiv \frac{v}{\sqrt{2}}$, where v is the vacuum expectation value. In fact, there is an infinite number of degenerate states wich are related to each other via the following U(1) transformation $\phi = \frac{v}{\sqrt{2}}\exp(i\theta)$. We can choose everyone of this states. For simplicity we choose $\theta = 0$ and the symmetry is spontaneously broken. In order to investigate the particle spectrum we have to move in a perturbative way around the vacuum. We can decompose the initial field ϕ as follows $\phi(x) = \frac{1}{\sqrt{2}}(\phi_1(x) + i\,\phi_2(x))$, and using the shift $\varphi_1 \equiv \phi_1 - v$ along ϕ_1 direction and $\varphi_2 \equiv \phi_2$ along the ϕ_2 direction,

we obtain $\phi(x) = \frac{1}{\sqrt{2}}(v + \varphi_1(x) + i\,\varphi_2(x))$. In terms of the new fields φ_1 and φ_2 the Lagrangian above has the following form:

$$\begin{aligned}
\mathcal{L} &= \frac{1}{2}\partial_\mu\varphi_1\,\partial^\mu\varphi_1 + \frac{1}{2}\partial_\mu\varphi_2\,\partial^\mu\varphi_2 - \frac{\mu^2}{2}\Big((v+\varphi_1)^2+\varphi_2^2\Big) - \frac{\lambda}{4}\Big((v+\varphi_1)^2+\varphi_2^2\Big)^2 = \\
&= \frac{1}{2}\partial_\mu\varphi_1\,\partial^\mu\varphi_1 + \frac{1}{2}\partial_\mu\varphi_2\,\partial^\mu\varphi_2 - \lambda\,v^2\varphi_1^2 - 0\,\varphi_2^2 - \\
&- \lambda\Big(v\,\varphi_1^3 + v\,\varphi_1\,\varphi_2^2 + \frac{1}{2}\varphi_1^2\,\varphi_2^2 + \frac{1}{4}(\varphi_1^4+\varphi_2^4) - \frac{v^4}{4}\Big) = \\
&= \Big[\frac{1}{2}\partial_\mu\varphi_1\,\partial^\mu\varphi_1 - \lambda\,v^2\varphi_1^2\Big] + \Big[\frac{1}{2}\partial_\mu\varphi_2\,\partial^\mu\varphi_2 - 0\,\varphi_2^2\Big] + \text{interaction terms}, \qquad (1.24)
\end{aligned}$$

where the relation $\mu^2 = -\lambda v^2$ has been used. Comparing the last line of the Lagrangian above with the Lagrangian of a scalar particle $\mathcal{L} = \frac{1}{2}\partial_\mu\phi\,\partial^\mu\phi - \frac{1}{2}m^2\,\phi^2$, with mass m, it is clear that eq. (1.24) describes a massive scalar particle φ_1 with mass $m_{\varphi_1} = \sqrt{2\lambda v^2}$ and a massless scalar φ_2. The spontaneous breaking of the global gauge symmetry has generated massless excitations, a result related to Goldstone's theorem [32]: for each broken generator of a continuous symmetry there appears a massless scalar particle.

1.4.5 Spontaneous Breaking of a local gauge Symmetry. The Higgs mechanism. Gauge boson masses

In this section we will investigate what happens when a local gauge symmetry is spontaneously broken. Local gauge invariance requires the Lagrangian to be invariant under the transformation $\phi'(x) = \exp(i\,\alpha(x))\phi(x)$ and also, through the covariant derivative, introduces gauge fields that have a special transformation rule. We are interested for the case of $SU(2)_L \otimes U(1)_Y$ Lagrangian, since we expect the spontaneous breaking of local gauge symmetry will generate mass terms for weak gauge bosons. In this point we introduce the Higgs boson field, a doublet of complex scalar fields:

$$\phi(x) = \begin{pmatrix} \phi^+(x) \\ \phi^{(0)}(x) \end{pmatrix} \qquad (1.25)$$

and eq. (1.23) reads:

$$\mathcal{L} = (D_\mu\phi^\dagger)(D^\mu\phi) - \mu^2\phi^\dagger\phi - \lambda\,(\phi^\dagger\phi)^2, \qquad (1.26)$$

where $D_\mu\phi = \Big(\partial_\mu - i\,g A_\mu^a\tau^a - i\frac{1}{2}\,g' B_\mu\Big)\phi$ and as previously $\mu^2 < 0$ and $\lambda > 0$. This Lagrangian is invariant under the local gauge transformation $\phi'(x) = \exp(i\,\alpha(x))\phi(x)$ and those described in eq. (1.20). The potential term guarantees that there is an infinity of degenerate ground states located at $|\phi_0|^2 = \sqrt{\frac{-\mu^2}{2\lambda}}$. We can choose one of them by parametrizing the field ϕ ,"ala Kibble", as follows:

$$\phi(x) = \exp\{i\frac{\sigma^i}{2}\,\theta_i(x)\}\frac{1}{\sqrt{2}}\begin{pmatrix} 0 \\ v + h(x) \end{pmatrix}, \qquad (1.27)$$

where $\theta_i(x)$ and $h(x)$ are real fields. We can simplify the situation by working in the unitary gauge where $\theta_i(x) = 0$. This is allowed by the local $SU(2)$ invariance of the Lagrangian since we can rotate away any $\theta_i(x)$ dependence. The potential term in eq. (1.26) will generate self-interactions of Higgs boson and also a mass term for it. The gauge boson mass terms should come from the first term of eq. (1.26) evaluated at the scalar field expectation value. We work out only the relevant terms:

$$\Delta\mathcal{L} = D_\mu\phi^\dagger D^\mu\phi \sim \frac{1}{2}(0,v)\Big(gA^a_\mu\tau^a + \frac{1}{2}g'B_\mu\Big)\Big(gA^{b\,\mu}\tau^b + \frac{1}{2}g'B^\mu\Big)\begin{pmatrix}0\\ v\end{pmatrix}. \quad (1.28)$$

Considering that $\tau^a = \sigma^a/2$ and using the explicit form of Pauli matrices (for properties of Pauli matrices see Appendix A), we find:

$$\Delta\mathcal{L} = \frac{1}{2}\frac{v^2}{4}\Big[g^2(A^1_\mu)^2 + g^2(A^2_\mu)^2 + (-gA^3_\mu + g'B_\mu)^2\Big]. \quad (1.29)$$

It is convenient to define the following linear combinations of fields:

$$W^\pm_\mu = \frac{\Big(A^1_\mu \mp iA^2_\mu\Big)}{\sqrt{2}}, \quad Z^0_\mu = \frac{\Big(gA^3_\mu - g'B_\mu\Big)}{\sqrt{g^2+g'^2}}, \quad A_\mu = \frac{\Big(g'A^3_\mu + g\,B_\mu\Big)}{\sqrt{g^2+g'^2}}. \quad (1.30)$$

Now eq. (1.29) takes the form:

$$\Delta\mathcal{L} = \frac{1}{2}\Big(\frac{g\,v}{2}\Big)^2(W^+_\mu)^\dagger\,W^{+\mu} + \frac{1}{2}\Big(\frac{g\,v}{2}\Big)^2(W^-_\mu)^\dagger\,W^{-\mu} + \Big(\frac{g^2+g'^2}{2}\Big)(\frac{v}{2})^2 Z^0_\mu\,Z^{0\mu} + 0\,A_\mu A^\mu. \quad (1.31)$$

From this expression it is clear that the combinations $W^\pm_\mu$ acquire a mass $m_W = \frac{g\,v}{2}$, the Z^0_μ acquires a mass $m_{Z^0} = \frac{v}{2}\sqrt{g^2+g'^2}$, since in the Lagrangian a general mass term for the massive gauge bosons has the form $\frac{1}{2}m^2\,V_\mu V^\mu$. The last combination A_μ remains massless. The $W^\pm_\mu$ and Z^0_μ are identified with the weak gauge bosons and the field A_μ with the photon. In this way it is evident that the spontaneous breaking of a local gauge symmetry has generated massive gauge bosons and also a massless particle as well. In the general case of considering the coupling of vector fields to fermions the covariant derivative takes the form:

$$D_\mu = \partial_\mu - ig\,A^a_\mu T^a - ig'YB_\mu, \quad (1.32)$$

where $T^a = \frac{1}{2}\sigma^a$ and Y the $U(1)$ hypercharge. We are interested in writing this expression as a function of mass eigenstate fields $W^\pm$, Z^0 and A_μ. First we define $T^\pm = T^1 \pm i\,T^2 = \frac{1}{2}(\sigma^1 \pm i\,\sigma^2)$. Therefore the expression for the covariant derivative becomes:

$$\begin{aligned} D_\mu &= \partial_\mu - i\frac{g}{\sqrt{2}}\Big(W^+_\mu T^+ + W^-_\mu T^-\Big) - i\frac{1}{\sqrt{g^2+g'^2}}Z^0_\mu\Big(g^2T^3 - g'^2Y\Big) - \\ &\quad -i\frac{g\,g'}{\sqrt{g^2+g'^2}}A_\mu\Big(T^3+Y\Big). \end{aligned} \quad (1.33)$$

In this expression it is clear that the massless gauge boson couples to the gauge generator $T^3 + Y$. This leaves the vacuum unaffected. Since the gauge boson A_μ corresponds

to the photon, the mediator of electromagnetism, we conclude that the symmetry related to the electromagnetism leaves the vacuum invariant, which has as a consequence the presence of the massless photon. In order to simplify the eq. (1.33) further, we define the factor next to A_μ field as the electron charge $e = \frac{g\,g'}{\sqrt{g^2+g'^2}}$ and also identify the quantum number of the electric charge as $Q = T^3 + Y$. In terms of T^3 and Q, the term next to Z_μ field in eq. (1.33), takes the form $g^2T^3 - g'^2Y = (g^2+g'^2)T^3 - g'^2Q$ and also define $\cos\theta_w = \frac{g}{\sqrt{g^2+g'^2}}$ and $\sin\theta_w = \frac{g'}{\sqrt{g^2+g'^2}}$, where θ_w is the weak mixing angle. After the above definitions and abbreviations eq. (1.33) is written in a simplified form:

$$D_\mu = \partial_\mu - i\frac{g}{\sqrt{2}}\Big(W_\mu^+ T^+ + W_\mu^- T^-\Big) - i\frac{g}{\cos\theta_w} Z_\mu^0 \Big(T^3 - \sin^2\theta_w\Big) - ieA_\mu Q. \quad (1.34)$$

We can use the angle θ_w to express different useful relations as for example the parametrization of mixing between (Z^0, A) and (A^3, B) gauge fields through the change from one basis to the other as follows:

$$\begin{pmatrix} Z^0 \\ A \end{pmatrix} = \begin{pmatrix} \cos\theta_w & -\sin\theta_w \\ \sin\theta_w & \cos\theta_w \end{pmatrix} \begin{pmatrix} A^3 \\ B \end{pmatrix}, \quad (1.35)$$

or the relation $e = g\,\sin\theta_w$, between the electron charge and $SU(2)$ coupling, or finally the relation between the W and Z^0 masses: $m_W = m_{Z^0}\cos\theta_w$. From the last relation we can define the ρ parameter:

$$\rho \equiv \frac{m_W^2}{m_{Z^0}^2\cos^2\theta_w}, \quad (1.36)$$

and $\rho = 1$ at the lowest order of perturbation theory. The experimental measurements of m_W, m_{Z^0} and $\cos\theta_w$ confirm this relation. It is interesting that the total number of degrees of freedom remains the same before and after symmetry breaking. Before breaking there where four massless gauge fields (A^1, A^2, A^3, B) each one with two degrees of freedom due to the two possible transverse polarizations and four real scalar fields (the components of the complex Higgs field). In total $4 \times 2 + 4 = 12$ degrees of freedom. After spontaneous symmetry breaking appear three massive gauge bosons, each one with three degrees of freedom, a massless photon with two degrees of freedom and the remaining Higgs field with one degree of freedom, in total $3\times3+2+1 = 12$. So far we have described how the introduction of a scalar field with non-zero expectation value allows the system to reach in a spontaneously broken state and this mechanism generates the gauge boson masses and a massless photon. But this mechanism provides a mass term for the Higgs boson, the quantum of Higgs field, describes Higgs boson's self-interaction and interactions of Higgs boson and gauge bosons, and finally explains how fermions acquire their mass.

1.4.6 Interactions between fermions and gauge bosons. Fermion masses

So far the model we have described, contains massless fermions, since any mass term for fermions is forbidden by the gauge invariance. For example, a term in the Lagrangian of the form $\Delta\mathcal{L} = -m_e(\overline{e}_L e_R + \overline{e}_R e_L)$ contains fields that have different transformation properties under $SU(2)$ or $U(1)$ transformation groups. This information is encoded in the fermionic part of the Lagrangian in eq. (1.22):

$$\Delta\mathcal{L}_f \sim \overline{E}_L(i\not{D})E_L + \overline{e}_R(i\not{D})e_R + \overline{Q}_L(i\not{D})Q_L + \overline{u}_R(i\not{D})u_R + \overline{d}_R(i\not{D})d_R, \qquad (1.37)$$

where in general $D_\mu = \partial_\mu - igA^a\tau^a - ig'YB_\mu$. Since the different fermionic fields in the Lagrangian above belong to different representations, they have different values for the hypercharge Y. Using the relation $Q = T^3 + Y$, the hypercharge is chosen in such a way to reproduce the correct electric charge. For example, for right handed fermions the hypercharge coincides with the electric charge since in this case $T^3 = 0$. For the left handed fermions it is determined from the relation $Y = Q - T^3$, where we have considered that $T^3 = \pm 1/2$ for the upper and lower component of fermionic doublet respectively. Therefore the left handed doublets:

$$E_L = \begin{pmatrix} \nu_e \\ e^- \end{pmatrix}_L, \qquad Q_L = \begin{pmatrix} u \\ d \end{pmatrix}_L, \qquad (1.38)$$

have hypercharge $Y = -1/2$ and $Y = +1/6$ respectively. We can use the expression of covariant derivative as a function of mass eigenstates gauge fields, in order to express eq. (1.37) as follows:

$$\begin{aligned} \Delta\mathcal{L}_f &\sim \overline{E}_L(i\not{\partial})E_L + \overline{e}_R(i\not{\partial})e_R + \overline{Q}_L(i\not{\partial})Q_L + \overline{u}_R(i\not{\partial})u_R + \overline{d}_R(i\not{\partial})d_R + \\ &+ g\Big(W^+_\mu J^{\mu+}_W + W^-_\mu J^{\mu-}_W + Z^0_\mu J^\mu_Z\Big) + eA_\mu J^\mu_{EM}, \end{aligned} \qquad (1.39)$$

where the corresponding currents are:

$$\begin{aligned} J^\mu_{W^+} &= \frac{1}{\sqrt{2}}\Big(\overline{\nu}_L\gamma^\mu e_L + \overline{u}_L\gamma^\mu d_L\Big), \\ J^\mu_{W^-} &= \frac{1}{\sqrt{2}}\Big(\overline{e}_L\gamma^\mu \nu_L + \overline{d}_L\gamma^\mu u_L\Big), \\ J^\mu_{EM} &= \overline{e}\gamma^\mu(-1)e + \overline{u}\gamma^\mu(+\frac{2}{3})u + \overline{d}\gamma^\mu(-\frac{1}{3})d, \end{aligned} \qquad (1.40)$$

and

$$\begin{aligned} J^\mu_Z = \frac{1}{\cos\theta_W} \Big[&\frac{1}{2}\overline{\nu}_L\gamma^\mu\nu_L + \Big(-\frac{1}{2} + \sin^2\theta_W\Big)\overline{e}_L\gamma^\mu e_L + \sin^2\theta_W\overline{e}_R\gamma^\mu e_R + \\ + &\Big(\frac{1}{2} - \frac{2}{3}\sin^2\theta_W\Big)\overline{u}_L\gamma^\mu u_L + \Big(-\frac{2}{3}\sin^2\theta_W\Big)\overline{u}_R\gamma^\mu u_R + \\ + &\Big(-\frac{1}{2} + \frac{1}{3}\sin^2\theta_W\Big)\overline{d}_L\gamma^\mu d_L + \Big(\frac{1}{3}\sin^2\theta_W\Big)\overline{d}_R\gamma^\mu d_R\Big]. \end{aligned} \qquad (1.41)$$

Let see now how the introduction of the Higgs field produces a mass term for fermions. The scalar field must have $Y = 1/2$ and should be a spinor under $SU(2)$ in order to generate the correct gauge boson masses. It is interesting that the same scalar field, with these quantum numbers plays a crucial role in writing down a coupling term in the Lagrangian invariant under $SU(2)_L \otimes U(1)_Y$ of the form:

$$\Delta\mathcal{L}_e = -\lambda_e\,(\overline{E}_L \cdot \phi\; e_R + \overline{e}_R\,\phi^\dagger \cdot E_L), \tag{1.42}$$

where λ_e is a new dimensionless parameter. We notice that the hypercharges of the different fields sum to zero. If the scalar field has the form $\phi = \frac{1}{\sqrt{2}}\begin{pmatrix} 0 \\ v+h \end{pmatrix}$ then eq. (1.42) is written:

$$\begin{aligned}
\Delta\mathcal{L} &= \frac{-\lambda_e}{\sqrt{2}}\Big((\overline{\nu}_{e_L}, \overline{e}_L)\cdot\begin{pmatrix} 0 \\ v+h \end{pmatrix} e_R + \overline{e}_R(0, v+h)\cdot\begin{pmatrix} \nu_{e_L} \\ e_L \end{pmatrix}\Big) = \\
&= \frac{-\lambda_e}{\sqrt{2}}[v(\overline{e}_L e_R + \overline{e}_R e_L) + h(\overline{e}_L e_R + \overline{e}_R e_L)] = \\
&= -m_e \overline{e}\, e - \frac{\lambda_e}{\sqrt{2}} h\, \overline{e}\, e,
\end{aligned} \tag{1.43}$$

where $m_e = \frac{\lambda_e\, v}{\sqrt{2}}$ and $\overline{e}_L\, e_R + \overline{e}_R\, e_L = \overline{e}\, e$. From this expression it is clear that except of the fermionic mass term a coupling term between the Higgs boson and fermions has been generated. The eq. (1.42) seems to contribute to the mass generation of the lower component of the fermion doublet. In order to give mass to the upper component we write down the following $SU(2)_L \otimes U(1)_Y$ Lagrangian:

$$\Delta\mathcal{L}_u = -\lambda_u\Big(\overline{Q}_L \cdot \tilde{\phi}^c\, u_R + \overline{u}_R\,(\tilde{\phi}^c)^\dagger \cdot Q_L\Big), \tag{1.44}$$

where $\tilde{\phi}^c = i\sigma^2\phi^* = \frac{1}{\sqrt{2}}\begin{pmatrix} v+h \\ 0 \end{pmatrix}$. In this case the Lagrangian in eq. (1.44) takes the form:

$$\Delta\mathcal{L}_u = \frac{-\lambda_u}{\sqrt{2}}(v+h)\Big(\overline{u}_L\, u_R + \overline{u}_R\, u_L\Big) = -m_u \overline{u}\, u - \frac{\lambda_u}{\sqrt{2}} h\, \overline{u}\, u, \tag{1.45}$$

where $m_u = \frac{\lambda_u\, v}{\sqrt{2}}$ is the mass term for the u quark and $\overline{u}_L\, u_R + \overline{u}_R\, u_L = \overline{u}\, u$.

1.4.7 Higgs boson: mass, production and decay

By working out the terms in the potential part of eq. (1.26) for $\phi = \frac{1}{\sqrt{2}}\begin{pmatrix} 0 \\ v+h \end{pmatrix}$ and using the relation $-\mu^2 = \lambda\, v^2$ we find for the Higgs boson mass $m_H = \sqrt{2\lambda}v$. The vacuum expectation value is $v \approx 246\, GeV$ as it is evaluated from muon decay processes by taking into account the Fermi coupling and the relation $v = (\sqrt{2}G_F)^{-1/2}$. Also there appear interaction terms of the form $-\lambda v\, h^3 - \frac{\lambda\, h^4}{4}$ (some constant terms have been neglected) giving rise to third and fourth power self-interactions. From the

kinetic part of eq. (1.26) one also finds the interaction terms between the Higgs boson and weak gauge bosons. Manipulating the relevant terms one obtains:

$$\Delta\mathcal{L}_{kin.} \sim \frac{1}{2}\partial_\mu h\,\partial^\mu h + \left[m_W^2 W^{\mu^+} W_\mu^- + \frac{1}{2}m_Z^2 Z^\mu Z_\mu\right]\left(1+\frac{h}{v}\right)^2. \tag{1.46}$$

From this expression we conclude that there are four different couplings of the Higgs field to the gauge bosons (the triple and quartic interaction with each one gauge boson). There is no direct coupling of the Higgs boson to photon, since, as we know, the photon couples only to charged particles and the Higgs boson is a neutral one, or alternatively the Higgs boson couples to massive particles and the photon is massless. However, there appears a loop induced $h\gamma\gamma$ coupling involving fermions or W-bosons in the loop. On the other hand the coupling to the massive gauge bosons has the characteristic of being proportional to gauge boson's mass squared as it is clear from eq. (1.46).

At this point we want to discuss about Higss boson's production and decay. In previous sections we recognized the major role of the introduction of a scalar field in the theory, since it provides the framework where a mechanism that generates massive gauge bosons and also gives mass to fermions takes place. The quantum representative of this scalar field is the Higgs boson. The importance of the existence of the Higgs boson has rendered the search for this particle, one of the fundamental goals in physics last decades. These searches have been realized in Tevatron and LHC and seems to have given encouraging results with the discovery of a new boson which is at very high possibility, identified with the Higgs boson of the Standard Model [4, 5]. Before discussing about production and decay of the Higgs boson, let us provide some general information about the LHC. The main purpose of this accelerating machine is to shed light in some fundamental questions in modern physics:

1. Are the masses of elementary particles produced by the Higgs mechanism?
2. Is the recently discovered boson identified with the Higgs boson?
3. Are there supersymmetric partners of the SM particles ?
4. What is the possibility that extra dimensions exist?
5. What is the nature of dark matter?
6. Why the fundamental interactions have so different magnitude (the hierarchy problem)?
7. What is the deeper cause of matter-antimatter asymmetry?
8. What is the neutrino mass?

This thesis deals with points 1, 2 and 5. From the technical point of view, the LHC's "operating system" consists of a large underground tunnel ($\sim$ 27 km circumference), where two proton beams travel in opposite directions in extreme conditions (a pressure

of order $\sim 10^{-13}$ atm, 1.9 K temperature and ~ 8.3 T magnetic field). After accelerating in very high speeds, the two beams collide and the products of this collision are detected and analyzed. Each beam has a 7 TeV energy, giving a 14 TeV total collision energy. During the collision are created the conditions where some of the questions above will possibly find their answer.

After this short parenthesis about LHC, we return again to Higgs boson's production and decay features. The Higgs boson's production mechanism, at LHC, is dominated by gluon fusion, vector boson fusion and associative production with W boson or a top quark pair. Especially the gluon fusion has a major contribution to the Higgs boson's production, since the involved top quarks have a large coupling to Higgs boson due to their large mass. The Higgs boson, after its production is unstable and for a mass of about 126 GeV the Standard Model prediction is that its life time is about $1.6 \times 10^{-22} s$. The Higgs boson can decay through different channels with different probabilities. In general, more favorite are channels that contain heavy fermion-antifermion pairs, since the strength of interaction is proportional to fermion mass. Since for a Higgs boson with mass 126 GeV, the decay to top-antitop quark pair is forbidden (because $m_H \leq 346$ GeV which is twice the mass of top quark), the most probable decay channel contains a bottom-antibottom quark pair. An other alternative is the Higgs boson to decay into W and Z^0 gauge bosons, where each one of them subsequently decays into a pair of leptons. The products of these subsequent decays, provide information about the properties of the initial Higgs boson. The W boson decays into quarks which in general are very difficult to distinguish from the background, or decays into charged leptons and neutrinos that also have a detecting difficulty due to neutrinos very low detectability especially in collision experiments. On the other hand the Z^0-boson decays into a pair of charged fermions that in general are easy to detect. A third possibility is the Higgs boson to decay into a pair of gluons or a pair of photons. These two decay modes are indirect since the Higgs boson does not posses color or electric charge. It can be realized through loop induced interactions where are involved W-bosons or virtual heavy fermions. The case where the final particles are gluons, again expresses a difficulty due to the background. However the case of final photons is a very interesting process since the energy and momentum of these photons can be measured precisely and therefore this process plays a crucial role to the mass reconstruction of the initial decaying particle. In Chapter 4 we investigate an interesting behaviour of the last possibility where the loop involved particles are virtual W-bosons. The decay mode $h \to \gamma\gamma$ has definitively contributed to the identification of the recently discovered particle at the LHC, with the Higgs boson of the SM [4, 5].

1.5 Some selected topics

In what follows, we describe some selected topics related to the concepts and problems that we study in this thesis. This description serves as an introduction to issues that we analyze in more detail in the following Chapters. In particular we briefly describe some general aspects about the dark matter, chiral anomalies and dimensional regularization.

1.5.1 General aspects about the dark matter

There is an increasing number of facts about the existence of dark matter. It is believed that dark matter is a type of matter that does not emit or absorb electromagnetic radiation and its direct effects on the visible matter and radiation have gravitational nature. Among evidence about the existence of dark matter we refer the attempt to explain the rotational velocities of stars in the Milky Way or the evidence for the "missing mass" in the velocities of galaxies in clusters by Fritz Zwisky [10, 11], the "missing mass" in the explanation of rotational speed of galaxies by Vera Rubin in 1960-1970 [12, 13], the gravitational lensing effects in the background radiative structures, the distribution of anisotropies in the cosmic microwave background [14]. According to cosmological data our universe contains 4.9% ordinary matter, 26.8% dark matter and 68.3% dark energy [15].

This is a considerable percentage and has motivated several theoretical and experimental groups to focus on the search for dark matter [15–25]. Although the corpuscular nature of dark matter is still unknown, there are theories, such as supersymmetry or other extensions of the Standard Model of particle physics that provide possible candidates from a variety of subatomic particles (neutralinos, axions, heavy sterile neutrinos). The nature of dark matter however can not be baryonic. If this were the case then the cosmic microwave background will have a completely different form and also there would have been a conflict with the data about the abundance of light elements created during the big-bang nucleosynthesis. On the other hand, very light particles are also excluded since they are relativistic at early Universe and then escape rapidly from low density condensations. Any electric charge or magnetic moment are also forbidden since this would have allowed interactions with the photon-baryon plasma before recombination and clearly a different microwave background would have appeared. However, there are restrictions on this and we study models where dark sector gauge boson X_μ mixes to photon A_μ. The most accepted candidates are the WIMPs, (weakly interacting massive particles) [26] that interact with the rest of the ordinary matter via weak (possibly) and gravitational interactions. Since both these interactions are very weak, the detection of dark matter is extremely difficult, at least based on the detecting abilities that we possess so far.

There are two main kinds of detecting strategies: direct and indirect WIMP detection. The direct detection is based on the analysis of low background recoiling nuclei caused by the WIMP-nucleus scattering. The effectiveness of this method depends on the local dark matter density and velocity distribution. Two are the main techniques to detect recoiling nuclei: cryogenic detection, where the heat produced when a particle hits an atom in a crystal (Si, Ge) is measured and scintillator detection, where scintillation light is produced when a particle collides with the atoms in a liquid noble gas (Xe, Ar). The indirect detection techniques are based on the experimental search for particles that WIMPs could annihilate. The final particles may be photons, neutrinos, electrons, positrons or other Standard Model particles. Since the annihilation rate is proportional to the square of the WIMPs density, the ideal places to search for dark matter annihilation are dark matter dense objects (clusters of galaxies, galaxies

halos, dwarf galaxies) [27–29]. An alternative detecting choice provide particle colliders. Large Hadron Collider (LHC) is an ideal place to search for physics beyond the Standard Model. Future experiments in the LHC may be able to search for WIMP's production in proton-proton collisions. In principle, during a $p-p$ collision, quarks and gluons may annihilate in other colored particles (squarks, gluinos) and these particles may decay to WIMPs. Since the WIMP interacts extremely weak with the ordinary matter, it can be detected indirectly as missing energy and momentum.

However, alternative theories have been developed to explain the astronomical observations. Their philosophy is not to include large amounts of undetermined matter, but to modify laws of gravity.

1.5.2 Chiral anomalies

In quantum field theory there are phenomena that have not analog in classical theories. Their dynamics is affected completely by quantum effects. Such a problem is the decay rate of neutral pion $\pi^0 \to \gamma\gamma$ that leads to the concept of symmetry breaking anomalies. Here we will discuss the symmetry breaking of chiral anomalies. Chiral symmetry is a possible symmetry of the Lagrangian where the left and right handed fields transform independently. The massless Dirac Lagrangian has a symmetry related to the conservation of left and right handed fermions, leading to the conserved axial current $j^{\mu 5} = \overline{\Psi}\gamma^{\mu}\gamma^{5}\Psi$. In the massless case it is $\partial_{\mu} j^{\mu 5} = 0$. However, as we will see this equation is affected by quantum corrections. In order to understand this fact let us calculate the matrix element that corresponds to the creation of two photons by this axial current $j^{\mu 5}$. The matrix element for this process is :

$$\int d^4x\, e^{-iq\cdot x} \langle k_1 k_2 | j^{\mu 5}(x) | 0 \rangle = (2\pi)^4 \delta^{(4)}(k_1 + k_2 - q)\, \epsilon^*_{\lambda}(k_1)\, \epsilon^*_{\nu}(k_2)\, \mathcal{M}^{\mu\nu\lambda}(k_1, k_2), \quad (1.47)$$

where k_1, k_2 are the momenta of the outgoing photons, $\epsilon^*_{\lambda}(k_1)$, $\epsilon^*_{\nu}(k_2)$ their polarization vectors and $\mathcal{M}^{\mu\nu\lambda}$ the matrix element for the process shown in Fig. 1.2. The virtual

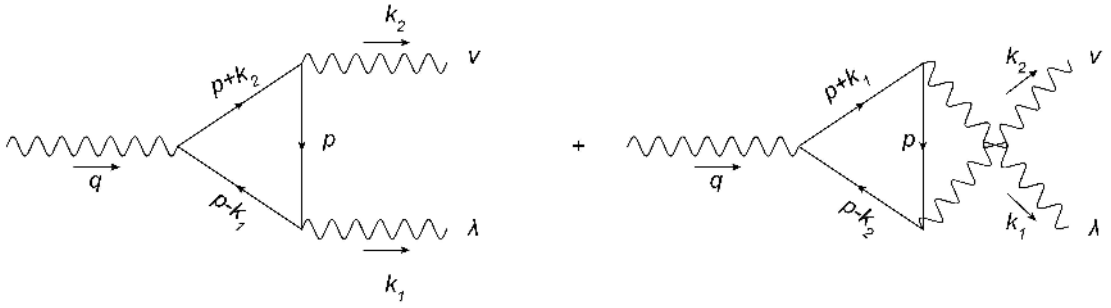

Figure 1.2: *Feynman diagrams contributing to two-photon matrix element of the divergence of the axial current.*

particles in the loop are fermions that we assume massless. For the contribution from

the first diagram one obtains:

$$\mathcal{M}_1^{\mu\nu\lambda} = -1(-ie)^2 \int \frac{d^4p}{(2\pi)^4} \mathbf{Tr}[\gamma^\mu\gamma^5 \frac{i\,(\not{p}-\not{k}_1)}{(p-k_1)^2}\gamma^\lambda \frac{i\,\not{p}}{p^2}\gamma^\nu \frac{i\,(\not{p}+\not{k}_2)}{(p+k_2)^2}]. \tag{1.48}$$

The minus sign corresponds to the fermion loop. From the second diagram one obtains the same result after interchanging (k_1, λ) with (k_2, ν). If in eq. (1.47) one takes the divergence, the result is similar to doting eq. (1.48) with iq_μ. In order to proceed we use the following identity:

$$q_\mu\gamma^\mu\gamma^5 = (\not{p}+\not{k}_2-\not{p}+\not{k}_1)\gamma^5 = (\not{p}+\not{k}_2)\gamma^5 + \gamma^5(\not{p}-\not{k}_1), \tag{1.49}$$

where we have used the fact that $q^\mu = k_1^\mu + k_2^\mu$ and the anti-commuting properties of gamma matrices (for properties of gamma matrices see Appendix A). Now, eq. (1.48), after doting with iq_μ and using the identity above, takes the form:

$$i\,q_\mu\mathcal{M}_1^{\mu\nu\lambda} = e^2 \int \frac{d^4p}{(2\pi)^4} \mathbf{Tr}[\gamma^5 \frac{(\not{p}-\not{k}_1)}{(p-k_1)^2}\gamma^\lambda \frac{\not{p}}{p^2}\gamma^\nu + \gamma^5\gamma^\lambda \frac{\not{p}}{p^2}\gamma^\nu \frac{(\not{p}+\not{k}_2)}{(p+k_2)^2}]. \tag{1.50}$$

Shifting the momentum of integration $p \to p + k_1$ in the first integral and using the cyclic property of trace and the anti-commutation property of γ^5 in the second integral, the eq. (1.50) takes the form:

$$i\,q_\mu\mathcal{M}_1^{\mu\nu\lambda} = e^2 \int \frac{d^4p}{(2\pi)^4} \mathbf{Tr}[\gamma^5 \frac{\not{p}}{p^2}\gamma^\lambda \frac{(\not{p}+\not{k}_1)}{(p+k_1)^2}\gamma^\nu - \gamma^5 \frac{\not{p}}{p^2}\gamma^\nu \frac{(\not{p}+\not{k}_2)}{(p+k_2)^2}\gamma^\lambda]. \tag{1.51}$$

This expression is obviously antisymmetric under $(k_1, \lambda) \to (k_2, \nu)$. Therefore, the contribution from the second diagram exactly cancels this result. Finally it seems that the total result is zero. But in the argument above there is something illegal. As we can see, the integrals in eq. (1.50) are divergent and the shift in divergent integrals is not allowed in general. One method to evaluate the integrals in eq. (1.50) is to use dimensional regularization. In principle, in the framework of dimensional regularization, any integral is performed in d dimensions and the physical result is obtained taking the limit $d \to 4$. But the anti-commutation relations of γ^5 with γ^μ in d dimensions should be used carefully. In their original paper t'Hooft and Veltman used the definition $\gamma^5 = i\gamma^0\gamma^1\gamma^2\gamma^3$ [33]. From this definition it is clear that γ^5 anticommutes with γ^μ for $\mu = 0, 1, 2, 3$ and commutes with γ^μ with other values of μ. In eq. (1.50) the external momenta k_1 and k_2 have at lest one non-zero component for $d = 0, 1, 2, 3$, but the internal momentum p has components in all dimensions. We can use the following decomposition $p = p_{||} + p_\perp$, where $p_{||}$ has zero components in $d-4$ dimensions and $p_\perp$ has zero components in $d = 0, 1, 2, 3$. Since γ^5 commutes with γ^μ in $d-4$ dimensions we can write the following identity:

$$q_\mu\gamma^\mu\gamma^5 = (\not{p}+\not{k}_1)\gamma^5 + \gamma^5(\not{p}-\not{k}_2) - 2\gamma^5\not{p}_\perp. \tag{1.52}$$

Since in the framework of dimensional regularization the shift is allowed, the first two terms after adding the contribution from the second diagram, vanish (we use the same

argument as above). However there is something that survives; the contribution from the third term. This contribution in eq. (1.48) is :

$$i\,q_\mu \mathcal{M}_1^{\mu\nu\lambda} = e^2 \int \frac{d^4p}{(2\pi)^4} \mathbf{Tr}\Big[-2\gamma^5 \not{p}_\perp \frac{(\not{p}-\not{k}_1)}{(p-k_1)^2}\gamma^\lambda \frac{\not{p}}{p^2}\gamma^\nu \frac{(\not{p}+\not{k}_2)}{(p+k_2)^2}\Big]. \tag{1.53}$$

In order to evaluate this integral we can introduce Feynman parameters x, y, and shift the integration variable $p \to p + x\,k_1 - y\,k_2$. The denominator takes the form $(p^2-\Delta)^3$, where Δ is a function of k_1, k_2 and x, y. In the numerator, terms with odd powers of p vanish due to symmetric integration. We can eliminate terms that give a non-zero result. This contribution comes from a term containing $\not{p}_\perp \not{p}_\perp$. Then, we have to evaluate the integral:

$$\int \frac{d^4p}{(2\pi)^4} \frac{\not{p}_\perp \not{p}_\perp}{(p^2-\Delta)^3}. \tag{1.54}$$

Using the fact that $\not{p}_\perp \not{p}_\perp = p_\perp^2 \to \frac{(d-4)}{d}\,p^2$ and standard dimensional regularization integrals we find:

$$\frac{i}{(4\pi)^{d/2}} \frac{(d-4)}{2} \frac{\Gamma(2-d/2)}{\Gamma(3)\,\Delta^{2-d/2}} \to \frac{-i}{2\,(4\pi)^2}, \tag{1.55}$$

when $d \to 4$. After a little standard algebra in eq. (1.53) we obtain:

$$i\,q_\mu \mathcal{M}_1^{\mu\nu\lambda} = e^2 \Big(\frac{-i}{2\,(4\pi)^2}\Big) \mathbf{Tr}[2\,\gamma^5(-\not{k}_1)\gamma^\lambda \not{k}_2 \gamma^\nu] = \frac{e^2}{4\,\pi^2}\epsilon^{\alpha\lambda\beta\nu} k_{1_\alpha} k_{2_\beta}. \tag{1.56}$$

The contribution from the second diagram is the same. Therefore the final result is:

$$\langle k_1, k_2 | \partial_\mu j^{\mu\,5}(0) | 0 \rangle = -\frac{e^2}{2\,\pi^2}\epsilon^{\alpha\nu\beta\lambda}(-i\,k_{2_\alpha})\epsilon^*_\nu(k_2)(-ik_{1_\beta})\epsilon^*_\lambda(k_1). \tag{1.57}$$

This equation shows an anomalous non-conservation of the four-dimensional axial current. It is correct to all orders of perturbation theory and does not receive any other radiative correction [30, 31]. This is a simple QED example where a chiral current appears a problem at one loop corrections. In general, theories that contain gauge bosons that couple to axial currents, are gauge invariant, only if the anomalous terms disappear. This is possible if the fermionic quantum numbers of all fermions are chosen in a suitable way, or if new particles are introduced in the particle spectrum of the theory. For three gauge bosons A^a_μ, A^b_ν and A^c_λ the anomalous term is proportional to the quantity $\mathbf{Tr}[\gamma^5\,t^a\{t^b, t^c\}]$, where the trace is taken over all fermions and t^a, t^b, t^c are group representation matrices. The anticommutator is related to the sum of two diagrams where internal fermions circle in opposite directions. The γ^5 expresses the fact that the anomaly comes from chiral currents. Gauge theories satisfying the condition that the trace above is zero, are called anomaly free. In Chapter 3 we present a systematic method in order to generalize this result in the case of a triple gauge boson vertex. We use a different approach to derive the generalization of the result above. Instead of working in d dimensions, we prefer to perform the calculation in $d = 4$ dimensions and introduce some arbitrary vectors to handle the divergencies that appear during the calculations (for details about these calculations see Appendix H).

1.5.3 Dimensional Regularization

Dimensional Regularization is a method that enables us to evaluate integrals related to calculations that involve Feynman diagrams containing loops. In fact it is a set of self-consistent formal rules that respect the gauge invariance and the renormalizability of a theory. The method has been developed in early 70s by t'Hooft and Veltman [33]. The basic idea behind dimensional regularization is the modification of divergent integrals that appear often in calculations in such a way that the infinities that they involve, are isolated from their finite parts. The main ingredient of this modification is the analytic continuation of the integral $\int d^d\,\mathbf{p} f(\mathbf{p})$, which is considered a function of the complex parameter d, from a region that it converges to a meromorphic[1] function of all values of d. In general the parameter d is a complex number, not necessarily identified with the number of space-time dimensions. This identification occurs only in the case that d is a positive integer number. The following axioms constitute the foundations that dimensional regularization is based on:

1. Linearity: For every a and b complex numbers,

$$\int d^d\mathbf{p}\,[af(\mathbf{p}) + bg(\mathbf{p})] = a\int d^d\mathbf{p}\,f(\mathbf{p}) + b\int d^d\mathbf{p}\,g(\mathbf{p}). \tag{1.58}$$

2. Scaling: For any number s,

$$\int d^d\mathbf{p}\,f(s\,\mathbf{p}) = s^{-d}\int d^d\mathbf{p}\,f(\mathbf{p}). \tag{1.59}$$

3. Translation Invariance: For any vector $\mathbf{q}$,

$$\int d^d\mathbf{p}\,f(\mathbf{p}+\mathbf{q}) = \int d^d\mathbf{p}\,f(\mathbf{p}). \tag{1.60}$$

In order to obtain the result that corresponds to the physical case, one should take the limit $d \to 4$ in the dimensional regularization result. In exactly $d = 4$, some surface integrals appear and the obtained result is not gauge invariant. This case requires a special treatment and it is discussed in more detail in Chapter 4. Also, some d-dimensional integrals and mathematical tricks relevant to dimensional regularization, are presented in Appendix A. Although we have used a different method to perform the four-dimensional integrals especially in Chapters 3 and 4 (shifting the integration variable by arbitrary constant vectors and requiring the result to be gauge invariant), we have used the dimensional regularization method to check our results in several intermediated calculational steps.

[1] A function defined on an open subset D of the complex plane, is called meromorphic, if it is differentiable on all D except a set of isolated points, the poles of this function, where there exists a Laurent series.

Chapter 2

Direct Detection of Dark Matter

Motivated by cosmic ray experimental results, in this Chapter we propose a scenario where a secluded dark matter particle annihilates, primarily, into Standard Model leptons through a low mass mediator particle. We consider several varieties of this scenario depending on the type of mixing among gauge bosons and we study the implications in direct dark matter experiments for detecting low energy recoiling electrons. We find significant event rates and time modulation effects, especially in the case where the mediator is massless, that may be complementary to those from recoiling nuclei. This Chapter is based on the published work [35].

2.1 Introduction

The analysis of the positrons excess (vs electrons) seen in cosmic ray spectra from PAMELA [16,17] in the energy region above 10 GeV confirming previous results from HEAT [18, 19] and AMS-01 [36] experiments together with results from FERMI [20] and HESS [21] collaborations seems to suggest the presence of a WIMP that annihilates into leptons without any indication of annihilation into $(p, \overline{p})$ pairs or other hadrons (see Refs. [37,38] for relevant analysis). This is also reinforced by ATIC [22] experiment which reports excess of electron plus positron cosmic ray events in the energy region $300 \lesssim E \lesssim 800$ GeV and also by signals from WMAP and EGRET [39–41] experiments. These phenomena can be explained by a scenario, originally proposed in ref. [42] - a subset of the so called *secluded Dark Matter* scenarios [43] - involving a new gauge boson X_μ [45][1], which couples to Standard Model (SM) particles and the WIMP through kinetic vector boson mixing with the following properties [46–48] :

$$2\, m_e \lesssim m_X \lesssim m_\chi\, \beta \lesssim m_\chi\, \alpha_{\rm DM}\ , \tag{2.1}$$

where $m_\chi \beta$ is a typical non-relativistic WIMP momentum and velocity $\beta \sim 10^{-3}$ inside the galactic halo and $\alpha_{\rm DM}$ is the dark matter coupling. It has been shown that if eq. (2.1) is satisfied then dark matter annihilation to leptons inside the halo is

[1] In earlier models [44] of secluded dark matter, WIMPs could be annihilated into new light scalar and gauge bosons.

enhanced by a Sommerfeld factor of $\mathcal{O}(\alpha_{\rm DM}/\beta)$ [49], while annihilation to protons is simply kinematically forbidden. A typical range of parameters that are going to be exploited in our analysis and satisfy eq. (2.1) are : $m_X = 0.1 - 1$ GeV, $\alpha_{\rm DM} = \alpha_{\rm em}$ and $m_\chi = 0.1 - 1$ TeV. The new force mediated by the X-boson is a long range force indeed. We must note here that there is a choice of another viable possibility with an even lighter mediator in MeV range that has been studied in ref. [50]. Our results for detecting low energy electrons are even more pronounced in this case.

There is also a possibility for the gauge boson mediator X_μ that couples to the SM gauge bosons through a mass mixing matrix in a generalized gauge invariant way. These models are frequently called Stückelberg models [51,52] and are denoted as model type II in our classification. A characteristic of these models is that the electromagnetic current couples to the dark sector through a massless pole identified as the physical photon. As we shall see, this results in considerable and comparable rates in both nucleon or electron recoiling experiments. Alternatively, it could be that there is a symmetry that renders dark matter particles leptophylic [53–57]. This symmetry is spontaneously broken, resulting in a massive gauge boson X_μ that couples directly to both leptons and WIMP at tree level. Again Sommerfeld enhancement dictates the mass of the X-boson to be in the GeV (or sub GeV) range. This is the model III that is considered in section 2.2.

Within the three model categories mentioned above we want :

1. to study the implications of this new force carrier on both traditional nucleon recoil, and non traditional electron recoil direct dark matter searches, and,

2. to suggest new dark matter experiments involving the detection of electrons scattered by this carrier providing a direct link to observed cosmic ray anomalous electron/positron events.

So far there is a dedicated analysis for electron recoils in DAMA experiment [58] with energies approximately 5 KeV. Our analysis investigates recoiling electrons with energies as low as 10 eV, and suggests an experimental method on how to reach such low energies. It is therefore complementary to the analysis of ref. [58].

In what follows we present a field theory setup which helps to categorize three representative model examples that have been studied in detail and we present event rate predictions for conventional nucleon recoil detection for the models studied. Also we deal with the not so familiar methods of electron recoil detection rates together with time modulation effects and make a proposition of a prototype experiment to be exploited in discovering low energy electrons ejected from WIMP + atom collisions.

2.2 Theory Setup and Model Categories

In this section, we formulate the problem of the Standard Model coupled to, for simplicity, an abelian dark sector with arbitrary kinetic or mass mixing terms allowed by Lorentz, gauge symmetries and renormalizability. Our formulae are then applied in subsequent sections to make predictions for event rates in dark matter detection experiments.

To read out the gauge boson propagators we write the general renormalizable form of the Lagrangian :

$$\mathscr{L} \;=\; -\frac{1}{4}\,\mathbf{\Phi}^T_{\mu\nu}\,\mathcal{K}\,\mathbf{\Phi}^{\mu\nu} \;+\; \frac{1}{2}\,\mathbf{\Phi}^T_{\mu}\,\mathcal{M}^2\;\mathbf{\Phi}^{\mu} \;-\; \frac{1}{2}\,\partial^{\mu}\mathbf{\Phi}^T_{\mu}\,\Xi\,\partial^{\nu}\mathbf{\Phi}_{\nu} \;+\; \mathbf{J}_{\mu}{}^T\,\mathbf{\Phi}^{\mu}\;, \tag{2.2}$$

where $\mathbf{\Phi}_{\mu\nu} = (\partial_\mu \mathbf{\Phi}_\nu - \partial_\nu \mathbf{\Phi}_\mu)$ is a N-column matrix field strength tensor corresponding to an N-column $\mathbf{\Phi}_\mu$ vector field, "T" denotes the transpose of a matrix, $\mathcal{K}$ and $\mathcal{M}^2$ are real and symmetric $N \times N$ matrices with model dependent elements to be specified below, and Ξ is the gauge fixing $N \times N$ symmetric matrix necessary to remove unphysical gauge degrees of freedom. Interaction terms are encoded in the last term of eq. (2.2) where an external current $\mathbf{J}_\mu$, associated with symmetries, couples to the gauge fields.

One has to notice that elements of the mass matrix $\mathcal{M}^2$ should be further restricted by electromagnetic gauge invariance. Phenomenologically speaking, there should always be a pole on the propagator $\langle \mathbf{\Phi}_\mu \mathbf{\Phi}_\nu \rangle$ corresponding to the massless photon i.e., the determinant of the inverse propagator at zero momentum must be exactly zero. Furthermore, without loss of generality, we can always assume that the diagonal elements of matrix $\mathcal{K}$ are normalized to unity.

In Appendix B we calculate the Feynman propagator, $\widetilde{\mathcal{D}}_{\mu\nu}(p)$ with momentum p, for the gauge field $\mathbf{\Phi}^\mu$ which in momentum space reads,

$$i\,\widetilde{\mathcal{D}}_{\mu\nu}(p) \;=\; (\mathcal{K}\,p^2 - \mathcal{M}^2)^{-1}\,\left(g_{\mu\nu} - \frac{p_\mu\,p_\nu}{p^2}\right) \;+\; \left(\Xi\,p^2 - \mathcal{M}^2\right)^{-1}\,\frac{p_\mu\,p_\nu}{p^2}\;. \tag{2.3}$$

At lowest order in $\hbar$, interactions among fields are stored in the action functional

$$S[\widetilde{\mathbf{J}}] \;=\; \frac{1}{2}\int \frac{d^4p}{(2\pi)^4}\,\widetilde{\mathbf{J}}^T_\mu(p)\,[i\widetilde{\mathcal{D}}^{\mu\nu}(p)]\,\widetilde{\mathbf{J}}_\nu(-p)\;, \tag{2.4}$$

where $\widetilde{\mathbf{J}}_\mu(p)$ is the vector current in momentum space. Equations (2.3) and (2.4) are what we actually need to describe observables that arise from mixing dark (or hidden) and visible gauge bosons. As a simple example, we consider the electromagnetic and the dark gauge boson current. Then in eq. (2.2), it is $\mathbf{J}^T_\mu = (eJ^{\rm e.m}_\mu\,,\, g_X J^{\rm dark}_\mu)^T$. It is then clear from eq. (2.4) that interactions between the visible and the dark sector will involve off diagonal elements of the propagator (2.3). Observables, like nucleon recoil event rates can easily be described using the above propagator mixing formalism [59], by simply finding the inverse matrices such in eq. (2.3) for a given model. We remark here that the propagator mixing formalism works equally well in different current basis such as $Q - T_3$ or $Y - T_3$, where Q and Y are the charge and hypercharge of the particles respectively.

Figure 2.1: *Diagramatic form of Feynman propagator appeared in eq. (2.3) between gauge boson "flavours" i and j. For explicit expressions in model I see eqs.(2.6)-(2.11); for model II see eq. (2.14).*

2.2.1 Model I : Non-standard Kinetic Mixing $\mathcal{K}$

Models in this category [42, 43] have been exploited in ref. [47] as candidates for explaining positron excess in cosmic ray data experiments. In its simplest form, the dark matter particle, χ, is charged under a 'dark' $U(1)_X$ and the corresponding 'dark' gauge boson X_μ mixes with the photon A_μ and Z-gauge boson, Z_μ. Annihilations of dark matter particles into *only* SM leptons (and not quarks) are kinematically allowed when the intermediate gauge boson has a mass at the GeV scale.

In notation of ref. [60] and in basis (A_μ, X_μ, Z_μ) (or else $Q - T_3$) our matrices $\mathcal{K}$ and $\mathcal{M}^2$ appeared in eq. (2.3), become:

$$\mathcal{K} \;=\; \begin{pmatrix} 1 & -\epsilon\cos\theta_W & 0 \\ -\epsilon\cos\theta_W & 1 & \epsilon\sin\theta_W \\ 0 & \epsilon\sin\theta_W & 1 \end{pmatrix} \quad , \quad \mathcal{M}^2 \;=\; \begin{pmatrix} 0 & 0 & 0 \\ 0 & m_X^2 & 0 \\ 0 & 0 & m_Z^2 \end{pmatrix}, \quad (2.5)$$

where m_X is the mass of the exotic gauge boson, m_Z is the mass of Z-boson, θ_W is the weak mixing angle and ϵ is a small ($\approx 10^{-3}$) mixing parameter between $U(1)_Y$ and $U(1)_X$ field strength tensors. Working in Feynman gauge ($\Xi = \mathbf{1}_{3\times 3}$) and keeping up to ϵ^2-terms it is easy to work out the mixed propagators $\widetilde{\mathcal{D}}^{ij}_{\mu\nu}(p)$, depicted in Fig.2.1,

between photon, X and Z-gauge bosons, labeled 1,2,3, respectively :

$$i\,\widetilde{\mathcal{D}}^{11}_{\mu\nu}(p) = \frac{g_{\mu\nu}}{p^2} + \frac{\epsilon^2\,\cos^2\theta_W}{p^2-m_X^2}\left(g_{\mu\nu}-\frac{p_\mu p_\nu}{p^2}\right) + \mathcal{O}(\epsilon^3)\,, \tag{2.6}$$

$$i\,\widetilde{\mathcal{D}}^{12}_{\mu\nu}(p) = \frac{\epsilon\cos\theta_W}{p^2-m_X^2}\left(g_{\mu\nu}-\frac{p_\mu p_\nu}{p^2}\right) + \mathcal{O}(\epsilon^3)\,, \tag{2.7}$$

$$i\,\widetilde{\mathcal{D}}^{13}_{\mu\nu}(p) = -\frac{\epsilon^2\,p^2\,\cos\theta_W\sin\theta_W}{(p^2-m_X^2)(p^2-m_Z^2)}\left(g_{\mu\nu}-\frac{p_\mu p_\nu}{p^2}\right) + \mathcal{O}(\epsilon^3)\,, \tag{2.8}$$

$$i\,\widetilde{\mathcal{D}}^{22}_{\mu\nu}(p) = \frac{g_{\mu\nu}}{p^2-m_X^2} + \frac{\epsilon^2\,p^2\,(p^2-\cos^2\theta_W m_Z^2)}{(p^2-m_X^2)^2(p^2-m_Z^2)}\left(g_{\mu\nu}-\frac{p_\mu p_\nu}{p^2}\right) + \mathcal{O}(\epsilon^3), \tag{2.9}$$

$$i\,\widetilde{\mathcal{D}}^{23}_{\mu\nu}(p) = -\frac{\epsilon\,p^2\sin\theta_W}{(p^2-m_X^2)\,(p^2-m_Z^2)}\left(g_{\mu\nu}-\frac{p_\mu p_\nu}{p^2}\right) + \mathcal{O}(\epsilon^3)\,, \tag{2.10}$$

$$i\,\widetilde{\mathcal{D}}^{33}_{\mu\nu}(p) = \frac{g_{\mu\nu}}{p^2-m_Z^2} + \frac{\epsilon^2\,p^4\,\sin^2\theta_W}{(p^2-m_X^2)(p^2-m_Z^2)^2}\left(g_{\mu\nu}-\frac{p_\mu p_\nu}{p^2}\right) + \mathcal{O}(\epsilon^3). \tag{2.11}$$

Some remarks are in order : *i)* among the three physical masses only m_X^2 mass is shifted by an amount of $m_X^2\epsilon^2$ that we ignore, *ii)* gauge invariance for the off diagonal propagator terms is preserved as should be the case. As far as the effective action in eq. (2.4) is concerned, additional statements are in order:

- The single pole $[1/p^2]$ appears only in $J_{\rm e.m}\cdot J_{\rm e.m}$ exchange as usual in the SM.
- A pole $[1/(p^2-m_X^2)]$ for the exotic boson X_μ appears, apart from $J_X\cdot J_X$ exchange, also in $J_{\rm em}\cdot J_X$ exchange at $\mathcal{O}(\epsilon)$.
- There is exchange of current $J_X\cdot J_Z$ i.e., neutrinos and dark matter particles, through a double pole of X and Z at order ϵ.
- There is exchange of $J_{\rm em}\cdot J_Z$ at order ϵ^2 via double pole of X and Z.

The $\epsilon\approx 10^{-3}$-term in the kinetic mixing can naturally arise as a result of mixing two $U(1)$'s at high energies - a mechanism first proposed in ref. [42]. Furthermore, X-boson contributions to the muon anomalous magnetic moment relative to the SM expectation, $\Delta\alpha_\mu=\alpha_\mu^{\rm exp}-\alpha_\mu^{\rm SM}=(290\pm 90)\times 10^{-11}$ [61], are easily found using eq. (2.6) to be

$$\Delta\alpha_\mu = \frac{\alpha_{\rm em}}{3\pi}\,\epsilon^2\cos^2\theta_W\left(\frac{m_\mu}{m_X}\right)^2, \qquad \text{for} \quad \frac{m_\mu}{m_X}\ll 1\,. \tag{2.12}$$

This requires $\epsilon\lesssim 3\times 10^{-2}$ for $m_X\simeq 1$ GeV, where the equality accounts for the 2σ upper limit on $\Delta\alpha_\mu$. Of course there are many other constraints on the mixing parameter ϵ from direct or indirect collider searches and we refer the reader to refs. [62–65]. For example, as we see from eqs. (2.6), (2.9) and (2.11) corrections to oblique electroweak observables arise at order ϵ^2 similar to the case of muon anomalous magnetic moment.

2.2.2 Model II : Non-standard Mass Mixing, $\mathcal{M}^2$

Models belonging to this category are usually referred to as Stueckelberg models [51]. An account on "Stueckelberg" extensions of the Standard Model can be found in [66]. Here, it is more convenient to work on $Y - Y_X - T_3$ basis (B_μ, X_μ, A^3_μ). We now assume that only the matrix $\mathcal{M}^2$ is nontrivial,

$$\mathcal{K} \;=\; \begin{pmatrix} 1 & 0 & 0 \\ 0 & 1 & 0 \\ 0 & 0 & 1 \end{pmatrix}, \qquad \mathcal{M}^2 \;=\; \begin{pmatrix} \frac{1}{4}\, g_Y^2 v^2 + m_Y^2 & m_Y\, m_X & -\frac{1}{4}\, g_Y g\, v^2 \\ m_Y\, m_X & m_X^2 & 0 \\ -\frac{1}{4}\, g_Y g\, v^2 & 0 & \frac{1}{4}\, g^2 v^2 \end{pmatrix}, \tag{2.13}$$

where g_Y, g are the $U(1)_Y, SU(2)_L$ gauge couplings respectively, m_Y^2 is a mass term for the hypercharge gauge field B_μ and v is the vacuum expectation value. The form of the upper left 2×2 $\mathcal{M}^2$ matrix guarantees electromagnetic gauge invariance i.e., massless photon. Furthermore, the zero elements (23) and (32) guarantee that neutrinos are not charged under electromagnetism. Demanding that the inverse propagator has poles at the physical masses, $\det[p^2 - \mathcal{M}^2]|_{p^2=m_i^2} = 0$ where $m_i = 0, m_X, m_Z$, we find that the photon mass is zero to all orders in m_Y, the dark gauge boson and the Z-boson masses are not altered up to $\mathcal{O}(m_Y^2)$, and thus $m_Z^2 = \frac{1}{4}(g^2 + g_Y^2)v^2 + \mathcal{O}(m_Y^2)$.

Following eq. (2.4), we obtain the following effective action (see Appendix C):

$$\begin{aligned} S[J] \;=\; & \frac{1}{2}\int \frac{d^4p}{(2\pi)^4}\, \left\{ \left[e^2\, J_{\rm e.m}(p)\cdot J_{\rm e.m}(-p) - 2\, e^2\, \frac{g_X}{g_Y}\frac{m_Y}{m_X}\, J_{\rm e.m}(p)\cdot J_X(-p) \right] \frac{1}{p^2} + \right. \\ & + \left[g_X^2\, J_X(p)\cdot J_X(-p)\, \left(1 - \frac{m_X^2}{m_Z^2}\right) \;+\; 2\, e^2 \frac{g_X}{g_Y}\frac{m_Y}{m_X}\, J_{\rm e.m}(p)\cdot J_X(-p) \;- \right. \\ & - \left. 2\, g_Y g_X \frac{m_X\, m_Y}{m_Z^2}\, J_X(p)\cdot J_Y(-p) \right] \frac{1}{p^2 - m_X^2}\, \left(\frac{m_Z^2}{m_Z^2 - m_X^2}\right) + \\ & + \left[g^2\, J_Z(p)\cdot J_Z(-p) \left(1 - \frac{m_X^2}{m_Z^2}\right) - 2\, e^2 \frac{g_X}{g_Y}\frac{m_X\, m_Y}{m_Z^2}\, J_{\rm e.m}(p)\cdot J_X(-p) \;+ \right. \\ & + \left. \left. 2 g_Y g_X \frac{m_X\, m_Y}{m_Z^2}\, J_X(p)\cdot J_Y(-p) \right] \frac{1}{p^2 - m_Z^2}\, \left(\frac{m_Z^2}{m_Z^2 - m_X^2}\right) \right\} \;+ \mathcal{O}(m_Y^2), \end{aligned} \tag{2.14}$$

where $e \equiv g_Y g/\sqrt{g_Y^2 + g^2}$ is the electron charge.
Furthermore, $J_{\rm e.m}(p) = J_{A_3}(p) + J_Y(p)$ is the momentum space Fourier transform of the electromagnetic current, i.e., $J^\mu_{\rm e.m} = \sum_f Q_f \overline{f}\gamma^\mu f$ with $Q_f e$ being the charge of a generic fermion f. The dark current J_X obtains an analogous formula with obvious replacement of charge $Q_f e$ by another (hyper)charge, Q_X. Of course, if fermions under consideration are Majorana particles then the corresponding current has only axial-vector form. In addition, J_Z denotes the Fourier transform of the Standard Model neutral current $J^\mu_Z = \frac{1}{\cos\theta_w}(J^\mu_{A_3} - \sin^2\theta_w\, J^\mu_{\rm e.m})$, where the electromagnetic current is, as usual in the SM, the sum of the third component of the isospin $J^\mu_{A_3}$ and hypercharge currents J^μ_Y.

The physics of eq. (2.14) is now transparent : to order $\mathcal{O}(m_Y)$, there are interactions between the electromagnetic $J_{\rm e.m}$ and dark current J_X mediated by the photon *i.e.,* the dark matter particle is charged, and interactions between the hypercharge J_Y and dark current J_X mediated by (X or Z) gauge bosons, respectively. An estimate of the dominant contribution to $\Delta\alpha_\mu$ results in an upper bound $\frac{m_Y}{m_X} \lesssim 9 \times 10^{-4}$, where a 2σ bound on $\Delta\alpha_\mu$ is taken from ref. [61]. As normal in the SM, when the limit of $g_Y \to 0$ is taken, weak currents in eq. (2.14) exhibit a global $SU(2)$ "custodial" symmetry. In present, this symmetry is further enhanced to a global $SO(4) \sim SU(2) \otimes SU(2)$ if, in addition to $g_Y \to 0$, we take the limits $g_X \to g$ and $m_X \to m_Z$ or $m_X \to 0$. In the former case the "hypercharge-dark" current mixing cancels out in the effective action, eq. (2.14). However, there is still $J_{e.m} \cdot J_X$ current mixing. In the latter case ($m_X \to 0$) the off-diagonal, "e.m - dark" currents cancel out to all orders in m_Y, even for general values of gauge couplings since the remaining gauge symmetry is now $U(1)_{e.m} \otimes U(1)_X$. In this limit, eq. (2.13) tells us there is no connection between the SM and the Dark sector.

2.2.3 Model III : Direct coupling, no mixing

In this model, some of the SM leptons (but not quarks) ℓ_L, e_R and the WIMP particle χ are coupled directly to the dark gauge boson X_μ, in principle with different couplings[2]:

$$J^\mu_X \;=\; g'\, Y'(e_L)\, \overline{\ell}_L \gamma^\mu \ell_L \;+\; g'\, Y'(e_R)\, \overline{e}_R \gamma^\mu e_R \;+\; g_X\, Y'(\chi)\, \overline{\chi}\gamma^\mu \chi \;, \tag{2.15}$$

where $Y'(e_L, e_R) = (1, -1)$ denotes the particle hypercharge under the new gauge symmetry. As it has been suggested in Refs. [37,53,54,56,57], this could be an anomaly free gauged $U(1)_{L_e - L_\tau}$. Of course, a new Dirac fermion χ would be playing the role of dark matter particle is also gauged under this symmetry with $Y'(\chi) = 1$. Because we have already discussed the effects of the kinetic and mass mixing in the previous models, without loss of generality, we assume that these mixing matrices are trivial in this model at tree level[3]. If X_μ does not couple to the muon, then the most important constraint on $\alpha' = g'^2/4\pi$ will arise from the $\nu - e$ scattering at low q^2 (ref. [67]):

$$\frac{\alpha'}{m_X^2} \;\lesssim\; 7 \times 10^{-7} \;. \tag{2.16}$$

We shall use this bound when discussing electron recoil detection rates in section 2.4 as is typically comparable with other direct experimental bounds arising from LEP or meson factories. If the X_μ vector boson couples to electrons and muons instead, there is a comparable bound to eq. (2.16) from the muon anomalous magnetic moment. Following $\Delta\alpha_\mu = \frac{\alpha'}{3\pi}\frac{m_\mu^2}{m_X^2}$ for $m_\mu \ll m_X$, there is a bound

$$\frac{\alpha'}{m_X^2} \;\lesssim\; 4.4 \times 10^{-6} \;. \tag{2.17}$$

[2]Various possibilities on how this is realized can be found in ref. [53].

[3]Of course mixing of the X_μ gauge boson with the $U(1)_Y$ is inevitable at one loop. Its magnitude is calculable : $\epsilon \simeq \alpha'^2 \log\frac{m_\tau}{m_\mu} = 2 \times 10^{-4}$ for $\alpha' = \alpha_{\rm em}$. The rest will proceed following eqs.(2.6 - 2.11) of model I.

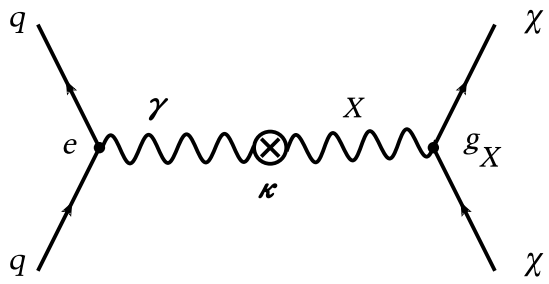

Figure 2.2: *A Feynman diagram leading to the direct interaction of the WIMP χ to the quarks relevant for direct detection of dark matter. The process is mediated by the physical photon. The cross indicates merely that the exotic gauge boson has a small admixture of the photon. Similarly the WIMP can also couple to electrons.*

2.3 Conventional WIMP searches

Conventional DM searches deal with phenomena of WIMPs scattered of a nucleus. The study of the recoil energy spectrum is the primary goal of experiments such as CDMS [23], XENON [24] and DAMA [25]. For models we described in the previous section there are two cases which have been discussed in the literature that could explain the anomalous cosmic ray events:

a) The lightest mediator is massless and

b) the lightest mediator is massive with mass around the proton mass (m_p),

in addition to the assumption that

$$m_p \ll m_\chi \,, \tag{2.18}$$

where m_χ is the WIMP mass. Only model II belongs to the first category and models I, II belong to the second since by definition, there is no direct coupling of X-boson to quarks in model III. In the following subsections we present the WIMP-nucleon cross section for both cases (a) and (b).

2.3.1 Massless Mediator

The differential WIMP-proton cross section in the rest frame of the initial proton is given by:

$$d\sigma = \frac{s(\beta)}{\beta} \frac{e^2 \left(g_X \kappa\right)^2}{q^4} \frac{d^3\mathbf{p}'}{(2\pi)^3} \frac{d^3\mathbf{q}}{(2\pi)^3} (2\pi)^3 \, \delta^{(3)} \left(\mathbf{p} - \mathbf{p}' - \mathbf{q}\right) (2\pi) \, \delta(T - T' - T_q) \,. \tag{2.19}$$

In the equation above $\mathbf{p}', \mathbf{p}$ are the momenta of the incoming and outgoing WIMP respectively, $\mathbf{q}$ the momentum transfer to the nucleon and $T = p^2/2m_\chi$, $T' = (p')^2/2m_\chi$ and $T_q = q^2/2m_p$, are respectively the corresponding kinetic energies in the non relativistic limit. Furthermore, β is the WIMP velocity and $s(\beta) = 1$ for a WIMP which is a Dirac fermion, while $s(\beta) = \beta^2$ in case it is Majorana one [68] (For a detailed derivation of this result see Appendix F) [4]). One finds that the momentum transfer and the final nucleon energy are given by:

$$q = 2\,\mu_r \upsilon\,\xi \approx 2\,m_p \upsilon\,\xi \quad , \quad T_q \approx 2\,m_p\,\upsilon^2 \xi^2 \,, \tag{2.20}$$

where μ_r is the WIMP-nucleon reduced mass, m_p is the proton mass and $0 \leq \xi \leq 1$ is the cosine of the angle between the incoming WIMP and the outgoing nucleon. Integrating over the momentum of the outgoing WIMP and the magnitude of the momentum of the final hadron as well as the ϕ-angle one finds :

$$d\sigma \;=\; \frac{s(\beta)}{\beta}\,\frac{e^2\,(g_X\kappa)^2}{2\pi}\,\frac{1}{(2m_p)^2}\,\frac{d\xi}{\upsilon^3\xi^3}\,. \tag{2.21}$$

The above expression exhibits, of course, the infrared divergence. We will impose a low momentum cut off $E_{\rm th}/A$ provided by the energy threshold $E_{\rm th}$, where A is the mass number of the target, i.e.

$$\xi_{\rm min} = \sqrt{\frac{E_{\rm th}}{(2Am_p\beta^2)}}\,. \tag{2.22}$$

Thus the total cross-section for a Majorana WIMP is given by:

$$\sigma \;=\; \frac{\alpha}{2}\,(g_X\kappa)^2\,\frac{1}{(m_p)^2}\left(\frac{A\,m_p}{E_{\rm th}} - \frac{m_p}{T_{\rm max}}\right) \approx \frac{\alpha}{2}\,(g_X\kappa)^2\,\frac{1}{(m_p)^2}\frac{A\,m_p}{E_{\rm th}}\,. \tag{2.23}$$

Equation 2.23 shows a much stronger dependence of the event rate on the threshold energy $E_{\rm th}$ due to the adopted cut-off $E_{\rm cut-off} = E_{\rm th}/A$. It is interesting to note that this cross section is independent of the WIMP velocity (in the case of a Dirac WIMP the extracted from the data cross section must be multiplied by β^2). We distinguish two cases :

1. The case of Majorana WIMP. We find:

$$\sigma \approx 1.6 \times 10^{-30}\ {\rm cm}^2\,(g_X\kappa)^2\,\frac{2\,A\,m_p}{E_{th}}\,. \tag{2.24}$$

[4]The Majorana fermion does not possess electromagnetic properties. Hence only the $\gamma_\mu\gamma_5$ of the WIMP –X-boson interaction contributes.

The direct dark matter experiments have set on the coherent nucleon cross section the limits:

- The CDMSII experiment [23]:
  The best limit is 6.6×10^{-44} cm^2. The extracted value depends, however, on the WIMP mass. It can vary between 6.6×10^{-44} and 6.6×10^{-42} cm^2.
- The XENON10 collaboration [24]
  They extract 8.8×10^{-44} cm^2 and 4.5×10^{-44} cm^2 for WIMP masses of 100 and 30 GeV respectively.[5]

For our purposes we will assume that the extracted from the data nucleon cross section is $10^{-7}\text{pb} = 10^{-43}\text{cm}^2$. Furthermore, we will take as a reference a threshold energy of 5.0 KeV and examine the sensitivity of our results to the experimental threshold. Using the experimental limit, $\sigma_p \leq 1.0 \times 10^{-43}$ cm^2, we can write:

$$\frac{\text{Rate(new)}}{\text{Rate(conventional)}} = 1.6 \times 10^6 \frac{Z^2}{A^2} \left(g_X \kappa\right)^2 \frac{A\, m_p}{E_{th}} \ . \tag{2.25}$$

Note that the coherence factor now is Z^2, since in the case of the photon only the protons of the target contribute. Adopting a threshold value of 5 KeV, we get

$$\frac{\text{Rate(new)}}{\text{Rate(conventional)}} = 3.0 \times 10^{18} \frac{Z^2}{A} \left(g_X \kappa\right)^2 \ . \tag{2.26}$$

For the Ge target $(A = 73, Z = 32)$ we get

$$\frac{\text{Rate(new)}}{\text{Rate(conventional)}} = 4.3 \times 10^{19} \left(g_X \kappa\right)^2 \ , \tag{2.27}$$

which leads to the limit:

$$|g_X \kappa| \leq \sqrt{\frac{1}{0.43 \times 10^{19}}} = 1.6 \times 10^{-10} \ . \tag{2.28}$$

From the second term in eq. (2.14) and assuming that $\alpha_{\text{DM}} = g_X^2/4\pi = \alpha_{\text{em}}$, one can easily translate this into bounds on the model II parameters for Majorana WIMP :

$$Q_X \frac{m_Y}{m_X} \lesssim 0.54 \times 10^{-10} \ , \qquad \text{(model II)} \ . \tag{2.29}$$

2. <u>The case of a Dirac WIMP</u>. We find:

$$\sigma \approx \frac{1}{\beta^2} \frac{\alpha}{2} \frac{1}{(m_p)^2} \left(g_X \kappa\right)^2 \frac{A\, m_p}{E_{th}} \ . \tag{2.30}$$

[5]These limits however, have been improved for WIMP mass lower than 10 GeV. For the CDMSII experiment the extracted value is 2.4×10^{-41} cm^2 for WIMP mass ~ 10 GeV with 90% upper confidence level. For XENON10 the spin independent dark matter-nucleon cross section is $> 3.5 \times 10^{-42}$ cm^2 for a dark matter particle with mass 8 GeV.

If we knew the coupling $|g_X\kappa|$ we could incorporate this into the evaluation of the nuclear cross section, fold it with the velocity distribution and proceed with the evaluation of the event rate. Since, however, we like to constrain the parameter $|g_X\kappa|$ we will employ an average velocity:

$$\sigma \to <\sigma> \approx <\frac{1}{\beta^2}> \frac{\alpha}{2}\frac{1}{(m_p)^2}\,(g_X\kappa)^2\,\frac{Am_p}{E_{th}}\ . \tag{2.31}$$

But for a Maxwell - Boltzmann distribution *i.e.,* $<\frac{1}{\beta^2}> \to \frac{3}{<\beta^2>}$, we obtain the constraint:

$$|g_X\kappa| \leq 1.6\times 10^{-10}\frac{\sqrt{<\beta^2>}}{\sqrt{3}} \approx 0.8\times 10^{-13}\ , \tag{2.32}$$

from which the bound on model II for $\alpha_{\rm DM}=\alpha_{\rm em}$:

$$Q_X\,\frac{m_Y}{m_X} \lesssim 0.27\times 10^{-13}\ , \qquad \text{(model II)}\ , \tag{2.33}$$

is found. As expected the limit is now more stringent than in eq. (2.29).

The results for the Xe target are similar. This bound is by many orders of magnitude stronger than the one obtained from electroweak fits [66] or $(g-2)_\mu$ [see discussion towards the end of section (2.2.2)]. The corresponding bound for Dirac WIMP is about three orders of magnitude more stringent. This means that additional mechanisms should be added in model II (Stückelberg type of ref. [66] for example) in order to efficiently depleting the WIMP in the early universe.

Although eq. (2.29) [or eq. (2.33)] provides a very stringent limit, we should not forget that in this case we have a much stronger dependence of the rates on the energy threshold through the need for a low energy cut off on the elementary cross section.

Alternatively we may extract from the data for Xe ($A=131, Z=54$) an elementary cross section assuming it to be of the form[6] :

$$\sigma^S_{N,\chi^0}\,(A,E_{\rm th}) \ =\ \sigma_0\frac{A}{131}\frac{5\ {\rm keV}}{E_{\rm th}}\ , \tag{2.34}$$

where σ_0 is the elementary cross section obtained in the particle model for a target with nuclear mass number A and threshold energy $E_{\rm th}$. Then by fitting to the experiment we obtain:

$$(131/54)^2\sigma^S_{N,\chi^0} = 0.5\times 10^{-7} \Rightarrow \sigma_0 = 2.9\times 10^{-7}{\rm pb} = 2.9\times 10^{-43}\ {\rm cm}^2\ . \tag{2.35}$$

In spite of the $(Z/A)^2$ factor we obtain a smaller value than in the standard experiment. This is due to the small cut off energy $E_{\rm th}/A$ employed. With the above ingredients the number of events in time T due to the coherent scattering [69], can be cast in the form:

$$R \simeq 1.07\ 10^{-5}\times\frac{T}{1{\rm y}}\frac{\rho(0)}{0.2\ {\rm GeVcm}^{-3}}\ \frac{100\ {\rm GeV}}{m_{\chi^0}}\ \frac{m}{1\ {\rm kg}}\ \frac{\sqrt{\langle v^2\rangle}}{280\ {\rm km\ s}^{-1}}\ \frac{\sigma^S_{N,\chi}}{10^{-43}\ {\rm cm}^2}\ f_{\rm coh}(A,\mu_r(A)), \tag{2.36}$$

[6]This treatment does not distinguish between a Majorana and a Dirac WIMP.

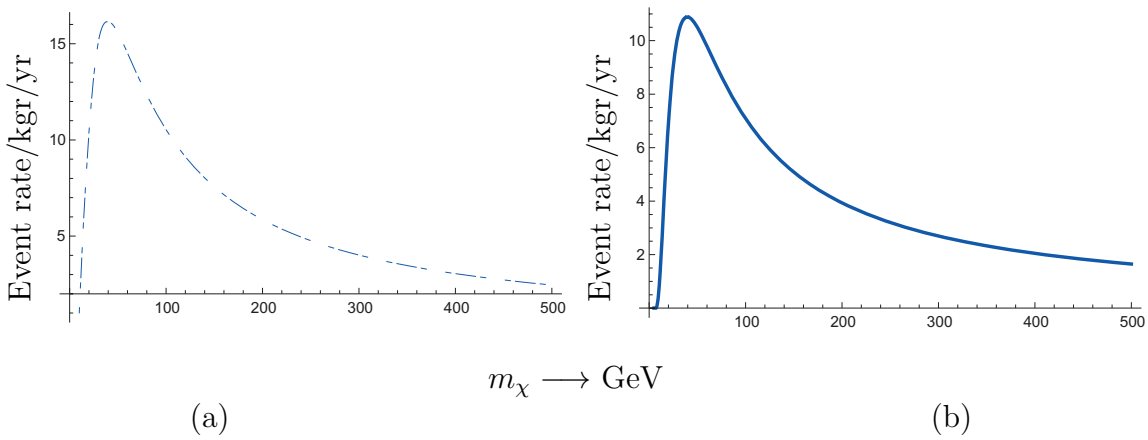

Figure 2.3: *The total rates for traditional WIMP searches assuming a nucleon cross section* $\sigma_N = 10^{-43}$ cm^2 *in (a). The case of the photon mediated process considered in this work is exhibited in (b). Both refer to the case of a heavy target (A=131) and were computed assuming an energy threshold of 5 KeV. The results for the Iodine target used by the DAMA experiment are almost identical.*

where the elementary cross section $\sigma^S_{N,\chi}$ can be treated as a phenomenological parameter independent of the WIMP mass in units of 10^{-43} cm^2. The quantity $f_{\rm coh}(A, \mu_r(A))$ can be obtained from the published in ref. [69] values of t for the standard MB velocity distribution (n=1). For the photon mediated mechanism examined here, the above equation must be modified by multiplying $f_{\rm coh}(A, \mu_r(A))$ with the factor Z^2/A^2 and employing eq. (2.34) for the elementary cross section (in units of 10^{-43} cm^2). The event rate per kg of target per year for the traditional experiments for a heavy isotope like Xe and a light isotope like ^{19}F, as a function of the WIMP mass is exhibited in Figs 2.3 and 2.4. On the same plots we show the event rate for the photon mediated process examined in the present work. It is not surprising that the agreement is good since the elementary cross section was fitted to the data. The small difference is understood, since in the extraction of the elementary cross section from the data, a zero threshold value was used in the phase space integrals. The event rates are sensitive functions of the threshold energy, $R = R(E_{\rm th})$. In the case of the Xe isotope the ratio $R(E_{\rm th})/R((E_{\rm th})_{\rm min}$ is exhibited in Fig. 2.5. The threshold dependence is much more profound in the case of the light WIMP, since, then, the average energy transfered is small. As expected the threshold dependence is more dramatic in the case of the present model (this is a bit obscured in the figure since in this case the graphs are normalized at 5 keV). In the case of a Dirac fermion the extracted limit will be smaller, but the traditional calculations are not adequate for the analysis, due to the different velocity dependence of the elementary cross section.

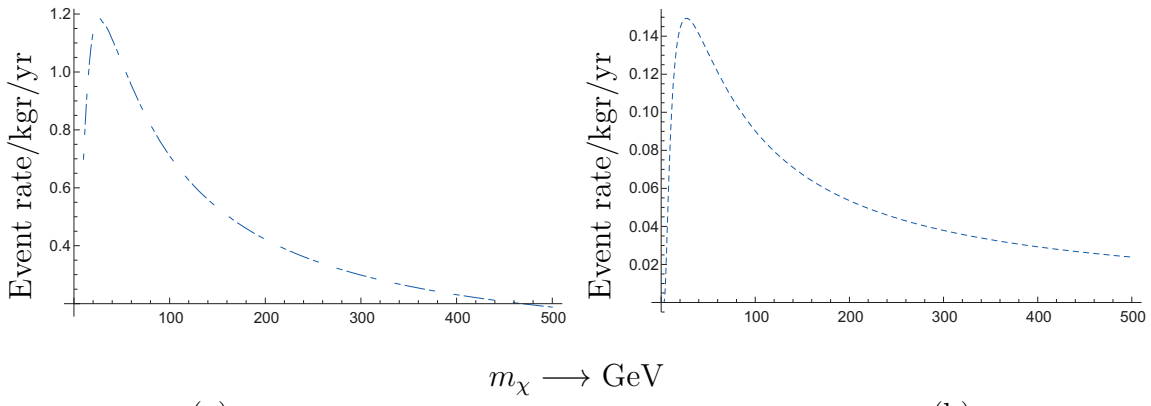

Figure 2.4: *The same as in Fig. 2.3 in the case of the light target* ^{19}F.

2.3.2 Massive Mediator

In this case the WIMP - nucleon cross section reads :

$$\begin{aligned}\sigma &= s(\beta)\,\frac{16\pi\alpha_{\rm em}\,\kappa^2\,\alpha_{\rm DM}\,m_p^2}{m_X^4} \\ &= 1.2\times 10^{-30}\ {\rm cm}^{\,2}\, s(\beta)\,\frac{\alpha}{137^{-1}}\,\frac{\alpha_{\rm DM}}{137^{-1}}\,\kappa^2\left(\frac{m_p}{m_X}\right)^4 , \end{aligned} \tag{2.37}$$

where the cross section refers to Dirac (Majorana) WIMP and $s(\beta) = 1(\beta^2)$ respectively. Taking $\beta^2 \ \to < \beta^2 > \approx \ 10^{-3}$ we find:

$$\kappa \lesssim 3\times 10^{-7}\ (3\times 10^{-4})\,. \tag{2.38}$$

From these we obtain bounds for parameters in models I, II [see eqs. (2.8) and (2.14)],

$$\epsilon \ \lesssim \ 3.0\times 10^{-7}\,(3.0\times 10^{-3})\,, \qquad \text{(model I)} \tag{2.39}$$

$$Q_X\,\frac{m_Y}{m_X} \ \lesssim \ 1.6\times 10^{-6}\,(1.6\times 10^{-3})\,, \qquad \text{(model II)}\,, \tag{2.40}$$

where the number in parenthesis corresponds to Majorana WIMP dark matter particle. These limits are less stringent than those obtained in the case of the massless mediator. In the case of the massive mediator, with the possible exception of the velocity dependence in the case of Majorana WIMP, the cross section behaves as in the standard CDM case, since in this case we do not encounter an energy cutoff. Since, however, we do not know the values of the parameters ϵ and $\frac{m_Y}{m_X}$, we cannot make predictions about the event rates. Instead we have used the present experimental limits to constrain these parameters. Thus we saw that the current experimental limits impose the most stringent limits on these parameters. If, on the other hand, we use the previous constrains we can conclude that WIMPs in models I, II scatter off nuclei too many times.

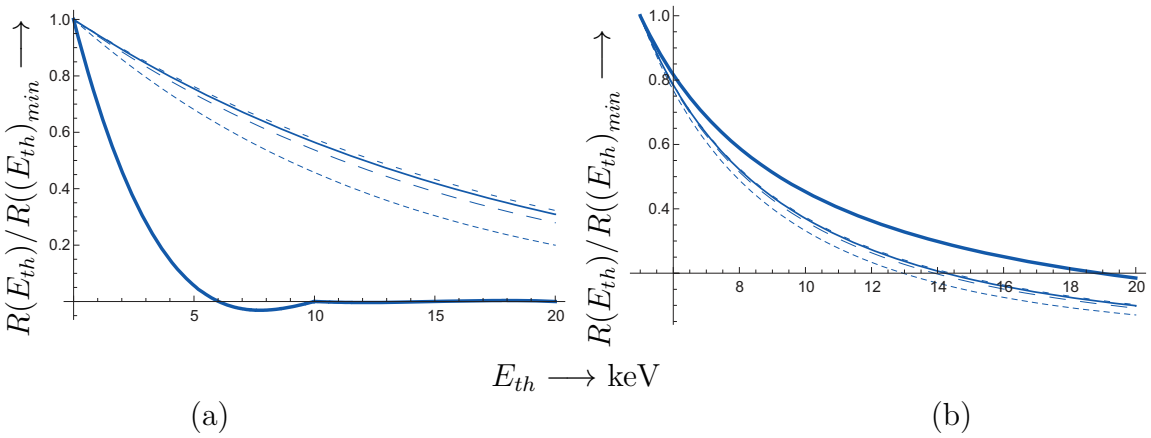

Figure 2.5: *The quantity $R(E_{\rm th})/R((E_{\rm th})_{min}$, i.e. the ratio of the event rate at a given threshold divided by that at the lowest threshold considered, as a function of the threshold energy. In (a) as predicted by traditional mechanisms (lowest threshold assumed zero). In (b) as predicted by the present model (now due to the need for a cut off the lowest threshold energy employed was 5 keV). The thick line, short dash, long dash, fine line and long short dash correspond to WIMP masses 10, 50, 100, 200 and 500 GeV respectively.*

These effects should have been seen in experiments [23, 24] (or may have already been seen [25]). An exception is a Majorana WIMP candidate in model I which results in current sensitivity event rates.

2.4 Unconventional WIMP searches

2.4.1 Cross Section

The other possibility is the direct scattering of WIMPs by electrons that are bounded in atoms. The relevant Feynman diagram is obtained replacing the quarks by electrons. In this case only the electron flavour can be detected since the other flavours are not energetically allowed. Since the outgoing electrons are expected to have energies in the eV region one cannot ignore atomic binding effects. The binding energy b is found from the tables of ionization potential (energy) of an atom.[7]

The problem is to find the cross section for WIMP scattered off an electron bounded in an atom. In order to proceed we shall make two simplifying assumptions :

1. As a working example, we shall assume that the target is a hydrogenic atom denoted by H *i.e.,* a nucleus with charge $+Ze$ and a single bounded electron

[7]Tables are normally given in kJ/mol, but they can easily be translated in eV, since we can use the fact that 96.485 kJ/mol = 1 eV. Thus for Cs we find $b = 375.7/96.485 = 3.89$ eV.

with charge $-e$. We shall discuss deviations from this assumption throughout.

2. The gauge boson mediator X couples *only* to WIMP and leptons but not to quarks. This is a necessary condition to explain PAMELA positron excess of events. Therefore, this discussion refers strictly to model III in eq. (2.15)

There are four processes that could take place in WIMP + H-like atom collisions :

$$\chi + H \longrightarrow \chi + H \quad \text{(elastic)}\,, \tag{2.41}$$
$$\chi + H \longrightarrow \chi + H^* \quad \text{(inelastic)}\,, \tag{2.42}$$
$$\chi + H \longrightarrow \chi + e^- + H^+ \quad \text{(production)} \tag{2.43}$$
$$\chi + H \longrightarrow (\chi + H) \quad \text{(bound state)}\,. \tag{2.44}$$

For the rest we shall consider only the situation (2.43). The elastic scattering (2.41) cannot be detected, and although we cannot exclude the inelastic one (2.42) from being experimentally probed through final state photons, we believe that it would be easier to detect the electrons from (2.43). We shall assume that the electron emerges with high momenta, $\mathbf{p'_e}$, such that in the final state its interaction with the Coulomb potential in H-like atom is negligible, i.e, we can use plane wave states for incoming and outgoing particles. Using standard textbook [34] wavepacket analysis our starting point will be the cross section formula in the lab frame:

$$\begin{aligned} d\sigma \;=\; & \frac{1}{2E_\chi\, 2E_e}\,\frac{1}{|v|}\,\frac{d^3\mathbf{p'}_\chi}{(2\pi)^3 2E'_\chi}\,\frac{d^3\mathbf{p'_e}}{(2\pi)^3 2E'_e}\,|\overline{\mathcal{M}}|^2\,(2\pi)\,\delta(T_\chi - T'_\chi - T'_e - b)\,\times \\ & \times\, d^3\mathbf{p_e}\,(2\pi)^3\,\delta^{(3)}(\mathbf{p}_\chi + \mathbf{p_e} - \mathbf{p'}_\chi - \mathbf{p'_e})\,|\phi(Z,\mathbf{p_e})|^2, \end{aligned} \tag{2.45}$$

where $\mathbf{p}_\chi, \mathbf{p_e}$ ($\mathbf{p'}_\chi, \mathbf{p'_e}$) are the incoming (outgoing) three vector momenta of the WIMP and electron respectively, and $\overline{\mathcal{M}}$ is the matrix element of the process $\chi + e \to \chi + e$ averaged over the spins of the initial states calculated in Born approximation. We also ignore local velocity effects from the bound electron in the (static in lab frame) atom i.e., that is the relative velocity is $v \simeq v_\chi$. $T_i = p_i^2/2m_i$, $i = \chi, e$ are the kinetic energies and b is the binding energy of the electron in H-atom ($b \approx 13.6$ eV). Moreover, in the non-relativistic limit $E_\chi \simeq E'_\chi \approx m_\chi$ and $E_e \simeq E'_e \approx m_e$ with $m_\chi \gg m_e$, while $\phi_{n\ell m_\ell}(\mathbf{p})$, normalized at $\int_V d^3p\,|\phi_{n\ell m_\ell}(\mathbf{p})|^2 = 1$, is the Fourier transform of the coordinate wave function $\psi_{n\ell m_\ell}(\mathbf{r})$. Using the $\delta^{(3)}$-function to perform the integration over $\mathbf{p_e}$, we obtain:

$$\begin{aligned} d\sigma \;=\; & \frac{|\overline{\mathcal{M}}|^2}{16 m_\chi^2 m_e^2 \beta}\,\frac{d^3\mathbf{p'}_\chi\, d^3\mathbf{p'_e}}{(2\pi)^2}\,\delta\!\left(\frac{|\mathbf{p}_\chi|^2}{2m_\chi} - \frac{|\mathbf{p'}_\chi|^2}{2m_\chi} - \frac{|\mathbf{p'_e}|^2}{2m_e} - b(Z)\right)\,\times \\ & \times\,|\phi_{n\ell m_\ell}(Z, \mathbf{p'}_\chi + \mathbf{p'_e} - \mathbf{p}_\chi)|^2, \end{aligned} \tag{2.46}$$

where the energy conservation delta-function has been written out explicitly. The result of eq. (2.46) is a product of two parts : a part that contains the dynamics of the WIMP-electron interaction through the matrix element $|\overline{\mathcal{M}}|$ times the probability of

finding the target electron with momentum $\mathbf{p_e} = \mathbf{p}'_\chi + \mathbf{p}'_\mathbf{e} - \mathbf{p}_\chi$ in H-atom. In addition the matrix element of the process $\chi + e \to \chi + e$ averaged over the spins of the initial states in Born approximation reads :

$$|\overline{\mathcal{M}}|^2 \;\simeq\; \frac{(16\pi)^2 \alpha_{\rm DM} \alpha' m_e^2 m_\chi^2}{(|\mathbf{p}_\chi - \mathbf{p}'_\chi|^2 - m_X^2)^2}\, s(\beta)\;, \tag{2.47}$$

where the factor $s(\beta) \equiv 1\,(\beta^2)$ for Dirac WIMP (Majorana WIMP) particle. Note that the cross section for Majorana WIMP is always smaller by a factor of β^2 compared to the one involving Dirac WIMP (details in Appendix F). We now use the kinetic energy δ-function appearing in eq. (2.46) in order to perform the $|\mathbf{p}'_\chi|$ integration and arrive at:

$$d\sigma \;=\; \frac{16\pi^2 \alpha_{\rm DM} \alpha' m_\chi^2\, s(\beta)}{(|\mathbf{p}_\chi - \mathbf{p}'_\chi|^2 - m_X^2)^2}\, \frac{|\mathbf{p}'_\chi|}{|\mathbf{p}_\chi|}\, |\mathbf{p}'_\mathbf{e}|^2 d|\mathbf{p}'_\mathbf{e}|\; |\phi_{n\ell m_\ell}(Z, \mathbf{p}'_\chi + \mathbf{p}'_\mathbf{e} - \mathbf{p}_\chi)|^2\, d\xi\, d\eta, \tag{2.48}$$

where the initial WIMP momentum is $|\mathbf{p}_\chi| = m_\chi \beta$ and the scattering angles are defined as

$$\xi = \widehat{p}_\chi \cdot \widehat{p}'_\chi\;, \qquad \eta = \widehat{p}_\chi \cdot \widehat{p}'_e\;, \qquad \xi, \eta \in [-1, 1]\;. \tag{2.49}$$

The integration over the azimuthal angles has been carried out trivially in eq. (2.48) and the momentum $|\mathbf{p}'_\chi|$ of the scattered WIMP is found to be

$$|\mathbf{p}'_\chi| \;=\; \sqrt{m_\chi^2\, \beta^2 \;-\; 2\, m_\chi\, b(Z) \;-\; \frac{m_\chi}{m_e}\, p'^2_e}\;, \quad \text{with} \qquad p'_e \;=\; \sqrt{2\, m_e\, E'_e}\;, \tag{2.50}$$

where $b(Z)$ is the ground state energy for hydrogenic atoms:

$$b(Z) \;=\; \frac{Z^2}{2a}\frac{e^2}{4\pi} \;=\; \frac{Z^2}{2} m_e\, \alpha_{\rm em}^2\;, \qquad a \simeq \frac{1}{m_e\, \alpha_{\rm em}}\;, \tag{2.51}$$

in the approximation $\mu \simeq m_e$, where μ is the reduced mass, with $\alpha_{\rm em} = \frac{e^2}{4\pi} \approx 1/137$, $m_e \simeq 0.5$ MeV and $a = a_0 \approx 0.5$ Å being the Bohr radius for $Z = 1$. Throughout this Chapter, we are going to use the ground state momentum distribution of hydrogenic atoms which reads:

$$\phi_{100}(Z, p) \;=\; \frac{2^{3/2}}{\pi a}\, \frac{(Za)^{5/2}}{(Z^2 + p^2\, a^2)^2}\;. \tag{2.52}$$

Notice that $\phi_{100}(p)$ depends on $|p|^2$ and therefore on the scattering angles η and ξ and electron energy E'_e. A term in eq. (2.48), $\frac{|\mathbf{p}'_\chi|}{|\mathbf{p}_\chi|} = \frac{|\mathbf{v}'_\chi|}{|\mathbf{v}_\chi|}$, arises from the fact that we treated the H-atom as a brick wall potential. Had we not done so, the influence of the Coulomb potential on the emerging electron would not have been uniquely correlated to $\mathbf{p}'_\chi$, $\mathbf{p}_\chi$ and the back reaction of the proton should have been taken into account.

Exactly the same result as in eq. (2.48) can be found by using simpler time-dependent perturbation theory for transitions to continuum in non-relativistic quantum

mechanics [70] (for more details see Appendix E). In a more refined analysis however, when the recoiling energy is in the neighborhood of the binding energy of the atom, one should take into account effects from the continuum hydrogenic wave functions instead of treating the final electron as plane wave. This analysis, though more accurate, is far more complicated and does not change the qualitative features of our results. We analyze below the corresponding cross sections for a massless and a massive mediator as we did in section 2.3 for the nucleons.

Event Detection Rates

In general for an atom, due to binding energy effects, only the loosely bound electrons can contribute to the process (2.43). So, we will convolute the elementary cross section with the WIMP velocity distribution, which, with respect to the galactic center, we will take to be Maxwell-Boltzmann form:

$$f(\beta) \;=\; \left(\frac{3}{2<\beta^2>}\right)^{3/2} \frac{1}{\pi^{3/2}}\, e^{-\frac{3\beta^2}{2<\beta^2>}}\,. \tag{2.53}$$

Transforming this into the local coordinate system:

$$\beta \to \beta\widehat{\beta} + \beta_0\widehat{z} = \beta\widehat{\beta} + \sqrt{\frac{2<\beta^2>}{3}}\widehat{z}, \quad \beta^2 \to \beta^2 + \frac{2}{3}<\beta^2> + 2\beta\cos(\theta)\sqrt{\frac{2}{3}<\beta^2>}\,, \tag{2.54}$$

where θ is the angle between $\widehat{\beta}$ and $\widehat{z}$ and $\beta_0 = \sqrt{\frac{2<\beta^2>}{3}}$ is the sun's velocity with respect to the center of the galaxy and $<\beta^2> \approx 10^{-6}$. Then we obtain the local distribution of speeds $f_\ell(\beta)$ relative to the detector to be:

$$f_\ell(\beta) = \left(\frac{3}{2<\beta^2>}\right)^{3/2} \frac{1}{\pi^{3/2}} e^{-\left(\frac{3\beta^2}{2<\beta^2>} \,+\, 2\,\beta\,\cos(\theta)\,\sqrt{\frac{3}{2<\beta^2>}} \,+\, 1\right)}. \tag{2.55}$$

The integration over the angles of the distribution can be done analytically. In evaluating the rate one has to incorporate the incoming flux. So, adopting appropriate normalization, in the convolution we introduce the factor $1/\sqrt{<\beta^2>}$. This way, as we find in Appendix D, the rate is proportional to :

$$\frac{\beta\, f_\ell(\beta)\, d^3\beta}{\sqrt{<\beta^2>}} \;=\; \left(\frac{3}{2<\beta^2>}\right)^{3/2} \frac{2}{\sqrt{\pi}} e^{-\left(\frac{3\beta^2}{2<\beta^2>}+1\right)} \frac{\beta^3}{\sqrt{<\beta^2>}} \frac{\sinh\left(2\beta\sqrt{3/(2<\beta^2>)}\right)}{\beta\sqrt{3/(2<\beta^2>)}} d\beta\,. \tag{2.56}$$

Combining this with the cross section of eq. (2.48) obtained previously we arrive at:

$$\left\langle \frac{d\sigma}{dE'_e} \frac{\beta}{\sqrt{<\beta^2>}} \right\rangle \;=\; \int_{\beta_{\rm min}}^{\beta_{\rm esc}} d\beta\, \frac{\beta f_\ell(\beta)}{\sqrt{<\beta^2>}}\, \frac{d\sigma}{dE'_e}\,, \tag{2.57}$$

where the lower velocity in the integral can be read from the positivity of the square root quantity in eq. (2.50):

$$\beta_{\rm min} = \sqrt{\frac{2E'_e}{m_\chi} + \frac{2b(Z)}{m_\chi}}\,, \tag{2.58}$$

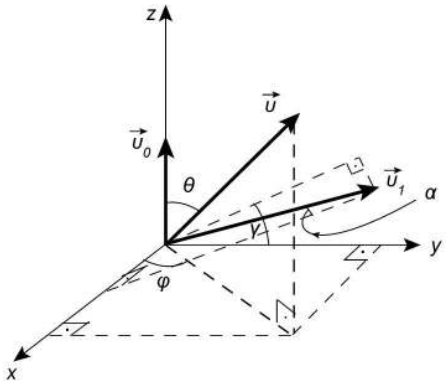

Figure 2.6: *The kinematics relevant to time modulation effects.*

and $\beta_{esc} = 2.84\sqrt{(2/3) < \beta^2 >}$ is the escape velocity. It is now easy to calculate the differential event rate per eV ejected electron energy per year and per kilogram of target material, to be

$$\frac{dR}{dE'_e} \;=\; \frac{\rho_0}{m_\chi}\sqrt{< \beta^2 >}N_e \left\langle \frac{d\sigma}{dE'_e}\,\frac{\beta}{\sqrt{< \beta^2 >}} \right\rangle \;, \tag{2.59}$$

where $\rho_0 = 0.2$ GeV/cm^3 is the WIMP energy density and N_e is the number of target electrons. Integration of eq. (2.59) upon E'_e over the region from $E'_{e_{min}} = 0$ to $[m_\chi \beta^2_{\rm esc}/2 - b(Z)]$ results in the total event number per unit time and mass of the target which among other parameters depends on the mass and atomic numbers of the target atom. Moreover, we shall display results on the total event rate $R(Z)$ when $E'_{e_{min}} = E_{\rm th}$ with varying experimental threshold energy $E_{\rm th}$.

Time Modulation Effects for Electrons

In the convolution of the elementary cross section we have so far considered only the motion of the sun with respect to the center of galaxy. More realistically, one should consider also the Earth's velocity and then find the modulated event rate that might be detected on Earth. In this case the WIMP velocity is read from

$$\mathbf{v'} \;=\; \mathbf{v} \;+\; v_0\,\widehat{\mathbf{z}} \;+\; v_1\,(\sin\alpha\,\widehat{\mathbf{x}} \;+\; \cos\alpha\cos\gamma\,\widehat{\mathbf{y}} \;+\; \cos\alpha\sin\gamma\,\widehat{\mathbf{z}})\;, \tag{2.60}$$

where v_0 is Sun's velocity, v_1 is Earth's annual velocity, $\gamma \approx \frac{\pi}{6}$ is the angle between the projection of vector $\mathbf{v_1}$ on the plane yOz and the $\widehat{\mathbf{y}}$ direction and $\alpha = \alpha(t)$ is the complementary angle of the angle between $\mathbf{v_1}$ and $\widehat{\mathbf{x}}$ (see Fig. 2.6 above). Then the WIMP cross section has to be convoluted with

$$\left(\frac{\beta\, f_\ell(\beta)\, d\beta}{\sqrt{< \beta^2 >}}\right) \;=\; \left(\frac{\beta\, f_\ell(\beta)\, d\beta}{\sqrt{< \beta^2 >}}\right)_0 (1 + k\,\delta\,\cos\alpha)\;, \tag{2.61}$$

where the expression with the subscript "0" refers to eq. (2.56) with $\delta = \frac{v_1}{v_0} \approx 0.135$ and

$$k \;=\; \left(2\beta \sqrt{\frac{3}{2<\beta^2>}}\, \frac{\cosh\left(2\beta\sqrt{\frac{3}{2<\beta^2>}}\right)}{\sinh\left(2\beta\sqrt{\frac{3}{2<\beta^2>}}\right)} - 3 \right) \sin\gamma \; . \tag{2.62}$$

It is now trivial to extend the distribution with energies event rate of eq. (2.59) with

$$\frac{dR}{dE'_e} \;=\; \left\langle \frac{dR}{dE'_e} \right\rangle_0 \;+\; \left\langle \frac{dR}{dE'_e} \right\rangle_{\rm mod} \times \cos\alpha, \tag{2.63}$$

where $\left\langle \frac{dR}{dE'_e} \right\rangle_0$ is the unmodulated differential event rate, while $\left\langle \frac{dR}{dE'_e} \right\rangle_{\rm mod}$ contains also the factor k in eq. (2.62). A detailed derivation of these expressions, is presented in Appendix D.

2.4.2 Massless Mediator

In this case dark matter scattering happens via the coupling of the exotic gauge boson to the photon (model II). In the general case the WIMP-electron cross section is not independent of the velocity. Thus, we will first estimate the cross section by using an average velocity $\sqrt{<\beta^2>} = 10^{-3}$. Following eq. (2.48) for a photonic mediator we find the differential cross section:

$$\frac{d\sigma}{dE'_e} \;=\; s(\beta) 16\pi^2 \alpha' \alpha_{\rm DM}\, \kappa^2\, m_\chi^2 m_e\, \frac{|\mathbf{p}'_\chi|}{|\mathbf{p}_\chi|}\, |\mathbf{p}'_\mathbf{e}| \int_{-1}^{1} d\xi \int_{-1}^{1} d\eta\, \frac{|\phi_{n\ell m_\ell}(Z, \mathbf{p}'_\chi + \mathbf{p}'_\mathbf{e} - \mathbf{p}_\chi)|^2}{(\mathbf{p}'_\chi - \mathbf{p}_\chi)^4}, \tag{2.64}$$

where $\mathbf{q} = \mathbf{p}'_\chi - \mathbf{p}_\chi$ is the WIMP momentum transfer which is ξ dependent. The cross section peaks up the most from the forward direction $\xi \approx 1$. It should be mentioned that since the initial electron is bound, there is no infrared divergence in this case. Moreover, the momentum transfer can be as low as :

$$|\mathbf{q}| \;\simeq\; 2\, \frac{b(Z) + E'_e}{\beta} \; . \tag{2.65}$$

This relation is important for explaining our numerical results below. Furthermore, in presenting the results we assume a Dirac WIMP fermion i.e. $s(\beta) = 1$. We choose a benchmark scenario inspired by our findings in nucleon decay :

$$\beta = \sqrt{<\beta^2>} = 10^{-3} \; , \; Z = 1 \; , \; \alpha_{\rm DM} = \alpha' = \alpha_{\rm em} \; , \; m_\chi = 100 \text{ GeV} \; , \; \kappa = 10^{-10} \; . \tag{2.66}$$

As it is obvious from eq. (2.64) it is very easy to apply our numerical results to any other parameters, β, $\alpha_{\rm DM}$, α', κ than those shown in eq. (2.66). We must note here that there is no parameter analogous to κ in model III. This parameter is used here as a rescale factor and its very small value is adjusted so that we obtain rates of few events.

In Fig. 2.7a are shown the results for the $d\sigma/dE'_e$ as a function of final electron's energy E'_e for three different cases of hydrogenic atoms with $Z = 1$, $Z = 3$ and

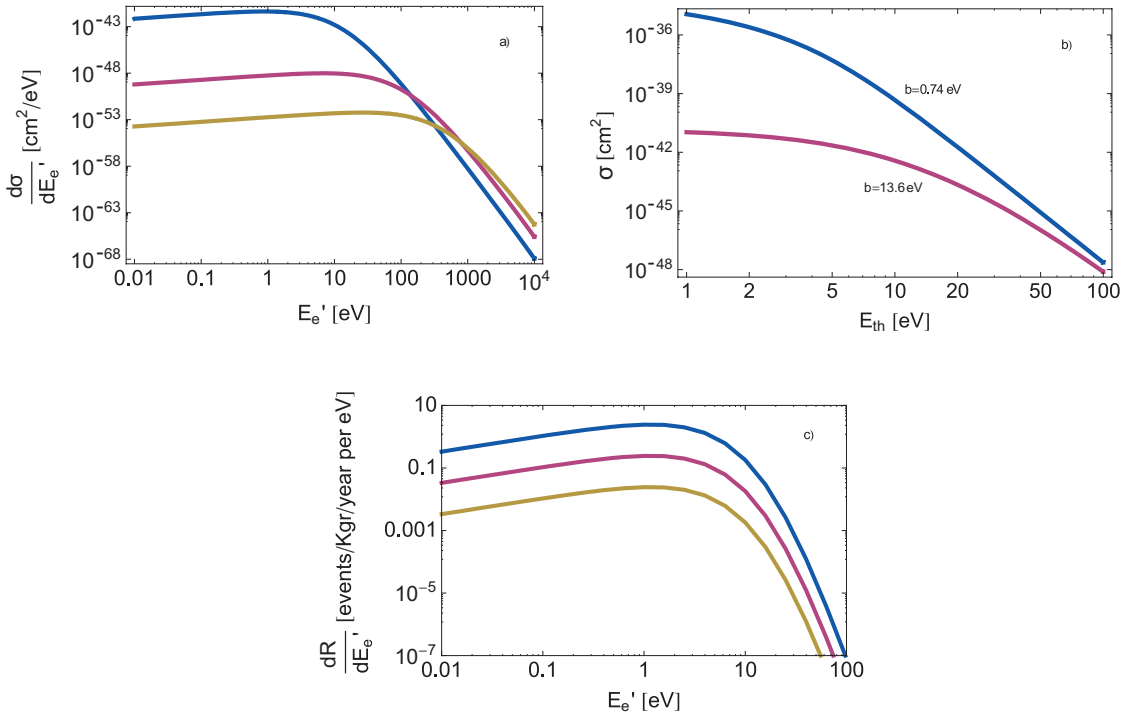

Figure 2.7: *a) Predictions for $d\sigma/dE'_e$ as a function of the ejected electron energy E'_e. The target is assumed to be a hydrogenic atom in the ground state with $Z = 1, 3, 6$ (from top to bottom). b) The total cross section for process (2.43) as a function of the experimental threshold energy for two binding energies. c) The differential event rate as a function of the electron energy and various WIMP masses* (10, 100, 1000) *GeV from (top to bottom). Other parameters not shown, are taken from eq. (2.66).*

$Z = 6$ respectively. The differential cross section takes on its maximum values for final electron energy of around few eV for $Z = 1$, around few tens of eV for $Z = 3$ and around a hundred eV for $Z = 6$. For the case $Z = 1$, the extremum happens because of a fast increase of the term $\frac{|\mathbf{p}'_\chi|}{|\mathbf{p}_\chi|}\,|\mathbf{p}'_\mathbf{e}| \sim \sqrt{E'_e}$ and the almost constant value of $|\phi_{100}|^2$ until 5 eV. For higher electron energies, e.g., $E'_e \gtrsim 10$ eV, the probability density factor $|\phi_{100}|^2$ drops fast as $1/E_e^{'8}$ and the term in the denominator of the integral increases as $E_e^{'2}$, resulting in overall decreasing of the cross section as $E_e^{'-19/2}$. The same analysis can be used to describe the behaviour of $d\sigma/dE'_e$ in the other cases ($Z = 3$, $Z = 6$). We must note here that in the limit $E'_e \to 0$ we obtain $d\sigma/dE'_e \to 0$ as the case should be. This is obscured in Fig. 2.7 due to the range choice of E'_e.

Corresponding to the input parameters noted in (2.66) we calculate the total cross section from eq. (2.64) after integrating over E'_e in the region $[E_{\rm th}, m_\chi\,\beta^2/2 - b(Z)]$. Our results for σ vs. the threshold energy $E_{\rm th}$ are depicted in Fig. 2.7b. We have chosen two extreme cases of binding energies : $b = 0.74$ eV that is the binding energy of the electron bounded in the two electron atom H^-, and $b = 13.6$ eV that is the one corresponding to the H-atom we have been dealing so far. For $E_{\rm th} \lesssim 10$ eV the

E'_e [eV]	$\left\langle \frac{dR}{dE'_e} \right\rangle$ [events/kgr target/year/eV]		
	unmod.	mod.	H
0.1	0.11	0.01	0.09
1	0.24	0.03	0.13
10	0.02	0.002	0.10
100	8.21×10^{-9}	1.04×10^{-9}	0.13

Table 2.1: *Time modulation effects in case of a photonic mediator following eq. (2.63) in the text. Various input parameters are given in eq. (2.66). H is the ratio of the modulated divided by the unmodulated differential rate.*

difference in cross section is about three to six orders of magnitude, while for higher threshold energies becomes unimportant.

Following eq. (2.64) it turns out that the total cross section for process (2.43) is WIMP mass independent. It is experimentally useful to know how the cross section depends on the threshold energy $E_{\rm th}$ that a given experiment can accomplish. This is plotted in Fig. 2.7b. For $E_{\rm th} \lesssim 1$ eV, the cross section is essentially independent of $E_{\rm th}$. When the threshold becomes 5 eV, in the case of $b(Z) = 13.6$ eV, the cross section drops by a factor of 5 while up to 10 eV by a factor of 50. For smaller binding energy though, i.e., $b(Z) = 0.74$ eV, and up to 10 eV the cross section decreases by three orders of magnitude.

Furthermore, the dependence of differential event rate dR/dE'_e on the ejected electron energy E'_e for three different WIMP masses, $m_\chi = 10$, 100, 1000 GeV, is shown in Fig. 2.7c. There is a maximum which follows the behaviour of differential cross section. The event rate falls as $1/m_\chi$ as the WIMP mass increases in accordance with eq. (2.59). For energy of few eV's and $m_\chi = 10$ GeV we obtain a handful of events for $\kappa = 10^{-10}$. A total event rate is obtained after integrating over the differential rate in Fig. 2.7c. As a typical value, for $m_\chi = 100$ GeV and the parameters in (2.66) we find $R(Z = 1, \kappa = 10^{-10}) \approx 1$ event/yr/target kgr. We must recall here that this assumes a mixing parameter as small as $\kappa = 10^{-10}$!!

Finally, following the theoretical discussion of the previous subsection we examine effects of the WIMP time modulation. In Table 2.1 we display both the unmodulated and modulated differential event rate for four representative values of E'_e in the case of a massless mediator and parameters of eq. (2.66). The dimensionless parameter H, which is the ratio of the modulated by the unmodulated differential amplitude, is constant around $9 - 13\%$ independent of the energy and the WIMP mass. The modulation $h = \delta \cdot k$ of the total rate is also going to be around 10%, which means that the difference between the maximum (here always in June 3-rd) and the minimum (here always in December) is $18 - 26\%$, a result should not to be overlooked.

2.4.3 Massive mediator

By taking the non-relativistic limit of eq. (2.48) and the assumption that the momentum transfer in eq. (2.65) is much less than the mediator's mass, $q^2 \ll m_X^2$, we arrive at:

$$\frac{d\sigma}{dE'_e} = \frac{16\pi^2\alpha'\alpha_{\rm DM}\kappa^2\, s(\beta)}{m_X^4}\, m_\chi^2 m_e\, \frac{|\mathbf{p}'_\chi|}{|\mathbf{p}_\chi|}\, |\mathbf{p}'_\mathbf{e}| \int_{-1}^{1} d\xi \int_{-1}^{1} d\eta\, |\phi_{n\ell m_\ell}(Z, \mathbf{p}'_\chi + \mathbf{p}'_\mathbf{e} - \mathbf{p}_\chi)|^2. \quad (2.67)$$

In what follows we assume a Dirac WIMP fermion, i.e., $s(\beta) = 1$. We assume the following input parameters :

$$\begin{aligned} \beta = \sqrt{<\beta^2>} &= 10^{-3}\,, \quad Z = 1\,, \quad \alpha_{\rm DM} = \alpha' = \alpha_{\rm em}\,, \\ m_X &= 1 \text{ GeV}\,, \quad m_\chi = 100 \text{ GeV}\,, \quad \kappa = 1\,. \end{aligned} \quad (2.68)$$

Although this parameter space violates the bounds in eqs. (2.16) and (2.17), it serves as a benchmark in comparing results with those of section 2.3 if possible. The value of κ is chosen such that the resulting rate presented in the figures assumes no mixing of the X-boson mediator which is formally the case of model III.

Results for the differential cross section $d\sigma/dE'_e$ for the electron in the ground state of three hydrogenic atoms are shown in Fig. 2.8a. The differential cross section takes on its maximum values for final electron energy of around few eV for $Z = 1$, ten of eV for $Z = 3$ and around hundred eV for $Z = 6$. For the case $Z = 1$, the extremum happens because of a fast increase of the term $\frac{|\mathbf{p}'_\chi|}{|\mathbf{p}_\chi|}\, |\mathbf{p}'_\mathbf{e}| \sim \sqrt{E'_e}$ and the almost constant value of $|\phi_{100}|^2$ until 5 eV [see eq. (2.67)]. For higher electron energies, e.g., $E'_e \gtrsim 10$ eV, the probability density factor $|\phi_{100}|^2$ drops fast as $1/E_e^{'8}$ resulting in overall decreasing of the cross section as $E_e^{'-15/2}$. In physical terms, the outgoing electrons of high energy demand high momenta in the initial electron wavefunction, which leads to suppression. The dependence on the Z is easily explained if we recall that for hydrogenic atoms, $\langle p^2\rangle_{n=1} = Z^2 p_0^2$ where p_0 is the Bohr momentum for Hydrogen. Furthermore, despite appearances in eq. (2.67), the differential cross section depends only very mildly on the WIMP mass. One can show analytically that the double integral over the wave function squared, is approximately proportional to $1/m_\chi^2$ which cancels the m_χ^2 in the numerator.

Corresponding to the input parameters noted in (2.68) we calculate the total cross section from eq. (2.67) after integration over E'_e in the region $[E_{\rm th}, m_\chi\beta^2/2 - b(Z)]$. For fixed velocity, $\beta = 0.001$, and $E_{\rm th} = 0$ eV we find the following representative values :

Z	$\sigma[\text{cm}^2]$
1	3×10^{-40}
10	2×10^{-44}
50	3×10^{-48}

The total cross section increases by a factor of about 32 when $\beta = \beta_{\rm esc}$ is taken. The cross section decreases with Z [see also Fig.2.8a], the reason being the fact that the binding energy increases with Z^2 [see eq. (2.51)] and therefore we need to go to larger

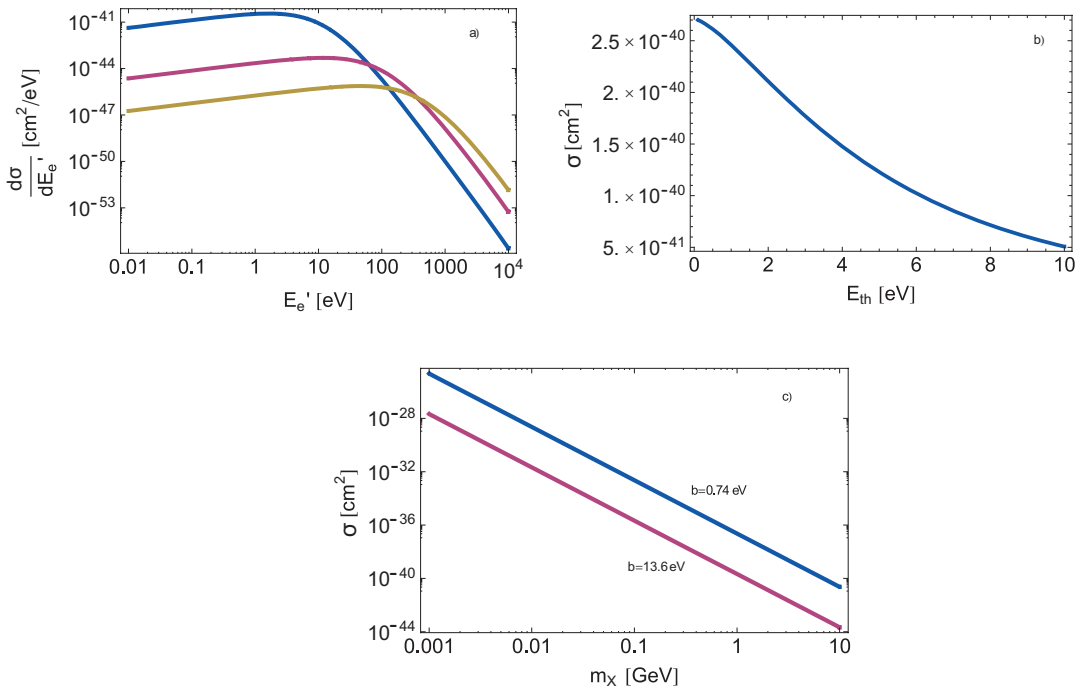

Figure 2.8: *a) Predictions for $d\sigma/dE_e'$ as a function of the ejected electron energy E_e'. The target is assumed hydrogenic atom with $Z = 1, 3, 6$ (from top to bottom) in the ground state. b) The total cross section as a function of threshold energy. c) The total cross section as a function of m_X for two different binding energies. We assume a Dirac WIMP, $E_{\rm th} = 0$ eV and input parameters from eq. (2.68) if not stated otherwise.*

- compared to ground state - momenta where the wavefunction is small despite their maximum value displacement towards larger momenta.

Assuming that the sensitivity of detecting low energy electrons will be analogous to the ongoing experiments ($\approx 10^{-43}$ cm^2), we could even extract bounds on various parameters in models I, II or III. From all running experiments, DAMA [25, 58] is the one that triggers on final state electrons with energy around 5 KeV. From Fig. 2.8a one obtains that, around that energy, the cross section is too small for $m_X = 1$ GeV and all other inputs in eq. (2.68). However, $d\sigma/dE_e' \propto m_X^{-4}$ and therefore for $m_X \approx 1$ MeV *i.e.,* model types proposed in ref. [50], DAMA is a relevant experiment. Additionally, this is demonstrated in Fig. 2.8c where the total cross section as a function of m_X is plotted for two reference values of binding energy. In Fig. 2.8b we examine the total cross section as a function of the experimental energy threshold for low energies, relevant to our proposal. As we can see, the total cross section reduces by a factor of six in the region $0 \lesssim E_{\rm th} \lesssim 10$ eV. Above 10 eV the cross section drops drastically [see total rate in Fig. 2.9b].

Although not shown, we have also examined departures of the wavefunction from the ground state. The maximum value $d\sigma/dE_e'|_{max}$ approximately appears at the same region in $E_e' \approx 1 - 10$ eV. As an example, the difference in $d\sigma/dE_e'|_{max}$ is an

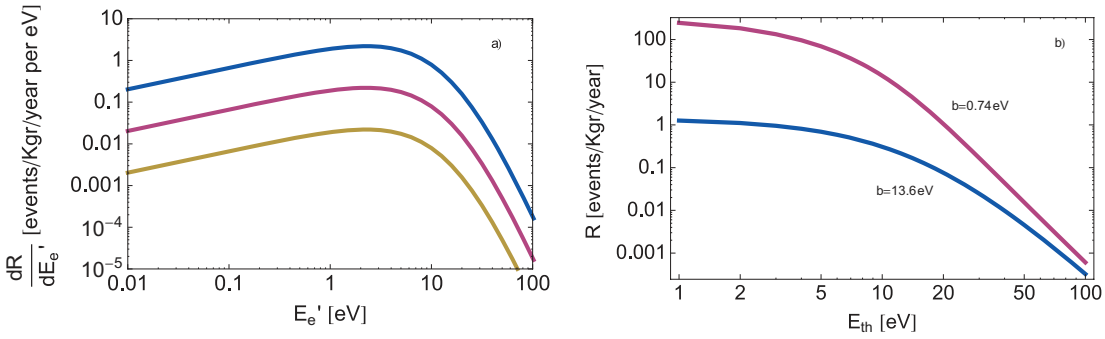

Figure 2.9: *a) Differential event rate of Dirac WIMP, scattered by electrons in a hydrogenic ($Z = 1, A = 1$) target, per year per Kgr as a function of ejected electron energy E'_e in eV. We assume three different WIMP masses : $m_\chi = 10$, 100, 1000 GeV, from top to bottom, respectively. b) The total event rate as a function of the experimental threshold energy for $m_\chi = 100$ GeV for two different binding energies. Other input parameters are taken from eq. (2.68) for the massive mediator.*

enhancement by a factor 20 when going from $1s \to 2s$. Furthermore, the size of the momentum transfer in conjunction with the non-zero binding energy are such that never let the wavefunctions to reach their zero nodes. Assuming one electron per target atom, and the average cross section of Fig. 2.8a for $Z = 1$, the differential event rate per eV of electrons energy per year per Kgr of hydrogen material as a functions of E'_e for various WIMP masses is depicted in Fig. 2.9a. The differential event rate again exhibits a maximum which follows that of the differential cross section calculated in Fig. 2.8a. The event rate is of course higher for smaller WIMP mass [recall eq. (2.59)] and for electron energy of few eV's it varies from 0.01 up to 2 events/yr/kgr/eV for $m_\chi = 1000$, 10 GeV respectively. For electron energy of around 100 eV the role of the wave function is to reduce the differential rate by an order of magnitude i.e., from $10^{-4} \div 10^{-3}$ events/yr/kgr/eV. The total event rate for $m_\chi = 100$ GeV and the other parameters in eq. (2.68) is predicted to be:

$$R(Z = 1,\, \kappa = 1) \;\simeq\; 2 \text{ [events/yr/target kgr]} \,. \tag{2.69}$$

It is useful to know how the total rate (2.69) varies with the experimental threshold energy. This information can be extracted from Fig. 2.9b for two different but judiciously chosen, values of binding energy. As in the case of the total cross section in Fig. 2.8b, the total rate drops by only a factor of five until $E_{\rm th} \approx 10$ eV while it drops very rapidly after about this scale. For example, it drops by a factor of 10^4 for $E_{\rm th} = 100$ eV. Smaller binding energies [upper line in Fig. 2.9b] result in up to two orders of magnitude bigger rates but for threshold energies as low as $E_{\rm th} \lesssim 5$ eV. Finally, in Table 2.2 we calculate the effects of time modulation and present the differential event rate for four different values of E'_e in the case of massive mediator with $m_X = 1$ GeV. We assume also a WIMP mass $m_\chi = 100$ GeV and $Z = 1$. The H ratio is constant around 10% independent of the energy and the WIMP mass. The modulation h of the total

E'_e [eV]	$\left\langle \frac{dR}{dE'_e} \right\rangle$ [events/kgr target/year/eV]		
	unmod.	mod.	H
0.1	0.06	0.01	0.17
1	0.19	0.02	0.11
10	0.079	0.008	0.10
100	1.84×10^{-5}	1.78×10^{-6}	0.097

Table 2.2: *Time modulation effects in case of a massive mediator following eq. (2.63) and various input parameters in eq. (2.68). H is the ratio of the modulated by the unmodulated differential amplitude.*

rate is also going to be around $10 - 17\%$, which means that the difference between the maximum (here always in June 3rd) and the minimum (here always in December) is $20 - 34\%$.

2.4.4 Experiment : The prospects of detecting single ultra low energy electrons

As discussed in a previous section observation of light X-boson would require detectors with sub-keV sensitivities. The development of such detectors, having a low energy threshold and low noise, remains generally a daunting challenge for present-day and future low background experiments. As shown in Fig. 2.9 the signal of low energy electrons produced by an elastic collision process exhibits a maximum at energies around or even lower than 10 eV. At such energies a detector with single electron sensitivity will be required to reach a reasonable efficiency. A notable effort to develop ultra low threshold detectors in order to address low energy neutrino physics [71–74] is going on. This has been achieved for low mass detectors. We are, however, seeking an even lower energy threshold.

Usual solid state detectors employed for dark matter projects have typical thresholds of a few keV. It is very difficult to combine sub-keV and big mass at the same time. For instance Ultra-Low-Energy Germanium detectors [23] are able to reach a threshold of a few hundred eV's, but they are limited to a modular mass of a few grams. Anyway, the achieved energy threshold is still below our requirements.

Single electron efficiency is achieved using detectors reaching very-high gains in order to cope with electronic noise. Gaseous detectors are good candidates. In such detectors high gains may easily be achieved. Having been conceived as a TPC Micromegas detector (•MS) [75], it is compatible with large drift volumes and operation at high pressure, an example of which are the HELLAZ [76] prototypes. A great advantage of this detector is the versatility of target material: various gases from the lightest (H_2) to heaviest (Xe) could be used offering a large choice.

One idea to increase the mass of the target material is to use the recently developed Spherical Proportional Counter (SPC) [79]. This detector consists of a large spherical

gas volume with a central electrode and radial electric field. Charges deposited in the drift volume are drifting to the central sensor where are amplified and collected. A novel concept of a proportional sensor, a metallic ball having a radius of about 15 mm, located at the center of curvature, acting as a proportional amplification structure is used. It allows to reach high gas gains ($\geq$ 104) and operates from low to high gas pressure. At such gains, provided the low electronic noise of this detector, single electron efficiency is easily achieved. The main advantages of the new structure relevant to our project are:

- Simplicity of the design.
- A single channel is used to read-out a large volume.
- Robustness
- The depth of the interaction, related to the rise time of the signal, is measured. This is important to apply fiducial cuts for background rejection purpose.
- Low detector capacity $\leq$ 0.1 pF, independent of the vessel size, allows very-low electronic noise, which is a key point toward achieving low energy threshold.
- Versatility of the target material and density; the detector is compatible with a large variety of gases and could operate from low pressure to high pressure. This could be a precious tool to identify a possible signal out of background.

A main concern of the proposed detection scheme is the minimal background level that will be reached by our system. By this, one means that the detector body and appropriate shield will be built with materials which are screened for low levels of natural and man-made radioactive impurities. Ordinary construction and shielding materials, however, do contain trace amounts of naturally occurring and man-made radionuclides which result in elevated background level; we need to design and fabricate the detector by careful material selection made out of low level activity.

Unfortunately, however, there exists very little experience at the very low energy (sub keV) region where our detector will be operating. An example is a low background gaseous detector with sub KeV energy threshold developed for solar axion search [78]. The reached background level is quite low and is flat in the sub KeV energy range down to 250 eV. Our purpose is to further decrease the energy threshold down to the region of 10 eV. This region has never been explored and therefore reaching the desired low level activity becomes a new experimental challenge. Single electron backgrounds could be emitted by materials pulled by the electric field through thermionic emission. The advantage of the spherical detector is that at the external vessel the electric field is extremely low and therefore highly reduced thermionic emission is expected.

The present prototype having a volume of $1\,m^3$, filled with a gas at high pressure with a target mass of the order of 10 kg could fulfill sensitivity requirements for our project. We will search appropriate molecular gases having low binding energy and compatible with operation in the Spherical Proportional Counter detector [79].

At present it looks realistic to soon have a sphere of radius of 5 meters, which can be under a pressure of 5 bars. Thus, if one fills it with 80% Ar and 20% Isobutane (C_4H_{10}), one can have 212 Kg of Hydrogen. With this much Hydrogen using eq. (2.69) and a threshold of ≈10 eV, we expect around 200 events per year for the parameters in (2.68). In models [50] where the mediator mass is very low, *e.g.* $m_X \approx 1$ MeV, we expect an increase of the event rate by almost six orders of magnitude. Therefore, if a low energy experiment will be built it would possibly set the best limits on these kind of models.

2.5 Conclusions

Cosmic ray results from PAMELA, HESS and FERMI collaborations show an unexpected rising of positron events with energy that may be due to Dark Matter particle (χ) annihilations in the halo of our Galaxy. This Dark Matter particle "sees" the SM ones only through its interactions with an X-boson that couples to the SM gauge sector. Depending on the model, the mediator can be massless or massive with different couplings. We have studied direct detection of this secluded type of dark matter employing nucleons or electrons with main emphasis in the latter case.

Due to the small momentum transfer[8] the massless case results in a large number of events that should have been seen by current nucleon recoiling direct detection experiments and therefore strong bounds on mixing parameters and couplings exist. Our work emphasizes the role of the low energy electron recoil in direct detection experiments and proposes a novel experimental avenue on how to proceed in searching for such low energy electrons. For simple hydrogenic atoms, at low energy, $E'_e \approx 10$ eV, the cross section is enhanced by orders of magnitude compared to KeV recoil energies. In the neighborhood of low energies, the results depend highly on the binding energy of the ejected electron: the more loose the electron is, the bigger the event rate becomes as expected. In this regard we considered two possibilities:

1. The process is mediated by the massive mediator X (our model III). In this case we do not have scattering off hadrons at tree level. Therefore, we do not have dominant constraints on the parameters of the model coming from the ongoing WIMP searches. Using the parameters of eq. (2.68) we have obtained fairly large cross sections for a Dirac WIMP. Employing the spherical TPC detector described above with a radius of 5 m under a pressure of 5 Atm we have found that we could have about 200 counts in a year, assuming a threshold of 10 eV. It is possible, however, that our choice of parameters is a bit optimistic and we may have not considered all available constraints. Our results are also applicable to model-I. In this case however, due to the fact that couplings of the X-boson to hadrons appear at tree level, there exist strong constraints on the mixing parameter already from the nucleon direct searches [see eq. (2.38)].

[8]For nucleons, the momentum transfer is ≈ 2 MeV and the energy transfer is ≈ 2 KeV, while for low energy electron recoils they are ≈ 50 KeV and ≈ 10 eV, respectively.

2. The process is accommodated by the massless mediator (leptophylic version of model II). This mechanism is similar to that involving hadrons in section 2.3, one simply replaces the quarks by leptons. In this case we have found that the most stringent constraints on the parameters come from the standard WIMP searches. Thus, using the parameters of eq. (2.66) we have obtained with the above detector hundreds of events per year even with a (reduction) mixing coupling constant as low as $\kappa = 10^{-10}$ for a Dirac WIMP. *Such a huge signal cannot be seen by current experiments either due to lack of low energy threshold or because, experiments, like CDMS and XENON, are keeping only nuclear recoil events.* We were surprised to find so large cross section. We now understand it, however, to be due to the photon propagator $(1/q^2)^2$, which is favored by the fact that the momentum transfer is very low in the case of electrons. We should mention that, since the initial electron is bound, there is no infrared divergence and no need for a low energy cut off. It should be also noted that quark couplings to X-boson will come back through loop corrections even if they are forbidden at tree level by a symmetry which is eventually broken. Then current nucleon recoil experiments will be as important [see eq. (2.32)] and complementary to the electron ones.

In conclusions above the assumption that the WIMP is a Dirac particle has been made. If the WIMP is Majorana particle, as we have shown (see Appendix F) the rates are suppressed by approximately a factor $\beta^2 \approx 10^{-6}$. For both the above cases, annual time modulation effects are of the order of 20-30%, important enough to be noticed.

We have limited the discussion of the rates in the case of hydrogen, since our cross section was evaluated using hydrogenic wave functions. Certainly the obtained rates will increase, if one can exploit the other atomic electrons with smaller binding energy. This situation was made manifest in our work with a judicious change of the binding energy [see Figs. 2.7 b, 2.8 c, 2.9 b]. But then one should employ realistic wave functions.

In a similar fashion one can treat other dark matter candidates like right handed neutrinos, which arise in models in which the ordinary Dirac type mass is forbidden due to a discreet symmetry, but communication with leptons is allowed via exotic scalars [80–82] with masses in the 50 GeV region. It may also apply to other models involving exotic fermions and scalars proposed and reviewed in ref. [83].

Chapter 3

Heavy Fermion Non-Decoupling Effects

In the previous Chapter we analyzed different varieties of a scenario where a dark matter particle could annihilate in other particles, especially into Standard Model fermions. In this Chapter, within a spontaneously broken gauge group, we carefully analyze and calculate triple gauge boson vertices dominated by triangle one-loop Feynman diagrams involving heavy fermions compared to external momenta and gauge boson masses. Since a complete one particle irreducible vertex for three off-shell gauge bosons is a useful tool in analyzing low energy inelastic scattering processes, we can use it to study scattering processes with a photon in the final state, as an example. This can be useful in dark matter scattering off atomic electrons and nuclei, mediated by light gauge boson particles, as one application among many (see refs. [35,85,86]). This is an other possible scenario that constitutes an alternative to the effects that we studied in the previous Chapter. We perform our calculation strictly in four dimensions and derive a general formula for the off-shell, one-particle irreducible (1PI) effective vertex which satisfies the relevant Ward Identities and the Goldstone Boson Equivalence Theorem (GBET). In the technical level we introduce arbitrary four-vectors in our calculation. These vectors are associated with different types of divergences that appear during the calculation and help in the reduction of these divergencies as much as possible. Our goal is to search for non-decoupling heavy fermion effects highlighting their synergy with gauge chiral anomalies. Particularly in the Standard Model, we find that when the arbitrary anomaly parameters are fixed by gauge invariance and/or Bose symmetry, the heavy fermion contribution cancels its anomaly contribution leaving behind anomaly and mass independent contributions from the light fermions. We apply these results in calculating the corresponding CP-invariant one-loop induced corrections to triple gauge boson vertices in the SM, minimal Z'-models as well as their extensions with a fourth fermion generation, and compare with experimental data. This Chapter is based on the published work [87].

3.1 Introduction

In general, the Appelquist-Carazzone [88] theorem states that the effect from a heavy fermion mass m at low energy observables is suppressed by powers of m. However, this theorem does not hold for theories with chiral gauge couplings or large mass splitting within gauge multiplets, a situation known to take place in the minimal Standard Model (SM) of particle physics [1–3]. Failure of the decoupling of heavy fermion from radiative corrections requires breaking of a local gauge symmetry and, in addition, breaking of a global symmetry by these corrections [89, 90].

Another aspect of theories with chiral gauge couplings is the Adler-Bell-Jackiw or chiral anomaly [30, 31, 91, 92]. This is the situation where certain classical Ward Identities (WIs) are violated by quantum corrections (for reviews see [93–95]). For a model that is non-anomaly free, anomalous Ward Identities render it non-renormalizable and non-unitary. This problem shows up in every symmetry breaking stage of the model. In order to cancel chiral anomalies associated with axial (AAA) or vector-axial (VVA) currents in gauge theories, we either need to stick to only by-construction anomaly-free gauge groups, or, to introduce additional chiral femionic fields [96, 97].

An energy region of experimental interest corresponds to the case where a fermion mass m is very heavy, $m_Z^2 < s \ll m^2$, so that it cannot be pair-produced at Tevatron, LHC or a future lepton-collider. If this fermion is chiral *i.e.*, it receives its mass from the Higgs mechanism which is also responsible for the gauge boson mass, then the question of the decoupling of this particle would cause a problem in anomaly cancellation and therefore to gauge invariance. This question has been tackled in many papers in the literature most notably by D'Hoker and Farhi in ref. [98, 99]: decoupling of a fermion whose mass is generated by a Yukawa coupling induces an action functional of the Higgs field and gauge boson fields term, analogous to Wess-Zumino-Witten (WZW) term [100, 101] in chiral Lagrangian. Then D'Hoker and Farhi showed that the theory without the decoupled fermion but with the WZW term is gauge invariant. Applications of this non-decoupling effect have been utilised in many physics projects from hadronic up to electroweak physics of the SM and beyond, see for example refs. [102–108]. However, to our knowledge, the above conclusion has not been drawn in the broken phase of theories with spontaneous gauge symmetry breaking like the SM. It is after all meaningful to discuss non-decoupling effects *only* in theories where the physical masses appear explicitly.

The problem when discussing decoupling effects or in general physics associated with the fermionic triangle graph is related to the question : *what is the correct result for such a graph?* The answer depends on the physical set-up in which it arises [109]. For example, as we shall show below in the case of SM, gauge invariance and Bose symmetry are enough to set the triple neutral gauge boson vertices finite and well defined. Only then can we reach the conclusions for the theory at the heavy fermion mass limit.

If the SM gauge group is extended by extra $U(1)$'s then anomaly cancellation conditions become more involved. Recently, the authors of refs. [110, 111] noted that such cancellations may occur inside a "cluster" of anomaly-free heavy fermion sector which

is not accessible by the current colliders, leaving behind non-decoupling effects in trilinear gauge boson vertices of the extra massive gauge boson Z' and those of the SM $Z'ZZ$, $Z'WW$, $Z'Z\gamma$ that may be observable at low energies. These effects are visible in the energy region where $M_{Z'} \sim gv < \sqrt{s} \ll m \sim \lambda v$. For these non-decoupling effects to occur it is necessary for fermions and gauge bosons to receive mass from the same Higgs boson and there must be a hierarchy between Yukawa and gauge coupling, $\lambda \sim \mathcal{O}(1) \gg g$. In this Chapter we also elaborate on this issue categorising conditions among couplings where such a situation occurs. A few toy-model examples with two or three different external gauge bosons are presented. We note in passing that, within field theory, mixed anomaly cancellations via 4d Green-Shwartz mechanism have been discussed and analysed phenomenologically in the literature e.g. [112–117].

Our goal here is to construct a perturbative, gauge invariant, one-loop proper effective vertex for three external gauge bosons that incorporates both chiral anomaly ambiguities together with non-decoupling effects induced by heavy fermions in an explicit manner. We would like to apply this effective vertex in order to:

- investigate the interplay between chiral anomaly effects and non-decoupling effects of individual particles in trilinear gauge boson vertices in the SM and its extensions,
- categorise all possible models of mixed anomaly cancellations and non-decoupling effects of very heavy fermions that are directly unreachable at LHC,
- search for phenomenological implications at colliders.

General Lorentz-invariant expressions for three gauge boson vertices have been analysed in detail in refs. [118, 119]. One-loop corrections in the SM for the VWW, where $V = Z$, γ using dimensional regularisation were considered in [89] with special emphasis on the non-decoupling effects due to large doublet mass splittings. The first correct calculation for the $Z\gamma\gamma$ vertex was performed in ref. [120], while for $ZZ\gamma$ in ref. [121]. Phenomenological studies including expectations for those interactions at hadron and lepton colliders were studied in detail in refs. [122–125].

We first present the 1PI effective action for the triple gauge boson vertex and then we discuss all possible and general non-decoupling effects from heavy fermions. A variety of applications of the general vertex in the SM, in minimal Z' models and their extensions with a fourth sequential fermion generation, is presented.

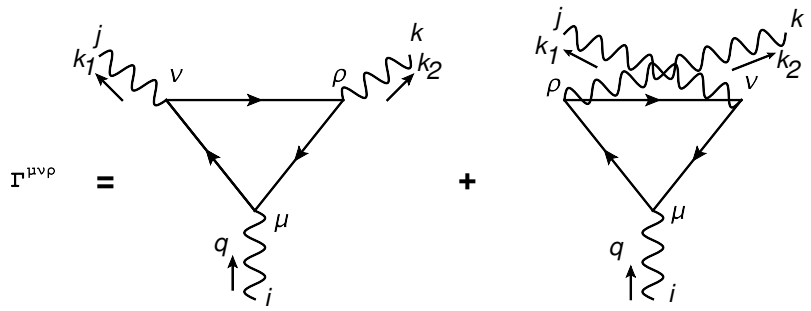

Figure 3.1: *The one-loop effective trilinear gauge boson vertex, $\Gamma^{\mu\nu\rho}$. The crossed diagram is obtained with the replacement $\{\nu,\rho\} \leftrightarrow \{\rho,\nu\}$ and $k_1 \leftrightarrow k_2$. Indices $\{i,j,k\}$ denote distinct external gauge bosons in general.*

3.2 The Trilinear Gauge Boson Vertex

In this section we briefly present the main results for the three gauge boson 1PI vertex, $\Gamma^{\mu\nu\rho}$. The details of this calculation are given in Appendices G and H. Furthermore, the behaviour of $\Gamma^{\mu\nu\rho}(s)$ at high energies s, and issues on gauge invariance and Goldstone Boson Equivalence Theorem are discussed in the subsequent subsections.

3.2.1 The construction of $\Gamma^{\mu\nu\rho}$

The relevant diagrams are depicted in Fig. 3.1 and their evaluation is developed in Appendix H. What we basically need in order to calculate the diagrams in Fig. 3.1 is the interaction part of the Lagrangian

$$\mathscr{L}_{int} \supset e\,\overline{\Psi}\,\gamma^{\mu}\,(\alpha+\beta\,\gamma_5)\,\Psi\,A_{\mu}\,, \tag{3.1}$$

where $\Psi(x)$ is a 4-component spinor consisting of a pair of two Dirac fermions coupled chirally to a vector field $A_\mu(x)$. Flavour or spinor indices are silently implied. We shall assume a model interaction for eq. (3.1) that arises from a spontaneously broken Abelian gauge theory. A toy model as such is described in Appendix G. Then α and β in eq. (3.1) are real numbers (in units of e) related to linear combinations of hypercharges [see for instance eq. (G.8)].

The integral representation for this diagram is given in eq. (H.1). By naive power counting this integral is linearly divergent. This means that when we make a shift of integration variable, e.g., $p \to p+a$, the result depends upon the choice of the arbitrary vector a^μ. This change is only reflected in the form factors proportional to k_1 and k_2 in Lorentz invariant expansion of $\Gamma^{\mu\nu\rho}$ [see eq. (3.2) below]. As a result, the naive Ward Identities (WIs), eqs. (H.15), (H.16) and (H.18) are violated by terms that contain the arbitrary four vector a^μ. It is useful to write this four vector as a linear combination of the two independent external momenta : $a^\mu = z\,k_1^\mu + w\,k_2^\mu$, with z, w arbitrary real parameters.

In order to write out an explicit form for the trilinear gauge boson vertex, say for three identical massive gauge bosons, we make use of an explicit expression for the triangle graphs first calculated by Rosenberg [120]. The most general form of the axial tensor $\Gamma^{\mu\nu\rho}$ consistent with Lorentz and parity symmetry is:

$$\begin{aligned}\Gamma^{\mu\nu\rho}(k_1,k_2;w,z) = \Big[& A_1(k_1,k_2;w)\,\varepsilon^{\mu\nu\rho\sigma}\,k_{2\sigma} + \\ & + A_2(k_1,k_2;z)\,\varepsilon^{\mu\nu\rho\sigma}\,k_{1\sigma} + A_3(k_1,k_2)\,\varepsilon^{\mu\rho\beta\delta}\,k_2^\nu\,k_{1\beta}\,k_{2\delta} + \\ & + A_4(k_1,k_2)\,\varepsilon^{\mu\rho\beta\delta}\,k_1^\nu\,k_{1\beta}\,k_{2\delta} + A_5(k_1,k_2)\,\varepsilon^{\mu\nu\beta\delta}\,k_2^\rho\,k_{1\beta}\,k_{2\delta} + \\ & + A_6(k_1,k_2)\,\varepsilon^{\mu\nu\beta\delta}\,k_1^\rho\,k_{1\beta}\,k_{2\delta}\Big]\,. \end{aligned} \tag{3.2}$$

By naive power counting the dimensionless form factors $A_{1,2}$ are infinite. They can be rendered finite by forcing them to obey the relevant, albeit anomalous, Ward Identities. However, $A_{1,2}$ are in general *undetermined* since they depend on arbitrary parameters w and z. This arbitrariness can be fixed by physical requirements like for example conservation of charge. On the other hand the form factors (or integrals) $A_{3,..6}$ are finite having dimension of inverse mass square. The latter can be found independently by direct diagrammatic methods. The whole procedure is described in Appendix H.

Therefore, non-decoupling effects should originate solely from the A_1 and A_2 parts of $\Gamma^{\mu\nu\rho}$ but without any further physical input they are undetermined. A direct calculation of $A_{1,2}$ with dimensional regularisation [33] or with Pauli-Villars regularisation is not a good choice when shifting integration variables within linearly (and above) divergent Feynman integrals in four dimensions [126–128]. The outcome for a single external gauge boson ($i = j = k$ in Fig. 3.1) triangle graph is appended in eqs. (H.26), (H.27) and (H.28). From these expressions and from eq. (3.2) we obtain $A_1(k_1,k_2;w)$ and $A_2(k_1,k_2;z)$ in terms of the finite integrals $A_{3..6}$. The corresponding results, in the case of three identical external gauge bosons, are given by eqs. (H.37) and (H.38) while the finite integrals $A_{3..6}$ by eqs. (H.33), (H.34) and (H.35).

Furthermore, although Bose symmetry could constrain the arbitrary numbers w and z, it is not enough to eliminate them altogether: a physical condition is needed, e.g., conservation of electric charge for fermions coupled to external photons or vanishing triangle graph for on-shell momenta of massive gauge bosons or, even, a pure theoretical reason, like the decoupling property. It is straightforward, albeit tedious, to generalize $\Gamma^{\mu\nu\rho}$ in eq. (3.2) to the case of three distinct external, massive or massless, gauge bosons ($i \neq j \neq k$ in Fig. 3.1).

With the assignments depicted in Fig. 3.1, the generalised Ward Identities for vertices μ, ν, ρ are written respectively as[1]

$$q_\mu\,\Gamma^{\mu\nu\rho}(k_1,k_2,w,z) = i\,m_{A_i}\,\Gamma^{\nu\rho}(k_1,k_2) + \\ + \frac{e^3[(\alpha_i\alpha_j+\beta_i\beta_j)\beta_k+(\alpha_i\beta_j+\alpha_j\beta_i)\alpha_k]}{4\pi^2}\varepsilon^{\lambda\nu\rho\sigma}k_{1\lambda}k_{2\sigma}(w-z), \tag{3.3a}$$

$$-k_{1\nu}\,\tilde{\Gamma}^{\nu\rho\mu}(k_1,k_2,w,z) = i\,m_{A_j}\,\tilde{\Gamma}^{\rho\mu}(k_1,k_2) + \\ + \frac{e^3[(\alpha_j\alpha_k+\beta_j\beta_k)\beta_i+(\alpha_j\beta_k+\alpha_k\beta_j)\alpha_i]}{4\pi^2}\varepsilon^{\lambda\mu\rho\sigma}k_{1\lambda}k_{2\sigma}(w-1), \tag{3.3b}$$

$$-k_{2\rho}\,\widehat{\Gamma}^{\rho\mu\nu}(k_1,k_2,w,z) = i\,m_{A_k}\,\widehat{\Gamma}^{\mu\nu}(k_1,k_2) + \\ + \frac{e^3[(\alpha_k\alpha_i+\beta_k\beta_i)\beta_j+(\alpha_k\beta_i+\alpha_i\beta_k)\alpha_j]}{4\pi^2}\varepsilon^{\lambda\mu\nu\sigma}k_{1\lambda}k_{2\sigma}(z+1), \tag{3.3c}$$

where the corresponding Γ, $\tilde{\Gamma}$, and $\widehat{\Gamma}$ are appended in eqs. (H.47) and (H.48). It is remarkable here to note the i'th gauge boson mass factor $m_{A_i} = -2\beta_i\,e\,v$ in front of the pseudoscalar 1PI function $\Gamma^{\nu\rho}$ is explicitly given in eq. (H.48). This term and the analogous in eqs. (3.3b) and (3.3c) are the source of heavy fermion mass non-decoupling effects since in the formal limit of $m \to \infty$ there is a remaining piece of order $e^3\varepsilon^{\lambda\nu\rho\sigma}k_{1\lambda}k_{2\sigma}/4\pi^2$ in $\Gamma^{\mu\nu\rho}$ for example. On the other hand it shows that currents which are associated to unbroken symmetry generators *i.e.*, to massless gauge bosons, do not provide any non-decoupling effect in $\Gamma^{\mu\nu\rho}$. Moreover, $\Gamma^{\nu\rho}$, $\tilde{\Gamma}^{\rho\mu}$, $\widehat{\Gamma}^{\mu\nu}$ depend linearly upon the Yukawa coupling λ, that is responsible for the fermion mass through the Higgs mechanism and vanishes in the limit of $\lambda \to 0$[2].

Using the WI's for the vertices ν and ρ, *i.e.*, eqs. (3.3b) and (3.3c) as well as eq. (3.2), we obtain the following expressions for the integrals A_1 and A_2:

$$A_1(k_1,k_2;w) = (k_1\cdot k_2)A_3 + k_1^2A_4 - \frac{e^3m^2\beta_j}{\pi^2}I_1(k_1,k_2,m) + \\ + \frac{e^3[(\alpha_j\alpha_k+\beta_j\beta_k)\beta_i+(\alpha_j\beta_k+\alpha_k\beta_j)\alpha_i]}{4\pi^2}(w-1)\,, \tag{3.4a}$$

$$A_2(k_1,k_2;z) = (k_1\cdot k_2)A_6 + k_2^2A_5 - \frac{e^3m^2\beta_k}{\pi^2}I_2(k_1,k_2,m) + \\ + \frac{e^3[(\alpha_i\alpha_k+\beta_i\beta_k)\beta_j+(\alpha_i\beta_k+\alpha_k\beta_i)\alpha_j]}{4\pi^2}(z+1)\,, \tag{3.4b}$$

[1] In order not to clutter the notation we suppress indices i, j, k in the following expressions for Γ's.

[2] Throughout, we assume chiral fermions that receive masses via Yukawa interactions with the Higgs field.

where the "non-decoupled" integrals are given by

$$I_1(k_1,k_2,m)=\int_0^1 dx\int_0^{1-x} dy\frac{-(\alpha_i\alpha_k+\beta_k\beta_i)+2x\beta_i\beta_k}{\Delta}\,, \tag{3.5a}$$

$$I_2(k_1,k_2,m)=\int_0^1 dx\int_0^{1-x} dy\frac{(\alpha_i\alpha_j+\beta_i\beta_j)-2y\beta_i\beta_j}{\Delta}\,, \tag{3.5b}$$

with

$$\Delta\equiv\Delta(k_1,k_2)=x(x-1)k_2^2+y(y-1)k_1^2-2xyk_1\cdot k_2+m^2. \tag{3.6}$$

The following limits,

$$\lim_{m\to\infty} m^2 I_1(k_1,k_2,m)=-\frac{1}{6}\left(3\,\alpha_i\alpha_k+\beta_i\beta_k\right)\,, \tag{3.7a}$$

$$\lim_{m\to\infty} m^2 I_2(k_1,k_2,m)=\frac{1}{6}\left(3\,\alpha_i\alpha_j+\beta_i\beta_j\right)\,, \tag{3.7b}$$

are also useful in simplifying formulae when discussing synergies of anomaly and non-decoupling terms. We are now ready to complete $\Gamma^{\mu\nu\rho}$ in eq. (3.2), by reading directly from eq. (H.47) the finite (in four dimensions) terms $A_{3..6}$. We find:

$$A_3(k_1,k_2)=-\frac{e^3[(\alpha_i\alpha_j+\beta_i\beta_j)\beta_k+(\alpha_i\beta_j+\beta_i\alpha_j)\alpha_k]}{\pi^2}\int_0^1 dx\int_0^{1-x} dy\,\frac{xy}{\Delta}\,, \tag{3.8a}$$

$$A_4(k_1,k_2)=\frac{e^3[(\alpha_i\alpha_j+\beta_i\beta_j)\beta_k+(\alpha_i\beta_j+\beta_i\alpha_j)\alpha_k]}{\pi^2}\int_0^1 dx\int_0^{1-x} dy\,\frac{y(y-1)}{\Delta}\,, \tag{3.8b}$$

$$A_5(k_1,k_2)=-\frac{e^3[(\alpha_i\alpha_j+\beta_i\beta_j)\beta_k+(\alpha_i\beta_j+\beta_i\alpha_j)\alpha_k]}{\pi^2}\int_0^1 dx\int_0^{1-x} dy\,\frac{x(x-1)}{\Delta}\,, \tag{3.8c}$$

$$A_6(k_1,k_2)=-A_3(k_1,k_2)\,. \tag{3.8d}$$

One could guess the expressions above with $i\neq j\neq k$ from the ones with a single identical gauge boson $i=j=k$ by exploiting simple combinatoric algebra in eqs. (H.33), (H.34) and (H.35) and eqs. (H.37) and (H.38). One can check that all the above form factors obey the Bose symmetry specified in eqs. (H.39a), (H.39b) and (H.39c).

In summary, our main result is the trilinear gauge boson vertex $\Gamma^{\mu\nu\rho}$ of eq. (3.2), supplemented by form factor components $A_{i=1..6}$ read from eqs. (3.4) and (3.8). Equation (3.2) satisfies the relevant Ward Identities stated in eq. (3.3) which originate from the partial conservation of vector and axial vector symmetries in (G.9).

3.2.2 Unitarity

We can make full use of the effective vertex $\Gamma^{\mu\nu\rho}$ in order to calculate, as an example, the matrix element for the process $ZZ \longrightarrow ZZ$ with an intermediate massive vector boson Z'. We perform the calculation in the center of mass frame with the following kinematics:

$$
\begin{aligned}
&p_1 = (E, 0, 0, p) \ , \quad p_2 = (E, 0, 0, -p) \\
&k_1 = (E, p\sin\theta, 0, p\cos\theta) \ , \quad k_2 = (E, -p\sin\theta, 0, -p\cos\theta) \ , \\
&\varepsilon(p_1) = \frac{1}{m_Z}(p, 0, 0, E) \ , \quad \varepsilon(p_2) = \frac{1}{m_Z}(p, 0, 0, -E) \ , \\
&\varepsilon^*(k_1) = \frac{1}{m_Z}(p, E\sin\theta, 0, E\cos\theta) \ , \quad \varepsilon^*(k_2) = \frac{1}{m_Z}(p, -E\sin\theta, 0, -E\cos\theta) \ ,
\end{aligned}
$$

where p_1 and p_2 are the four-momenta of incoming particles, k_1 and k_2 the four-momenta of outgoing particles, $\varepsilon(p_1)$, $\varepsilon(p_2)$, $\varepsilon^*(k_1)$, $\varepsilon^*(k_2)$ are the polarisation vectors of the incoming and outgoing particles respectively and θ is the scattering angle of the outgoing Z-boson in the center of mass frame. Non-zero contributions arise only from t and u-channels since the s-channel amplitude vanishes in this frame. Working in the unitary gauge, we find a contribution to $ZZ \to ZZ$ due to loop-induced $\Gamma^{\mu\nu\rho}_{Z'ZZ}$ of eq. (3.2) as,

$$
\begin{aligned}
\mathscr{M} \ = \ \mathscr{M}_t + \mathscr{M}_u \quad &= \quad \left(\frac{E^2\sin^2\theta}{t - m_{Z'}^2}\right)\Big[(A_1 - A_2) + p^2\,(1 - \cos\theta)\,(A_3 - A_6)\Big]^2 \\
&+ \quad \left(\frac{E^2\sin^2\theta}{u - m_{Z'}^2}\right)\Big[(A_1 - A_2) + p^2\,(1 + \cos\theta)\,(A_3 - A_6)\Big]^2 , \qquad (3.9)
\end{aligned}
$$

where $t = (p_1 - k_1)^2 = -2\,p^2(1 - \cos\theta)$ and $u = (k_1 - p_2)^2 = -2\,p^2(1 + \cos\theta)$. The factors A_1 and A_2 in eq. (3.4) are dimensionless and, in the limit of $E^2 \to \infty$ vary at worse as constants while from eq. (3.8) we have $A_3 = -A_6$ which asymptotically go like E^{-2}. Therefore, at high energies $E^2 \to \infty$, terms inside the square brackets in eq. (3.9) behave like constants and so the amplitude does at high energies. This means that unitarity is satisfied as is of course expected for a renormalised theory. It is worthwhile noting that in the limit $E^2 \to \infty$ we obtain $(A_1 - A_2) \propto c(w - z)$ where c is an anomaly pre-factor present in the second term in the r.h.s of eq. (3.3a). There is still however a finite and non-vanishing constant contribution from the $A_{3,6}$ form factors in eq. (3.9) which for every particle contribution reads,

$$
\lim_{E^2\to\infty} \mathscr{M} = -\left(\frac{c}{4\pi^2}\right)^2 \sin^2\theta \left[1 + 2(w - z) + \frac{(w - z)^2}{2\sin^2\theta}\right] \ . \qquad (3.10)
$$

We observe that the unknown parameters w and z still remain in the amplitude. Only the relation $w = z$ removes them from the asymptotic limit. We shall come back at this point when discussing the Z'^*ZZ-vertex in section 3.4.3.

3.2.3 Goldstone boson Equivalence Theorem and R_ξ - independence

There are several ways to derive the Ward Identities of eq. (3.3). A classical method is to demand invariance of the path integral under the combined local vector and axial-vector gauge transformations (G.9). We can then represent these WI's diagrammatically to prove the Goldstone Boson Equivalence Theorem [129–131]. This is most clearly explained in Lorentz gauge ($\xi = 0$) where the gauge fixing term (G.10) does not involve the Goldstone boson field φ. Then conservation of the gauge current implies

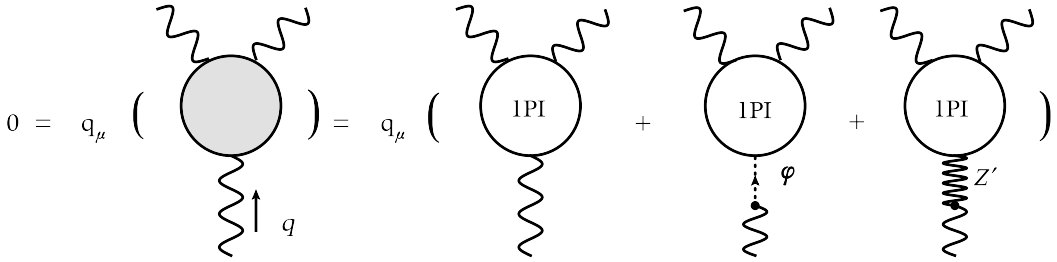

Figure 3.2: *Graphical representation of the WI in eq. (3.3a).*

that q^μ can be contracted directly with $\Gamma^{\mu\nu\rho}$ and also with the derivatively coupled Goldstone boson to $\Gamma^{\nu\rho}$. In principle there is a third contribution from possible mixings with other gauge bosons, say Z', that couple to the same fermions in the vertex. This last mixing must necessarily be proportional to $(g_{\mu\lambda} - q_\mu q_\lambda/q^2)$ and when contracted with q^μ, vanishes. Therefore, by using rules from the toy model in Appendix G, it is straightforward to see that we recover the classical WI (3.3a), without the anomaly term. While a possible gauge boson mixing contributes to $\Gamma^{\mu\nu\rho}$, it does not contribute to WIs in eq.(3.3). At very high energy, the longitudinal polarization vector is $\varepsilon_{L\mu}(q) \simeq q_\mu/m_A$, where m_A is the gauge boson mass. In other words for an anomaly-free model, eq. (3.3a) or the sum of the diagrams in Fig. 3.2, can be written as,

$$\epsilon_{L\mu}(q)\,\Gamma^{\mu\nu\rho} \;=\; i\,\Gamma^{\nu\rho}\;. \tag{3.11}$$

This equation tells us that at the high energy limit, the physical amplitude with the gauge boson in vertex μ is replaced by the vertex with a Goldstone boson that 'has been eaten'. However, as is evident from eq. (3.3a) the relation (3.11) is broken by possible gauge anomalies. This is another reason why the latter should be absent.

One can easily check by studying for example the fermion-antifermion annihilation process to two gauge bosons with the toy model of Appendix G, that eq. (3.11) is the required condition for the amplitude to be gauge ξ-independent. Again the anomaly-term *must* be absent.

3.3 Non-Decoupling Effects

Heavy fermion non-decoupling effects can be cast in two classes :

A) effects that arise from a large mass splitting between particles within an anomaly-free multiplet.

B) *anomaly driven* effects that originate from decoupling a whole anomaly-free multiplet.

In case (A), formal decoupling of the heavy particle that participates in the anomaly cancellation mechanism will leave at low energies an effective Lagrangian $\Delta\Gamma^{\mu\nu\rho}$ that accounts for the anomaly cancellation missing piece [98,99,103]. In case (B), the Higgs coupling to fermions will be much larger than the gauge coupling with the latter being approximately zero when the fermion mass is going to infinity [110,111].

3.3.1 Non-Decoupling due to large mass splitting

We are going to focus first on the simplest case with three identical external gauge bosons. This means we set $i = j = k$ in the Ward Identities of eq. (3.3), or else we look directly at expressions, (H.26) - (H.28). In order to carry out a systematic study of non-decoupling effects and their interplay with chiral anomalies, it is essential to keep track of the anomalous terms that depend on the arbitrary parameters w and z. By exploiting Bose symmetries for on-shell external gauge bosons, and specifically, (H.39) among legs j and k we find $w = -z$, while with (H.40) among legs i and j we find (after some tedious algebra) $2\,w - z - 1 = 0$. The solution of this system,

$$w \;=\; -z \;=\; \frac{1}{3}\,, \tag{3.12}$$

finally fixes the arbitrary parameters w and z. Our observation is that these fixed values for the arbitrary parameters correspond to the case of a particle decoupling from the effective action, *i.e.*,

$$\lim_{m\to\infty} \Gamma^{\mu\nu\rho}(k_1, k_2; w, z) = 0 \;\Rightarrow w = -z = \frac{1}{3}\,. \tag{3.13}$$

We elaborate this point in what follows. The WIs now take the form:

$$\begin{aligned} q_\mu \Gamma^{\mu\nu\rho}(k_1,k_2;w=1/3) &= -\frac{e^3\beta m^2}{\pi^2}\,\varepsilon^{\lambda\nu\rho\sigma}\,k_{1\lambda}\,k_{2\sigma}\,I_0(k_1,k_2;m)+ \\ &+ \frac{e^3(\beta^3+3\alpha^2\beta)}{6\pi^2}\,\varepsilon^{\lambda\nu\rho\sigma}\;k_{1\lambda}\,k_{2\sigma}\;. \end{aligned} \tag{3.14a}$$

$$\begin{aligned} -k_{1\nu}\widetilde{\Gamma}^{\nu\rho\mu}(k_1,k_2;w=1/3) &= -\frac{e^3\beta m^2}{\pi^2}\,\varepsilon^{\lambda\mu\rho\sigma}\,k_{1\lambda}\,k_{2\sigma}\,I_1(k_1,k_2;m)- \\ &- \frac{e^3(\beta^3+3\alpha^2\beta)}{6\pi^2}\varepsilon^{\lambda\mu\rho\sigma}\;k_{1\lambda}k_{2\sigma}\;, \end{aligned} \tag{3.14b}$$

$$\begin{aligned} -k_{2\rho}\widehat{\Gamma}^{\rho\mu\nu}(k_1,k_2;w=1/3) &= -\frac{e^3\beta m^2}{\pi^2}\,\varepsilon^{\lambda\mu\nu\sigma}\,k_{1\lambda}\,k_{2\sigma}\,I_2(k_1,k_2;m)+ \\ &+ \frac{e^3(\beta^3+3\alpha^2\beta)}{6\pi^2}\,\varepsilon^{\lambda\mu\nu\sigma}\,k_{1\lambda}k_{2\sigma}\;, \end{aligned} \tag{3.14c}$$

where the integrals $I_{0,1,2}$ are defined in eqs. (H.5), (H.22) and (H.23) respectively. The anomalous terms in eq. (3.14) are then allocated "democratically" in the three legs of $\Gamma^{\mu\nu\rho}$ as one would have naively expected. Note also that since we find the following limits, $\lim_{m\to\infty} m^2 I_0 = -\lim_{m\to\infty} m^2 I_1 = \lim_{m\to\infty} m^2 I_2 = \frac{1}{6}(\beta^2+3\alpha^2)$, the r.h.s of eqs. (3.14a), (3.14b) and (3.14c) cancel identically, verifying our statement in eq. (3.13). Therefore, for a Dirac fermion pair circulating the loop as shown in Fig. 3.1 and for three identical external gauge bosons, *at the formal decoupling limit, the finite contributions are equal and opposite to the anomaly contributions in the vertex.* In a Lorentz gauge, terms in $\Gamma^{\mu\nu\rho}$ proportional to $I_{0,1,2}$ arise from the mixing between the Goldstone boson φ and the gauge boson as it is shown in Fig. 3.2. We should notice however, that our calculation of WIs in eq. (3.14) given in Appendix H contains no reference to a particular gauge choice.

For a Lorentz-invariant and renormalizable chiral gauge theory the anomaly terms *i.e.,* the last terms on the r.h.s of eqs. (3.14), have to be absent. The only way[3], consistent with renormalizability[4] [96,97], to remove the anomaly terms, is to add a new Dirac fermion pair with opposite β *i.e.*, opposite hypercharges Y_L and Y_R. A consistent way to describe heavy fermion decoupling effects is to perform the calculation directly in the broken phase of the theory where physical masses appear explicitly. Assuming that the mass of the second (heavy) pair and the c.m energy, $s=(k_1+k_2)^2$, is much bigger than the first (light) fermion, say, $m_2^2 \gg s \gg m_1^2 \approx 0$, there is a non-decoupled term in the 1PI effective action which can be read off from eqs. (H.32), (H.37) and (H.38) [or eqs. (3.2) and (3.4) for $i=j=k$] to be,

$$\Delta\Gamma^{\mu\nu\rho}(k_1,k_2) \approx \frac{e^3\,(\beta^3+3\alpha^2\beta)}{6\pi^2}\,\varepsilon^{\mu\nu\rho\sigma}\,(k_1-k_2)_\sigma\;. \tag{3.15}$$

[3]Of course there is the trivial case of vector multiplets *i.e.*, $\beta=0$.

[4]We are not going to consider here the situation [112] of incorporating non-renormalizable counterterms to cancel the anomalies at the expense of introducing a cut-off scale $\Lambda \sim 4\pi v$.

This term remains in the 1PI effective function for the light particle. In the heavy mass limit ($m_2 \to \infty$), the form factors $A_{i=3,\ldots 6}(k_1, k_2)$ vanish as $1/m^2$ leaving only the term eq. (3.15) in the low energy effective action which has no 'memory' anymore from the heavy mass m_2. Although, the exact non-kinematic prefactor in eq. (3.15), depends upon model details, its magnitude (in e-units) is approximately, α/π and could be observable. Furthermore, the non-decoupling term eq. (3.15) does not depend on the regularization scheme, *i.e.*, on the parameters w and z in eqs. (H.37) and (H.38), since the model is by construction anomaly-free.

3.3.2 Anomaly Driven non-decoupling effects

This is a category of possible non-decoupling effects for models possessing an anomaly-free cluster of heavy particles just above those known from the Standard Model. We systematically then check anomaly cancellation conditions in Ward Identities (eq. 3.3) by demanding the pre-factors of $I_{1,2}$ integrals in eqs. (3.4a) and (3.4b) to be non-zero. We are seeking for minimal models with up-to three different gauge bosons and up to the least n-Dirac fermions.

A model that contains one gauge boson X, with V-A couplings as in eq. (3.1), coupled to only one fermion is impossible to exist because it is anomalous (except the trivial case of a vector-like particle where $\beta = 0$). Adding an extra fermion with the same mass but with opposite axial-vector coupling (β) renders the model anomaly-free. Such a simple particle content does not lead to non-decoupling effects because all these effects are proportional to an odd power of the axial-vector coupling ($\sim \beta^{2k+1}$) and therefore the sum over the two fermions vanishes. A similar situation arises when more fermions are circulating in the loop.

More interesting is the case where one has two, distinct, external gauge bosons, X and Y, either massive or massless. The cancelation of trilinear anomalies requires the existence of at least two fermions with opposite axial-vector couplings but again it is impossible to satisfy instantaneously the mixed anomaly and non-decoupling conditions [see below]. We first obtain the general conditions for an anomaly free model with two gauge bosons X and Y. In notation of eq. (3.1) these conditions read:

$$\sum_{i=1}^{n}(\beta_X^3 + 3\alpha_X^2\beta_X)_i = 0\,, \tag{3.16a}$$

$$\sum_{i=1}^{n}(\beta_Y^3 + 3\alpha_Y^2\beta_Y)_i = 0\,, \tag{3.16b}$$

$$\sum_{i=1}^{n}(\beta_X^2\beta_Y + 2\alpha_X\alpha_Y\beta_X + \alpha_X^2\beta_Y)_i = 0\,, \tag{3.16c}$$

$$\sum_{i=1}^{n}(\beta_Y^2\beta_X + 2\alpha_X\alpha_Y\beta_Y + \alpha_Y^2\beta_X)_i = 0\,, \tag{3.16d}$$

where n is the total number of fermions. Starting from trilinear anomalies eq. (3.16a) or eq. (3.16b) we see that the case $n = 1$ requires only vectorial couplings, $\beta_X = \beta_Y = 0$.

	ψ_1	ψ_2	ψ_3
$U(1)_X$	$\alpha = e, \beta = -e$	$\alpha = e, \beta = e$	$\alpha = 0, \beta = 0$
$U(1)_Y$	$\alpha = -e, \beta = -e$	$\alpha = 0, \beta = 0$	$\alpha = e, \beta = e$

Table 3.1: *Charges of an anomaly-free model with non-decoupling remnants in three gauge boson vertices XXY and YYX.*

Therefore for $n = 1$ there is no non-trivial solution. For $n = 2$ the non-zero couplings must satisfy the following conditions:

$$\begin{aligned} \beta_{X2} &= -\beta_{X1}, \qquad \alpha_{X2} = \pm\alpha_{X1} \\ \beta_{Y2} &= -\beta_{Y1}, \qquad \alpha_{Y2} = \pm\alpha_{Y1} \ . \end{aligned} \tag{3.17}$$

Turning to mixed anomalies, eq. (3.16c) and eq. (3.16d), it is amusing first that they are satisfied even with one internal fermion ($n = 1$), iff

$$\beta_X = \alpha_X \ , \qquad \beta_Y = -\alpha_Y \ , \tag{3.18}$$

or

$$\beta_X = -\alpha_X \ , \qquad \beta_Y = \alpha_Y \ . \tag{3.19}$$

Non-decoupling conditions are derived by the requirement that the pre-factors of I_1 and I_2 integrals in eqs. (3.4a) and (3.4b) are non-zero. Hence, in the limit of $k_1^2,\, k_2^2 \simeq s \ll m^2$ at least one of the following algebraic expressions,

$$\begin{aligned} &\sum_{i=1}^{n}(\beta_X^2\beta_Y + 3\alpha_X\alpha_Y\beta_X)_i \ , \qquad \sum_{i=1}^{n}(\beta_X^2\beta_Y + 3\alpha_X^2\beta_Y)_i \ , \\ &\sum_{i=1}^{n}(\beta_Y^2\beta_X + 3\alpha_X\alpha_Y\beta_Y)_i \ , \qquad \sum_{i=1}^{n}(\beta_Y^2\beta_X + 3\alpha_Y^2\beta_X)_i \ , \end{aligned} \tag{3.20}$$

must be non-vanishing. For $n = 1$ the choice of eq. (3.18) [or eq. (3.19)] which eliminates the mixed anomalies, sets also eqs. (3.20) to a non-zero value. However, to cancel the XXX and YYY anomalies one needs at least $n = 2$ fermions to satisfy the conditions in eq.(3.17). These set the non-decoupling expressions (3.20) back to zero. The first non-trivial solution of the system of eqs. (3.16) and (3.20) arises with three pairs of chiral Dirac fermions ($n = 3$) with an example of quantum numbers given in Table 3.1. Here, we use eq. (3.18) and eq. (3.19) to cancel mixed anomalies for ψ_1. The other two particles ψ_2 and ψ_3 are singlets under $U(1)_Y$ and $U(1)_X$, respectively. Plug these into eqs. (H.32), (3.4) and (3.7), we obtain the non-vanishing operators at the decoupling limit:

$$\Gamma^{\mu\nu\rho}_{XYY} = \Gamma^{\mu\nu\rho}_{YXX} = \frac{e^3}{3\pi^2}\varepsilon^{\mu\nu\rho\sigma}\,(k_2 - k_1)_\sigma \ , \tag{3.21a}$$

$$\Gamma^{\mu\nu\rho}_{XYX} = \Gamma^{\mu\nu\rho}_{YXY} = -\frac{e^3}{3\pi^2}\varepsilon^{\mu\nu\rho\sigma}\,(2k_2 + k_1)_\sigma \ , \tag{3.21b}$$

$$\Gamma^{\mu\nu\rho}_{XXX} = \Gamma^{\mu\nu\rho}_{YYY} = 0 \ . \tag{3.21c}$$

	ψ_1	ψ_2	χ_1	χ_2
$U(1)_X$	$\alpha = e_1, \beta = 0$	$\alpha = e_2, \beta = 0$	$\alpha = \frac{e_3+e_4}{2}, \beta = \frac{e_3-e_4}{2}$	$\alpha = \frac{e_3+e_4}{2}, \beta = -\frac{e_3-e_4}{2}$
$U(1)_Y$	$\alpha = 0, \beta = -q_1$	$\alpha = 0, \beta = q_1$	$\alpha = q_2, \beta = 0$	$\alpha = -q_2, \beta = 0$

Table 3.2: *Charges of all fermions with respect to the gauge groups* $U(1)_X \times U(1)_Y$.

Next is a model example with $n = 4$ Dirac fermions charged under the product of gauge groups $U(1)_X \times U(1)_Y$. This toy model has been examined in ref. [110]. Charge assignments are given in Table 3.2. They are chosen in such a way that triangular anomalies $[U(1)_X]^3$ and $[U(1)_Y]^3$ are canceled separately. The cancelation of mixed anomalies requires the extra condition $q_2 = q_1 \frac{(e_1^2 - e_2^2)}{(e_3^2 - e_4^2)}$. Charges in Table 3.2 follow the general rules of eqs. (3.17). If we assume that all extra fermions have a common mass m and are all very heavy, then in the low energy limit we find the following expressions for the effective vertices with different combinations of external gauge bosons:

$$\Gamma^{\mu\nu\rho}_{XXX} = \Gamma^{\mu\nu\rho}_{YYY} = 0 \,, \tag{3.22a}$$

$$\Gamma^{\mu\nu\rho}_{XXY} = \frac{q_1(e_1^2 - e_2^2)}{4\pi^2}(2k_1 + k_2)_\sigma \varepsilon^{\mu\nu\rho\sigma} \,, \tag{3.22b}$$

$$\Gamma^{\mu\nu\rho}_{YXX} = \frac{q_1(e_1^2 - e_2^2)}{4\pi^2}(k_2 - k_1)_\sigma \varepsilon^{\mu\nu\rho\sigma} \,, \tag{3.22c}$$

$$\Gamma^{\mu\nu\rho}_{XYY} = \Gamma^{\mu\nu\rho}_{YXY} = 0 \,. \tag{3.22d}$$

These contributions arise from terms that are proportional to I_1 and I_2-integrals taking into account that this model is anomaly-free. Such a situation should never occur in the SM. The basic difference is that neither gauge bosons X and Y is purely vector-like for the entire fermionic sector *i.e.,* X and Y must be *strictly massive*. This is a crucial difference that leads to the existence of remnants in the low energy limit. On the contrary, the existence of the photon in the SM leads to a term related to I_1 or I_2 which always vanishes for an anomaly-free model.

We have also worked out the case with three different gauge bosons. The corresponding 10 independent anomaly-free, and, 18 independent non-decoupling conditions, are quite involved and are presented separately in Appendix K. Again the non-decoupling effects arise for $n \geq 3$. The new feature that appear in this category is the fact that one can exploit non-decoupling effects where one of the gauge bosons is massless. Such a minimal ($n = 3$) example comes into sight if we adopt the charge assignments shown in Table 3.3. Notice that all fermions have $\beta_Y = 0$ *i.e.*, the Y couples purely to a vector current.

We can easily check that the conditions (K.1) for an anomaly-free model are satisfied while at the same time some of the expressions in (K.2) are non zero.

	ψ_1	ψ_2	ψ_3
$U(1)_X$	$\alpha = e, \beta = e$	$\alpha = e, \beta = -e$	$\alpha = 0, \beta = 0$
$U(1)_Y$	$\alpha = e, \beta = 0$	$\alpha = e, \beta = 0$	$\alpha = e, \beta = 0$
$U(1)_Z$	$\alpha = e, \beta = -e$	$\alpha = 0, \beta = 0$	$\alpha = e, \beta = e$

Table 3.3: *Charges of an anomaly-free model with non-decoupling remnants in three gauge boson vertex XYZ.*

The non-zero effective vertices can be written in the form,

$$\Gamma^{\mu\nu\rho}_{XXZ} = -\Gamma^{\mu\nu\rho}_{ZZX} = \frac{e^3}{3\pi^2}(2k_1 + k_2)_\sigma \varepsilon^{\mu\nu\rho\sigma} \ , \tag{3.23a}$$

$$\Gamma^{\mu\nu\rho}_{XZX} = -\Gamma^{\mu\nu\rho}_{ZXZ} = -\frac{e^3}{3\pi^2}(2k_2 + k_1)_\sigma \varepsilon^{\mu\nu\rho\sigma} \ , \tag{3.23b}$$

$$\Gamma^{\mu\nu\rho}_{ZXX} = -\Gamma_{XZZ} = \frac{e^3}{3\pi^2}(k_1 - k_2)_\sigma \varepsilon^{\mu\nu\rho\sigma} \ , \tag{3.23c}$$

$$\Gamma^{\mu\nu\rho}_{YXZ} = \Gamma^{\mu\nu\rho}_{YZX} = \frac{e^3}{2\pi^2}(k_1 + k_2)_\sigma \varepsilon^{\mu\nu\rho\sigma} \ , \tag{3.23d}$$

$$\Gamma^{\mu\nu\rho}_{XYZ} = -\Gamma^{\mu\nu\rho}_{ZYX} = \frac{e^3}{2\pi^2} k_{1_\sigma} \varepsilon^{\mu\nu\rho\sigma} \ , \tag{3.23e}$$

$$\Gamma^{\mu\nu\rho}_{XZY} = \Gamma^{\mu\nu\rho}_{ZXY} = -\frac{e^3}{2\pi^2} k_{2_\sigma} \varepsilon^{\mu\nu\rho\sigma} \ . \tag{3.23f}$$

We observe that heavy fermion non-decoupling effects appear in eq. (3.23e) and (3.23f). If a model like this, with $X = Z'$, $Y = \gamma$, $Z = Z$ can be embedded in the SM, then it would in principle allow for decays like $Z' \to Z\gamma$ that do not depend on the heavy fermion masses.

We should finally remark that in models considered in Tables 3.1-3.3, gravitational anomalies cancel out since it is always $\sum_f \beta_f^X = 0$ for a given axial vector coupling between a vector boson X and a fermion f.

3.4 Applications

3.4.1 Standard Model

Focusing first in the Standard Model with neutral, Z or γ triple gauge boson vertices, we need only to consider the interaction Lagrangian with fermions. This reads as:

$$\mathscr{L}_{int} = \sum_f \alpha_f^\gamma A_\mu \overline{\Psi}_f \gamma^\mu \Psi_f + \sum_f Z_\mu \overline{\Psi}_f \gamma^\mu (\alpha_f^Z + \beta_f^Z \gamma_5) \Psi_f \ , \tag{3.24}$$

where the factors α_f^V, β_f^V with $V = \gamma, Z$ are

$$\begin{aligned} &\alpha_f^\gamma = e\, Q_f \ , \quad \beta_f^\gamma = 0 \ , \\ &\alpha_f^Z = \frac{g_Z}{2}\,(T_{f_L}^3 - 2\, s_w^2\, Q_f) \ , \quad \beta_f^Z = -\frac{g_Z}{2}\, T_{f_L}^3 \ , \end{aligned} \tag{3.25}$$

and $T_{f_L}^3$ and Q_f are the third component of weak isospin and charge of the SM Dirac fermions $f = \nu, e, u, d$, respectively. Explicitly in the SM, the prefactors α_f^V and β_f^Z take the form:

$$\begin{aligned} &\alpha_u^\gamma = \frac{2}{3} e \ , \quad \alpha_u^Z = \frac{g_Z}{2}(\frac{1}{2} - \frac{4}{3} s_w^2) \ , \quad \beta_u^Z = -\frac{g_Z}{4} \ , \\ &\alpha_d^\gamma = -\frac{1}{3} e \ , \quad \alpha_d^Z = \frac{g_Z}{2}(-\frac{1}{2} + \frac{2}{3} s_w^2) \ , \quad \beta_d^Z = \frac{g_Z}{4} \ , \\ &\alpha_e^\gamma = -e \ , \quad \alpha_e^Z = \frac{g_Z}{2}(-\frac{1}{2} + 2 s_w^2) \ , \quad \beta_e^Z = \frac{g_Z}{4} \\ &\alpha_\nu^\gamma = 0 \ , \quad \alpha_\nu^Z = \frac{g_Z}{4} \ , \quad \beta_\nu^Z = -\frac{g_Z}{4} \ , \end{aligned} \tag{3.26}$$

where $g_Z = e/s_w$ is the weak boson gauge coupling and $s_w,\ c_w$ are the sinus and cosinus of the weak mixing angle.

V^*ZZ

Our first application refers to the vertex V^*ZZ with $V = \gamma$, Z being off-shell. This interaction has been searched for at LEP and Tevatron while is currently under scrutiny at the LHC. At one loop level the only CP-conserving contribution arises from the triangle graph in Fig. 3.1. Applying our general form of the 1PI vertex in eq. (3.2) and making use of the Bose symmetry $\nu \leftrightarrow \mu, k_1 \leftrightarrow k_2$ as in eq. (H.39), we find:

$$\Gamma^{\mu\nu\rho}_{V^*ZZ}(k_1, k_2; w) = \left[\epsilon^{\mu\nu\rho\sigma}(k_1 - k_2)_\sigma \left(-A_1 + \frac{s}{2} A_3\right) + A_3\, q^\mu \epsilon^{\rho\beta\nu\delta} k_{1\beta} k_{2\delta}\right] , \tag{3.27}$$

where the polarization vectors $\epsilon_\nu^*(k_1)$, $\epsilon_\rho^*(k_2)$ outside the square brackets have been omitted, and also, we set $A_1(k_1, k_2) \equiv A_1, ...$ etc for simplicity. More specifically, A_1 is ambiguous: it depends on how the momentum is routing the loop *i.e.*, the parameter w. This arbitrariness (or regularization scheme dependence if you wish) is further fixed by exploiting the fact that the ZZZ on-shell boson vertex vanishes by Bose symmetry.

The latter requires $w = 1/3$. On the other hand, for the vertex γZZ, conservation of the vector current and Bose symmetry implies that $w = z = 0$.

Having specified the arbitrary parameters w and z we apply our general expressions for A_1 and A_3 found in eqs. (3.4a) and (3.8a), specifically to the vertices Z^*ZZ and γ^*ZZ and sum over all SM fermions. By ignoring (see below however), the last term proportional to q^μ in eq. (3.27), we can easily find,

$$\begin{aligned}\Gamma^{\mu\nu\rho}_{Z^*ZZ}(k_1,k_2) &= \epsilon^{\mu\nu\rho\sigma}(k_1-k_2)_\sigma \times \\ &\times \sum_{f=u,d,e,\nu}\left[m_Z^2(A_{3f}-A_{4f}) + \frac{m_f^2\beta_f^Z}{\pi^2}\,I_{1f} + \frac{1}{6\pi^2}\left(\beta_f^{Z\,3}+3\beta_f^Z\alpha_f^{Z\,2}\right)\right] \\ &\equiv \epsilon^{\mu\nu\rho\sigma}(k_1-k_2)_\sigma\,\Gamma_{Z^*ZZ}(s)\,, \end{aligned} \tag{3.28}$$

$$\begin{aligned}\Gamma^{\mu\nu\rho}_{\gamma^*ZZ}(k_1,k_2) &= \epsilon^{\mu\nu\rho\sigma}(k_1-k_2)_\sigma \sum_{f=u,d,e,\nu}\left[m_Z^2(A_{3f}-A_{4f}) + \frac{m_f^2\beta_f^Z}{\pi^2}\,I_{1f} + \frac{1}{2\pi^2}\alpha_f^\gamma\alpha_f^Z\beta_f^Z\right] \\ &\equiv \epsilon^{\mu\nu\rho\sigma}(k_1-k_2)_\sigma\Gamma_{\gamma^*ZZ}(s)\,, \end{aligned} \tag{3.29}$$

where $s = (k_1+k_2)^2$ and I_{1f} is given by eq. (3.5a). The last term in eqs. (3.28) and (3.29) is the anomaly contribution, while the second term is a non-decoupling one in the limit of heavy fermion mass, $m_f \to \infty$. Again we should notice here that in this limit and for one fermion contribution, the last two terms mutually cancel while the first term vanishes as m_Z^2/m_f^2. Therefore, the decoupling of heavy fermions in V^*ZZ vertex is operative even if those fermions have vastly different, but always much greater than the EW scale, masses among each other. In the SM for example, what is left behind after the decoupling of the top quark is a theory with an anomalous (sometimes called *Chern-Simons*) term that is necessary to render the effective low energy theory gauge invariant.

Especially for γ^*ZZ one can go one step further and write the whole effective vertex in terms of one integral only, namely

$$\Gamma_{\gamma^*ZZ}(s) = \frac{s}{2}\sum_{f=u,d,e,\nu} A_{3f}(s)\,. \tag{3.30}$$

Now bringing back the last term on the r.h.s of eq. (3.27) we find a perfectly fine and gauge invariant form for γ^*ZZ vertex,

$$\Gamma^{\mu\nu\rho}_{\gamma^*ZZ}(s) = \sum_f \frac{sA_{3f}}{2}\times\left[\epsilon^{\mu\nu\rho\sigma}(k_1-k_2)_\sigma - \frac{\epsilon^{\nu\rho\beta\sigma}q^\mu q_\beta}{s}(k_1-k_2)_\sigma\right]. \tag{3.31}$$

This vertex *must* be proportional to s in order to cancel the pole contribution arising at $s = q^2 = 0$ [118]. This is a generic statement for all γ^*VV vertices we address below. One should recall that this expression has been derived only after fixing the anomaly coefficients, w and z, by symmetry requirements. We could have done the reverse: to fix w, z from the requirement of no pole contribution in eq. (3.31). In a way, the anomaly and the non-decoupled terms have been absorbed in the finite integral A_3.

It is now evident from eqs. (3.30) and (3.8) that $\Gamma_{\gamma^* ZZ}(s \to 0) = 0$ for every fermion contribution, independently. Furthermore, as expected, for asymptotic values of s we also observe that $\Gamma_{\gamma^* ZZ}(s \to \infty) = 0$ after summing over all SM fermion contributions.

Within one generation of fermions, the SM is a chiral, gauge, and anomaly-free Quantum Field Theory (QFT). As a result, contributions to $\Gamma_{V^* ZZ}$ from (approximately) massless generations, vanish identically (recall that form factors $A_{3,\,4}$ are proportional to the anomaly factors, [see eqs. (3.8a) and (3.8b)] and the second term vanishes in the massless case). Therefore to a good approximation, for $\sqrt{s} \gtrsim 2M_Z$, the only non-negligible contribution to $\Gamma_{V^* ZZ}$ arises from the third generation and is due to the large mass difference between the top quark and all other fermions. The top quark influences mainly the last two terms in the square bracket of $\Gamma_{Z^* ZZ}$ and $\Gamma_{\gamma^* ZZ}$ in eqs. (3.28) and (3.29). If we make the (numerically crude) approximation of $m_Z^2 \ll s < m_t^2$ and exploit eq. (J.12c) from Appendix J, we find ($N_c = 3$ is the color factor),

$$\frac{m_t^2 \beta_t^Z}{\pi^2} I_{1t} \approx -\frac{N_c}{6\pi^2} \left(\beta_t^{Z\,3} + 3\beta_t^Z \alpha_t^{Z\,2} \right) - \frac{N_c}{120\pi^2} \left(\beta_t^{Z\,3} + 5\beta_t^Z \alpha_t^{Z\,2} \right) \frac{s}{m_t^2} \,. \tag{3.32}$$

The first term is just the opposite of the top quark anomaly contribution in $\Gamma_{Z^* ZZ}$ and they both cancel out in the limit of heavy top quark. One can prove easily this statement for all SM vertices, $\Gamma_{V^* VV}, V = Z, \gamma$ appearing below in this Chapter and we claim, following the arguments of section 3.3, that this is a general theorem: *a heavy particle cancels its own anomaly contribution in a triple gauge boson vertex and at the (non-perturbative) limit of $m \to \infty$ leaving no trace from itself behind*. Of course in the top-less SM the last term in $\Gamma_{Z^* ZZ}$ does not vanish since the particle content (τ, ν_τ, b) is now anomalous. It is also evident from eq. (3.32) that the behaviour of $\Gamma_{Z^* ZZ}(s)$ at $s \approx m_t^2$ rises approximately linearly with s as s/m_t^2. This is also verified from our numerical result shown in Fig.3.3a. Similar conclusions one can derive for $\Gamma_{\gamma^* ZZ}$ as it is shown in Fig.3.3b, but this is rather obvious now because of eq. (3.30).

Furthermore, it is also instructive to study the behaviour of the vertices $\Gamma_{V^* ZZ}(s)$ in the asymptotic region, $s \gg m_t^2 > m_Z^2$. By exploiting eq. (J.13) and keeping only terms of order m_f^2/s we arrive at the following expression,

$$\begin{aligned} \Gamma_{Z^* ZZ}(s \gg m_t^2) \approx N_c \frac{m_t^2}{s} \Bigg\{ & \frac{2\beta_t^{Z\,3}}{\pi^2} \left(2 - \ln \frac{s}{m_t^2} - i\pi \right) + \\ & + \frac{\beta_t^{Z\,3} + \alpha_t^{Z\,2} \beta_t^Z}{\pi^2} \left(\frac{1}{2} \ln^2 \frac{s}{m_t^2} - \frac{\pi^2}{2} + i\pi \ln \frac{s}{m_t^2} \right) \Bigg\} , \end{aligned} \tag{3.33}$$

in which both real and imaginary parts vanish at asymptotic values of s as they should following unitarity arguments. The effect of a "heavy" particle (here the top quark) is to just delay the "falling off" of $|\Gamma_{Z^* ZZ}(s)|$ [see Fig.3.3a.] as $s \to \infty$. Finally it is also obvious that the real and imaginary part of $\Gamma_{Z^* ZZ}$ are of the same order of magnitude, a situation which remains true everywhere after the threshold energy, $s \gtrsim 4m_t^2$.

Translating our numerical results for the SM to the notation of ref. [118][5] that is usually followed by the theoretical and experimental literature, we find for LEP energies and $m_t = 173$ GeV, that

$$f_5^Z(\sqrt{s} = 200 \text{ GeV}) = 1.8 \times 10^{-4} , \tag{3.34}$$
$$f_5^\gamma(\sqrt{s} = 200 \text{ GeV}) = 2.1 \times 10^{-4} , \tag{3.35}$$

where we have neglected small imaginary part contributions from light quark and lepton mass thresholds. These results agree with those quoted in ref. [124]. Unfortunately, they are too small to have been reached by LEP [132].

Just above the top quark threshold energies $s \geq 4m_t^2$, the vertex develops a significant absorptive part. This is apparent from our analytical expressions in Appendix J for integrals $A_{3..6}$ and $I_{1,2}$ and the discussion above. For $\sqrt{s} = 500$ GeV we find :

$$f_5^Z(\sqrt{s} = 500 \text{ GeV}) = (0.4 - 0.5i) \times 10^{-4} , \tag{3.36}$$
$$f_5^\gamma(\sqrt{s} = 500 \text{ GeV}) = (-0.3 + 0.3i) \times 10^{-4} . \tag{3.37}$$

Note again that the imaginary part of the amplitude is of the same order of magnitude as the real part.

$V^*\gamma Z$

Another non-trivial class among trilinear neutral gauge boson vertices that have been and being searched for at colliders, is the amplitude $V^*\gamma Z$. In the notation of Fig. 3.1, we assign $V_\mu^*(q)$, $\gamma_\nu(k_1)$ and $Z_\rho(k_2)$ to the 1PI effective vertex $\Gamma^{\mu\nu\rho}_{V^*\gamma Z}$ of eq. (3.2) with $V = Z, \gamma$. When the photon and the Z-gauge boson are both on-shell we find:

$$\begin{aligned}\Gamma^{\mu\nu\rho}_{V^*\gamma Z}(k_1, k_2) &= \epsilon^{\mu\nu\rho\sigma}\, k_{1\sigma} \left(A_2 + \frac{s + m_Z^2}{2}\, A_3 \right) + \\ &+ \epsilon^{\mu\rho\beta\delta} q^\nu\, q_\beta\, k_{2\delta}\, (A_3 + A_6) + \epsilon^{\nu\rho\beta\delta} q^\mu k_{1\beta} k_{2\delta}\, A_3 \,. \end{aligned} \tag{3.38}$$

We have seen however in eq. (3.8d) that $A_3 = -A_6$ and therefore the second term in eq. (3.38) vanishes at one-loop. Furthermore, the last term when coupled to a light quark or lepton vector current, is proportional to the mass of the incoming fermions and for current collider architectures this contribution is negligible[6]. Hence, only the first term remains with potentially visible effects. When *all* external particles are on-shell, Bose symmetry and gauge invariance require the vertex $V\gamma Z$ to vanish. Bose symmetry relations among form factors and gauge invariance fix the arbitrary parameters w and z to be:

$$Z\gamma Z \; : \qquad w = 1 \,, \quad z = 0 \,, \tag{3.39}$$
$$\gamma\gamma Z \; : \qquad w = 1 \,, \quad z = 1 \,. \tag{3.40}$$

[5] We multiply $\Gamma_{V^*ZZ}(s)$ in eqs. (3.28) and (3.29) with $e\, m_Z^2/(s - m_V^2)$.

[6] This term however is important for gauge invariance to be preserved, as in eq. (3.31) before.

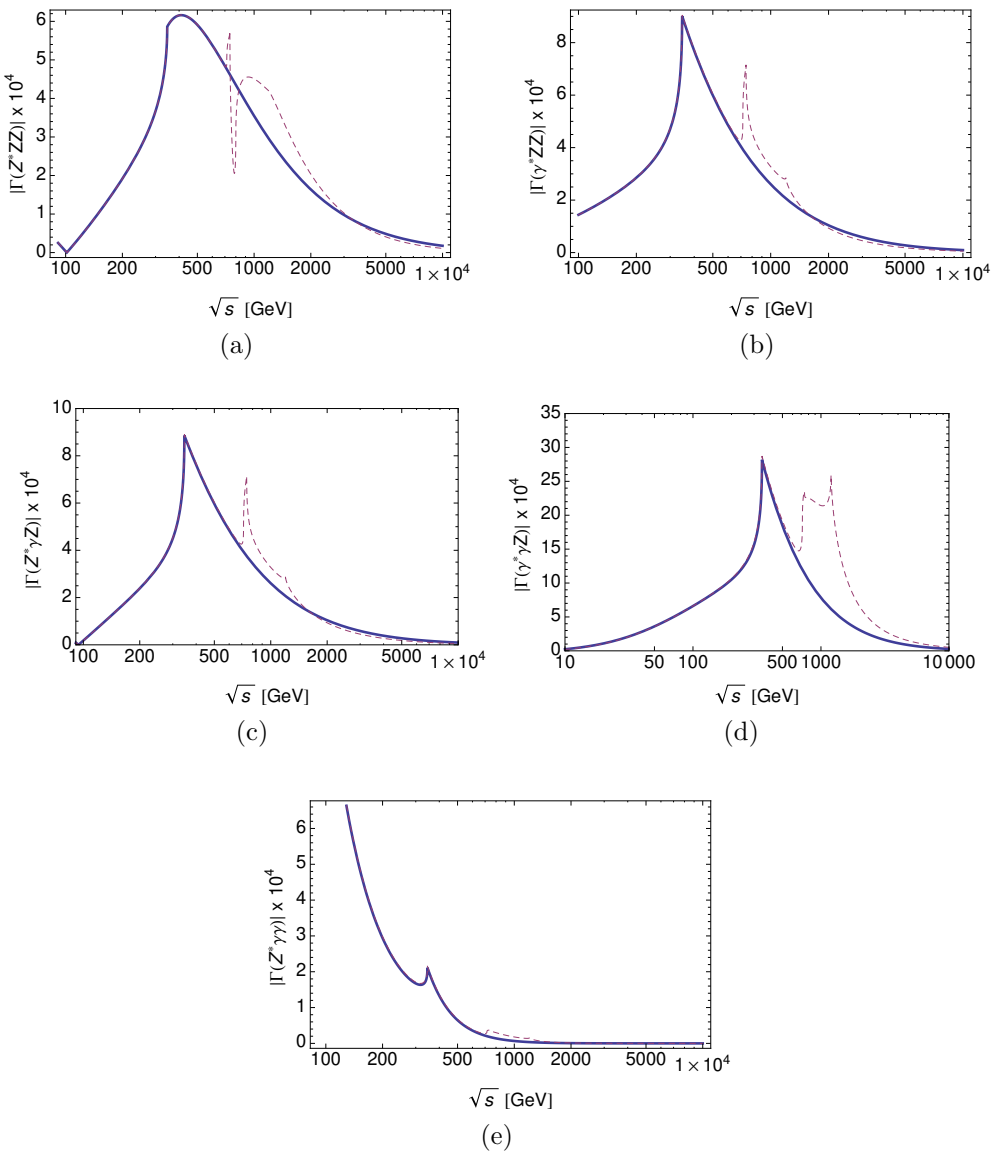

Figure 3.3: *The dependence of* $|\Gamma_{V^*VV}(s)|$ *with* $\sqrt{s}$ *for different gauge bosons combinations,* $V = \gamma, Z$ *: (a)* Z^*ZZ*, (b)* γ^*ZZ*, (c)* $Z^*\gamma Z$*, (d)* $\gamma^*\gamma Z$*, (e)* $Z^*\gamma\gamma$*. The solid curve corresponds to the SM, the dashed curve corresponds to the SM + 4th generation fermion model. Masses for light quarks and leptons are neglected while* $m_t = 173$ GeV*. Fourth generation quarks and lepton masses are taken as in eq. (3.66).*

By substituting the form in A_2 from the general expression of eq. (3.4b) we obtain:

$$\Gamma^{\mu\nu\rho}_{Z^*\gamma Z}(k_1,k_2) = \epsilon^{\mu\nu\rho\sigma}k_{1\sigma}\sum_{f=u,d,e,\nu}\left[m_Z^2(A_{3f}+A_{5f}) - \frac{m_f^2\beta_f^Z}{\pi^2}\,I_{2f} + \frac{1}{2\pi^2}\alpha_f^Z\alpha_f^\gamma\beta_f^Z\right]$$
$$\equiv \epsilon^{\mu\nu\rho\sigma}k_{1\sigma}\,\Gamma_{Z^*\gamma Z}(s)\,, \tag{3.41}$$

$$\Gamma^{\mu\nu\rho}_{\gamma^*\gamma Z}(k_1,k_2) = \epsilon^{\mu\nu\rho\sigma}k_{1\sigma}\sum_{f=u,d,e,\nu}\left[m_Z^2(A_{3f}+A_{5f}) - \frac{m_f^2\beta_f^Z}{\pi^2}\,I_{2f} + \frac{1}{2\pi^2}\alpha_f^\gamma\alpha_f^\gamma\beta_f^Z\right]$$
$$\equiv \epsilon^{\mu\nu\rho\sigma}k_{1\sigma}\,\Gamma_{\gamma^*\gamma Z}(s)\,. \tag{3.42}$$

One should notice that the square bracket of $\Gamma_{Z^*\gamma Z}$ is approximately equal to $\Gamma_{\gamma^* ZZ}$ since in this case $A_5 \simeq -A_4$ and $I_1 \simeq -I_2$.

It is amazing to see how greatly the $\gamma^*\gamma Z$-vertex is simplified. Placing back the last term of eq. (3.38) in order to restore gauge invariance, we find,

$$\Gamma^{\mu\nu\rho}_{\gamma^*\gamma Z}(s) = \sum_f s\, A_{3f} \times \left[\epsilon^{\mu\nu\rho\sigma} k_{1\sigma} - \frac{\epsilon^{\nu\rho\beta\sigma} q^\mu k_{2\beta} k_{1\sigma}}{s}\right] . \tag{3.43}$$

The s-factor outside the vertex is expected because it must cancel the pole behaviour of the second term in the square bracket. Once again, the "physical" choice of w, z in the anomalous terms played a crucial role in eq. (3.43) like in the case of $\gamma^* ZZ$ vertex. Regarding decoupling effects, eq. (3.43) is self explained: for every particle contribution, a synergy between anomaly and non-decoupling terms results in a well defined integral $s\, A_{3f}$ that vanishes asymptotically due to the anomaly-free condition. If however, the energy $\sqrt{s}$ is between two particle masses which combined render the model anomaly-free, then there should be non decoupling effects in this regime. On the other hand, adding to the SM, anomaly-free and heavy chiral fermions, there should be no-nondecoupling effect remaining in the low energy regime where $\sqrt{s} \lesssim 2m_t$.

One can go one step further also in the case of $Z^*\gamma Z$ in eq. (3.41). In fact, we can eliminate I_{2f} and the anomaly factors from eq. (3.41) leaving only the finite integrals A_3 and A_5, as:

$$\Gamma_{Z^*\gamma Z}(s) = \frac{1}{2}\sum_f \left[(s + m_Z^2)A_{3f} + m_Z^2 A_{5f}\right] . \tag{3.44}$$

After using few integral tricks, like for example the ones of eq. (H.44), it is easy to show that $\Gamma_{Z^*\gamma Z}(s)$ behaves like $(s - m_Z^2)A_{3f}$ near the Z-pole and $\Gamma_{V^*\gamma Z} \propto \sum_f (s - m_V^2)A_{3f}$. This is clearly verified when performing the full numerical evaluation of the integrals as in Figs. 3.3c, 3.3d.

One can easily see from further working out eqs. (3.41) and (3.42) that due to the fact that the SM is an anomaly free QFT, the whole contribution arises to a very good approximation from particles of the third generation. Numerically, in the conventions of ref. [118] [see also footnote 4], we find for LEP energies

$$h_3^Z(\sqrt{s} = 200\ \text{GeV}) = 2.1 \times 10^{-4} , \tag{3.45}$$
$$h_3^\gamma(\sqrt{s} = 200\ \text{GeV}) = 7.2 \times 10^{-4} , \tag{3.46}$$

up to tiny small imaginary parts. These results are in agreement with those presented in ref. [124]. As we have noticed above it is also confirmed numerically that $|f_5^\gamma| \simeq |h_3^\gamma|$. SM predictions of eqs. (3.47) and (3.48) are in the best case [for h_3^γ] two orders of magnitude below the published LEP bounds [132].

For comparison, at higher energies the SM predicts:

$$h_3^Z(\sqrt{s} = 500\ \text{GeV}) = (0.3 - 0.6\, i) \times 10^{-4} , \tag{3.47}$$
$$h_3^\gamma(\sqrt{s} = 500\ \text{GeV}) = (0.9 - 1.8\, i) \times 10^{-4} . \tag{3.48}$$

Full numerical results for $|\Gamma_{V^*\gamma Z}(s)|$ are represented by solid lines in Figs. 3.3c, 3.3d. We observe that in the neighborhood of the top threshold, $|\Gamma_{\gamma^*\gamma Z}(s)|$ is one order of magnitude bigger than $|\Gamma_{Z^*\gamma Z}(s)|$. They are both however far below the current Tevatron and LHC sensitivity [133,134]. Following the projecting sensitivity calculated in ref. [122], observation at the LHC (14 TeV) seems extremely difficult within SM, even for the $\gamma\gamma Z$ vertex.

$V^*\gamma\gamma$

We now turn our discussion to the last SM neutral triple gauge boson vertex, the $V^*\gamma\gamma$. Of course, thanks to Furry's theorem only the case $V = Z$ is valid (for $V = \gamma$ all three currents are vector-like, *i.e.*, $\beta_i = 0$). However, even in $Z^*\gamma\gamma$ there are no non-decoupling effects since there is no would be Goldstone boson associated with the unbroken $U(1)_{\rm em}$, *i.e.*, the final particles are massless. Nevertheless, one can write a simple $Z^*\gamma\gamma$ 1PI vertex. We obtain:

$$\Gamma^{\mu\nu\rho}_{Z^*\gamma\gamma}(k_1,k_2) \;=\; \epsilon^{\nu\rho\beta\delta} q^\mu k_{1\beta} k_{2\delta}\,[A_3] + \frac{\beta_f^Z(\alpha_f^\gamma)^2}{4\pi^2}\,\epsilon^{\mu\nu\rho\sigma}\left[(w-1)\,k_2 + (z+1)\,k_1\right]_\sigma \;. \quad (3.49)$$

Landau [135] and Yang [136] say that the on-shell amplitute, $\epsilon_\mu(q)\Gamma^{\mu\nu\rho}_{Z^*\gamma\gamma}(k_1,k_2)$ must vanish due to selection rules on space inversion and angular momentum conservation. This fixes the arbitrary parameters $w = -z = 1$ for every fermion contribution f. One obtains the same values for w and z from $U(1)_{em}$ gauge invariance, *i.e.*, satisfaction of Ward Identities. Although it is necessary to preserve gauge invariance, this remaining contribution is negligible for light s-channel incoming particles e.g., $e^+e^- \to \gamma\gamma$, but nevertheless it may be important for heavy external particles like for example dark matter particles or heavy neutrinos annihilating into photons (see related work in refs. [137, 138]).

Defining $\Gamma_{Z^*\gamma\gamma}(s) \equiv \sum_f m_Z^2\, A_{3f}(s)$ and summing over the SM particles, we find numerically,

$$\Gamma_{Z^*\gamma\gamma}(\sqrt{s} \;=\; 200\ \text{GeV}) = 2.9\times10^{-4}\;, \quad (3.50)$$

$$\Gamma_{Z^*\gamma\gamma}(\sqrt{s} \;=\; 500\ \text{GeV}) = (3.2 - 5.6\,i)\times10^{-5}\;. \quad (3.51)$$

For various values of s, the function $|\Gamma_{Z^*\gamma\gamma}(s)|$ is plotted in Fig. 3.3e. Notably, at very small s this quantity behaves like $1/s$ and in contrary to the previous Z^*VV vertices does not vanish at $s = m_Z^2$. For general values of s, and $k_1^2 = k_2^2 = 0$, $\Gamma_{Z^*\gamma\gamma}(s)$ is easily written as:

$$\Gamma_{Z^*\gamma\gamma}(s) = \sum_f \frac{\beta_f^Z(\alpha_f^\gamma)^2}{2\pi^2}\,\frac{m_Z^2}{s}\,\xi_f\,J(\xi_f)\;, \quad (3.52)$$

where $\xi_f \equiv 4m_f^2/m_Z^2$ and the function $J(\xi_f)$ is appended in eq. (J.2).

For energies (s) below the top quark threshold, $\Gamma_{Z^*\gamma\gamma}(s)$, approximately takes the form,

$$\Gamma_{Z^*\gamma\gamma}(s) \equiv \sum_f m_Z^2 A_{3f}(m_Z^2 < s < m_t^2) \approx$$

$$\approx -N_c \frac{\beta_t^Z {\alpha_t^\gamma}^2}{\pi^2} \left[\frac{m_Z^2}{2s} + \left(\frac{m_Z^2}{m_t^2}\right)\left(\frac{1}{24} + \frac{1}{180}\frac{s}{m_t^2}\right)\right], \tag{3.53}$$

a behaviour which shows decoupling of a heavy top-quark mass. This follows our general statement just below eq. (3.32): since the anomaly term in eq. (3.49) vanishes due to the physical choice of w and z there is no non-decoupled remnant to cancel it. In the asymptotic region we find:

$$\Gamma_{Z^*\gamma\gamma}(s \gg m_Z^2, m_t^2) \approx N_c \frac{\beta_t^Z {\alpha_t^\gamma}^2}{2\pi^2} \left(\frac{m_Z^2 m_t^2}{s^2}\right) \left[\ln^2 \frac{s}{m_t^2} - \pi^2 + 2i\pi \ln \frac{s}{m_t^2}\right]. \tag{3.54}$$

Therefore, $\Gamma_{Z^*\gamma\gamma}(s)$ behaves asymptotically as $1/s^2$ while all other neutral vertices behave like $1/s$. This fast drop with s is also verified by comparing the solid lines between Figs. 3.3a, b, c, d and Fig. 3.3e.

$V^*W^-W^+$

Just for completeness, we study the chiral CP-invariant part of the $(\gamma, Z)^*WW$ vertex. For on-shell W's and in momentum space this corresponds to operators of the form,

$$f_5^V \epsilon^{\mu\nu\rho\sigma} (k_1 - k_2)_\sigma \ . \tag{3.55}$$

There are of course CP-invariant, non-chiral operators generated from our fermion triangle graph that have the form [118, 119],

$$f_1^V (k_1 - k_2)^\mu g^{\nu\rho} - \frac{f_2^V}{m_W^2}(k_1 - k_2)^\mu q^\nu q^\rho + f_3^V (q^\nu g^{\mu\rho} - q^\rho g^{\mu\nu}) \ . \tag{3.56}$$

In the SM, note that both f_1 and f_3, exist at tree level. We are interested here only on chiral, one-loop (triangle) induced operators in eq. (3.55).

The numerical calculation of the $(\gamma^*, Z^*)W^-W^+$ effective vertices are somehow more complicated than the neutral ones. There are two masses and two different neutral vertices involved, making the triangle diagram looking differently than its crossed counterpart (see Fig. 3.4). We follow the same steps as we did for the neutral vertices and present our results (and technical details) in Appendix I. The chiral CP-invariant part of the effective vertex, $\Gamma^{\mu\nu\rho}$, is the same as in eq. (3.2). The finite form factors $A_{3..6}$ need to be slightly modified by the mass difference of the two fermions involved; analogously for $A_{1,2}$. Our main conclusion for a general vertex that contains external charged gauge bosons is given by eqs. (I.2) and (I.3).

The relevant couplings $\alpha_{ff'}^W$, and $\beta_{ff'}^W$ can be read from the charged current part of the SM Lagrangian,

$$\mathscr{L} \supset g_Z (W_\mu^+ J_W^{\mu +} + W_\mu^- J_W^{\mu -}) \ , \tag{3.57}$$

with the $J_W^{\pm}$-currents being

$$J_W^{\mu\,+} = (J_W^{\mu\,-})^\dagger = \frac{1}{2\sqrt{2}}\,\left[\overline{\nu}\gamma^\mu(1-\gamma_5)e + \overline{u}\gamma^\mu(1-\gamma_5)d\right]\,. \tag{3.58}$$

Hence $\alpha^W_{ff'} = -\beta^W_{ff'} = \frac{g_Z}{2\sqrt{2}}$ for the pairs $(ff') = (\nu, e), (u, d)$, respectively. For simplicity, we ignore quark and lepton mixing effects, but these can easily be included.

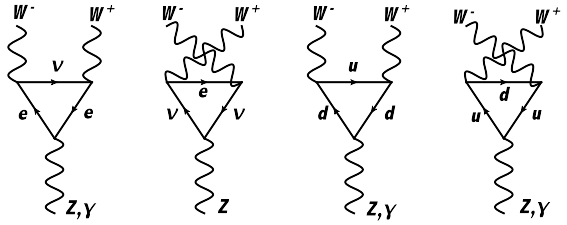

Figure 3.4: *Standard Model fermion contributions to $(Z, \gamma)WW$ one loop vertex.*

We therefore set $\alpha_{j,k} = -\beta_{j,k} = \frac{g_Z}{2\sqrt{2}}$ in eqs. (I.2) and (I.3). The neutral gauge boson-fermion couplings, α_f^V, β_f^V, are taken from eq. (3.26). Assuming CP-conservation, the 1PI effective action $\Gamma^{\mu\nu\rho}_{V^*WW}$ with $V = \gamma$, Z looks exactly the same as in eq. (3.27) with the only difference being the form factors $A_{1,3}$ must be replaced by those given in eq. (I.2) [and the paragraph below (I.2)]. Therefore we write[7] ,

$$\Gamma^{\mu\nu\rho}_{V^*W^-W^+}(k_1, k_2) \equiv \epsilon^{\mu\nu\rho\sigma}\,(k_1 - k_2)_\sigma\,\Gamma_{V^*W^-W^+}(s)\,, \tag{3.59}$$

where

$$\begin{aligned}\Gamma_{V^*W^-W^+}(s) \;=\; \sum_{\text{doublets}} \Big[m_W^2(A_3 - A_4) \;+\; \frac{g_Z^2\alpha^V_{f_d}}{16\pi^2}\,\mathcal{I}_1 \;+\; \frac{g_Z^2\beta^V_{f_d}}{16\pi^2}\,\mathcal{I}_2 + \\ +\; \frac{g_Z^2}{32\pi^2}\,(\alpha^V_{f_d} - \beta^V_{f_d})\,(w-1) + (f_u \leftrightarrow f_d)\Big]\,.\end{aligned} \tag{3.60}$$

In this formula we abbreviate $A_{3,4} \equiv A_{3,4}(m^2_{f_u}, m^2_{f_d})$ and $\mathcal{I}_{1,2} \equiv \mathcal{I}_{1,2}(m^2_{f_u}, m^2_{f_d})$, with

$$\mathcal{I}_1 = \int_0^1 dx \int_0^{1-x} dy\, \frac{-(x+y)\Delta m^2 + m^2_{f_u}}{x(x-1)m_W^2 + y(y-1)m_W^2 - xy(s-2m_W^2) - (x+y)\Delta m^2 + m^2_{f_u}}\,, \tag{3.61a}$$

$$\mathcal{I}_2 = \int_0^1 dx \int_0^{1-x} dy\, \frac{2x\,m^2_{f_d} + (x+y)\Delta m^2 - m^2_{f_u}}{x(x-1)m_W^2 + y(y-1)m_W^2 - xy(s-2m_W^2) - (x+y)\Delta m^2 + m^2_{f_u}}\,, \tag{3.61b}$$

[7] Our notation for $\Gamma_{V^*W^-W^+}(s)$ is related to the standard form factor of ref. [118], as $\Gamma_{V^*W^-W^+}(s) = -g_{VWW} f_5^V(s)$.

where $\Delta m^2 \equiv m^2_{f_u} - m^2_{f_d}$. In the limit of heavy masses, $m^2 = m^2_{f_u} = m^2_{f_d} \gg s, m^2_W$, we obtain:

$$\lim_{m^2\to\infty} \mathcal{I}_1 = \frac{1}{2}\,, \quad \lim_{m^2\to\infty} \mathcal{I}_2 = -\frac{1}{6}\,. \tag{3.62}$$

Let us examine the $\gamma^* W^- W^+$ case first. We must set $\beta^\gamma_{f_{u,d}} = 0$. In this case gauge invariance [see eq. (I.4)] implies $w = z$ and CP-invariance $w = -z$, and therefore $w = z = 0$. Having fixed the anomaly term, the result for this vertex turns out to be simply,

$$\Gamma_{\gamma^* W^- W^+}(s) = \frac{1}{2}\, s \sum_{\text{doublets}} \Big[A_3(m^2_{f_u}, m^2_{f_d}) + (f_u \leftrightarrow f_d) \Big]\,, \tag{3.63}$$

where A_3 is a form factor defined in Appendix I. Here $\Gamma_{\gamma^* W^- W^+}(s = 0) = 0$ as it should be [118, 119], *i.e.*, there is no pole at $q^2 = 0$. This is a special case where the anomaly term conspires with $\mathcal{I}_1$-term such that the final result contains no non-decoupling terms. In order for gauge invariance to be non-anomalous, the last terms in the WIs system (I.4), must vanish. This implies a relation among fermion charges,

$$\sum_{f=e,\nu,d,u} \alpha^\gamma_f = Q_e + Q_\nu + 3\,Q_d + 3\,Q_u = 0\,, \tag{3.64}$$

which is exactly the charge conservation condition. Then, in the asymptotic limit, $s \gg m^2_W, m^2_{f_{u,d}}$, the amplitude for $\Gamma_{\gamma^* W^- W^+}(s \to \infty)$ vanishes, thanks to eq. (3.64). This is obvious from the numerical outcome in Fig. 3.5. It also shows an enhanced threshold behaviour around $\sqrt{s} \approx 2\, m_t$ (solid line).

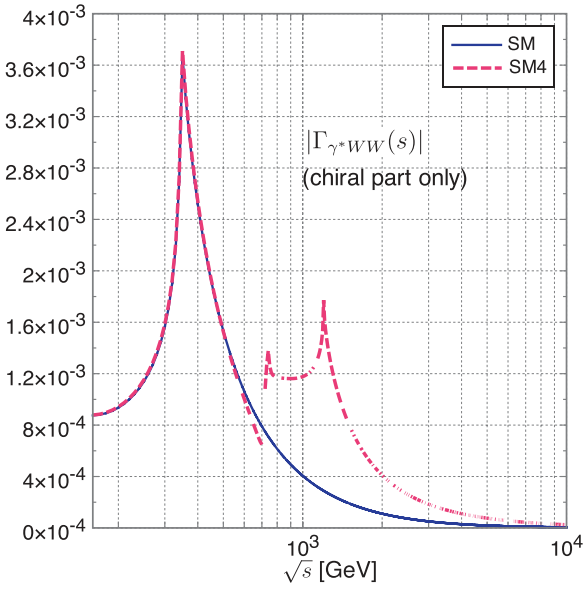

Figure 3.5: *The effective vertex* $|\Gamma_{\gamma^* WW}(s)|$ *in the minimal SM (solid line) and in SM with an extra fourth (SM4) generation (dashed line).*

Quantitatively, this can be seen from eq. (3.63) by expanding A_3 around the threshold. Compared to $\Gamma_{\gamma^* ZZ}(s)$, there is an additional contribution due to the large mass difference $\Delta m^2 = m_t^2 - m_b^2 \approx m_t^2$, in the numerical factor that multiplies s/m_t^2. Our evaluation of integrals contains one numerical integration and follows the procedure of Appendix B in ref. [89]. Our analytic formulae in Appendix J, at the limit of $m_W = 0$, are in full agreement with these results. Few representative values are,

$$\begin{aligned} \Gamma_{\gamma^* WW}(\sqrt{s} = 200 \text{ GeV}) &= (6.8 - 6.4\, i) \times 10^{-4} \,, \\ \Gamma_{\gamma^* WW}(\sqrt{s} = 500 \text{ GeV}) &= (-1.5 + 15\, i) \times 10^{-4} \,. \end{aligned}$$

Comparing with $\gamma^* ZZ$ vertex we see here that the mass splitting generates a sizeable absorptive part that dominates the vertex after $\sqrt{s} \gtrsim 2\, m_W$.

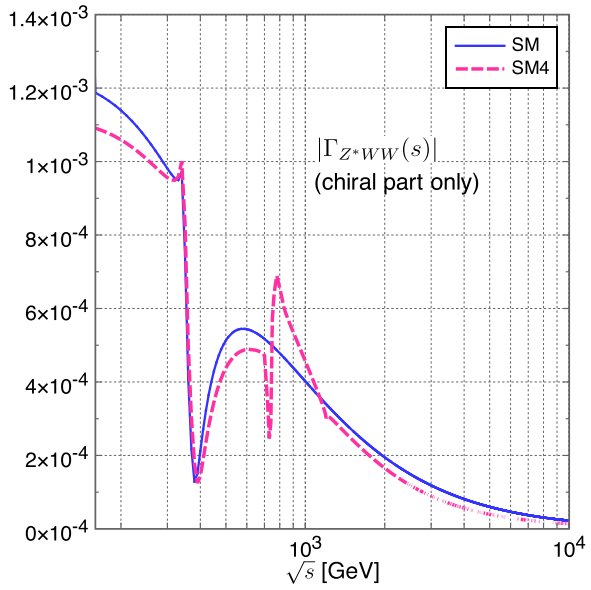

Figure 3.6: *The effective vertex* $|\Gamma_{Z^*WW}(s)|$ *in the minimal SM (solid line) and in SM with an extra fourth (SM4) generation (dashed line).*

We now turn to the $Z^* W^- W^+$ vertex. This time we have only CP-symmetry at our disposal which sets only the constraint $w = -z$. At the broken limit there is no other symmetry remaining in order to fix the parameter w alone. However, in the exact $SU(2)$ limit where $[g', s_w \to 0,\ \alpha_f = -\beta_f]$ this vertex should be exactly the same as the $Z^* ZZ$. Therefore, the arbitrary parameters are fixed by Bose symmetry to be $w = -z = 1/3$. For this choice of w and at the heavy mass limit, $m^2 = m_{f_u}^2 = m_{f_d}^2 \gg s,\, m_W^2$, the vertex is proportional to $\alpha_f + \beta_f \propto s_w^2$ for every fermion contribution, a combination which is proportional to $SU(2)$ breaking effects. Another, equally good, choice would be $w = 0$, for example. The physical requirement here is the decoupling of a particle from the Γ_{Z^*WW} vertex.

In conclusion, the $Z^* WW$ vertex is *undetermined*: there is only CP-symmetry, that is not enough to fix two arbitrary parameters. However, for the anomaly-free SM this

arbitrariness is irrelevant since it is cancelled when the whole fermion contribution is taken into account. We shall meet this situation again in the $Z'VV$-vertex below.

Our numerical evaluation of the SM $|\Gamma_{Z^*WW}(s)|$ is shown in Fig. 3.6. This time, the top quark threshold destructively adds to the vertex. As in previous cases, we present few representative values,

$$\begin{aligned}\Gamma_{Z^*WW}(\sqrt{s}=200\ \text{GeV}) &= -(8.5+7.6\,i)\times 10^{-4}\ ,\\ \Gamma_{Z^*WW}(\sqrt{s}=500\ \text{GeV}) &= -(3.8+3.5\,i)\times 10^{-4}\ ,\end{aligned}$$

that show similar order of magnitude values for the real part as in the Z^*ZZ vertex but an enhanced absorptive part. The latter is due to custodial symmetry breaking effects *i.e.*, the large mass difference between the top and the bottom quarks. Although there is an intense experimental ongoing analysis at LEP [139], Tevatron [140] and LHC [141,142] for the first three CP-invariant non-chiral operators, $f^V_{i=1..3}$ of eq. (3.56), we are not aware of a similar experimental search on the chiral f^V_5 of eq. (3.55).

3.4.2 Models with a sequential fourth fermion generation

In our first departure from the SM we assume a fourth generation matter of quarks and leptons. Apart from the fact that the 4th generation neutrino has to weight more than 45 GeV, a certain tuning to avoid EW constraints is needed. More specifically, one extra doublet of degenerate leptons contributes a piece of approximately $1/6\pi \approx 0.05$ into the S-parameter [143] while the current fit [144] to the EW data gives,

$$S \;=\; 0.04 \pm 0.10\ . \tag{3.65}$$

Therefore, a 4th, mass degenerate, fermion generation will contribute a $4/6\pi \approx 0.2$ piece to S-parameter which is incompatible with the fit. A certain mass difference or else a certain weak isospin violation is needed which is parameterized by the T parameter [143]. A consistent parameter space with EW precision data and published direct searches is

$$\begin{aligned} m_{\nu 4} &= 400\ \text{GeV}\ , \quad \mathrm{m_{e4}} = 660\ \text{GeV}\ ,\\ m_{t4} &= 358\ \text{GeV}\ , \quad \mathrm{m_{b4}} = 372\ \text{GeV}\ . \end{aligned} \tag{3.66}$$

This mass spectrum corresponds to Tevatron experiments allowed region where the analyses from CDF [145] have excluded t_4 and b_4 quarks to have masses smaller than the values quoted above[8]. The leptons mass spectrum is chosen such that it does

[8]Currently, the sequential 4th generation is under siege from LHC [146]. If there exist new heavy SM type quarks, they will contribute a factor of up to $N_c^2 = 9$ into the Higgs production cross section for the (triangle) process $gg \to H$. The current cross section sensitivity at LHC is within a few of the SM prediction and therefore it sets an indirect bound over the whole exclusion Higgs area, up to 550-600 GeV. Other direct bounds from LHC on 4th generation top and bottom quarks involve assumptions about their mass difference to be smaller than the W-boson mass. These caveats are discussed in some detail with complete references in ref. [147]. However, even more stringent constraints have been obtained from direct searches at the LHC. Searching for short-lived b-quarks, CMS ruled out $m_{b4} < 611$ GeV at 95% CL (ref. [148]). Also, the inclusive search in ref. [149] set a strong limit on a degenerate fourth generation, $m_{t4} > 495$ GeV at 95% CL, assuming a minimal off-diagonal mixing between the third and the fourth generation.

not contribute significantly to the oblique parameters, e.g., for these values of lepton masses one has $\Delta S_l \simeq 0$ [144].

Due to the fact that the charges are the same as in the SM, the anomalies are canceled in each generation. It is important to notice here that if all the extra fermions were very heavy and had the same mass, no effect would be left back and the decoupling would work perfectly. The reason is, first of all, that the sum over all extra fermions of expressions that contain the finite integrals A_3, A_4 or A_5 vanishes because the integrand factors out a term $\sum_i c_i$, where c_i is the pre-anomaly factor of each fermion. But, this sum is equal to zero for an anomaly free generation. On the other hand, terms proportional to I_1 or I_2 in eq. (3.4), in the limit of large fermion mass, are canceled exactly with the anomaly term for special values of w and z parameters that are fixed by the Bose symmetry in each case. But this constraint is not necessary, e.g., if an anomaly free generation of very heavy mass degenerate chiral fermions is added to the SM, it has no effects at low energies, no matter what the values of w and z are. This is guaranteed by the fact that the extra generation is anomaly free.

The numerical analysis for the three gauge bosons vertices is the same as previously. Using the approximate integral expressions from Appendix J, we draw plots for the amplitudes $|\Gamma_{V^*VV}(s)|$ and $|\Gamma_{V^*WW}(s)|$ versus $\sqrt{s}$ in different combinations of the external gauge bosons $V = \gamma$, Z. These plots are collected in Fig. 3.3, and Figs. 3.5, 3.6, respectively [dashed line].

The extra generation has a significant contribution in the region near twice the threshold of each extra fermion where the amplitude rises until those values (shown as peaks in every combination of external gauge bosons) and drops fast as $1/s$ (apart from $V^*\gamma\gamma$ which drops as $1/s^2$). We see that for small values of energy the two curves (the curve that corresponds to the SM case and the curve that corresponds both to the SM and the 4th generation) have the same form. In this energetic region ($\sqrt{s} \lesssim 600\,\mathrm{GeV}$) the dominant feature is the first peak that corresponds to the threshold energy for the creation of the top quark ($\sqrt{s} \approx 350\,\mathrm{GeV} \approx 2\,m_t$). In addition, the contribution from the extra fermionic generation is negligible, because all the extra fermions are heavy compared to the energy, ($2\,m_f > \sqrt{s}$), where f runs over the extra fermions. These extra fermions have more or less similar masses. As before with the top-quark mass, there is a cancellation between the anomaly contributions and the $I_{1,2}$ parts of the amplitude for each fermion separately. As a result, the total contribution from the fourth generation is negligible as we can see from Fig. 3.3. The situation is different when $\sqrt{s}$ runs over the mass spectrum of the extra fermionic generation. Firstly for ($\sqrt{s} \gtrsim 600\,\mathrm{GeV}$) we see different peaks that correspond to the threshold energy for the creation of the extra fermions ($\sqrt{s} \approx 2\,m_i$). When ($2\,m_i < \sqrt{s} < 2\,m_j$), there is a non-zero contribution to the total amplitude. In this case, fermions whose masses are very heavy compared to $\sqrt{s}$, exhibit the same behaviour as previously *i.e.*, the anomaly term cancels out against the finite contribution.

3.4.3 Minimal Z' models

Grand Unified Theories (GUTs) with rank larger than four, could break to the SM gauge group times additional $U(1)'$s : $SU(3)\times SU(2)\times U(1)\times U(1)'^n$. This symmetry is broken down to $U(1)_{em}$ and therefore there is a possibility of additional forces mediated by the Z' gauge bosons associated with the broken $U(1)'$ symmetries (for a review see ref. [150]).

We shall concentrate here on minimal models with one additional neutral gauge boson, the Z'. Minimal here means models that contain no-additional *i.e.*, no exotic, matter particles apart from the SM ones and right handed neutrinos. The latter play a crucial role in cancelling anomalies due to the additional $U(1)'$ and in producing viably small neutrino masses. These models were devised first in ref. [151] and later elaborated in refs. [152, 153]. Following the notation of ref. [152] we can describe these models with three additional parameters: the mass of the new gauge boson, $M_{Z'}$, and the couplings g_Y and g_{BL}. The latter enter into the current which couples to the unmixed Z'_0 gauge boson as:

$$E_k - \lambda_p(n) J^{\mu}_{Z'_0} = \sum_{f=f_L,f_R} \left[g_Y Y_f + g_{BL} \left(B-L\right)_f \right] \overline{f} \gamma^{\mu} f \ . \tag{3.67}$$

From this, it is easy to construct $\mathscr{L}_{int}$ in eq. (3.24) with

$$\alpha_f^Z = \cos\theta' \, \alpha_f^{Z_0} - \sin\theta' \, \alpha_f^{Z'_0} \ , \tag{3.68a}$$

$$\alpha_f^{Z'} = \sin\theta' \, \alpha_f^{Z_0} + \cos\theta' \, \alpha_f^{Z'_0} \ , \tag{3.68b}$$

$$\beta_f^Z = \cos\theta' \, \beta_f^{Z_0} - \sin\theta' \, \beta_f^{Z'_0} \ , \tag{3.68c}$$

$$\beta_f^{Z'} = \sin\theta' \, \beta_f^{Z_0} + \cos\theta' \, \beta_f^{Z'_0} \ , \tag{3.68d}$$

where θ' is the mixing angle between Z and Z' gauge bosons given by,

$$\tan\theta' \ = \ -\frac{g_Y}{g_Z} \, \frac{M^2_{Z_0}}{M^2_{Z'} - M^2_{Z_0}} \ , \tag{3.69}$$

with $M^2_{Z_0} = g_Z^2 v^2/4$ the 'SM' Z-boson mass. Also in eq. (3.68) we obtain for $\alpha_f^{Z'_0}, \beta_f^{Z'_0}$,

$$\begin{aligned}
\alpha_u^{Z'_0} &= \frac{1}{2}\left(\frac{5}{6} g_Y + \frac{2}{3} g_{BL}\right) \quad , \quad \beta_u^{Z'_0} = \frac{g_Y}{4} \ , \\
\alpha_d^{Z'_0} &= \frac{1}{2}\left(-\frac{1}{6} g_Y + \frac{2}{3} g_{BL}\right) \ , \quad \beta_d^{Z'_0} = -\frac{g_Y}{4} \ , \\
\alpha_e^{Z'_0} &= \frac{1}{2}\left(-\frac{3}{2} g_Y - 2 g_{BL}\right) \ , \quad \beta_e^{Z'_0} = -\frac{g_Y}{4} \ , \\
\alpha_\nu^{Z'_0} &= \frac{1}{2}\left(-\frac{1}{2} g_Y - 2 g_{BL}\right) \ , \quad \beta_\nu^{Z'_0} = \frac{g_Y}{4} \ ,
\end{aligned} \tag{3.70}$$

while the corresponding expressions for $\alpha_f^{Z_0}, \beta_f^{Z_0}$ are given by eq. (3.26). This parameterisation through g_Y and g_{BL} helps us to very easily incorporate several models

that have been studied in the literature: Z_{B-L} when the $U(1)_{B-L}$ charges of the SM fermions are proportional to $(B-L)$ quantum numbers, Z_χ a GUT inspired $SO(10) \to SU(5) \times U(1)_\chi$ model and finally, Z_{3R} where the corresponding $U(1)_{3R}$ charges are proportional to T_{3R} generator of the global $SU(2)_R$ symmetry. We summarise the couplings of these models in the following table:

	Z_{B-L}	Z_χ	Z_{3R}
g_Y	0	$-\frac{2}{\sqrt{10}} g_{Z'}$	$-g_{Z'}$
g_{BL}	$\sqrt{\frac{3}{8}} g_{Z'}$	$\frac{5}{2\sqrt{10}} g_{Z'}$	$\frac{1}{2} g_{Z'}$

Here, we wish to calculate the effective vertices $\Gamma_{Z'^*\gamma Z}$ and $\Gamma_{Z'^* ZZ}$ for those models. Recalling eqs. (3.38) and (3.27) with $i = Z'$, $j = \gamma$ or Z and $k = Z$ respectively, we obtain:

$$\begin{aligned}
\Gamma^{\mu\nu\rho}_{Z'^*\gamma Z}(s) &\approx \epsilon^{\mu\nu\rho\sigma} k_{1\sigma} \sum_{f=u,d,e,\nu} [m_Z^2 (A_{3f} + A_{5f}) - \frac{m_f^2 \beta_f^Z}{\pi^2} I_{2f} + \\
&+ \frac{(z+1)}{4\pi^2} (\alpha_f^{Z'} \beta_f^Z + \alpha_f^Z \beta_f^{Z'}) \alpha_f^\gamma] \\
&\equiv \epsilon^{\mu\nu\rho\sigma} k_{1\sigma} \Gamma_{Z'^*\gamma Z}(s) \,, \qquad (3.71)
\end{aligned}$$

$$\begin{aligned}
\Gamma^{\mu\nu\rho}_{Z'^* ZZ}(s) &= \epsilon^{\mu\nu\rho\sigma} (k_1 - k_2)_\sigma \sum_{f=u,d,e,\nu} \Big[m_Z^2 (A_{3f} - A_{4f}) + \frac{m_f^2 \beta_f^Z}{\pi^2} I_{1f} - \\
&\quad - \frac{(w-1)}{4\pi^2} [(\alpha_f^Z)^2 \beta_f^{Z'} + (\beta_f^Z)^2 \beta_f^{Z'} + 2\, \alpha_f^{Z'} \alpha_f^Z \beta_f^Z] \Big] \equiv \\
&\equiv \epsilon^{\mu\nu\rho\sigma} (k_1 - k_2)_\sigma \Gamma_{Z'^* ZZ}(s) \,, \qquad (3.72)
\end{aligned}$$

with α_f, and β_f given in eqs. (3.68) and (3.70). Again the last terms on the r.h.s of eqs. (3.71) and (3.72) arrive from the chiral anomaly of individual fermion contributions. These anomaly terms cancel out when we sum over all SM fermions (here we also need the right handed neutrino). This also removes the arbitrariness due to the unknown parameters w, z. Contrary to the SM vertices, we cannot use here any physical argument in order to remove completely both w and z parameters. We only have $U(1)_{em}$ gauge invariance for $Z'^*\gamma Z$ and Bose symmetry for $Z'^* ZZ$ while in the SM we have two neutral gauge bosons and two symmetries.

But let us for the moment keep the anomalous terms. Obviously they are multiplied by the arbitrary parameters $(z+1)$ (for $Z'^*\gamma Z$) and $(w-1)$ (for $Z'^* ZZ$). Focusing on the Z'_{B-L} model, where the mixing angle θ' vanishes, we observe that for any single heavy fermion contribution the 2nd and the 3rd term on the r.h.s of eqs. (3.71) and (3.72) mutually cancel and what remains back is the effective theory with the low mass fermion contributions but *together with* their anomalous terms included. The latter do not depend on particle masses. The choices for the arbitrary parameters are $w = z = 1$ for $Z'\gamma Z$ and $w = z = 0$ for $Z'ZZ$.

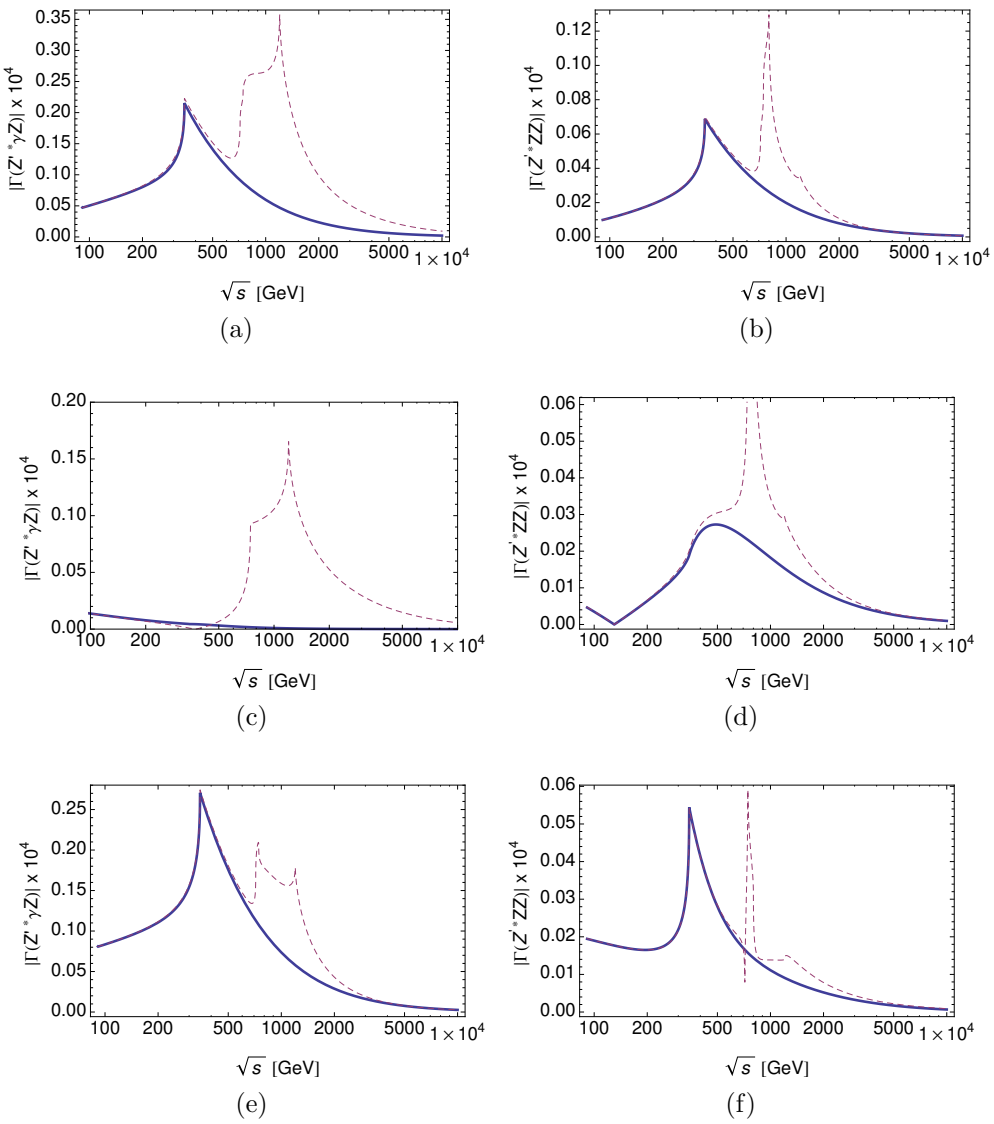

Figure 3.7: *a, b)* $|\,\Gamma_{Z'VV}(s)\,|$ *versus* $\sqrt{s}$ *for different gauge bosons combinations as they are given by eqs. (3.71) and (3.72). The solid curve corresponds to the SM spectrum with an extra* $U(1)_{B-L}$*, while the dashed curve corresponds to the same but with a 4th sequential fermion generation added as in Fig. 3.3. We take* $M_{Z'} = 1$ TeV *and* $g_{Z'} = \alpha_{\rm em}$*. c, d) The same as (a, b) but with* $U(1)_\chi$*. e, f) The same as (a, b) but with* $U(1)_{3R}$*.*

The last condition can be interpreted as follows: for the amplitude $ZZ \to ZZ$ to hold for asymptotic values of energies, eq. (3.10) requires $w = z$ but Bose symmetry requires $w = -z$. This conclusion does not stand firm in the case of mixing between Z and Z' *i.e.*, in models Z_χ, Z_{3R} of the table above, and the contribution of a heavy mass particle is undetermined. Of course anomalies do cancel when *all* model fermions are added. In Fig. 3.7 we display numerical results for the absolute value of the scalar part of the 1PI effective vertices $Z'^*\gamma Z$ and Z'^*ZZ in eqs. (3.71) and (3.72) for $M_{Z'} = 1$ TeV

and $g_{Z'} = \alpha_{em}$. Figs. (3.7a, b) refer to Z_{B-L} model, Figs. (3.7c, d) to Z_χ models and, finally, Figs. (3.7e, f) to Z_{3R} models. For the values of $M_{Z'}$ and $g_{Z'}$ chosen, fits to electroweak observables and direct searches are satisfied. We also present results when adding a sequential 4th generation of fermions with the same masses (and the reasoning) as we did for the SM case of section 3.4.1. We observe that there is an enhancement of the vertices by a factor of 2 for Z_{B-L}, and a factor of 10-15 for Z_χ. Numerically, we can define analogous quantities $h_3^{Z'}$ and $f_5^{Z'}$ by simply replacing Z with Z' in the correspondind definitions. As an example, for the $B-L$ model we obtain,

$$\begin{aligned}
&h_3^{Z'}(\sqrt{s} = 200 \text{ GeV}) = -2.7 \times 10^{-5} \,, \\
&h_3^{Z'}(\sqrt{s} = 500 \text{ GeV}) = (-2.7 + 5.3i) \times 10^{-4} \,, \\
&f_5^{Z'}(\sqrt{s} = 200 \text{ GeV}) = -7.2 \times 10^{-6} \,, \\
&f_5^{Z'}(\sqrt{s} = 500 \text{ GeV}) = (-7.7 + 18i) \times 10^{-5} \,.
\end{aligned} \tag{3.73}$$

Numerical results for the vertices presented above and in Fig. 3.7 are based on various analytical approximations for form factors described in Appendix J.

Now that Z' can be heavy, it is interesting to study its decay width into $Z\gamma$ and ZZ modes. Based on eq. (3.1) and on eqs. (3.71) and (3.72) the decay widths of the Z' can be read from

$$\begin{aligned}
\Gamma(Z' \to \gamma Z) = \frac{1}{48\pi} \Big| \sum_{f=u,d,e,\nu} & [m_Z^2 (A_{3f} + A_{5f}) - \frac{m_f^2 \beta_f^Z}{\pi^2} I_{2f} + \\
& + \frac{(z+1)}{4\pi^2} (\alpha_f^{Z'} \beta_f^Z + \alpha_f^Z \beta_f^{Z'}) \alpha_f^\gamma] \Big|^2 \times \\
& \times \frac{m_{Z'}^3}{m_Z^2} (1 - \frac{m_Z^2}{m_{Z'}^2})^3 (1 + \frac{m_Z^2}{m_{Z'}^2}) \,,
\end{aligned} \tag{3.74}$$

$$\begin{aligned}
\Gamma(Z' \to ZZ) = \frac{1}{96\pi} \Big| \sum_{f=u,d,e,\nu} & \big[m_Z^2 (A_{3f} - A_{4f}) + \frac{m_f^2 \beta_f^Z}{\pi^2} I_{1f} - \\
& - \frac{(w-1)}{4\pi^2} [(\alpha_f^Z)^2 \beta_f^{Z'} + (\beta_f^Z)^2 \beta_f^{Z'} + 2\, \alpha_f^{Z'} \alpha_f^Z \beta_f^Z] \big] \Big|^2 \times \\
& \times \frac{m_{Z'}^3}{m_Z^2} (1 - \frac{4\, m_Z^2}{m_{Z'}^2})^{5/2} \,,
\end{aligned} \tag{3.75}$$

$$\Gamma(Z' \to W^+ W^-) = \frac{\alpha_{em}\, m_{Z'}\, \sin^2\theta'}{48 \tan^2\theta_w} \left(1 - 4\, \frac{m_W^2}{m_{Z'}^2}\right)^{3/2} \left[1 + 20\, \frac{m_W^2}{m_{Z'}^2} + 12 \frac{m_W^4}{m_{Z'}^4}\right] \left(\frac{m_W^2}{m_{Z'}^2}\right)^{-2} , \tag{3.76}$$

$$\Gamma(Z' \to \overline{f} f) = \frac{N_c\, m_{Z'}}{12\, \pi} \left[(\alpha_f^{Z'\,2} + \beta_f^{Z'\,2}) - \frac{3 m_f^2}{m_{Z'}^2} (\alpha_f^{Z'\,2} - \beta_f^{Z'\,2}) \right] \sqrt{1 - \frac{4 m_f^2}{m_{Z'}^2}} \,, \tag{3.77}$$

where N_c is the color factor (3 for quarks and 1 for leptons) and the tree level decay width for $Z' \to WW$ has been taken from ref. [154] and is dominant over the loop-induced ones. For $g_{Z'} = \alpha_{em}$, $M_{Z'} = 1$ TeV and SM spectrum with three generations

we obtain for the $B-L,\ (\chi),\ [3R]$ models:

$$\begin{aligned}
\mathrm{Br}(Z' \to \nu\nu) &= 37.7\ (42.3)\ [12.5]\ \%\ , \\
\mathrm{Br}(Z' \to \ell\ell) &= 37.7\ (12.5)\ [12.6]\ \%\ , \\
\mathrm{Br}(Z' \to qq) &= 24.5\ (45.1)\ [74.8]\ \%\ , \\
\mathrm{Br}(Z' \to WW) &= 0.03\ (3.2)\ [8.1] \times 10^{-5}\ , \\
\mathrm{Br}(Z' \to Z\gamma) &= 5.8\ (\sim 10^{-3})\ [8.7] \times 10^{-6}\ , \\
\mathrm{Br}(Z' \to ZZ) &= 3.0\ (2.5)\ [0.9] \times 10^{-7}\ .
\end{aligned} \tag{3.78}$$

These results are pretty much the same for bigger $M_{Z'}$ values. As we can see, the branching fraction for $Z' \to \gamma Z$ is in the region of $10^{-5} - 10^{-6}$, while for $Z' \to ZZ$ in the region $\sim 10^{-7}$. These are very challenging numbers even for LHC@14 TeV.

In coordinate space representation, the vertices in eqs.(3.71) and (3.72) arise on-shell from the following operators:

$$\mathcal{O}_{Z'\gamma Z} \sim \varepsilon^{\mu\nu\rho\sigma} Z'_\mu Z_\nu\, F_{\rho\sigma}\ , \tag{3.79}$$

$$\mathcal{O}_{Z'ZZ} \sim \varepsilon^{\mu\nu\rho\sigma} Z'_\mu Z_\nu\, \partial_\rho Z_\sigma\ , \tag{3.80}$$

which are both P-odd but CP-invariant. Although not present in the SM and in the Z'-model under consideration, there may be P-even but CP-violating operators of the form $\mathcal{O}_{Z'ZZ} \sim Z'^{\mu}(\partial^\nu Z_\mu)Z_\nu$ induced by a triple scalar loop instead. The latter would interfere with eq. (3.80) and there is a proposal in ref. [155] on how their effects can be separated at the LHC. However, within minimal Z'-models considered here, this looks very difficult due to tiny $\mathrm{Br}(Z' \to VV)$ of eq. (3.78).

3.5 Conclusions

We construct an effective 1PI vertex for triple gauge bosons for every renormalized theory making explicit mentioning to the chiral anomalies and their synergy with heavy fermion decoupling phenomena. Our method for calculating the vertex is based on ref. [120]. It is quite general and can be divided in four steps:

1. Write down the most general, Lorentz (and/or possibly other symmetry) invariant effective vertex $\Gamma^{\mu\nu\rho}$ [like eq. (3.2)] with unknown form factors.

2. Isolate the -potentially- infinite form factors and calculate only the finite parts.

3. Derive Ward Identities arising from the underlying spontaneously broken gauge symmetries at the quantum level. Apply them to $\Gamma^{\mu\nu\rho}$ and calculate the ambiguous form factors, thus forcing them to be finite.

4. If the vertex is still undetermined *i.e.*, if arbitrary parameters still remain, try to fix them by physical requirements. If nevertheless arbitrariness persists, then the model needs completion, perhaps with new particles or new dynamics.

This method, explained in detail in Appendix H and in section 3.2, does not require dimensional regularisation or other integral regularisation techniques. It may require, however, "shifting momenta" techniques like eq. (H.11). The above steps can be enriched with additional relations. Instead of WIs, one could use other identities like for example those arising from perturbative unitarity sum rules or the Goldstone Boson Equivalence Theorem e.g., eq. (3.11).

All the above steps are realized when calculating triple gauge boson vertices in spontaneously broken gauge theories, like for example the SM or its extensions like minimal Z'-models. The anomaly terms are arbitrary and can only be fixed by physics. Only then can we discuss non-decoupling effects in the broken limit. We observe that for V^*VV, $V = \gamma$, Z and for γ^*WW vertices, there are two arbitrary parameters that are completely determined by two physical symmetries: $U(1)_{em}$ and Bose symmetry or CP-invariance. We find that at the limit of heavy fermion masses, non-decoupled terms cancel exactly those that arise from anomalies. For example, in the SM, decoupling of the top quark will leave behind anomalous-terms of light quarks and leptons plus finite parts. On the other hand vertices like Z^*WW, Z'^*VV are in general undetermined because there are no enough symmetries to fix the arbitrary parameters. Of course, for anomaly free models, this arbitrariness is removed when adding up all fermion contributions.

We performed a numerical analysis for SM and minimal Z' model vertices. To this end we made an effort to calculate finite integrals in terms of standard functions that are easy to handle. For example in Appendix J, we solved analytically the integrals for $V^*\gamma V$-vertices. We then proceeded to SM predictions for the triple gauge boson vertices. Unfortunately, it turns out that within the SM these are rather small to be discovered even at the LHC with $\sqrt{s} = 14$ TeV. Similar results are obtained in the SM extended by a sequential fourth fermion generation. The difference w.r.t the SM, is that $|\Gamma_{V^*VV}(s)|$ is "delayed" to vanish for large $\sqrt{s}$ due to the heavy, 4th generation thresholds (see Figs. 3.3). In the best case, the SM + 4th generation predicts a maximum of a few$\times 10^{-3}$ for $|\Gamma_{\gamma^*\gamma Z}|$ [see dashed lines in Figs. 3.3].

We have performed a numerical analysis, shown in Fig. 3.7, for minimal Z'-models with $U(1)_{B-L}$ symmetry, SO(10)-like and $U(1)_{3R}$ also extended with a 4th fermion generation. For a conservative choice of $M_{Z'} = 1$ TeV and $g_Z = \alpha_{em}$, we find $|\Gamma_{Z'ZZ}|$ and $|\Gamma_{Z'\gamma Z}|$ in the regime below a few$\times 10^{-5}$. We also briefly discussed Z'-decays to $Z\gamma$ and ZZ. Adopting the parameter space above, their branching ratio come out to be in the neighborhood of $\sim 10^{-5}$ and $\sim 10^{-7}$, respectively.

In section 3.3.2 and Appendix K, we calculated non-decoupling effects that arise instantaneously with vanishing anomalies. We constructed several toy models with two or three external gauge bosons and a number of fermions where this situation could take place. In principle, these models can be used as a basis towards realistic extensions of the SM.

Our main result, the effective triple gauge boson vertex obtained in section 3.2 can be used in various ways: *i)* in models with anomalous spectrum, *ii)* in realistic anomaly driven models of section 3.3.2, *iii)* in MSSM and its extensions, *iv)* in dark matter or neutrino - nucleon scattering processes with a photon in the final state.

Chapter 4

Anatomy of the $H \to \gamma\,\gamma$ in the unitary gauge

In this Chapter, we review and clarify computational issues about the W-gauge boson one-loop contribution to the $H \to \gamma\gamma$ decay amplitude, in the unitary gauge and in the Standard Model. As in the previous Chapter, we introduce arbitrary four-vectors in order to shift the integral momentum variable. We find that highly divergent integrals depend upon the choice of these arbitrary vectors. One particular combination of these arbitrary vectors reduces the superficial divergency down to a logarithmic one. The remaining ambiguity is then fixed by exploiting gauge invariance and the Goldstone Boson Equivalence Theorem (GBET). Again, as we operated in the previous Chapter, the method is strictly realised in four-dimensions. The result for the amplitude agrees with the "famous" one obtained using dimensional regularization (DR) in the limit $d \to 4$, where d is the number of spatial dimensions in Euclidean space. At the exact equality $d = 4$, a three-sphere surface term appears that renders the Ward Identities and the equivalence theorem inconsistent. We also examined an alternative four-dimensional regularization scheme and found agreement with the DR outcome.

After presenting the problem about the ambiguities that appear in the calculation of $H \to \gamma\,\gamma$ amplitude in the unitary gauge and introducing the basic steps of our method, we present the calculation of the W-loop contribution[1] to $H \to \gamma\gamma$ amplitude, its ambiguities and the resolution within physics arising from GBET. We also examine details of the amplitude calculation within an alternative regularization method (four dimensional regularization scheme FDR) ref. [172], the one that resembles most closely the symmetry approach taken here. This Chapter is based on ref. [173].

[1]Note that the calculation of the fermion triangle contribution is well defined i.e., it is independent of arbitrary vectors and finite.

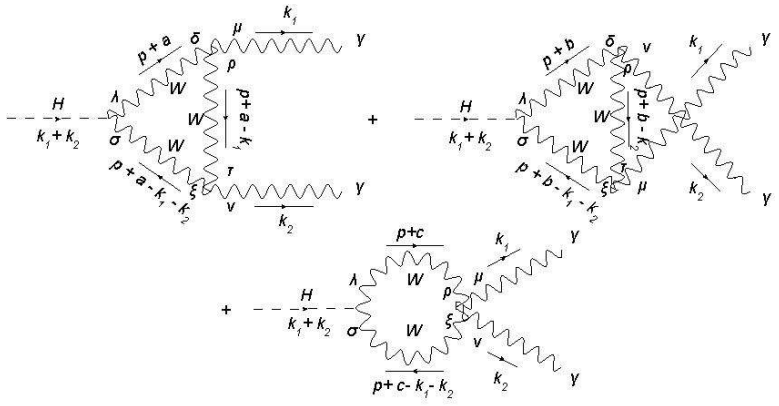

Figure 4.1: *W-gauge boson contribution to the $H \to \gamma\gamma$ amplitude. Momentum flow together with relevant shift vectors are indicated.*

4.1 Introduction

Today one of the main focal points at the Large Hadron Collider (LHC) is to search for the Higgs boson (H) (refs. [6–8]) through its decay into two photons, $H \to \gamma\gamma$ (for reviews see refs. [159, 160]). Indeed, the recent (refs. [4, 5]) observation by ATLAS and CMS experiments of a resonance, that could be the Standard Model (SM) Higgs boson, is based on data mainly driven by $H \to \gamma\gamma$. In the (SM) [1–3], this particular decay process goes through loop induced diagrams involving either charged fermions or W-gauge bosons. Their calculation was first performed in ref. [161] in the limit of light Higgs mass $m_H \ll m_W$, using dimensional regularisation in the 't Hooft-Feynman gauge. Since then, there are numerous works spent on improving this calculation including finite Higgs mass effects in linear and non-linear gauges (refs. [162–164]), different regularisation schemes (refs. [165–168]) and/or different gauge choices (ref. [169]).

The $H \to \gamma\gamma$ amplitude is originated, in broken (unbroken) phase, by a dimension-5 (dimension-6) SM gauge invariant operator(s) and, therefore, its expression, within a renormalizable theory, must be finite, gauge invariant and independent of any gauge choice. The amplitude should also be consistent with the Goldstone Boson Equivalence Theorem (GBET) (refs. [129–131]) since the SM is a renormalizable, spontaneously broken, gauge field theory.

A problem arises when the W-gauge boson contribution (see Fig. 4.1) to $H \to \gamma\gamma$ produces "infinite" results at intermediate steps. These problems are usually treated by using a gauge invariant regulator method, e.g., dimensional regularization. In the unitary gauge (ref. [170]), this indeterminacy is more pronounced and more difficult to handle with[2] due to the particular form of the W-gauge boson propagator. On the other hand it is much simpler to work with only few diagrams, that involve physical

[2]However, using DR and unitary gauge with modern computer algorithms this may not be a hard problem today (see ref. [169]).

particle masses, rather than many.

More specifically, in the unitary gauge, one encounters divergencies up to the sixth power. It is well known that, in four-dimensions, shifting momenta in integrals that are more than logarithmically divergent is a "tricky business" - recall the calculation of linearly divergent fermion triangles in chiral anomalies [30, 91] - that requires keeping track of several "surface" terms for these integrals. There is also the situation we face here where apparent logarithmically divergent integrals turn out to be finite but discontinuous at $d = 4$.

We would like to bypass those ambiguities and at the same time to present a "regularisation" method, by performing the calculation for the $H \to \gamma\gamma$ amplitude strictly in 4-dimensions and in the physical unitary gauge. Our method is similar to the one used in the previous Chapter for calculating triple gauge boson amplitudes (see refs. [87, 120]), or Lorentz non-invariant amplitudes [109], and consists of three steps:

1. We write down the most general Lorentz invariant $H \to \gamma\gamma$ amplitude.

2. We introduce arbitrary vectors that account for the "shifting momentum" indeterminacy. We show that a particular choice of those "shifting vectors" cancel higher powers of infinities leaving still behind at most logarithmically divergent integrals that are treated as undetermined variables.

3. We exploit physics, i.e., gauge invariance (Ward Identities) and the GBET in order to fix the last undetermined variables.

This method is quite general and can be applied to other observables within a renormalizable theory. Following these steps we arrive at the same result for the $H \to \gamma\gamma$ amplitude obtained by J. Ellis et.al [161] and by M. Shifman et.al [163] almost 35 years ago. Our analysis, among other issues, highlights that the recent observation [4, 5] of the $H \to \gamma\gamma$ at the LHC signifies the validity of the Goldstone Boson Equivalence Theorem. As a further clarification we also make a remark on the direct calculation in the following three cases: we first perform the integrals in exactly $d = 4$ (with no regularisation method beyond the one discussed in point 2 above), second, by exploiting Dimensional Regularisation (DR) as defined in refs. [33, 171] and then taking the limit $d \to 4$, and finally third by using a four-dimensional regularization scheme introduced in ref. [172].

Our calculation is complementary to, but somewhat different than, the two existing ones, performed in the unitary gauge (refs. [169, 174, 175]) . It is not our intend to redo the calculation in unitary gauge with DR as in ref. [169]. On the contrary, we want to clarify subtle issues related to the amplitude in unitary gauge and $d = 4$ raised in part by refs. [174, 175]. We find, using arbitrary vectors, that divergencies (up to 6th power) are reduced down to logarithmic ones. This is a new result that is not obvious when working in unitary gauge and cannot be seen when using dimensional regularization. This fact was stated incorrectly in refs. [174, 175].

4.2 The W-loop contribution to $H \to \gamma\gamma$ in SM

In this section we present the calculation of the W-loop contribution[3] to $H \to \gamma\gamma$ amplitude. The most general, Lorentz and CP-invariant, form of the of-shell amplitude is:

$$\mathcal{M}_1\, g^{\mu\nu} + \mathcal{M}_2\, k_1^\nu\, k_2^\mu + \mathcal{M}_3\, k_1^\mu\, k_2^\nu + \mathcal{M}_4\, k_1^\mu\, k_1^\nu + \mathcal{M}_5\, k_2^\mu\, k_2^\nu\ , \tag{4.1}$$

where k_1 and k_2 are the outgoing photon momenta shown in Fig. 4.1, and the coefficients $\mathcal{M}_{i=1..5} \equiv \mathcal{M}_{i=1..5}(k_1, k_2)$ are scalar functions of k_1^2, k_2^2, and $k_1 \cdot k_2$. By considering that all particles are on-mass-shell, that is $k_1^2 = k_2^2 = 0,\ k_1 \cdot k_2 = m_H^2/2,\ k_1 \cdot \epsilon^*(k_1) = 0 = k_2 \cdot \epsilon^*(k_2)$, we obtain an amplitude $\mathcal{M} = \mathcal{M}^{\mu\nu}\epsilon^*_\mu(k_1)\epsilon^*_\nu(k_2)$ with only two, undetermined (for the time being), coefficients,

$$\mathcal{M}^{\mu\nu} = \mathcal{M}_1\, g^{\mu\nu}\ +\ \mathcal{M}_2\, k_1^\nu\, k_2^\mu\ . \tag{4.2}$$

In unitary gauge, the Feynman diagrams that contribute to $\mathcal{M}_1$ and $\mathcal{M}_2$ are displayed in Fig. 4.1. In order to calculate them, we introduce three arbitrary four-vectors a, b and c, one for each diagram. These vectors shift the integration momentum, i.e., $p \to p+a$ for the first diagram, $p \to p+b$ for the second diagram and $p \to p+c$ for the third diagram. As we shall see, these arbitrary vectors operate as regulators capable to handle highly divergent integrals related to unitary gauge choice. Furthermore, the vectors a, b and c, linearly depend upon the external momenta k_1 and k_2. Hence a, b and c are not linearly independent [*c.f.* eq. (4.4)]. This is an important fact leading to the cancellation of infinities.

We first calculate the less divergent part of $\mathcal{M}^{\mu\nu}$ in eq. (4.2) which is the $\mathcal{M}_2$ coefficient[4]. By naive power counting, we see that $\mathcal{M}_2$ diverges by at most four powers. Then we perform the Feynman integral calculations strictly in 4-dimensions. For reasons that will become clear later, we shall keep the number of dimensions general in all intermediate steps of the calculation i.e., $g^{\mu\nu}g_{\mu\nu} = d$. As we will see, d contributes only in finite pieces of $\mathcal{M}_2$ [*c.f.* eq. (4.9)][5].

With all the above definitions, we can write down the total amplitude in the form

$$\begin{aligned}
\mathcal{M}^{\mu\nu}\ \sim\ & \int \frac{d^4p}{(2\pi)^4}\,\big[\mathcal{A}_{11}\, g^{\mu\nu} \\
+\ & \mathcal{A}_{21}\,(p+a)^\mu\,(p+a)^\nu + \mathcal{A}_{22}\,(p+b)^\mu\,(p+b)^\nu + \mathcal{A}_{23}\,(p+c)^\mu\,(p+c)^\nu \\
+\ & \mathcal{A}_{31}\,(p+a)^\mu\,k_1^\nu + \mathcal{A}_{32}\,(p+b)^\mu\,k_1^\nu + \mathcal{A}_{33}\,(p+c)^\mu\,k_1^\nu \\
+\ & \mathcal{A}_{41}\,(p+a)^\nu\,k_2^\mu + \mathcal{A}_{42}\,(p+b)^\nu\,k_2^\mu + \mathcal{A}_{43}\,(p+c)^\nu\,k_2^\mu \\
+\ & \mathcal{A}_{51}\,k_2^\mu\,k_1^\nu\,\big]\ ,
\end{aligned} \tag{4.3}$$

where the coefficients $\mathcal{A}_{ij} = \mathcal{A}_{ij}(p^n; k_1, k_2; a; b; c)$ with $-6 \le n \le 0$, are given in Appendix L, and the $\sim$ sign is the proportionality factor: $-\frac{2ie^2}{v}$. Note that $\mathcal{M}^{\mu\nu}$ is a

[3]Note that the calculation of the fermion triangle contribution is well defined i.e., it is independent of arbitrary vectors and finite. We are not going to repeat this calculation here and refer the reader to the reviews in refs. [159, 160].

[4]The coefficient $\mathcal{M}_1$ will be fixed later on by the requirement of gauge invariance.

[5]On the contrary, we shall see that there are non-trivial d-contributions into $\mathcal{M}_1$-coefficient.

(superficially) 6th power divergent amplitude in the unitary gauge. We can see that $\mathcal{A}_{11}$ in eq. (4.3) solely contributes to $\mathcal{M}_1$, while all other $\mathcal{A}$-elements contribute to both $\mathcal{M}_1$ and/or $\mathcal{M}_2$ in eq. (4.2).

First we focus on the calculation of the "less divergent" coefficient $\mathcal{M}_2$ of eq. (4.2). Based on naive power counting, we observe that the $\mathcal{A}_{21}$, $\mathcal{A}_{22}$, $\mathcal{A}_{23}$-terms in eq. (4.3), lead to at the most quartic divergent integrals. However, when adding all these pieces together, we find that quartic divergent integrals vanish for every arbitrary vectors a, b and c leaving behind an expression with integrals of third power (in momenta) plus integrals with smaller divergencies. Then, the cubically divergent integrals are proportional to all possible Lorentz invariant combinations like: $[(a+b-2c)\cdot p]\, p^\mu p^\nu$, $[(a+b-2c)^\nu p^\mu]\, p^2$ and $[(a+b-2c)^\mu p^\nu]\, p^2$. Therefore, choosing

$$a + b - 2\,c \;=\; 0\;, \tag{4.4}$$

we ensure that third order divergent integrals related to $\mathcal{A}_{21}$, $\mathcal{A}_{22}$, $\mathcal{A}_{23}$-terms, vanish identically. In the same way, by naive power counting, $\mathcal{A}_{31}$ and $\mathcal{A}_{33}$-terms - these terms in eq. (4.3) together with $\mathcal{A}_{32}$ contribute solely to $\mathcal{M}_2$ - lead again to at most third order divergent integrals. However, in the sum of $\mathcal{A}_{31}$ and $\mathcal{A}_{33}$-terms in eq. (4.3), third order divergent integrals vanish for arbitrary a, b and c, leading to an expression, that when added to $\mathcal{A}_{32}$-term, consists of at most quadratically divergent integrals, proportional to $[(c-a)\cdot p]\, p^\mu k_1^\nu$ and $[(c-a)^\mu k_1^\nu]\, p^2$. We choose,

$$c - a = \;0\;, \tag{4.5}$$

for the quadratically divergent integrals to vanish. Likewise, when we add $\mathcal{A}_{42}$ and $\mathcal{A}_{43}$-terms - these terms, together with $\mathcal{A}_{41}$, solely contribute to $\mathcal{M}_2$ in eq. (4.2) - the third order divergent integrals vanish for every choice of a, b, c leading to an expression, that when added to $\mathcal{A}_{41}$, consists of at most quadratically divergent integrals proportional to $[(c-b)\cdot p]\, p^\nu k_2^\mu$ and $[(c-b)^\nu k_2^\mu]\, p^2$. Therefore, we choose

$$c - b = \;0\;, \tag{4.6}$$

for infinities to vanish identically. From eqs. (4.4), (4.5) and (4.6) we arrive at the final relation among the three introduced vectors:

$$a \;=\; b \;=\; c\;. \tag{4.7}$$

Equation (4.7) suggests that the rest of the divergent integrals depend by, at most, one arbitrary vector, say the a-vector. Note that $\mathcal{A}_{51}$ contributes only to the finite part of $\mathcal{M}_2$. Now, if we impose conditions of eq. (4.7) onto the remaining expressions for $\mathcal{A}_{21}$, $\mathcal{A}_{22}$, ..., $\mathcal{A}_{51}$-terms of eq. (4.3), we find that *all* quadratically and linearly divergent integrals vanish, independently of the direction of the a-vector. We stress here the fact that *the cancellation of divergencies down to logarithmic ones is a highly non-trivial, almost "miraculous", result. These cancellations only take place for a particular choice of the momentum-variable shift vectors, [eq. (4.7)]*[6]. Of course this is an expected outcome for an observable within a renormalizable theory.

[6] As a corollary, if for instance, we had split the $WW\gamma$-vertex into three pieces, each one associated with three different arbitrary vectors, then the generalised condition (4.7) would again downgrade the divergency of the amplitude to a logarithmic one.

The final result contains *at most logarithmically divergent integrals*. Despite of the fact that the resulting expressions so far contain the shift $p + a$ instead of p with an arbitrary vector a, its presence is irrelevant since logarithmically divergent integrals are momentum-variable shift independent [126]. This result is different with the one obtained in refs. [174, 175], where there is a quadratically divergent term remaining and is tuned to zero by appropriate choice of loop momentum.[7] Summing up all the above contributions to $\mathcal{M}_2$, we find a particularly nice and symmetric form for $\mathcal{M}^{\mu\nu}$,

$$
\begin{aligned}
\mathcal{M}^{\mu\nu} \;\sim\; & \int \frac{d^4p}{(2\pi)^4}\, p^\mu p^\nu \left\{ \frac{4(d-1)\, m_W^2 + 2\, m_H^2}{[p^2 - m_W^2][(p-k_1)^2 - m_W^2][(p-k_1-k_2)^2 - m_W^2]} \right. \\
+ \; & \left. \frac{4(d-1)\; m_W^2 + 2\, m_H^2}{[p^2 - m_W^2][(p-k_2)^2 - m_W^2][(p-k_1-k_2)^2 - m_W^2]} \right\} \\
+ \; & \int \frac{d^4p}{(2\pi)^4}\, p^\mu k_1^\nu \left\{ \frac{-4(d-1)\, m_W^2 - 4\,(p\cdot k_2)}{[p^2 - m_W^2][(p-k_1)^2 - m_W^2][(p-k_1-k_2)^2 - m_W^2]} \right. \\
+ \; & \left. \frac{-4\,(p\cdot k_2)}{[p^2 - m_W^2][(p-k_2)^2 - m_W^2][(p-k_1-k_2)^2 - m_W^2]} \right\} \\
+ \; & \int \frac{d^4p}{(2\pi)^4}\, p^\nu k_2^\mu \left\{ \frac{-4\,(p\cdot k_1)}{[p^2 - m_W^2][(p-k_1)^2 - m_W^2][(p-k_1-k_2)^2 - m_W^2]} \right. \\
+ \; & \left. \frac{-4(d-1)\, m_W^2 - 4\,(p\cdot k_1)}{[p^2 - m_W^2][(p-k_2)^2 - m_W^2][(p-k_1-k_2)^2 - m_W^2]} \right\} \\
+ \; & \int \frac{d^4p}{(2\pi)^4}\, k_1^\nu k_2^\mu \left\{ \frac{6\, m_W^2 + 2\, p^2}{[p^2 - m_W^2][(p-k_1)^2 - m_W^2][(p-k_1-k_2)^2 - m_W^2]} \right. \\
+ \; & \left. \frac{6\, m_W^2 + 2\, p^2}{[p^2 - m_W^2][(p-k_2)^2 - m_W^2][(p-k_1-k_2)^2 - m_W^2]} \right\} . \qquad (4.8)
\end{aligned}
$$

Introducing Feynman parameters, shifting momentum variable from p to ℓ and ignoring all terms that contribute to $\mathcal{M}_1$ [8] we find that the contribution to $\mathcal{M}_2$ in eq. (4.2) arises

[7] Following eq.(11) in Gastmans *et.al* paper [174], or eq.(3.36) in their sequel paper [175], and unless there is a typo in both their formulae, we find that there is a missing quadratically divergent term proportional to $k^2 k_\mu k_\nu$. Moreover, their formulae contain a linearly divergent term that is referred to by the authors claiming that this term reduces to a logarithmically divergent integral by changing the momentum $k \to -k$ and further manipulating the integral. Note that in our calculation all divergent integrals are reduced to at most logarithmically divergent ones *without* any further manipulation nor any assumption other than eq. (4.7) for every arbitrary vectors a, b and c. Finally the authors in refs. [174, 175] have made a specific choice for routing the internal loop momentum corresponding to $a = b = c = \frac{1}{2}(k_1 + k_2)$ and therefore their result should be the same with ours.

[8] These terms will be used later in arriving at eq. (4.24).

solely from the term,

$$\mathcal{M}_2\, k_1^\nu\, k_2^\mu \;\sim\; 8\int_0^1 dx\int_0^{1-x} dy\int \frac{d^4\ell}{(2\pi)^4}\,\frac{\ell^2\, k_1^\nu\, k_2^\mu - 2\,(\ell\cdot k_2)\,\ell^\mu\, k_1^\nu - 2\,(\ell\cdot k_1)\,\ell^\nu\, k_2^\mu}{(\ell^2-\Delta)^3}$$

$$+\;\; 8\, m_W^2\int_0^1 dx\int_0^{1-x} dy\int \frac{d^4\ell}{(2\pi)^4}\,\frac{3-2\,(d-1)\,x\,(1-x-y)}{(\ell^2-\Delta)^3}\, k_1^\nu\, k_2^\mu\;, \quad (4.9)$$

with $\Delta = x(x+y-1)\, m_H^2 + m_W^2$. Obviously, the first integral in eq. (4.9) is (superficially) logarithmically divergent while the second one is finite. The number of dimensions (d) appears only at the finite integral and therefore we can fearlessly set $d = 4$ everywhere. This means that we do not use dimensional regularisation in what follows (see however the discussion below). We state here few additional remarks to be exploited later on: a) we observe that the top line in the integrand of eq. (4.9) *does not vanish* in the limit $m_W^2 \to 0$ and, b) despite of appearances in eq. (4.8), there is no m_H^2 in the numerators of the subsequent expression eq. (4.9). The whole m_H^2 contribution arises from the denominator's Δ-term.

Our next step is to parametrize the logarithmically divergent integral in eq. (4.9) by an unknown, dimensionless, parameter λ to be determined later by a physical argument. So we define,

$$\int_0^1 dx\int_0^{1-x} dy\int \frac{d^4\ell}{(2\pi)^4}\,\frac{\ell^2\, k_1^\nu\, k_2^\mu - 2\,(\ell\cdot k_2)\,\ell^\mu\, k_1^\nu - 2\,(\ell\cdot k_1)\,\ell^\nu\, k_2^\mu}{(\ell^2-\Delta)^3} \equiv \frac{i\lambda}{4(4\pi)^2}\, k_1^\nu\, k_2^\mu\;. \quad (4.10)$$

An important parenthesis here. We could of course promote $d^4\ell \to d^d\ell$ and use dimensional regularisation [33] by exploiting symmetric integration $\ell^\mu\ell^\nu \to \frac{1}{d}\ell^2 g^{\mu\nu}$ in d-dimensions. In this case, and after taking the limit $d \to 4$, one finds $\lambda = -1$ which is finite and non-zero, and, agrees with the one we find below in eq. (4.20) after imposing the GBET condition. This is also the result found in the original refs. [161–163]. However, according to refs. [174, 175], the integral in eq. (4.10) is discontinuous at $d = 4$; in fact, when symmetric integration, $\ell^\mu\ell^\nu \to \frac{1}{4}\ell^2 g^{\mu\nu}$ in $d = 4$ is used, one finds instead $\lambda = 0$. This is also understood in a slightly different context. It has long been known [126–128] that shifts of integration variables in linearly (and above) divergent integrals are accompanied by "surface" terms that appear only in four dimensions – a famous example being the integrals in chiral anomaly triangle graphs. For our purpose here let us start with the following shift of variables in a linearly divergent integral that has been generalised [128] to work in 2ω-dimensions following the expression,

$$\int d^{2\omega}\ell\,\frac{\ell_\mu}{[(\ell-k)^2-\Delta]^2} - \int d^{2\omega}\ell\,\frac{(\ell+k)_\mu}{(\ell^2-\Delta)^2} \;=\; -\frac{i\pi^2}{2}\, k_\mu\,\delta_{\omega,2}\;, \quad (4.11)$$

that is valid for $\omega < 5/2$ and Δ constant, possibly dependent on Feynman parameters, like the one given below eq. (4.9), and k_μ is an arbitrary constant four vector. By taking the derivative, $\frac{\partial}{\partial k^\nu}$, of both sides in eq. (4.11) and shifting the integration variable for

the logarithmically divergent integral encountered, and evaluating the finite one, we easily arrive at

$$\int d^{2\omega}\ell\,\frac{\ell^2\,g_{\mu\nu}-4\,\ell_\mu\,\ell_\nu}{(\ell^2-\Delta)^3}\;=\;-\frac{i\pi^2}{2}\,g_{\mu\nu}\left(\frac{\pi^{\omega-2}\,\Gamma(3-\omega)}{\Delta^{2-\omega}}-\delta_{\omega,2}\right). \tag{4.12}$$

For an alternative and detailed proof of eq. (4.12), see Appendix M.[9] Applying eq. (4.12) to $\ell^\sigma\ell^\rho$ terms of eq. (4.10) with $\frac{d^4\ell}{(2\pi)^4}\to\frac{d^{2\omega}\ell}{(2\pi)^{2\omega}}$, we find,

$$\lambda=\begin{cases}\;0\,, & \omega=2\\ -1\,, & \omega=2-\epsilon\quad(\text{DR})\end{cases}. \tag{4.13}$$

This is consistent with the symmetric integration in 4-dimensions ($\omega=2$), *but*, is also consistent with the usual tabulated textbook result [34] from dimensional regularisation in $4-2\epsilon$-dimensions ($\omega=2-\epsilon$). Equation (4.13) shows that λ is discontinuous at $d=2\,\omega=4$. Then the Question arises: *which λ value to believe in?* Answer: *the one that is indicated by well defined, calculable, boundary conditions and symmetries of the underlying theory.*

The above parenthesis to our calculation motivates us to avoid the direct calculation of integral (4.10) but set $d=4$ everywhere and treat λ as an unknown parameter to be defined later within a physical context or experiment. Substituting eq. (4.10) into eq. (4.9) we arrive at:

$$\mathcal{M}_2\sim\frac{i}{8\pi^2}\left\{\lambda-6\,m_W^2\int_0^1 dx\int_0^{1-x}dy\,\frac{1-2\,x\,(1-x-y)}{\Delta}\right\}. \tag{4.14}$$

Evaluating the double finite integral in eq. (4.14), and restoring the proportionality factor given below eq. (4.3), we obtain,

$$\mathcal{M}_2=-\frac{e^2g}{(4\pi)^2m_W}\left\{-2\,\lambda+\Big[3\,\beta+3\,\beta\,(2-\beta)\,f(\beta)\Big]\right\}, \tag{4.15}$$

where

$$\beta=\frac{4\,m_W^2}{m_H^2}\,,\quad\text{and,}\quad f(\beta)=\begin{cases}\arctan^2\left(\frac{1}{\sqrt{\beta-1}}\right)\,,\;\beta\geq1\\ -\frac{1}{4}\,\left[\ln\left(\frac{1+\sqrt{1-\beta}}{1-\sqrt{1-\beta}}\right)-i\,\pi\right]^2\,,\;\beta<1\end{cases}. \tag{4.16}$$

Our final step is to determine the unknown parameter λ in eq. (4.15). For this, we need physics that reproduces $\mathcal{M}_2$ in a different and unambiguous way. One choice, probably not the only one, is to adopt the Goldstone Boson Equivalence Theorem (GBET) [129–131] which states that the amplitude for emission or absorption of a longitudinally polarised W-boson at high energy becomes equivalent to the emission

[9] The same result is obtained by standard algebraic tricks. We would like to thank R. Jackiw for communicating his calculation to us.

or absorption of the Goldstone boson that was eaten. Mathematically, this is written by the following equation in ref. [176],

$$S[\, W_L^{\pm},\ \text{physical}\,] = i^n\, S[\, s^{\pm},\ \text{physical}\,]\,, \tag{4.17}$$

which says that the S-matrix elements for the scattering of the *physical* longitudinal vector bosons W_L with other physical particles are the same as the S-matrix elements of the theory where the W_L's have been replaced by *physical* Goldstone bosons ($s^{\pm}$).

According to ref. [176], within perturbation theory and in the limit of high energies, $m_W^2/s \to 0$, GBET can be expressed with physics in two different limits of the theory: (a) $g^2/\lambda_H \to 0$, or (b) $m_H^2/s \to 0$.

The limit (b) is irrelevant[10] for defining λ in eq. (4.15) so we completely focus on the limit (a). It is easy to see that, in the unitary gauge, the W_L's do not decouple[11] for vanishing gauge coupling g. Consider for example the diagrams in Fig. 4.1. There is always a m_W^2 from the HWW-vertex that cancels another m_W^2 sitting in the denominator of the longitudinal part for the internal W-boson propagator expression written in the unitary gauge. So, as it was already noted in the paragraph below eq. (4.9), in the limit $g \to 0$ there are remaining non-decoupled terms. Unfortunately, these effects may be obscured or misjudged by the regularisation method needed to handle divergent, intermediate, loop integrals. This is exactly what happens here when trying to calculate λ directly from its ambiguous form in eq. (4.10). On the other hand however, at the exact $g = 0$, with fixed v.e.v v and Higgs quartic coupling λ_H, eq. (4.17) suggests that the Goldstone bosons ($s^{\pm}$) should reappear at the physical spectrum of the theory, while the longitudinal components of W's become unphysical. At this limit, the SM is a spontaneously broken global $SU(2)_L \times U(1)_Y$-symmetry that couples, minimally, to electromagnetism. The interactions between the Higgs and photon with the Goldstone bosons are simply those of a spontaneously broken scalar QED with $U(1)_{\rm em}$,

$$H\, s^+\, s^- \ :\ -\frac{i m_H^2}{v}, \quad \gamma\, s^+(p_1)\, s^-(p_2) \ :\ -ie(p_1+p_2)^\mu, \quad \gamma\,\gamma\, s^+\, s^- \ :\ 2ie^2 g^{\mu\nu}\ . \tag{4.18}$$

Armed with these Feynman rules we calculate the diagrams in Fig. 4.2 below. By doing so, we introduce again three momentum variable shift vectors, one for each diagram, exactly in the same way we did for the calculation of the diagrams in Fig. 4.1. The Lorentz structure of the amplitude is completely analogous to eq. (4.2) with $\mathcal{M}_{1,2} \to \mathcal{M}_{1,2(\rm GBET)}$, but now due to the scalar propagators, the superficial degree of divergence, for diagrams contributing to $\mathcal{M}_{2(\rm GBET)}$, is $D = -2$. Hence, all integrals involved in $\mathcal{M}_{2(\rm GBET)}$ are finite and in addition, they are independent of any momentum integration shift vector variable.

As a consequence, $\mathcal{M}_{2(\rm GBET)}$ is well defined, calculable, independent of any regularisation method, and at the limit of $g \to 0$ (or $\beta = 4\, m_W^2/m_H^2 \to 0$) is

$$\mathcal{M}_{2(\rm GBET)} = -\frac{2\, e^2\, g}{(4\pi)^2 m_W}\ , \qquad \beta \to 0\ . \tag{4.19}$$

[10]The limit (b) simply says that matrix elements for the theory which contains the physical W_L's and zero v.e.v, are equal to those produced by scattering of massless physical Goldstone bosons (instead of W_L's) at high energies. We have checked that eq. (4.17) is satisfied in this limit.

[11]This is another advantage of calculating in the unitary gauge.

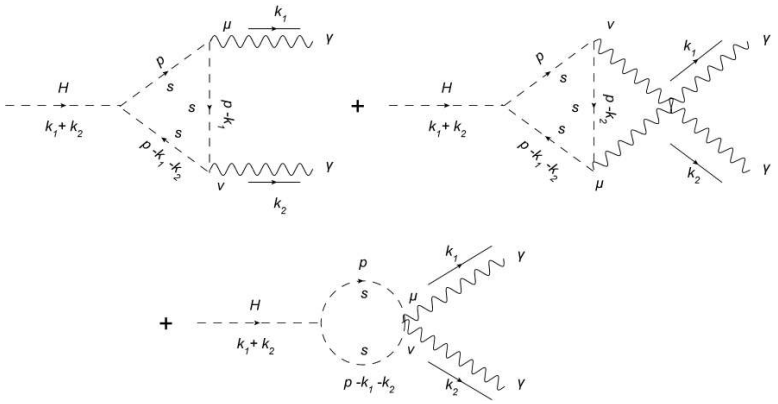

Figure 4.2: *Charged Goldstone boson contributions to $H \to \gamma\gamma$ in the limit of $g \to 0$.*

By equating eq. (4.15) (in the limit $\beta \to 0$) and eq. (4.19) which represent the l.h.s and r.h.s of the GBET condition (4.17), respectively, we find

$$\lambda = -1 \; . \tag{4.20}$$

This value agrees with dimensional regularization (ref. [33, 171]) when the limit $d \to 4$ is taken [see eq. (4.13)]. The final form of the $\mathcal{M}_2$ in eq. (4.2) is

$$\mathcal{M}_2 \;=\; -\frac{e^2 g}{(4\pi)^2\, m_W} \left\{ 2 + \left[3\,\beta + 3\,\beta\,(2-\beta)\, f(\beta) \right] \right\} , \tag{4.21}$$

with β, and $f(\beta)$ defined in eq. (4.16).

To complete the picture there is still the coefficient $\mathcal{M}_1$ in eq. (4.2) to be calculated. Naive power counting says that this is by two powers more divergent than $\mathcal{M}_2$ and, in general, undetermined. It can be fixed however by using quantum gauge invariance i.e., conservation of charge, for the $U(1)_{\rm em}$,

$$k_{1\mu}\mathcal{M}^{\mu\nu} = 0, \quad k_{2\nu}\mathcal{M}^{\mu\nu} = 0, \quad k_1^2 = k_2^2 = 0, \tag{4.22}$$

and thus from eq. (4.2),

$$\mathcal{M}_1 = -(k_1 \cdot k_2)\, \mathcal{M}_2 \; . \tag{4.23}$$

Equation (4.23) is substituted to eq. (4.2) with $\mathcal{M}_2$ read by eq. (4.21). This is exactly the same result for the W-boson contribution to $H \to \gamma\gamma$ amplitude, that has been obtained in refs. [161–164, 169] using dimensional regularisation in R_ξ-gauges.

It is interesting here to note the result from the explicit algebraic manipulation of $\mathcal{M}_1$ in the unitary gauge and check the validity of gauge invariance [eq. (4.23)]. Exactly as for $\mathcal{M}_2$, the condition $a = b = c$ for the arbitrary vectors given in eq. (4.7) is crucial in reducing the divergence of $\mathcal{M}_1$ down to a logarithmic one [see expression L.12].

In d-dimensions the expression for $\mathcal{M}_1$ is finally independent of any arbitrary vector and, up to a proportionality factor, reads:

$$\mathcal{M}_1 \sim 4\int_0^1 dx\int_0^{1-x} dy\int \frac{d^d\ell}{(2\pi)^d}\left\{\frac{4(\ell\cdot k_1)(\ell\cdot k_2)+2(\frac{2}{d}-1)\ell^2(k_1\cdot k_2)+(\frac{d-1}{d})(4-d)\,\ell^2\,m_W^2}{(\ell^2-\Delta)^3}+\right.$$
$$\left.+\frac{(d-1)\,m_W^4-3\,m_W^2\,m_H^2+(1-d)\,x(x+y-1)m_W^2\,m_H^2}{(\ell^2-\Delta)^3}\right\}. \quad (4.24)$$

Clearly the first integral in eq. (4.24) is ill-defined in four dimensions. If however, we insist in doing the calculation of eq. (4.24) in $d = 4$ with symmetric integration, like in refs. [174, 175], we find that gauge invariance [eq. (4.23)] is *not* satisfied. This is of course unacceptable. By going a little bit deeper, gauge invariance is lost because of the term proportional to $4 - d$ in eq. (4.24) which vanishes when $d = 4$. Quite the contrary in DR, this term results in a non-zero contribution when $m_W \neq 0$, since the (log-divergent) integral in front of $(4-d)$ contains a simple pole at $d = 4$. This changes the final result and renders eqs. (4.21), (4.24) and (4.23) consistent, only if $\lambda = -1$. This outcome is in agreement with ref. [169].

Few remarks are worth mentioning here. Had we started first by calculating $\mathcal{M}_1$, there would be no possibility of defining unambiguously λ without using a gauge invariant regulator: the $g_{\mu\nu}$ part of the amplitude at $g \to 0$ involving Goldstone bosons [see diagrams in Fig. 4.2] is not well defined - an integral as the one in eq. (4.12) appears again. Another remark is that the same expressions for the coefficients $\mathcal{A}_{ij}$ displayed in Appendix L in the unitary gauge, appear also when one exploits the R_ξ-gauge. In the latter there are in addition ξ-dependent terms (see ref. [169]) that vanish in the end from unphysical scalar contributions. Therefore, the logarithmic ambiguity in eq. (4.12), found here in the unitary gauge, is similar in every other gauge.

4.3 Four Dimensional Regularization (FDR)

So far we have proposed a regularization scheme which is four-dimensional and uses the basic symmetries and underlying physics of the SM. However, in more complicated models or observables with more parameters to adjust, such a scheme can become cumbersome. For example, it is not always obvious which physics argument will fix undefined integrals.

Very recently, R. Pittau (see ref. [172]) proposed a scheme that is fairly easy to handle and, to the best of our knoweledge, is the closest to four dimensional calculations, thereby coined four-dimensional regularisation/renormalization scheme or just FDR. According to this scheme, infinite bubble graph contributions, i.e., large loop momenta contributions that do not depend upon external momenta, are absorbed into the shift of the vacuum while the remaining finite corrections are calculable in four-dimensions in addition to being Lorentz and gauge invariant.

We have applied FDR into the calculation of the $H \to \gamma\gamma$ amplitude and found agreement with our physics approach and with DR results. In FDR, one introduces

an arbitrary scale μ which is considered to be much smaller than internal momenta and particle masses in loops. Self contracted loop momenta quantities like ℓ^2 become $\overline{\ell}^2 = \ell^2 - \mu^2$, while for gauge invariance to hold, vector momenta, p^μ, remain untouched. For example the integral of eq. (4.12) becomes,

$$\int [d^4\ell]\, \frac{\overline{\ell}^2\, g_{\mu\nu} - 4\,\ell_\mu\,\ell_\nu}{\overline{D}^3} \;= \int [d^4\ell]\, \frac{-\mu^2}{\overline{D}^3}\, g_{\mu\nu}\;, \tag{4.25}$$

where $\overline{D} = (\overline{\ell}^2 - \Delta)$ and $[d^4\ell]$ stands for integration over $d^4\ell$, dropping all divergent terms from the integrand (see below) and taking the limit $\mu \to 0$. In going from l.h.s to r.h.s of eq. (4.25) the symmetry property $\ell_\mu \ell_\nu = g_{\mu\nu}\,\ell^2/4$ has been used in four dimensions. Then, using the partial fractions identity,

$$\frac{1}{\overline{D}^3} = \left[\frac{1}{\overline{\ell}^6}\right] + \Delta\,\left(\frac{1}{\overline{D}^3\overline{\ell}^2} + \frac{1}{\overline{D}^2\overline{\ell}^4} + \frac{1}{\overline{D}\overline{\ell}^6}\right)\;, \tag{4.26}$$

the term in square bracket is recognised as divergent and therefore removed, and integrating the r.h.s of eq. (4.25) over $[d^4\ell]$ one obtains

$$\int [d^4\ell]\, \frac{-\mu^2}{\overline{D}^3} \equiv -\Delta \lim_{\mu\to 0} \mu^2 \int d^4\ell\, \left(\frac{1}{\overline{D}^3\overline{\ell}^2} + \frac{1}{\overline{D}^2\overline{\ell}^4} + \frac{1}{\overline{D}\overline{\ell}^6}\right) = -\frac{i\pi^2}{2}\;, \tag{4.27}$$

i.e., exactly the same result as in DR which eventually leads to $\lambda = -1$ consistent with gauge invariance and GBET. What in fact FDR scheme does, is to restate the correct DR answer through the regulator μ^2 keeping eq. (4.12) correct in $d = 4$. We therefore understand that the constant (β-independent) term of eq. (4.21) in FDR arises from the fact that the arbitrary scale, μ^2, *must* disappear from physical observables.

4.4 Discussion

It is evident that our calculation for the amplitude incorporates two physical inputs: one is the conservation of charge and the other is the equivalence theorem. They are both direct consequences of the gauge invariance of the underlying physical theory. The first one is experimentally indisputable while the second one is theoretical[12] and has been proven in ref. [179] that is valid in any spontaneously broken renormalizable theory, like for example the SM. One may think however that there is a loophole in our use of this second argument: so far, and, to our knowledge, the replacement of the W-bosons with Goldstone bosons at high energies has been proven to be valid only for external W-bosons (see refs. [176, 180, 181]) and *not* for internal ones which is the case exploited here. Although it has been tested in several phenomenological examples [182], a formal, to all orders, proof is still missing. Although this may be true, it is difficult to argue against the validity of decoupling limit $g \to 0$ (with fixed v.e.v and Higgs quartic coupling) discussed in the paragraph above eq. (4.18).

[12]This is not entirely correct. There is of course the high energy behaviour of $e^+e^- \to W^+W^-$ found at LEP [139] consistent with the GBET.

Is there another physics context from which one can define λ? One possibility is to exploit the low energy Higgs theorem (ref. [161, 183–185]) instead. Although this may serve as a consistency check, and indeed is compatible with $\lambda = -1$, we cannot use it to define λ. The reason here is threefold: first, when treating the Higgs field as an external background field with zero momentum, one needs to take partial derivative w.r.t m_W of the 2-point photon vacuum polarization amplitude, $\Pi_{\gamma\gamma}(q^2)$. The later, is notoriously difficult, if meaningful, to be calculated in the unitary gauge. Second, according to ref. [161], we know that to the lowest order in weak coupling, the amplitude for the process $\langle\gamma\gamma|H\rangle$ is proportional to $\langle\gamma\gamma|\Theta^\mu_\mu|0\rangle$, where $\Theta^\mu_\mu = 2\,m_W^2 W^+W^- + ...$ is the improved energy momentum tensor [186]. However, the calculation of $\langle\gamma\gamma|\Theta^\mu_\mu|0\rangle$ goes through the same steps as the calculation for the $H \to \gamma\gamma$ amplitude and therefore involves the same ambiguity for calculating λ. Third, one could examine the W-boson contribution to $H \to \gamma\gamma$ within the dispersion relation approach. It can be shown (ref. [187]) that the non-vanishing limit at $g_W \to 0$ is due to a finite subtraction induced by the corresponding trace anomaly [188]. However, in order to calculate unambigiously this finite piece, one has to make full use of a (physical) boundary condition of the theory.

As a final remark, suppose that we did not know DR and wanted to calculate a certain observable in 4-dimensions. In this observable we encounter singularities i.e., undefined and undetermined integrals. Then we use physics arguments to fix these ambiguities. However, we can always question whether we are using the right physics set up or not. In that sense the final judgement should come from the experiment. Therefore it may be not only academic to ask whether LHC could see the difference between $\lambda = -1$ and $\lambda = 0$? Setting the SM Higgs mass $m_H = 125$ GeV, and including the top-loop contribution, we find

$$\frac{\mathrm{Br}(H \to \gamma\gamma,\, \lambda = 0)}{\mathrm{Br}(H \to \gamma\gamma,\, \lambda = -1)} \;\approx\; 0.46\;. \tag{4.28}$$

This is certainly within LHC's sensitivity for 14 TeV c.m energy and luminosity of $30\,fb^{-1}$ (see for example Fig. 3 in ref. [189]). In fact, the recent observation by LHC experiments [4, 5] indicates a value $\frac{\mathrm{Br}(H\to\gamma\gamma,(\mathrm{exp}))}{\mathrm{Br}(H\to\gamma\gamma,\lambda=-1)} = 1.6 \pm 0.3$ (see ref. [190]) which highly disfavours the case $\lambda = 0$ by almost four standard deviations. We can turn this around and state that this is an indirect hint towards the validity of the equivalence theorem.

4.5 Conclusions

In this work we review the W-gauge boson loop contribution to the $H \to \gamma\gamma$ amplitude in the unitary gauge. Our objective is to fix intermediate step indeterminacies arising from divergent diagrams by making full use of physics at $d = 4$ much in the same way as in the calculation of the chiral anomaly triangle in the previous Chapter.

We anticipate a finite result for the loop induced $H \to \gamma\gamma$-amplitude in the renormalizable SM. Therefore the amplitude has to be independent of any shifting momentum variables we have originally introduced. But finite or even log-divergent integrals are independent of these vectors, so the vectors have to be accompanied only by infinite contributions, if at all. Therefore, infinities and arbitrary vectors are eliminated altogether by a certain combination among them [see eq. (4.7)].

The whole calculation in the unitary gauge boils down to a logarithmically divergent integral given by eq. (4.10). We find that, this integral results in two different values depending on whether $d \to 4$ or $d = 4$. This is due to a surface term remaining at the exact $d = 4$ case after the part-by-part integration in d-dimensions presented in Appandix M. To proceed, we identify this integral with an undefined parameter λ [see eq. (4.12)]. This parameter is then fixed unambiguously by assuming the validity of the Goldstone Boson Equivalence Theorem (GBET). Its value is consistent with DR in the limit $d \to 4$.

In our calculation we are very careful not to perform shifting of integration variables for highly divergent integrals by introducing three arbitrary momentum variable shift vectors straight from the beginning. Divergencies and arbitrariness from these unknown vectors are altogether removed, leaving behind a log-like divergent integral in $\mathcal{M}_2$ of eq. (4.2). This is defined by a physical input taken from the GBET and is connected to $\mathcal{M}_1$ by electromagnetic charge conservation.

As noted many times in the text, the key point towards deriving an unambiguous amplitude for $H \to \gamma\gamma$ in the unitary gauge is the limit of vanishing gauge couplings; this is an aspect of GBET [eq. (4.17)]. In this limit, the Goldstone boson loop contribution to the coefficient $\mathcal{M}_2$ is finite, i.e., independent of any regularisation scheme.

We also saw that DR (FDR), a regularisation scheme introduced to maintain Ward Identities at intermediate steps of a calculation, supports the GBET in the limit $d \to 4$ ($d = 4$). On the contrary, we find that, performing the integrals in $d = 4$ with symmetric integration is not a good choice because it leads to the violation of gauge invariance [see eq. (4.23) and the discussion below]. The main reason is due to surface terms that are developed in exactly $d = 4$ dimensions [see discussion below eq. (4.10) and Appendix M]. The latter are axiomatically discarded in DR [33, 171]. Another reason is the appearance of the $(d-4)$-term in the numerator of eq. (4.24).

In conclusion, the four-dimensional calculation of $H \to \gamma\gamma$ amplitude in the unitary gauge is ambiguous without introduction of a physics input beyond gauge invariance. As we have demonstrated, this physics, which uniquely defines the amplitude, may arise from the Goldstone Boson Equivalence Theorem (GBET). This effectively proves that GBET constitutes an additional important pillar of the Standard Model dynamics.

Chapter 5

Conclusions and future directions

Theories beyond the SM are worth studying since they provide possible answers to questions that in the SM framework remain open. In this thesis we deal with topics related to some of these questions such as the searches about the nature of dark matter, the mechanism of mass generation, the identification of the recently discovered particle at LHC with the Higgs boson of SM.

We used Quantum Field Theory tools throughout our work and developed a new method to handle different kind of divergences that appear during the calculations. In the basis of this method we showed a preference in performing the calculations in the physical choice of four dimensions and in the framework of the physical gauge (unitary gauge). We deliberately chose this gauge, although such a choice leads to difficulties coming from the high degree of divergences associated with it. We successfully applied this method in two different cases: the evaluation of chiral anomalies and their role to heavy fermion non-decoupling effects and the clarification of some issues in the decay of Higgs boson to two photons in the SM. In the last case, to the best of our knowledge, the use of this method constitutes a novel element. The encouraging fact is that we were able to verify well known results in the literature and received support from another recently proposed method (FDR) that also operates in the same four-dimensional basis. Another fact is that our method is applicable in every other gauge. The only negative fact so far, is the absence of calculational flexibility, since one has to handle a considerable amount of calculations. However, this can be bypassed by developing an appropriate computational program.

Our work constitutes a triptych with common element the use of QFT tools and the treatment of interesting topics of modern physics.

First, we presented a scenario where dark matter particles can decay into SM leptons through a light mediator. In this case we studied conventional dark matter searches, but a more detailed analysis has been performed for the case of unconventional dark matter searches, where low energy electrons are detected in the final state. We developed the theoretical framework where different models about this process, are presented. We showed that the dark sector "communicates" with the SM one, through interactions with an X-boson which couples to the SM gauge sector. This X boson could be massless or massive, depending on the model. We have also presented a detailed study

of time modulation effects and have considered that the dark matter particle can be a Dirac or Majorana fermion. In the second case the cross section for annihilation to fermions is suppressed by a factor of $\beta^2 \approx 10^{-6}$ compared with the corresponding cross section for the Dirac case. Studying the low energy electron recoil, we have considered only hydrogen-like atoms. However, we have found the cross section as a function of binding energy. This fact manifests indirectly how the cross section depends on the choice of the target material. For accurate results one should consider the real electronic wave-functions in the target's atoms. There was a proposal for the development of an experimental device with promising abilities in the dark matter non-conventional searches. Subsequently, astrophysical results which showed an excess in γ-ray emission in our galaxy, motivated us to study dark matter scattering processes where one or two photons were included in the final case.

Especially we were concerned about fermionic loop induced triple interactions of this type. This, naturally led us to generalize this special case and study the most general one loop triple gauge boson vertex. A complete one particle irreducible vertex for three off-shell gauge bosons is a useful tool in analyzing low energy inelastic scattering processes. We constructed the most general Lorentz invariant triple gauge boson vertex containing one fermionic loop. During this construction we encountered the case of linearly divergent integrals. In order to handle this problem we introduced arbitrary, constant four-vectors and performed the entire calculation in four dimensions. We chose this method instead of dimensional regularization in order to avoid any difficulty with the γ^5 anti-commutativity in the case of more than four dimensions. To determine the complete form of triple gauge boson vertex, we used Ward Identities and Bose symmetry and showed that the final result is not divergent, but ambiguous. This fact is directly connected with the chiral anomalies. The anomalous term is responsible for the anomaly that characterizes the vertex. In an anomalous free model this term does not exist and no ambiguity appears. In this basis we examined what happens in the case that the virtual fermions circulated in the loop become very heavy. In this case the anomalous term plays a crucial role in rendering the whole theory self-consistent. The reason is that, by integrating out the heavy fermions from an anomalous free theory, there is a surviving term. This term exactly cancels the anomalous term that appears in the low energy theory after integrating out the heavy particles. These heavy fermions non-decoupling effects render the low energy theory anomalous free. A next step was the presentation of different applications of the triple gauge boson vertex in the SM and some of its extensions. We constructed several anomalous free toy models with two or three different external gauge bosons and a number of fermions and also considered models with a fourth fermion generation and an extra gauge boson (Z'-boson models). In principle, these models can be used as a basis towards realistic extensions of the SM.

Subsequently we used the method of arbitrary four-vectors to clarify some issues about $H \to \gamma\gamma$ decay in the SM. We performed the calculation of the matrix element for this process, in exactly four-dimensions and in the unitary gauge. The choice of the unitary gauge renders the amplitude highly divergent, due to the form of W boson propagator. The arbitrary vectors play a crucial role in reducing these divergencies to

logarithmic one. However the final result is ambiguous. In order to unambiguously determine the result we used physics arguments, gauge invariance and the Goldstone Boson Equivalence Theorem. As an alternative choice we checked our calculation using the FDR method, a four-dimensional regularization scheme introduced to maintain the Ward Identities in the intermediate steps of calculations. In both cases we verified the well-known result in the literature for this process.

Certainly there are different extensions of this work. In the case of dark matter searches through electron recoil one can make use of the realistic wave functions instead of plane waves, to calculate the relevant cross section and event rates. An other direction is the study of the process $\chi + H \to (\chi + H)$ (bound state), where in the final state the WIMP, χ forms a bound state with the hydrogen atom. Furthermore, the dark matter scattering process involving a photon in the final state, is an interesting example of using the results from our analysis on triple gauge boson vertices.

Our study of triple gauge boson vertices opens a wide field of interesting applications with perspectives in extensions of SM. We can mention here the $(p, \overline{p})$ annihilation in W-bosons, the examination of decoupling or non-decoupling effects of heavy fermions in anomalous models by construction. In our work we studied several anomalous free models and revealed the synergy between chiral anomalies and non decoupling phenomena. The next step is to further extent this analysis in order to include chiral anomalous models and investigate if an analogous synergy takes place.

From the technical point of view, we are interested in applying the method of four-dimensional calculations using arbitrary vectors to other observables except from triple vertices that contain internal or external gauge bosons. Possible candidates are FCNC (Flavour Changing Neutral Currents) phenomena, such as top quark decays of the form $t \to c\,h$, $t \to c\,Z$, $t \to c\,\gamma$, the anomalous muon magnetic moment etc.

A big challenge constitutes the proof of renormalizability of a theory in the unitary gauge by using our four-dimensional approach. As we know, there is not so far a rigorous proof of renormalizability of a theory working in the unitary gauge from the beginning. The usual approach is to prove the renormalizability in the general R_ξ gauge and then to take the appropriate limits in order to obtain the desired property in the unitary gauge. It is evident that the calculational effort will be incomparable with that of the one loop calculation case. This manifests the necessity of developing and properly incorporating our method in the framework of a suitable computing program.

Appendix A: Dirac matrices and DR basics

Since we have repeatedly used some basic mathematical concepts in our calculations, we present in this first Appendix a short, representative collection of them. First of all some issues of basic Dirac algebra are presented, focusing on some properties of γ-matrices, especially on anticommutation relations and relations that traces of a set of γ-matrices obey. These have been used extensively in Chapters 2 and 3 during calculations of cross sections and triangular anomalies respectively. The notation used here, follows ref. [34]. In momentum space the Dirac equation has the following form:

$$\not{p} u^s(p) = m\, u^s(p), \tag{A.1}$$

where $u^s(p)$ represents a spinor with spin s, momentum p and mass m, and as usually $\not{p} \equiv \gamma^\mu p_\mu$. The γ^μ represent a set of four-dimensional matrices which satisfy the following anticommutation relation $\{\gamma^\mu, \gamma^\nu\} = 2\, g^{\mu\nu}$, where $g^{\mu\nu} = g_{\mu\nu} \equiv diag[1, -1, -1, -1]$ is the metric tensor and μ, $\nu = (0, 1, 2, 3)$. In a chiral basis these matrices have the form:

$$\gamma^\mu = \begin{pmatrix} 0 & \sigma^\mu \\ \overline{\sigma}^\mu & 0 \end{pmatrix}, \tag{A.2}$$

where $\sigma^\mu = (I, \vec{\sigma})$ and $\overline{\sigma}^\mu = (I, -\vec{\sigma})$. Here I represents the 2×2 unit matrix and $\vec{\sigma} = (\sigma^1, \sigma^2, \sigma^3)$, where σ^1, σ^2 and σ^3 are the Pauli matrices,

$$\sigma^1 = \begin{pmatrix} 0 & 1 \\ 1 & 0 \end{pmatrix}, \quad \sigma^2 = \begin{pmatrix} 0 & -i \\ i & 0 \end{pmatrix}, \quad \sigma^3 = \begin{pmatrix} 1 & 0 \\ 0 & -1 \end{pmatrix}. \tag{A.3}$$

We introduce the chirality matrix γ^5 as follows:

$$\gamma^5 = i\gamma^0\gamma^1\gamma^2\gamma^3 = -\frac{1}{4!}\epsilon^{\mu\nu\rho\sigma}\gamma_\mu\gamma_\nu\gamma_\rho\gamma_\sigma = \begin{pmatrix} -I & 0 \\ 0 & I \end{pmatrix}. \tag{A.4}$$

Some useful properties that γ-matrices obey *only* in four dimensions are:

$$\begin{gathered} \gamma^\mu\gamma_\mu = 4I_4,\ \gamma^\mu\gamma^\nu\gamma_\mu = -2\gamma^\nu,\ \gamma^\mu\gamma^\nu\gamma^\rho\gamma_\mu = 4g^{\nu\rho}, \\ \gamma^\mu\gamma^\nu\gamma^\rho\gamma^\sigma\gamma_\mu = -2\gamma^\sigma\gamma^\rho\gamma^\nu,\ \gamma^0(\gamma^\mu)^\dagger\gamma^0 = \gamma^\mu, (\gamma^0)^2 = I_4, (\gamma^0)^\dagger = \gamma^0, \\ \{\gamma^5, \gamma^\nu\} = 0,\ (\gamma^5)^2 = I_4,\ (\gamma^5)^\dagger = \gamma^5. \end{gathered} \tag{A.5}$$

Traces of γ-matrices satisfy the following relations:

$$\begin{aligned} &\mathbf{Tr}[I_4] = 4,\ \ \mathbf{Tr}[\gamma^\mu\gamma^\nu] = 4g^{\mu\nu},\ \mathbf{Tr}[\gamma^\mu\gamma^\nu\gamma^\rho\gamma^\sigma] = 4(g^{\mu\nu}g^{\rho\sigma} - g^{\mu\rho}g^{\nu\sigma} + g^{\mu\sigma}g^{\nu\rho}), \\ &\mathbf{Tr}[\gamma^5] = 0,\ \mathbf{Tr}[\gamma^\mu\gamma^\nu\gamma^5] = 0,\ \mathbf{Tr}[\gamma^\mu\gamma^\nu\gamma^\rho\gamma^\sigma\gamma^5] = -4i\epsilon^{\mu\nu\rho\sigma}, \\ &\mathbf{Tr}[\gamma^{\mu_1}\gamma^{\mu_2}\gamma^{\mu_3}....] = \mathbf{Tr}[.....\gamma^{\mu_1}\gamma^{\mu_2}\gamma^{\mu_3}], \\ &\mathbf{Tr}[\gamma^{\mu_1}\gamma^{\mu_2}\gamma^{\mu_3}.....\gamma^{\mu_n}] = 0 = \mathbf{Tr}[\gamma^{\mu_1}\gamma^{\mu_2}\gamma^{\mu_3}.....\gamma^{\mu_n}\gamma^5]. \end{aligned} \tag{A.6}$$

The relation in the third line above is the cyclic property of the trace, and the expression in the last line is valid when the number of γ matrices in the trace is an odd number.

Using the definition and properties of γ^5-matrix we can define two projection operators, useful in chiral representation of fermionic fields:

$$\Psi_L \equiv P_L\Psi, \qquad \Psi_R \equiv P_R\Psi, \tag{A.7}$$

where Ψ represents a four-component Dirac spinor, and P_L and P_R are the projection operators defined as:

$$P_L \equiv \frac{I_4 - \gamma^5}{2} = \begin{pmatrix} I & 0 \\ 0 & 0 \end{pmatrix}, \qquad P_R \equiv \frac{I_4 + \gamma^5}{2} = \begin{pmatrix} 0 & 0 \\ 0 & I \end{pmatrix}. \tag{A.8}$$

Since $(\gamma^5)^2 = I_4$ the following relations are obvious:

$$P_L P_L = P_L,\ P_R P_R = P_R,\ P_L P_R = P_R P_L = 0. \tag{A.9}$$

Secondly we append here some useful expressions about dimensional regularization. In order to deal with calculations of Feynman diagrams that contain loops, one introduces the Feynman parameters technique. The following decomposition of a combination of propagator denominators usually appears :

$$\frac{1}{A_1 A_2 ... A_n} = \int_0^1 dx_1 ... dx_n\, \delta\Big(\sum_{i=1}^{n} x_i - 1\Big) \frac{(n-1)!}{[x_1 A_1 + x_2 A_2 + ... + x_n A_n]^n}, \tag{A.10}$$

where A_1, $A_2, ... A_n$ are functions of the integration variable (loop momentum) and x_1, $x_2, ... x_n$ are real numbers such that $0 < x_i < 1$ and $x_1 + x_2 + ... + x_n = 1$, called Feynman parameters. In order to proceed, we complete the square in the denominator, shifting at the same time the integration variable p to absorb linear terms resulting to a shifted integration variable ℓ. Subsequently the denominator is simplified taking the form $(\ell^2 - \Delta)^n$, where Δ is a scalar function of internal loop masses and inner products of external momenta. The numerator is transformed in a function of even powers of ℓ, since all terms that contain odd powers of the integration variable ℓ vanish after symmetric integration. According to dimensional regularization we proceed from four to d dimensions and then we calculate d-dimensional loop integrals. Since we have completed the d-dimensional calculation, taking the limit $d \to 4$ we obtain the physical result.

A representative collection of some d-dimensional integrals in Minkowski space is the following:

$$\int \frac{d^d\ell}{(2\pi)^d}\frac{1}{(\ell^2-\Delta)^n} = \frac{(-1)^n\, i}{(4\pi)^{d/2}}\,\frac{\Gamma(n-\frac{d}{2})}{\Gamma(n)}\Big(\frac{1}{\Delta}\Big)^{n-\frac{d}{2}} \tag{A.11}$$

$$\int \frac{d^d\ell}{(2\pi)^d}\frac{\ell^2}{(\ell^2-\Delta)^n} = \frac{(-1)^{n-1}\, i}{(4\pi)^{d/2}}\,\frac{d}{2}\,\frac{\Gamma(n-\frac{d}{2}-1)}{\Gamma(n)}\Big(\frac{1}{\Delta}\Big)^{n-\frac{d}{2}-1} \tag{A.12}$$

$$\int \frac{d^d\ell}{(2\pi)^d}\frac{\ell^\mu\ell^\nu}{(\ell^2-\Delta)^n} = \frac{(-1)^{n-1}\, i}{(4\pi)^{d/2}}\,\frac{g^{\mu\nu}}{2}\,\frac{\Gamma(n-\frac{d}{2}-1)}{\Gamma(n)}\Big(\frac{1}{\Delta}\Big)^{n-\frac{d}{2}-1} \tag{A.13}$$

$$\int \frac{d^d\ell}{(2\pi)^d}\frac{(\ell^2)^2}{(\ell^2-\Delta)^n} = \frac{(-1)^n\, i}{(4\pi)^{d/2}}\,\frac{d(d+2)}{4}\,\frac{\Gamma(n-\frac{d}{2}-2)}{\Gamma(n)}\Big(\frac{1}{\Delta}\Big)^{n-\frac{d}{2}-2} \tag{A.14}$$

$$\begin{aligned}\int \frac{d^d\ell}{(2\pi)^d}\frac{\ell^\mu\ell^\nu\ell^\rho\ell^\sigma}{(\ell^2-\Delta)^n} &= \frac{(-1)^n\, i}{(4\pi)^{d/2}}\,\frac{\Gamma(n-\frac{d}{2}-2)}{\Gamma(n)}\Big(\frac{1}{\Delta}\Big)^{n-\frac{d}{2}-2}\times \\ &\times\ \frac{1}{4}(g^{\mu\nu}g^{\rho\sigma}+g^{\mu\rho}g^{\nu\sigma}+g^{\mu\sigma}g^{\nu\rho}),\end{aligned} \tag{A.15}$$

where $\Gamma(x)=\int_0^\infty t^{x-1}e^{-t}dt$ is the Euler Gamma function. This integral function is everywhere analytic except at non-positive integers where it has simple poles. For positive integers n it is $\Gamma(n)=(n-1)!$ and near its poles $x=-n$ it has the following expansion:

$$\Gamma(x)=\frac{(-1)^n}{n!}\Big(\frac{1}{x+n}-\gamma+1+...+\frac{1}{n}+\mathcal{O}(x+n)\Big), \tag{A.16}$$

where $\gamma\approx 0.5772$ is the Euler-Mascheroni constant. Often, as one takes the limit $d\to 4$, the following expression appears:

$$\frac{\Gamma(2-\frac{d}{2})}{(4\pi)^{d/2}}\Big(\frac{1}{\Delta}\Big)^{2-\frac{d}{2}}=\frac{1}{(4\pi)^2}\Big(\frac{2}{\epsilon}-\log\Delta-\gamma+\log(4\pi)+\mathcal{O}(\epsilon)\Big), \tag{A.17}$$

where $\epsilon=4-d$. To obtain eq. (A.17) we have used eq. (A.16) and the following expansion:

$$\Big(\frac{1}{\Delta}\Big)^{2-\frac{d}{2}}=1-(2-\frac{d}{2})\log\Delta+..., \tag{A.18}$$

when $d\to 4$. In the expression given by eq. (A.17) the pole is clearly isolated. This isolation is useful in order to guarantee the cancellations of infinite quantities when different Feynman diagrams are combined together.

Appendix B: Feynman propagator

In this Appendix we will clarify some computational issues related to expressions appearing in Chapter[2]. In order to find the Feynman propagator in eq. (2.3) we recall the definition of the action $S = \int d^4x\, \mathscr{L}$, where $\mathscr{L}$ is the Lagrangian density given by eq. (2.2). First of all in eq. (2.2) we assume that the field $\mathbf{\Phi}_\mu(x)$ has the following expansion as a Fourier integral, $\mathbf{\Phi}_\mu(x) = \int \frac{d^4p}{(2\pi)^4}\, \tilde{\mathbf{\Phi}}_\mu(p)\, e^{i\,p\cdot x}$, where $\tilde{\mathbf{\Phi}}_\mu(p)$ is the Fourier transform of $\mathbf{\Phi}_\mu(x)$. Then $\partial_\alpha \mathbf{\Phi}_\mu(x) = \int \frac{d^4p}{(2\pi)^4}\, \tilde{\mathbf{\Phi}}_\mu(p)\, (i\,p_\alpha)\, e^{i\,p\cdot x}$. Considering that the field strength tensor is $\mathbf{\Phi}_{\mu\nu} \equiv \partial_\mu \mathbf{\Phi}_\nu - \partial_\nu \mathbf{\Phi}_\mu$, and using the first three terms of eq. (2.2), the action takes the following form:

$$\begin{aligned} S &\sim \int d^4x \left[-\frac{1}{4} \left(\partial_\mu \mathbf{\Phi}_\nu^T - \partial_\nu \mathbf{\Phi}_\mu^T\right) \mathcal{K} \left(\partial^\mu \mathbf{\Phi}^\nu - \partial^\nu \mathbf{\Phi}^\mu\right) + \frac{1}{2}\, \mathbf{\Phi}_\mu^T\, \mathcal{M}^2\, \mathbf{\Phi}^\mu - \frac{1}{2}\, \partial^\mu \mathbf{\Phi}_\mu^T\, \Xi\, \partial^\nu \mathbf{\Phi}_\nu \right] = \\ &= \int d^4x \left[-\frac{1}{4} \Big(\partial_\mu \mathbf{\Phi}_\nu{}^T\, \mathcal{K}\, \partial^\mu \mathbf{\Phi}^\nu - \partial_\mu \mathbf{\Phi}_\nu{}^T\, \mathcal{K}\, \partial^\nu \mathbf{\Phi}^\mu - \partial_\nu \mathbf{\Phi}_\mu{}^T\, \mathcal{K}\, \partial^\mu \mathbf{\Phi}^\nu + \partial_\nu \mathbf{\Phi}_\mu{}^T\, \mathcal{K}\, \partial^\nu \mathbf{\Phi}^\mu \Big) + \right. \\ &\qquad \left. + \frac{1}{2} \mathbf{\Phi}_\mu^T\, \mathcal{M}^2\, \mathbf{\Phi}^\mu - \frac{1}{2} \partial^\mu \mathbf{\Phi}_\mu^T\, \Xi\, \partial^\nu \mathbf{\Phi}_\nu \right]. \end{aligned} \tag{B.1}$$

Using integration by parts one obtains:

$$\begin{aligned} S \sim\ &-\ \frac{1}{4} \Big(\oint_{\mathcal{S}} d^3x_\mu \mathbf{\Phi}_\nu^T\, \mathcal{K}\, \partial^\mu \mathbf{\Phi}^\nu - \int d^4x\, \mathbf{\Phi}_\nu^T\, \mathcal{K}\, \partial_\mu\, \partial^\mu \mathbf{\Phi}^\nu - \oint_{\mathcal{S}} d^3x_\mu \mathbf{\Phi}_\nu^T\, \mathcal{K}\, \partial^\nu \mathbf{\Phi}^\mu + \\ &+ \int d^4x\, \mathbf{\Phi}_\nu^T\, \mathcal{K}\, \partial_\mu\, \partial^\nu \mathbf{\Phi}^\mu - \oint_{\mathcal{S}} d^3x_\nu \mathbf{\Phi}_\mu^T\, \mathcal{K}\, \partial^\mu \mathbf{\Phi}^\nu + \int d^4x\, \mathbf{\Phi}_\mu^T\, \mathcal{K}\, \partial_\nu\, \partial^\mu \mathbf{\Phi}^\nu + \\ &+ \oint_{\mathcal{S}} d^3x_\nu \mathbf{\Phi}_\mu^T\, \mathcal{K}\, \partial^\nu \mathbf{\Phi}^\mu - \int d^4x\, \mathbf{\Phi}_\mu^T\, \mathcal{K}\, \partial_\nu\, \partial^\nu \mathbf{\Phi}^\mu \Big) + \frac{1}{2} \int d^4x\, \mathbf{\Phi}_\mu^T\, \mathcal{M}^2\, \mathbf{\Phi}^\mu - \\ &- \frac{1}{2} \Big(\oint_{\mathcal{S}} d^3x^\mu\, \mathbf{\Phi}_\mu^T\, \Xi\, \partial^\nu \mathbf{\Phi}_\nu - \int d^4x\, \mathbf{\Phi}_\mu^T\, \Xi\, \partial^\mu\, \partial^\nu \mathbf{\Phi}_\nu \Big), \end{aligned} \tag{B.2}$$

where $\oint_{\mathcal{S}}$ is the surface integral over a 3-dimensional sphere $\mathcal{S}$ with infinite radius. Considering that the fields $\mathbf{\Phi}_\mu(x)$ vanish at infinity, all the surface integrals vanish and the action reads:

$$\begin{aligned} S &\sim \frac{1}{2} \int d^4x \left[\mathbf{\Phi}_\mu^T\, \mathcal{K}\, \partial_\nu\, \partial^\nu \mathbf{\Phi}^\mu\ - \mathbf{\Phi}_\mu^T\, \mathcal{K}\, \partial_\nu\, \partial^\mu \mathbf{\Phi}^\nu + \mathbf{\Phi}_\mu^T\, \mathcal{M}^2\, \mathbf{\Phi}^\mu + \mathbf{\Phi}_\mu^T\, \Xi\, \partial^\mu\, \partial^\nu \mathbf{\Phi}_\nu \right] = \\ &= \frac{1}{2} \int d^4x\, \mathbf{\Phi}_\mu^T \left[g^{\alpha\beta} g^{\mu\nu}\, \mathcal{K}\, \partial_\alpha\, \partial_\beta - g^{\nu\alpha} g^{\mu\beta} \mathcal{K}\, \partial_\alpha\, \partial_\beta + g^{\mu\nu}\, \mathcal{M}^2 + g^{\mu\alpha}\, g^{\nu\beta}\, \Xi\, \partial_\alpha\, \partial_\beta \right] \mathbf{\Phi}_\nu = \\ &= \frac{1}{2} \int d^4x \int \frac{d^4p}{(2\pi)^4} \int \frac{d^4p'}{(2\pi)^4}\, \tilde{\mathbf{\Phi}}_\mu^T(p)\, e^{i\,p\cdot x} \left[g^{\alpha\beta} g^{\mu\nu}\, \mathcal{K}\, \partial_\alpha\, \partial_\beta - g^{\nu\alpha} g^{\mu\beta} \mathcal{K}\, \partial_\alpha\, \partial_\beta + \right. \\ &\qquad \left. + g^{\mu\nu}\, \mathcal{M}^2 + g^{\mu\alpha}\, g^{\nu\beta}\, \Xi\, \partial_\alpha\, \partial_\beta \right] \tilde{\mathbf{\Phi}}_\nu(p')\, e^{i\,p'\cdot x} = \\ &= \frac{1}{2} \int d^4x \int \frac{d^4p}{(2\pi)^4} \int \frac{d^4p'}{(2\pi)^4}\, \tilde{\mathbf{\Phi}}_\mu^T(p)\, e^{i\,p\cdot x} \left[g^{\alpha\beta} g^{\mu\nu}\, \mathcal{K}\, (-p'_\alpha\, p'_\beta) - g^{\nu\alpha} g^{\mu\beta} \mathcal{K}\, (-p'_\alpha\, p'_\beta) + \right. \\ &\qquad \left. + g^{\mu\nu}\, \mathcal{M}^2 + g^{\mu\alpha}\, g^{\nu\beta}\, \Xi\, (-p'_\alpha\, p'_\beta) \right] \tilde{\mathbf{\Phi}}_\nu(p')\, e^{i\,p'\cdot x}. \end{aligned} \tag{B.3}$$

Performing the integration over x and using the well-known integral representation of the Dirac $\delta^{(4)}$-functional $\int \frac{d^4x}{(2\pi)^4}\, e^{i\,x\cdot(p+p')} = \delta^{(4)}(p+p')$, one finds:

$$\begin{aligned} S \;\sim\; & \frac{1}{2}\int \frac{d^4p}{(2\pi)^4}\int d^4p'\,\tilde{\mathbf{\Phi}}^T_\mu(p)\Big[g^{\alpha\beta}g^{\mu\nu}\,\mathcal{K}\,(-p'_\alpha\,p'_\beta) - \; g^{\nu\alpha}g^{\mu\beta}\mathcal{K}\,(-p'_\alpha\,p'_\beta) + \\ & \qquad\qquad + g^{\mu\nu}\,\mathcal{M}^2 \;+\; g^{\mu\alpha}\,g^{\nu\beta}\;\Xi\,(-p'_\alpha\,p'_\beta)\Big]\tilde{\mathbf{\Phi}}_\nu(p')\,\delta^4(p+p') = \\ = \;& -\frac{1}{2}\int \frac{d^4p}{(2\pi)^4}\,\tilde{\mathbf{\Phi}}^T_\mu(p)\left[g^{\mu\nu}\,\mathcal{K}\,p^2 - \;\mathcal{K}\,p^\mu\,p^\nu \;- g^{\mu\nu}\,\mathcal{M}^2 \;+\; \Xi\,p^\mu\,p^\nu\right]\tilde{\mathbf{\Phi}}_\nu(-p) = \\ = \;& -\frac{1}{2}\int \frac{d^4p}{(2\pi)^4}\,\tilde{\mathbf{\Phi}}^T_\mu(p)\left[(\mathcal{K}\,p^2-\mathcal{M}^2)(g^{\mu\nu} \;-\frac{p^\mu\,p^\nu}{p^2}) + \;(\Xi\,p^2-\mathcal{M}^2)\frac{p^\mu\,p^\nu}{p^2}\;\right]\tilde{\mathbf{\Phi}}_\nu(-p), \end{aligned} \tag{B.4}$$

where in the third line the integration of $\delta^{(4)}$-function over p' has set $p' \to -p$. If we define

$$\Delta^{\mu\nu}(p) \equiv \; -\left(\mathcal{K}\,p^2-\mathcal{M}^2\right)\left(g^{\mu\nu} \;-\frac{p^\mu\,p^\nu}{p^2}\right) - \;\left(\Xi\,p^2-\mathcal{M}^2\right)\frac{p^\mu\,p^\nu}{p^2}, \tag{B.5}$$

then the Feynman propagator $\widetilde{\mathcal{D}}^{\mu\nu}(p)$ is required to satisfy the following equation in momentum space:

$$\Delta^{\mu\nu}(p)\,\widetilde{\mathcal{D}}_{\mu\alpha}(p) = i\,g^\nu{}_\alpha \tag{B.6}$$

Decomposing the propagator into a transverse and a longitudinal part as follows, $i\,\widetilde{\mathcal{D}}_{\mu\nu}(p) = (g_{\mu\nu} \;-\frac{p_\mu\,p_\nu}{p^2})\widetilde{\mathcal{D}}_T + \frac{p_\mu p_\nu}{p^2}\widetilde{\mathcal{D}}_L$, we can easily conclude that $\widetilde{\mathcal{D}}_T = (\mathcal{K}\,p^2-\mathcal{M}^2)^{-1}$ and $\widetilde{\mathcal{D}}_L = (\Xi\,p^2-\mathcal{M}^2)^{-1}$, verifying eq. (2.3). Applying eq. (2.3) in different models we can find in each case the corresponding form of the propagator.

Appendix C: Non-standard mass mixing

In this Appendix we find explicitly the effective action described in **Model II** (sec. 2.2.2). In **Model II** (Non-standard mass mixing), by working in Feynman gauge ($\Xi = \mathbf{1}_{3\times 3}$), assuming a trivial form for $\mathcal{K}$ and using eq. (2.13) for $\mathcal{M}^2$ we find for the propagator:

$$i\,\widetilde{\mathcal{D}}_{\mu\nu}(p) = g_{\mu\nu}\begin{pmatrix} p^2 - \frac{1}{4}\,g_Y^2 v^2 - m_Y^2 & -m_Y\,m_X & \frac{1}{4}\,g_Y g\,v^2 \\ -m_Y\,m_X & p^2 - m_X^2 & 0 \\ \frac{1}{4}\,g_Y g\,v^2 & 0 & p^2 - \frac{1}{4}\,g^2 v^2 \end{pmatrix}^{-1}. \tag{C.1}$$

Using eq. (2.4) for the effective action, by taking into account that $J_\mu(p) \equiv (g_Y J_Y(p),\, g_X J_X(p),\, g J_{A_3}(p))_\mu$, and considering the expression above for the propagator $i\,\widetilde{\mathcal{D}}_{\mu\nu}(p)$, we find up to order $\mathcal{O}(m_Y^2)$:

$$\begin{aligned} S[J] \;=\; & \frac{1}{2}\int \frac{d^4p}{(2\pi)^4}\Bigg\{ \frac{g_X^2 J_X(p)\cdot J_X(-p)}{p^2 - m_X^2} + \frac{g_Y^2\, J_Y(p)\cdot J_Y(-p)}{p^2 - m_Z^2} + \frac{g^2\, J_{A_3}(p)\cdot J_{A_3}(-p)}{p^2 - m_Z^2} - \\ & - \frac{g^2\, g_Y^2 v^2}{4\,p^2\,(p^2 - m_Z^2)}\Big(J_Y(p) + J_{A_3}(p)\Big)\cdot\Big(J_Y(-p) + J_{A_3}(-p)\Big) + \\ & + \frac{g_X\, g_Y\, m_X\, m_Y}{p^2\,(p^2 - m_X^2)(p^2 - m_Z^2)}\Bigg[p^2\Big(J_X(p)\cdot J_Y(-p) + J_X(-p)\cdot J_Y(p)\Big) - \\ & - \frac{1}{4}g^2 v^2\Big((J_{A_3}(p) + J_Y(p))\cdot J_X(-p) + (J_{A_3}(-p) + J_Y(-p))\cdot J_X(p)\Big)\Bigg]\Bigg\}, \end{aligned} \tag{C.2}$$

where $m_Z^2 = \frac{1}{4}v^2(g_Y^2 + g^2) + \mathcal{O}(m_Y^2)$. Changing the integration variable $p \to -p$, the terms in the second line and terms in the square bracket in the expression above are multiplied by a factor 2. Then the expression for $S[J]$ is simplifying further:

$$\begin{aligned} S[J] \;=\; & \frac{1}{2}\int \frac{d^4p}{(2\pi)^4}\Bigg\{ \frac{g_X^2 J_X(p)\cdot J_X(-p)}{p^2 - m_X^2} + \frac{g_Y^2\, J_Y(p)\cdot J_Y(-p)}{p^2 - m_Z^2} + \frac{g^2\, J_{A_3}(p)\cdot J_{A_3}(-p)}{p^2 - m_Z^2} - \\ & - \frac{g^2\, g_Y^2 v^2}{4\,p^2\,(p^2 - m_Z^2)}\Big(J_Y(p) + J_{A_3}(p)\Big)\cdot\Big(J_Y(-p) + J_{A_3}(-p)\Big) + \\ & + \frac{2\,g_X\, g_Y\, m_X\, m_Y}{p^2\,(p^2 - m_X^2)(p^2 - m_Z^2)}\Bigg[- \frac{1}{4}g^2 v^2\Big((J_{A_3}(p) + J_Y(p)\Big)\cdot J_X(-p) + \\ & + p^2\, J_X(p)\cdot J_Y(-p)\Bigg]\Bigg\}. \end{aligned} \tag{C.3}$$

As a next step we can analyze the expressions $\frac{1}{p^2\,(p^2 - m_X^2)(p^2 - m_Z^2)}$ and $\frac{1}{p^2(p^2 - m_Z^2)}$ in partial fractions as follows:

$$\begin{aligned} \frac{1}{p^2\,(p^2 - m_X^2)(p^2 - m_Z^2)} \;=\; & \frac{1}{m_X^2\,m_Z^2}\frac{1}{p^2} + \frac{1}{m_X^2\,(m_X^2 - m_Z^2)}\left(\frac{1}{p^2 - m_X^2}\right) - \\ & - \frac{1}{m_Z^2\,(m_X^2 - m_Z^2)}\left(\frac{1}{p^2 - m_Z^2}\right), \end{aligned} \tag{C.4a}$$

$$\text{and} \qquad \frac{1}{p^2(p^2 - m_Z^2)} \;=\; \frac{1}{m_Z^2}\left(\frac{1}{p^2 - m_Z^2} - \frac{1}{p^2}\right). \tag{C.4b}$$

Using the fact that $J_Y(p)+J_{A_3}(p) = J_{em}(p)$ for the electromagnetic current, and making use of eqs. (C.4a) and (C.4b), the eq.(C.3) takes the form:

$$\begin{aligned}
S[J] \;=\; & \frac{1}{2}\int \frac{d^4p}{(2\pi)^4}\Bigg\{\frac{1}{p^2}\Bigg[-\frac{g_X\, g_Y\, m_Y g^2 v^2}{2 m_X\, m_Z^2} J_{em}(p)\cdot J_X(-p) + \frac{g_Y^2\, g^2 v^2}{4\, m_Z^2} J_{em}(p)\cdot J_{em}(-p)\Bigg] + \\
& + \frac{1}{p^2-m_X^2}\Bigg[g_X^2 J_X(p)\cdot J_X(-p) + \frac{2\, g_X\, g_Y\, m_Y}{m_X\,(m_X^2-m_Z^2)}\, p^2\, J_X(p)\cdot J_Y(-p) \\
& - \frac{g_X\, g_Y\, m_Y g^2 v^2}{2\, m_X\,(m_X^2-m_Z^2)} J_{em}(p)\cdot J_X(-p)\Bigg] + \\
& + \frac{1}{p^2-m_Z^2}\Bigg[\frac{-2\, g_X\, g_Y\, m_X\, m_Y}{m_Z^2\,(m_X^2-m_Z^2)}\, p^2\, J_X(p)\cdot J_Y(-p) + \frac{g_X\, g_Y\, m_X\, m_Y\, g^2\, v^2}{2\, m_Z^2\,(m_X^2-m_Z^2)}\, J_{em}(p)\cdot J_X(-p) + \\
& + g_Y^2\, J_Y(p)\cdot J_Y(-p) + g^2\, J_{A_3}(p)\cdot J_{A_3}(-p) - \frac{g^2\, g_Y^2 v^2}{4\, m_Z^2}\, J_{em}(p)\cdot J_{em}(-p)\Bigg] \\
& + \frac{2\, g_X\, g_Y m_Y}{m_X\, m_Z^2} J_X(p)\cdot J_Y(-p)\Bigg\}. \qquad \text{(C.5)}
\end{aligned}$$

In what follows we can write the expression above as a function of the electric charge, considering that $e = \frac{g\, g_Y}{\sqrt{g^2+g_Y^2}}$ and absorb the vacuum expectation value using the relation $m_Z^2 = \frac{1}{4}v^2(g_Y^2+g^2) + \mathcal{O}(m_Y^2)$.

As a result we obtain:

$$\begin{aligned}
S[J] = & \frac{1}{2}\int \frac{d^4p}{(2\pi)^4}\Bigg\{\frac{1}{p^2}\Bigg[-\frac{2\, e^2\, g_X\, m_Y}{g_Y\, m_X} J_{em}(p)\cdot J_X(-p) + e^2\, J_{em}(p)\cdot J_{em}(-p)\Bigg] + \\
& + \frac{1}{p^2-m_X^2}\left(\frac{m_Z^2}{m_Z^2-m_X^2}\right)\Bigg[g_X^2 J_X(p)\cdot J_X(-p)\left(1-\frac{m_X^2}{m_Z^2}\right) - \frac{2\, g_X\, g_Y\, m_X\, m_Y}{m_Z^2}\, J_X(p)\cdot J_Y(-p) + \\
& + \frac{2\, e^2\, g_X\, m_Y}{g_Y\, m_X}\, J_{em}(p)\cdot J_X(-p)\Bigg] + \\
& + \frac{1}{p^2-m_Z^2}\left(\frac{m_Z^2}{m_Z^2-m_X^2}\right)\Bigg[g^2\, J_Z(p)\cdot J_Z(-p)\left(1-\frac{m_X^2}{m_Z^2}\right) + \frac{2\, g_X\, g_Y\, m_X\, m_Y}{m_Z^2}\, J_X(p)\cdot J_Y(-p) - \\
& - \frac{2\, e^2\, g_X\, m_X\, m_Y}{g_Y\, m_Z^2}\, J_{em}(p)\cdot J_X(-p)\Bigg]\Bigg\}, \qquad \text{(C.6)}
\end{aligned}$$

where $J_Z^\mu = \frac{1}{\cos\theta_W}\left(J_{A_3}^\mu - \sin^2\theta_W\, J_{em}^\mu\right)$ and also the following relation among different currents

$$\begin{aligned}
& g_Y^2\, J_Y(p)\cdot J_Y(-p) + g^2\, J_{A_3}(p)\cdot J_{A_3}(-p) - \frac{g^2\, g_Y^2 v^2}{4\, m_Z^2}\, J_{em}(p)\cdot J_{em}(-p) = \\
& = g^2\, J_Z(p)\cdot J_Z(-p), \qquad \text{(C.7)}
\end{aligned}$$

has been used.

Appendix D: Time modulation effects

In this Appendix we will show analytically how to obtain eq. (2.62) in the subsection "Event rates" in Chapter 2. Using eq. (2.53) for the WIMP's velocity distribution,

$$f_\ell(\beta) \;=\; \left(\frac{3}{2<\beta^2>}\right)^{3/2} \frac{1}{\pi^{3/2}}\, e^{-\frac{3\beta^2}{2<\beta^2>}}, \tag{D.1}$$

we can calculate the velocity's mean value in the unmodulated case:

$$\begin{aligned}\left(\frac{\beta f_\ell(\beta) d^3\beta}{\sqrt{<\beta^2>}}\right)_0 \;\rightarrow\; & \int d\Omega\, \frac{\beta^3 f_\ell(\beta) d\beta}{\sqrt{<\beta^2>}} = \left(\frac{2}{3<\beta^2>}\right)^{3/2} \frac{2\pi}{\pi^{3/2}} \frac{\beta^3 d\beta}{\sqrt{<\beta^2>}} e^{-\left(1+\frac{3\beta^2}{2\sqrt{<\beta^2>}}\right)} \times \\ & \times \int_0^\pi \sin\theta\, d\theta\, \exp\Big(-(2\,\beta\sqrt{\frac{3}{2<\beta^2>}}\cos\theta\Big),\end{aligned} \tag{D.2}$$

where $d\Omega$ is the infinitesimal solid angle in spherical coordinates and a factor of 2π has been included in the expression above due to integration over the azimuthal angle ϕ. Changing the integration variable, $\cos\theta \rightarrow \xi$, we find:

$$\begin{aligned}\left(\frac{\beta f_\ell(\beta) d^3\beta}{\sqrt{<\beta^2>}}\right)_0 \rightarrow \left(\frac{3}{2<\beta^2>}\right)^{3/2} \frac{2}{\sqrt{\pi}} \frac{\beta^3 d\beta}{\sqrt{<\beta^2>}} e^{-(1+\frac{3\beta^2}{2\sqrt{<\beta^2>}})} \int_{-1}^{1} d\xi\, e^{-\left(2\beta\sqrt{\frac{3}{2<\beta^2>}}\xi\right)} = \\ = \left(\frac{3}{2<\beta^2>}\right)^{3/2} \frac{2}{\sqrt{\pi}} \frac{\beta^3}{\sqrt{<\beta^2>}}\, e^{-\left(1+\frac{3\beta^2}{2\sqrt{<\beta^2>}}\right)} \frac{\sinh\left(2\beta\sqrt{\frac{3}{2<\beta^2>}}\right)}{\beta\sqrt{\frac{3}{2<\beta^2>}}} d\beta,\end{aligned} \tag{D.3}$$

verifying eq. (2.56).

In the case of time modulation effects, we consider the annual dependence of decay rate and assume the following expression for the WIMP velocity:

$$\mathbf{v'} \;=\; \mathbf{v} \;+\; v_0\,\widehat{\mathbf{z}} \;+\; v_1\,(\sin\alpha\,\widehat{\mathbf{x}} \;+\; \cos\alpha\cos\gamma\,\widehat{\mathbf{y}} \;+\; \cos\alpha\sin\gamma\,\widehat{\mathbf{z}})\,, \tag{D.4}$$

where $\mathbf{v}$ is the WIMP's velocity in the local system, $v_0 \rightarrow \beta_0 = \sqrt{\frac{2<\beta^2>}{3}}$ is the sun's velocity, v_1 is the Earth's velocity relative to the solar system, $\gamma \simeq \pi/6$ is the slope of the ecliptic and α is the time dependent angle that is the complementary angle of the angle between $\mathbf{v_1}$ and $\widehat{\mathbf{x}}$ (see Fig. 2.6). Analyzing the vector $\mathbf{v} = v\,\widehat{\mathbf{n}}$, where $\widehat{\mathbf{n}}$ the unit vector in the direction of $\mathbf{v}$, in spherical coordinates we find:

$$\begin{aligned}\mathbf{v'} \;=\; & (v\sin\theta\cos\phi + v_1\sin\alpha)\widehat{\mathbf{x}} + (v\sin\theta\sin\phi + v_1\cos\alpha\cos\gamma)\widehat{\mathbf{y}} + \\ & + (v\cos\theta + v_0 + v_1\cos\alpha\sin\gamma)\widehat{\mathbf{z}}.\end{aligned} \tag{D.5}$$

Squaring the expression above one obtains:

$$\begin{aligned}v'^2 \;=\; & v^2 + {v_0}^2 + {v_1}^2 + 2\,v\,v_1\sin\theta\cos\phi\sin\alpha + 2\,v\,v_1\sin\theta\sin\phi\cos\alpha\cos\gamma + \\ & + 2\,v\,v_0\cos\theta + 2\,v\,v_1\cos\theta\cos\alpha\sin\gamma + 2\,v_0\,v_1\cos\alpha\sin\gamma.\end{aligned} \tag{D.6}$$

Dividing by v_0^2 the expression above and using the abbreviations $\frac{v}{v_0} = \frac{\beta}{\beta_0} \equiv y$ and $\frac{v_1}{v_0} = \frac{v_1}{\beta_0} \equiv \delta$ we obtain the following expression relevant to convoluted decay rate:

$$\frac{\beta\, f_\ell(\beta) d^3\beta}{\sqrt{<\beta^2>}} \to \frac{1}{\sqrt{<\beta^2>}} \left(\frac{3}{2<\beta^2>}\right)^{3/2} \frac{\beta^3 d\beta}{\pi^{3/2}} \int d\Omega\, e^{-\frac{\beta'^2}{\beta_0^2}} =$$
$$= \left(\frac{3}{2(<\beta^2>)^{4/3}}\right)^{3/2} \frac{\beta^3 d\beta}{\pi^{3/2}} \int_0^{2\pi} d\phi\, \exp\Big[-2\,y\,\delta \sin\theta \big(\cos\phi \sin\alpha + \sin\phi\, \cos\alpha \cos\gamma\big)\Big] \times$$
$$\times \int_0^{\pi} \sin\theta\, d\theta\, \exp\Big[-\big(1 + y^2 + \delta^2 + 2\,y\, \cos\theta + 2\,y\,\delta \cos\theta \cos\alpha \sin\gamma + 2\,\delta \cos\alpha \sin\gamma\big)\Big]. \tag{D.7}$$

We can expand the integrand in the first line around δ, which is a perturbative parameter, and considering only terms of first power in this expansion we get:

$$\int_0^{2\pi} d\phi\, \exp\Big[-2\,y\,\delta \sin\theta \cos\phi \sin\alpha - 2\,y\,\delta \sin\theta \sin\phi \cos\alpha \cos\gamma\Big] \approx$$
$$\approx \int_0^{2\pi} d\phi \Big(1 - 2\,y\,\delta \sin\theta \cos\phi \sin\alpha - 2\,y\,\delta \sin\theta \sin\phi \cos\alpha \cos\gamma\Big) = 2\pi, \tag{D.8}$$

since terms that contain $\cos\phi$ and $\sin\phi$ vanish after the ϕ-integration. For the θ-integration we use $\cos\theta = \xi$ and neglecting δ^2-terms we obtain:

$$\int_0^{\pi} \sin\theta\, d\theta\, \exp\Big[-\big(1 + y^2 + 2\,y\, \cos\theta + 2\,\delta \cos\theta \cos\alpha \sin\gamma + 2\,\delta \cos\alpha \sin\gamma\big)\Big] =$$
$$= e^{-(1+y^2)} \int_{-1}^{1} d\xi\, \exp\Big[-\big(2\,y\,\xi + 2\,\delta \cos\alpha \sin\gamma\,(1 + y\,\xi)\big)\Big] \approx$$
$$\approx e^{-(1+y^2)} \int_{-1}^{1} d\xi\, \exp\Big(-(2\,y\,\xi)\Big)\Big[1 - 2\,\delta \cos\alpha \sin\gamma(1 + y\,\xi)\Big] =$$
$$= e^{-(1+y^2)} \left[\frac{\sinh(2\,y)}{y} - 2\,\delta \cos\alpha \sin\gamma \left(1 - \frac{y}{2}\frac{d}{dy}\right) \int_{-1}^{1} d\xi\, \exp(-2\,y\,\xi)\right] =$$
$$= e^{-(1+y^2)} \left[\frac{\sinh(2\,y)}{y} - 2\,\delta \cos\alpha \sin\gamma \left(1 - \frac{y}{2}\frac{d}{dy}\right) \frac{\sinh(2\,y)}{y}\right] =$$
$$= e^{-(1+y^2)} \left[\frac{\sinh(2\,y)}{y} - 2\,\delta \cos\alpha \sin\gamma \left(\frac{3\sinh(2\,y)}{2\,y} - \cosh(2\,y)\right)\right]$$
$$= e^{-(1+y^2)}\, \frac{\sinh(2\,y)}{y} \Big[1 + k\,\delta \cos\alpha\Big], \tag{D.9}$$

where

$$k = \left[2\,y\, \frac{\cosh(2\,y)}{\sinh(2y)} - 3\right] \sin\gamma = \left[2\,\beta \sqrt{\frac{3}{2<\beta^2>}}\, \frac{\cosh\left(2\,\beta\sqrt{\frac{3}{2<\beta^2>}}\right)}{\sinh\left(2\,\beta\sqrt{\frac{3}{2<\beta^2>}}\right)} - 3\right] \sin\gamma. \tag{D.10}$$

Finally, taking into account the values of ϕ and θ-integrals, the expression of eq. (D.7) for the mean value of WIMP's velocity relevant to time modulated effects, takes the following form:

$$\frac{\beta\, f_\ell(\beta) d^3\beta}{\sqrt{<\beta^2>}} \to \frac{1}{\sqrt{<\beta^2>}} \left(\frac{3}{2<\beta^2>}\right)^{3/2} \frac{\beta^3 d\beta}{\pi^{3/2}}\, 2\pi\, e^{-\left(1+y^2\right)}\, \frac{\sinh(2\,y)}{y} \Big[1 + k\,\delta\cos\alpha\Big] =$$

$$= \left(\frac{3}{2<\beta^2>}\right)^{3/2} \frac{\beta^2 d\beta}{\sqrt{<\beta^2>}}\, \frac{2}{\sqrt{\pi}}\, e^{-\left(1+\frac{3\beta^2}{2<\beta^2>}\right)}\, \frac{\sinh\left(2\,\beta\sqrt{\frac{3}{2<\beta^2>}}\right)}{\sqrt{\frac{3}{2<\beta^2>}}} \Big[1 + k\,\delta\cos\alpha\Big] =$$

$$= \left(\frac{\beta\, f_\ell(\beta) d^3\beta}{\sqrt{<\beta^2>}}\right)_0 \Big[1 + k\,\delta\cos\alpha\Big], \tag{D.11}$$

where $\left(\frac{\beta\, f_\ell(\beta) d^3\beta}{\sqrt{<\beta^2>}}\right)_0$ has been calculated in eq. (D.3) and is related to unmodulated effects.

Appendix E: Non relativistic cross section

This Appendix is based on ref. [84]. The problem is to find the WIMP - electron bounded in an atom, cross section. In order to proceed we shall make two simplified assumptions:

1. A hydrogen-like atom (H) is assumed i.e., a nucleus with charge $+Ze$ and a single bounded electron with charge $-e$.

2. The WIMP couples only to leptons and not to quarks. This is a sufficient condition to explain PAMELA/ATIC electron - positron excess events and it renders the following analysis fairly simple.

Furthermore, since the WIMP velocity, $\beta \approx 10^{-3}$ is small, we will frame the whole problem using non-relativistic quantum theory terms.

Although there are the following four processes that could take place in WIMP + H-like atom collisions:

$$\chi + H \longrightarrow \chi + H \quad \text{(elastic)}\,, \tag{E.1}$$
$$\chi + H \longrightarrow \chi + H^* \quad \text{(inelastic)}\,, \tag{E.2}$$
$$\chi + H \longrightarrow \chi + e^- + H^+ \quad \text{(production)}\,, \tag{E.3}$$
$$\chi + H \longrightarrow (\chi + H) \quad \text{(bound state)}, \tag{E.4}$$

we shall consider only the situation in (E.3), where the electron emerges with high momenta such that in the final state, $|\mathbf{p}'_\mathbf{e}\rangle$, its interaction with the Coulomb potential in H-like atom is negligible, i.e, we can use plane wave states for incoming and outgoing particles. The Hamiltonian of the system under consideration is :

$$\begin{aligned}\widehat{H}(\mathbf{r}_\chi, \mathbf{r_e}) &= \frac{\widehat{\mathbf{P}}^2(\mathbf{r}_\chi)}{2m_\chi} + \frac{\widehat{\mathbf{P}}^2(\mathbf{r_e})}{2m_e} + V_{Coul.}(|\mathbf{r_e}|) + V(|\mathbf{r}_\chi - \mathbf{r_e}|) \\ &= \widehat{\mathbf{K}}(\mathbf{r}_\chi) + \widehat{H}_0(\mathbf{r_e}) + V(|\mathbf{r}_\chi - \mathbf{r_e}|)\,, \end{aligned} \tag{E.5}$$

where we set the nucleus sitting at the origin of axes which is taken to be the lab frame with $\mathbf{r}_\chi$ and $\mathbf{r_e}$ pointing towards the positions of the WIMP χ, and electron e, respectively. $\widehat{\mathbf{K}}(\mathbf{r}_\chi)$ is the kinetic energy operator for χ particle with plane wave states

$$\langle \mathbf{r}_\chi | \mathbf{p}_\chi \rangle = \frac{1}{\sqrt{\Omega}}\, e^{i\mathbf{p}_\chi \cdot \mathbf{r}_\chi}\,, \tag{E.6}$$

with Ω being a finite cubic volume and our wave function in eq. (E.6) obeys periodic boundary conditions on Ω. In addition, $\widehat{H}_0(\mathbf{r_e})$, is the unperturbed Hamiltonian of the hydrogen like atoms. Obviously, we shall treat the potential $V(|\mathbf{r}_\chi - \mathbf{r_e}|)$ as perturbation in finding transitions between the initial state $|\alpha\rangle$ into the final state $|\beta\rangle$.

The initial state $|\alpha\rangle$ consists of a plane wave for χ and a bound electron state spectrum $|n\ell m_\ell\rangle$ with total energy E_α being :

$$\text{Initial State} \;:\quad |\alpha\rangle = |\mathbf{p}_\chi\rangle\,|n\ell m_\ell\rangle\;, \qquad E_\alpha = \frac{\hbar^2 p_\chi^2}{2m_\chi} + E_n(Z)\;, \tag{E.7}$$

whith $|E_n(Z)|$ the binding energy of the hydrogen like atom, $|E_1(Z=1)| = 13.6$ eV. Moreover, the final state consists of two continuum states, a χ-plane wave and an electron plane wave and together with its energy reads :

$$\text{Final State} \;:\quad |\beta\rangle = |\mathbf{p}'_\chi\rangle\,|\mathbf{p}'_\mathbf{e}\rangle\;, \qquad E_\beta = \frac{\hbar^2 p_\chi'^2}{2m_\chi} + \frac{\hbar^2 p_e'^2}{2m_e}\;, \tag{E.8}$$

where we assume implicitly that the nucleus has zero kinetic energy before and after the collision [recall assumption 2 above]. Obviously in eqs. (E.5), (E.7) and (E.8), we have neglected all angular momentum interactions in order to keep the discussion as simple as possible.

In order to calculate the transition probability for $|\alpha\rangle \to |\beta\rangle$ we need first to calculate the matrix element $\langle\beta|V(|\mathbf{r}_\chi - \mathbf{r_e}|)|\alpha\rangle$ and then essentially to square it. We find:

$$\langle\beta|V(|\mathbf{r}_\chi - \mathbf{r_e}|)|\alpha\rangle \;=\; \left(\frac{2\pi}{\Omega}\right)^{3/2} \widetilde{V}(\mathbf{q})\;\phi_{n\ell m_\ell}(\mathbf{q} - \mathbf{p}'_\mathbf{e})\;, \tag{E.9}$$

where

$$\widetilde{V}(\mathbf{q}) \;=\; \int_\Omega d^3r\, e^{i\mathbf{q}\cdot\mathbf{r}}\, V(|\mathbf{r}|)\;, \tag{E.10}$$

with $\mathbf{r} \equiv \mathbf{r}_\chi - \mathbf{r_e}$ and

$$\phi_{n\ell m_\ell}(\mathbf{q} - \mathbf{p}'_\mathbf{e}) \;=\; \left(\frac{1}{2\pi}\right)^{3/2} \int d^3r_e\, e^{i(\mathbf{q}-\mathbf{p}'_\mathbf{e})\cdot\mathbf{r_e}}\;\psi_{n\ell m_\ell}(\mathbf{r_e})\;, \tag{E.11}$$

is the momentum space wave function Fourier transform of the coordinate wave function $\psi_{n\ell m_\ell}(\mathbf{r_e})$ of the H-like atoms. In deriving eq. (E.9) we used the locality of the potential energy $V(\mathbf{r})$.

To finally write down Fermi's Golden rule we also need the density of final states which is given by

$$\rho_f(E_\beta) \;=\; \frac{1}{dE_\beta} \prod_{i=1}^{N} \frac{\Omega}{(2\pi\hbar)^3}\, d^3p_{\beta_i}\;, \qquad E_\beta = \sum_{i=1}^{N} E_{\beta_i}\;. \tag{E.12}$$

Then eq. (E.12) results in

$$\rho_f(E_\beta) \;=\; \frac{\Omega^2}{dE_\beta}\, \frac{d^3p'_\chi\, d^3p'_e}{(2\pi)^6}\;, \tag{E.13}$$

where in our case E_β is given by eq. (E.8). Which variables to use here depends on the experimental arrangement. Let us say an experimenter can measure the energy deposit of the ejected electron, E'_e. Then for fixed E'_e and eq. (E.8) we obtain $dE_\beta = dE'_\chi$ and thus,

$$\rho_f(E_\beta) \;=\; \frac{\Omega^2}{(2\pi)^6}\left(\frac{m_\chi|\mathbf{p}'_\chi|}{\hbar^2}\,d\Omega'_\chi\right)\left(\frac{m_e|\mathbf{p}'_\mathbf{e}|}{\hbar^2}\,d\Omega'_e\,dE'_e\right). \tag{E.14}$$

The differential cross section is then obtained by dividing the transition probability amplitude (first order in perturbation theory),

$$w^{(1)}_{\beta\alpha} = \frac{2\pi}{\hbar}\,\rho_f(E_\beta)\,|\langle\beta|V|\alpha\rangle|^2\,, \tag{E.15}$$

by the flux of the incoming particles, v_χ/Ω. Putting this together with eqs.(E.14, E.15), and (E.9) we arrive at

$$\frac{d\sigma}{dE'_e} \;=\; \left(\frac{m_\chi}{2\pi\hbar^2}\right)^2\frac{|\mathbf{p}'_\chi|}{|\mathbf{p}_\chi|}\left(\frac{m_e|\mathbf{p}'_\mathbf{e}|}{\hbar^2}\right)|\widetilde{V}(\mathbf{q})|^2\,|\phi_{n\ell m_\ell}(\mathbf{q}-\mathbf{p}'_\mathbf{e})|^2\,d\Omega'_\chi\,d\Omega'_e\,. \tag{E.16}$$

This can be written in a more transparent form as

$$d\sigma \;=\; \sigma(\mathbf{q})\,\frac{|\mathbf{p}'_\chi|}{|\mathbf{p}_\chi|}\,d\Omega'_\chi\,|\phi_{n\ell m_\ell}(\mathbf{p}_\chi-\mathbf{p}'_\chi-\mathbf{p}'_\mathbf{e})|^2\,d^3p'_e\,, \tag{E.17}$$

where $\sigma(\mathbf{q})$ is the Born approximation for the cross section arising from just the scattering between WIMP and electron particles. Apart from this, eq. (E.17) contains the probability density of finding a bounded electron in H-like atom with momentum $\mathbf{p_e} = \mathbf{p}_\chi - \mathbf{p}'_\chi - \mathbf{p}'_\mathbf{e}$, i.e., an electron that obeys the momentum conservation. These two terms come as not a surprise. What is a bit surprising is the ratio $\frac{|\mathbf{p}'_\chi|}{|\mathbf{p}_\chi|} = \frac{|\mathbf{v}'_\chi|}{|\mathbf{v}_\chi|}$ which is like a Sommerfeld enhancement term. This term comes around because we have treated WIMP scattering off a brick wall (the H-atom). Note also that $|\mathbf{p}'_\chi|$ *must* be taken from energy conservation $E_\alpha = E_\beta$ in eqs. (E.7) and (E.8).

Now we should compare eq. (E.17) with eqs. (2.45), (2.46) and (2.48). In eq. (2.48) we must follow three steps :

1. Use the δ-function of momenta to make a trivial integration on p_e.
2. Do not add an extra initial kinetic energy T_e in δ-function for energies.
3. Write the eq. (2.46) in terms of the matrix element squared to obtain eq. (2.48) and see if it agrees with eq. (E.17).

This should resolve the problem of finding the differential cross section and making the various phase space integrations.

Let us suppose we consider a Yukawa potential of the form[1]

$$V(r) \;=\; -\frac{g^2}{4\pi}\frac{e^{-m_X r}}{r}\,, \tag{E.18}$$

[1]From now on we are working in the units system where $\hbar = c = 1$.

where m_X is the mass of the $U(1)$-mediator we consider. By Fourier transforming this we obtain:

$$\widetilde{V}(q) \;=\; -\frac{g^2}{q^2+m_X^2}\;. \tag{E.19}$$

Replacing this in eq. (E.16), let $g^4 \to 16\pi^2\alpha'\alpha_{\rm DM}$, and taking the limit $q^2 \ll m_X^2$, we get

$$\frac{d\sigma}{dE'_e} \;=\; \frac{16\pi^2\alpha'\alpha_{\rm DM}}{m_X^4}\, m_\chi^2\, \frac{|\mathbf{p}'_\chi|}{|\mathbf{p}_\chi|}\, m_e|\mathbf{p}'_\mathbf{e}|\, |\phi_{n\ell m_\ell}(\mathbf{p}_\chi-\mathbf{p}'_\chi-\mathbf{p}'_\mathbf{e})|^2\, d\xi\, d\eta\;, \tag{E.20}$$

where the scattering angles are given by the following expressions:

$$\widehat{p}_\chi\cdot\widehat{p}'_\chi=\xi\;,\qquad \widehat{p}_\chi\cdot\widehat{p}'_e=\eta\;,\qquad \xi,\eta\in[-1,1]\;. \tag{E.21}$$

In this case we find that:

$$\begin{aligned}|\mathbf{p}_\chi-\mathbf{p}'_\chi-\mathbf{p}'_\mathbf{e})|^2 = p_\chi^2+p_\chi^{'2}+p_e^{'2}-2\,p_\chi p'_\chi\xi-2\,p_\chi p'_e\eta+\\ +2\,p'_\chi p'_e\,[\,\xi\,\eta-\sqrt{1-\xi^2}\,\sqrt{1-\eta^2}\cos(\phi_{\chi'}-\phi_{e'})],\end{aligned} \tag{E.22}$$

where $\phi_{\chi'}$ and $\phi_{e'}$ are the azimuthal angles of vectors $\widehat{p}'_\chi$ and $\widehat{p}'_e$ respectively. The azimuthal angles are equal i.e., $\phi_{\chi'}=\phi_{e'}$, however, because of the three vector momentum conservation the vectors $\mathbf{p_e}$, $\mathbf{p}_\chi$, $\mathbf{p}'_\chi$ are linearly dependent and therefore belong to the same plane.

Momentum and energy conservation of eqs. (E.7) and (E.8) results in

$$|\mathbf{p}'_\chi| \;=\; \sqrt{p_\chi^2-2\,m_\chi\,b(Z)\;-\;\frac{m_\chi}{m_e}\,p_e^{'2}}\;,\quad\text{with}\qquad p'_e\;=\;\sqrt{2\,m_eE'_e}\;, \tag{E.23}$$

where $b(Z)$ is the binding energy for hydrogenic atoms

$$b(Z)\;=\;\frac{Z^2}{2a}\frac{e^2}{4\pi}\;=\;\frac{Z^2}{2}m_e\,\alpha_{\rm em}^2\;,\qquad a\simeq\frac{1}{m_e\,\alpha_{\rm em}}\;, \tag{E.24}$$

with $\alpha_{\rm em}=\frac{e^2}{4\pi}\approx 1/137$ and $m_e\simeq 0.5$ MeV. Furthermore, the momentum distribution in the ground state of hydrogenic atoms reads:

$$\phi_{100}(q)\;=\;\frac{2^{3/2}}{\pi a}\,\frac{(Za)^{5/2}}{(Z^2+q^2a^2)^2}\;. \tag{E.25}$$

As we have seen in the case that the calculation of the cross section has been performed using a field theoretical approach, this cross section exhibits a maximum for final electron energy of around few eV. This happens because of a fast increase of the term $\frac{|\mathbf{p}'_\chi|}{|\mathbf{p}_\chi|}\,|\mathbf{p}'_\mathbf{e}|\sim\sqrt{E'_e}$ and the almost constant value of $|\phi_{100}|^2$ until 5 eV [see eq. (E.20)]. For higher electron energies, e.g., $E'_e\gtrsim 10$ eV, the probability $|\phi_{100}|^2$ drops fastly as $1/E_e^{'2}$ resulting in overall decreasing of the cross section as $E_e^{'-3/2}$. For $\beta=0.001$ and $Z=1$ we find,

$$\sigma\simeq 8\times10^{-40}\ {\rm cm}^2\;. \tag{E.26}$$

The cross section decreases with Z approximately as Z^{-4} for $Z\lesssim 40$.

Appendix F: Averaged amplitude squared

In this Appendix we calculate explicitly the averaged amplitude squared for the following process $e+\chi \to e+\chi$. First we assume that the WIMP interaction to X-gauge boson has the general form $ig_X\gamma^\nu(\tilde{\alpha}+\tilde{\beta}\,\gamma^5)$. Therefore if $\tilde{\alpha}=1$, $\tilde{\beta}=0$ the WIMP is considered a Dirac fermion, and if $\tilde{\alpha}=0$, $\tilde{\beta}=1$ it is considered a Majorana fermion respectively. The last choice of parameters $\tilde{\alpha}$ and $\tilde{\beta}$ reflects the fact that Majorana particles do not possess electromagnetic properties, thus only the axial component of the coupling contributes to the final result. The matrix element for the process $e+\chi \to e+\chi$ in the case of a massive gauge boson interchanged reads:

$$\begin{aligned} i\mathcal{M} &= \overline{u}(p'_\chi)\, i\, g_X\, \gamma^\nu(\tilde{\alpha}+\tilde{\beta}\,\gamma^5)u(p_\chi)\left(\frac{\epsilon\,\cos\theta_W}{(p_e-p'_e)^2-m_X^2}\right) \\ &\quad \left[g_{\mu\nu}-\frac{(p_e-p'_e)_\nu(p_e-p'_e)_\mu}{(p_e-p'_e)^2}\right]\overline{u}(p'_e)\, i\, e\,\gamma^\mu\, u(p_e), \end{aligned} \tag{F.1}$$

where we have used eq. (2.8) for the form of the propagator and p_χ, $p_e(p'_\chi,\, p'_e)$ are the incoming (outgoing) four-momenta of WIMPs and electron respectively. In order to compute the differential cross section, we need an expression for $|\overline{\mathcal{M}}|^2$, so we have to find the complex conjugate of the amplitude. Averaging over fermion spins we obtain the averaged amplitude squared:

$$\begin{aligned} |\overline{\mathcal{M}}|^2 &= \frac{1}{4}\left(\frac{\epsilon\, g_X\, e\,\cos\theta_W}{(p_e-p'_e)^2-m_X^2}\right)^2 \\ &\quad \sum_{spins}\left\{\overline{u}(p'_\chi)\gamma^\nu(\tilde{\alpha}+\tilde{\beta}\,\gamma^5)u(p_\chi)\left[g_{\mu\nu}-\frac{(p_e-p'_e)_\nu(p_e-p'_e)_\mu}{(p_e-p'_e)^2}\right]\overline{u}(p'_e)\,\gamma^\mu\, u(p_e)\right\} \\ &\quad \left\{\overline{u}(p'_\chi)\gamma^\lambda(\tilde{\alpha}+\tilde{\beta}\,\gamma^5)u(p_\chi)\left[g_{\lambda\xi}-\frac{(p_e-p'_e)_\lambda(p_e-p'_e)_\xi}{(p_e-p'_e)^2}\right]\overline{u}(p'_e)\,\gamma^\xi\, u(p_e)\right\}^* = \\ &= \frac{1}{4}\left(\frac{\epsilon\, g_X\, e\,\cos\theta_W}{(p_e-p'_e)^2-m_X^2}\right)^2 \\ &\quad \sum_{spins}\left\{\overline{u}(p'_\chi)\gamma^\nu(\tilde{\alpha}+\tilde{\beta}\,\gamma^5)u(p_\chi)\left[g_{\mu\nu}-\frac{(p_e-p'_e)_\nu(p_e-p'_e)_\mu}{(p_e-p'_e)^2}\right]\overline{u}(p'_e)\,\gamma^\mu\, u(p_e)\right\} \\ &\quad \left\{\overline{u}(p_\chi)\gamma^\lambda(\tilde{\alpha}+\tilde{\beta}\,\gamma^5)u(p'_\chi)\left[g_{\lambda\xi}-\frac{(p_e-p'_e)_\lambda(p_e-p'_e)_\xi}{(p_e-p'_e)^2}\right]\overline{u}(p_e)\,\gamma^\xi\, u(p'_e)\right\}, \end{aligned} \tag{F.2}$$

where has been made use of the fact that a bi-spinor product can be complex-conjugated as follows:

$$\begin{aligned} &\left(\overline{u}(p')\gamma^\lambda(\tilde{\alpha}+\tilde{\beta}\,\gamma^5)u(p)\right)^* = \left(u^\dagger(p')\,\gamma^0\,\gamma^\lambda\,(\tilde{\alpha}+\tilde{\beta}\,\gamma^5)u(p)\right)^\dagger = \\ &= u^\dagger(p)(\tilde{\alpha}+\tilde{\beta}\,(\gamma^5)^\dagger)\,(\gamma^\lambda)^\dagger\,(\gamma^0)^\dagger u(p') = \overline{u}(p)\,\gamma^0(\gamma^\lambda)^\dagger\,\gamma^0\,(\tilde{\alpha}+\tilde{\beta}\,\gamma^5)u(p') \\ &= \overline{u}(p)\,\gamma^\lambda\,(\tilde{\alpha}+\tilde{\beta}\,\gamma^5)u(p') \end{aligned} \tag{F.3}$$

since $(\gamma^0)^\dagger = \gamma^0$, $(\gamma^5)^\dagger = \gamma^5$, $\{\gamma^\lambda, \gamma^5\} = 0$ and $\gamma^0\,(\gamma^\lambda)^\dagger\,\gamma^0 = \gamma^\lambda$. If we take $\tilde{\alpha} = 1$ and $\tilde{\beta} = 0$ in the expression above we find $\Big(\overline{u}(q')\gamma^\xi u(q)\Big)^* = \overline{u}(q)\gamma^\xi u(q')$.
We can write the averaged amplitude squared in the form:

$$|\overline{\mathcal{M}}|^2 = \frac{1}{4}\left(\frac{\epsilon\, g_X\, e\, \cos\theta_W}{(p_e - p'_e)^2 - m_X^2}\right)^2 \Big(I + II + III + IV\Big), \tag{F.4}$$

where

$$\begin{aligned}
I &= \sum_{s,r,t,\ell} \overline{u}^s_\alpha(p'_\chi)\,\gamma^\nu_{\alpha\beta}\,(\tilde{\alpha} + \tilde{\beta}\,\gamma^5)_{\beta\gamma}\,u^r_\gamma(p_\chi)\overline{u}^t_\delta(p'_e)\,\gamma_{\nu_{\delta\varepsilon}}\,u^\ell_\varepsilon(p_e) \\
&\quad \overline{u}^r_\zeta(p_\chi)\,\gamma^\lambda_{\zeta\eta}\,(\tilde{\alpha} + \tilde{\beta}\,\gamma^5)_{\eta\theta}\,u^s_\theta(p'_\chi)\overline{u}^\ell_\iota(p_e)\,\gamma_{\lambda_{\iota\kappa}}\,u^t_\kappa(p'_e), \\
II &= -\sum_{s,r,t,\ell} \overline{u}^s_\alpha(p'_\chi)\,\gamma^\nu_{\alpha\beta}\,(\tilde{\alpha} + \tilde{\beta}\,\gamma^5)_{\beta\gamma}\,u^r_\gamma(p_\chi)\overline{u}^t_\delta(p'_e)\,\gamma_{\nu_{\delta\varepsilon}}\,u^\ell_\varepsilon(p_e) \\
&\quad \overline{u}^r_\zeta(p_\chi)\,\gamma^\lambda_{\zeta\eta}\,(\tilde{\alpha} + \tilde{\beta}\,\gamma^5)_{\eta\theta}\,u^s_\theta(p'_\chi)\overline{u}^\ell_\iota(p_e)\,\gamma^\xi_{\iota\kappa}\,u^t_\kappa(p'_e)\frac{(p_e - p'_e)_\lambda (p_e - p'_e)_\xi}{(p_e - p'_e)^2}, \\
III &= -\sum_{s,r,t,\ell} \overline{u}^s_\alpha(p'_\chi)\,\gamma^\nu_{\alpha\beta}\,(\tilde{\alpha} + \tilde{\beta}\,\gamma^5)_{\beta\gamma}\,u^r_\gamma(p_\chi)\overline{u}^t_\delta(p'_e)\,\gamma^\mu_{\delta\varepsilon}\,u^\ell_\varepsilon(p_e) \\
&\quad \overline{u}^r_\zeta(p_\chi)\,\gamma^\lambda_{\zeta\eta}\,(\tilde{\alpha} + \tilde{\beta}\,\gamma^5)_{\eta\theta}\,u^s_\theta(p'_\chi)\overline{u}^\ell_\iota(p_e)\,\gamma_{\lambda_{\iota\kappa}}\,u^t_\kappa(p'_e)\frac{(p_e - p'_e)_\mu (p_e - p'_e)_\nu}{(p_e - p'_e)^2}, \\
IV &= \sum_{s,r,t,\ell} \overline{u}^s_\alpha(p'_\chi)\,\gamma^\nu_{\alpha\beta}\,(\tilde{\alpha} + \tilde{\beta}\,\gamma^5)_{\beta\gamma}\,u^r_\gamma(p_\chi)\overline{u}^t_\delta(p'_e)\,\gamma^\mu_{\delta\varepsilon}\,u^\ell_\varepsilon(p_e) \\
&\quad \overline{u}^r_\zeta(p_\chi)\,\gamma^\lambda_{\zeta\eta}\,(\tilde{\alpha} + \tilde{\beta}\,\gamma^5)_{\eta\theta}\,u^s_\theta(p'_\chi)\overline{u}^\ell_\iota(p_e)\,\gamma^\xi_{\iota\kappa}\,u^t_\kappa(p'_e) \\
&\quad \frac{(p_e - p'_e)_\mu (p_e - p'_e)_\nu}{(p_e - p'_e)^2}\,\frac{(p_e - p'_e)_\lambda (p_e - p'_e)_\xi}{(p_e - p'_e)^2}.
\end{aligned} \tag{F.5}$$

Here indices s, r, t, ℓ correspond to particles spin and $\alpha, \beta, \gamma, \delta, \varepsilon, \zeta, \eta, \theta, \iota, \kappa$ correspond to matrix elements position. Making use of the completeness relation $\sum u^s(p)\overline{u}^s(p) = \not{p} + m$, we can compute each one of the coefficients I, II, III, IV separately.

$$\begin{aligned}
I &= \sum_{s,r,t,\ell} \overline{u}^s_\alpha(p'_\chi)\,\gamma^\nu_{\alpha\beta}\,(\tilde{\alpha} + \tilde{\beta}\,\gamma^5)_{\beta\gamma}\,u^r_\gamma(p_\chi)\overline{u}^t_\delta(p'_e)\,\gamma_{\nu_{\delta\varepsilon}}\,u^\ell_\varepsilon(p_e) \\
&\quad \overline{u}^r_\zeta(p_\chi)\,\gamma^\lambda_{\zeta\eta}\,(\tilde{\alpha} + \tilde{\beta}\,\gamma^5)_{\eta\theta}\,u^s_\theta(p'_\chi)\overline{u}^\ell_\iota(p_e)\,\gamma_{\lambda_{\iota\kappa}}\,u^t_\kappa(p'_e) = \\
&= \mathbf{Tr}[(\not{p}'_e + m_e)\gamma_\nu(\not{p}_e + m_e)\gamma_\lambda]\,\mathbf{Tr}[(\not{p}_\chi + m_\chi)\gamma^\lambda\,(\tilde{\alpha} + \tilde{\beta}\,\gamma^5)(\not{p}'_\chi + m_\chi)\gamma^\nu\,(\tilde{\alpha} + \tilde{\beta}\,\gamma^5)].
\end{aligned} \tag{F.6}$$

After a little standard trace algebra ($\mathbf{Tr}[\gamma^\mu\gamma^\nu\gamma^\rho\gamma^\sigma] = 4(g^{\mu\nu}g^{\rho\sigma} - g^{\mu\rho}g^{\nu\sigma} + g^{\mu\sigma}g^{\nu\rho})$ and $\mathbf{Tr}[\gamma^\mu\gamma^\nu\gamma^\rho\gamma^\sigma\gamma^5] = -4\,i\,\varepsilon^{\mu\nu\rho\sigma}$), we obtain :

$$I = 32\Bigg[(\tilde{\alpha}^2+\tilde{\beta}^2)\Bigg((p_\chi\cdot p_e)(p'_\chi\cdot p'_e) + (p_\chi\cdot p'_e)(p'_\chi\cdot p_e) - m_e^2(p_\chi\cdot p'_\chi)\Bigg) + \\ +m_\chi^2(\tilde{\alpha}^2-\tilde{\beta}^2)\Bigg(2\,m_e^2 - (p_e\cdot p'_e)\Bigg)\Bigg]. \tag{F.7}$$

Analogously for the coefficient II one finds:

$$II = \mathbf{Tr}[(\not{p}'_e + m_e)\gamma_\nu(\not{p}_e + m_e)\gamma^\xi]\,\mathbf{Tr}[(\not{p}_\chi + m_\chi)\gamma^\lambda\,(\tilde{\alpha}+\tilde{\beta}\,\gamma^5)(\not{p}'_\chi + m_\chi)\gamma^\nu\,(\tilde{\alpha}+\tilde{\beta}\,\gamma^5)]\times \\ \times\frac{(p_e-p'_e)_\lambda(p_e-p'_e)_\xi}{(p_e-p'_e)^2} = 0. \tag{F.8}$$

The above result has been obtained after performing the trace algebra and imposing the on-shell conditions $p_e^2 = m_e^2 = p_e'^2$. Similarly for the next coefficient:

$$III = \mathbf{Tr}[(\not{p}'_e + m_e)\gamma^\mu(\not{p}_e + m_e)\gamma_\lambda]\,\mathbf{Tr}[(\not{p}_\chi + m_\chi)\gamma^\lambda\,(\tilde{\alpha}+\tilde{\beta}\,\gamma^5)(\not{p}'_\chi + m_\chi)\gamma^\nu\,(\tilde{\alpha}+\tilde{\beta}\,\gamma^5)]\times \\ \times\frac{(p_e-p'_e)_\mu(p_e-p'_e)_\nu}{(p_e-p'_e)^2} = 0. \tag{F.9}$$

Finally for the coefficient IV, and after imposing the same on-shell conditions as above, we obtain:

$$IV = \mathbf{Tr}[(\not{p}'_e + m_e)\gamma^\mu(\not{p}_e + m_e)\gamma^\xi]\,\mathbf{Tr}[(\not{p}_\chi + m_\chi)\gamma^\lambda\,(\tilde{\alpha}+\tilde{\beta}\,\gamma^5)(\not{p}'_\chi + m_\chi)\gamma^\nu\,(\tilde{\alpha}+\tilde{\beta}\,\gamma^5)]\times \\ \times\left(\frac{(p_e-p'_e)_\mu(p_e-p'_e)_\xi}{(p_e-p'_e)^2}\right)\left(\frac{(p_e-p'_e)_\lambda(p_e-p'_e)_\nu}{(p_e-p'_e)^2}\right) = 0. \tag{F.10}$$

The averaged matrix element squared in eq. (F.4) now reads:

$$|\overline{\mathcal{M}}|^2 = 8\left(\frac{\epsilon\, g_X\, e\, \cos\theta_W}{(p_e-p'_e)^2 - m_X^2}\right)^2\Bigg[m_\chi^2\,(\tilde{\alpha}^2-\tilde{\beta}^2)\Bigg(2\,m_e^2 - (p_e\cdot p'_e)\Bigg) + \\ +(\tilde{\alpha}^2+\tilde{\beta}^2)\Bigg((p_\chi\cdot p_e)(p'_\chi\cdot p'_e) + (p_\chi\cdot p'_e)(p'_\chi\cdot p_e) - m_e^2(p_\chi\cdot p'_\chi)\Bigg)\Bigg]. \tag{F.11}$$

We can simplify eq. (F.11) by considering the following kinematics that holds for the non-relativistic case, where the initial electron is at rest:

$$p_\chi = (m_\chi + \frac{\vec{p_\chi}^{\,2}}{2\,m_\chi}, \vec{p_\chi}),\; p'_\chi = (m_\chi + \frac{\vec{p'_\chi}^{\,2}}{2\,m_\chi}, \vec{p'_\chi}),\; p_e = (m_e, \vec{0}),\; p'_e = (m_e + \frac{\vec{p'_e}^{\,2}}{2\,m_e}, \vec{p'_e}). \tag{F.12}$$

In the case that the WIMP is a Dirac fermion (e.g $\tilde{\alpha}=1$, $\tilde{\beta}=0$) from eq. (F.11) we find:

$$
\begin{aligned}
|\overline{\mathcal{M}}|^2 = 8\left(\frac{\epsilon\, g_X\, e\, \cos\theta_W}{(p_e-p_e')^2-m_X^2}\right)^2 \quad \Bigg[\quad & 2\,m_\chi^2\,m_e^2 + \frac{\vec{p_\chi}^{\,2}\,\vec{p_e'}^{\,2}}{2} + \frac{\vec{p_\chi'}^{\,2}\,\vec{p_e'}^{\,2}}{2} + \frac{m_\chi^2\,\vec{p_e'}^{\,2}}{2} - \\
& - \; m_\chi\, m_e\left((\vec{p_\chi'}\cdot\vec{p_e'}) + (\vec{p_\chi}\cdot\vec{p_e'})\right) + \\
& + \; \frac{m_e^2}{2}\left(\vec{p_\chi}^{\,2} + \vec{p_\chi'}^{\,2} + 2\,(\vec{p_\chi}\cdot\vec{p_\chi'})\right) - \\
& - \; \frac{m_e}{2m_\chi}\left(\vec{p_\chi}^{\,2}(\vec{p_\chi'}\cdot\vec{p_e'}) + \vec{p_\chi'}^{\,2}(\vec{p_\chi}\cdot\vec{p_e'})\right) + \\
& + \; \frac{\vec{p_\chi}^{\,2}\vec{p_\chi'}^{\,2}(\vec{p_e'}^{\,2}+m_e^2)}{4m_\chi^2}\Bigg]. \qquad \text{(F.13)}
\end{aligned}
$$

In the non-relativistic limit $|\vec{p_\chi}| \sim |\vec{p_\chi'}| = m_\chi\,\beta \ll m_\chi$ (since $\beta \sim 10^{-3}$) and also we assume $m_e \ll m_\chi$. Therefore we can neglect terms proportional to m_e/m_χ and $(m_e/m_\chi)^2$ in the expression above. Another fact is that the outgoing electron is moving with a very small velocity compared to WIMP's velocity, so terms that contain $\vec{p_e'}^{\,2}$ (or $\vec{p_e'}$ in any inner product), almost vanish. Taking into account all the assumptions above, the only surviving term in the square bracket of the expression eq. (F.13) is the first one. As a result we obtain for the averaged matrix element squared the following simple expression:

$$
|\overline{\mathcal{M}}|^2 \simeq 16\left(\frac{\epsilon\, g_X\, e\, \cos\theta_W}{(p_e-p_e')^2-m_X^2}\right)^2 m_\chi^2\, m_e^2. \qquad \text{(F.14)}
$$

If the WIMP is a Majorana fermion (e.g $\tilde{\alpha}=0$, $\tilde{\beta}=1$ since in this case the WIMP does not possess electromagnetic properties) from eq. (F.11) we find:

$$
\begin{aligned}
|\overline{\mathcal{M}}|^2 = 8\left(\frac{\epsilon\, g_X\, e\, \cos\theta_W}{(p_e-p_e')^2-m_X^2}\right)^2 \quad \Bigg[\quad & \frac{m_e^2}{2}\left(\vec{p_\chi}^{\,2} + \vec{p_\chi'}^{\,2} + 2\,(\vec{p_\chi}\cdot\vec{p_\chi'})\right) + \frac{\vec{p_\chi}^{\,2}\,\vec{p_e'}^{\,2}}{2} + \frac{\vec{p_\chi'}^{\,2}\,\vec{p_e'}^{\,2}}{2} - \\
& - \; m_\chi\, m_e\left((\vec{p_\chi'}\cdot\vec{p_e'}) + (\vec{p_\chi}\cdot\vec{p_e'})\right) - \\
& - \; \frac{m_e}{2m_\chi}\left(\vec{p_\chi}^{\,2}(\vec{p_\chi'}\cdot\vec{p_e'}) + \vec{p_\chi'}^{\,2}(\vec{p_\chi}\cdot\vec{p_e'})\right) + \\
& + \; \frac{3\,m_\chi^2\,\vec{p_e'}^{\,2}}{2} + \frac{\vec{p_\chi}^{\,2}\vec{p_\chi'}^{\,2}(\vec{p_e'}^{\,2}+m_e^2)}{4m_\chi^2}\Bigg]. \qquad \text{(F.15)}
\end{aligned}
$$

With the same assumptions as previously, the dominant contribution comes from the first term in the square bracket and is $\simeq 2\,m_\chi\,\beta^2$. In this case the averaged matrix element squared reads:

$$
|\overline{\mathcal{M}}|^2 \simeq 16\left(\frac{\epsilon\, g_X\, e\, \cos\theta_W}{(p_e-p_e')^2-m_X^2}\right)^2 m_\chi^2\, m_e^2\,\beta^2. \qquad \text{(F.16)}
$$

From this result we conclude that the cross section is suppressed by a factor $\beta^2 \simeq 10^{-6}$ in the case of a Majorana WIMP compared to the case of a Dirac WIMP.

Appendix G: Lagrangian for a toy model

In this Appendix we consider a toy model and present some general features of the relevant Lagrangian describing the three gauge boson vertex in Chapter 3. Consider a gauge theory that contains a complex scalar field Φ charged under a local $U(1)$ with charge Y_Φ (in units of e), a vector spin-1 abelian gauge boson A_μ and a pair of Dirac fermions E_L and e_R with $U(1)$-charges Y_L and Y_R respectively. This gauge theory is described by the Lagrangian [2],

$$\mathscr{L} = \mathscr{L}_g(\Phi, A_\mu) + \mathscr{L}_f(E_L, e_R, A_\mu) + \mathscr{L}_Y(E_L, e_R, \Phi) \ , \tag{G.1}$$

where the gauge boson-scalar interactions are

$$\mathscr{L}_g(\Phi, A_\mu) = -\frac{1}{4} F_{\mu\nu} F^{\mu\nu} - \frac{1}{2} (G)^2 + |D_\mu \Phi|^2 - V(\Phi) \ , \tag{G.2}$$

while the chiral fermion and the Yukawa interaction parts of the Lagrangian in eq. (G.1) are stored in:

$$\mathscr{L}_f(E_L, e_R, A_\mu) \ = \ \overline{E}_L \, (i \not{D}) \, E_L + \overline{e}_R \, (i \not{D}) \, e_R \ , \tag{G.3}$$

$$\mathscr{L}_Y(E_L, e_R, \Phi) \ = \ -\lambda_e \, (\overline{E}_L \, \Phi \, e_R \ + \ \overline{e}_R \, \Phi^* \, E_L) \ , \tag{G.4}$$

and $D_\mu \Phi = \partial_\mu \Phi + i e Y_\Phi A_\mu \Phi$, $D_\mu E_L = \partial_\mu E_L + i e Y_L A_\mu E_L$, and $D_\mu e_R = \partial_\mu e_R + i e Y_R A_\mu e_R$. $\mathscr{L}_g$ is invariant under the local, $U(1)$ gauge-transformation

$$\Phi(x) \to e^{i e Y_\Phi \Lambda(x)} \Phi(x) \ , \quad A_\mu(x) \to A_\mu(x) - \partial_\mu \Lambda(x) \ , \tag{G.5}$$

$$E_L(x) \to e^{i e Y_L \Lambda(x)} E_L(x) \ , \quad e_R(x) \to e^{i e Y_R \Lambda(x)} e_R(x) \ , \tag{G.6}$$

iff $Y_\Phi = Y_L - Y_R$. It is convenient to combine the left and right-handed fermions into a single Dirac four-component spinor $\Psi = (E_L, e_R)^T$. Then the interaction Lagrangian relevant to our study for triangle graphs reads:

$$\mathscr{L}_{int} \ = \ -\lambda_e \overline{\Psi} \Phi P_R \Psi - \lambda_e \overline{\Psi} \Phi^* P_L \Psi - e A_\mu \overline{\Psi} \gamma^\mu \, (\alpha + \beta \gamma_5) \Psi \ , \tag{G.7}$$

where

$$\alpha = \frac{Y_L + Y_R}{2} \ , \quad \beta = \frac{Y_R - Y_L}{2} \ . \tag{G.8}$$

Under gauge transformations the 4-component field Ψ transforms as

$$\Psi(x) \to e^{i e (\alpha + \beta \gamma_5) \Lambda(x)} \Psi(x) \ , \tag{G.9a}$$

$$\overline{\Psi}(x) \to \overline{\Psi}(x) e^{-i e (\alpha - \beta \gamma_5) \Lambda(x)} \ , \tag{G.9b}$$

which together with eq. (G.6) leave $\mathscr{L}$ invariant if $Y_\Phi = -2\beta$.

[2] Throughout we follow the notation and conventions of ref. [34].

We choose a renormalizable and gauge invariant potential $V(\Phi)$ such that the field Φ acquires a non-vanishing vacuum expectation value, $\langle\Phi\rangle = v/\sqrt{2}$, which breaks the local $U(1)$ symmetry spontaneously. We expand eq. (G.1) around the minimum, $\Phi = \frac{1}{\sqrt{2}}(v + h + i\varphi)$ and choose a gauge-fixing function in eq. (G.2),

$$G = \frac{1}{\sqrt{\xi}} \left(\partial_\mu A^\mu - \xi e v \varphi\right) , \tag{G.10}$$

which eliminates the Goldstone boson - gauge boson mixing term. The mass of the vector boson A_μ and of the unphysical Goldstone boson φ in this R_ξ-gauge become

$$m_A = e\, v\, Y_\Phi \ , \quad m_\varphi^2 = \xi\, m_A^2 \ . \tag{G.11}$$

The ghost part of $\mathscr{L}$ is not relevant to our discussion for the one-loop triangle graphs and is not presented. In terms of Ψ and $\overline{\Psi}$, $\mathscr{L}_f + \mathscr{L}_Y$ becomes

$$\begin{aligned} \mathscr{L}_f(\Psi, A_\mu) + \mathscr{L}_Y(\Psi, h, \varphi) \;\; &= \;\; \overline{\Psi} i\partial\!\!\!/ \Psi - e A_\mu \overline{\Psi}\gamma^\mu(\alpha + \beta\gamma^5)\Psi - \\ &\quad - m\overline{\Psi}\Psi - \tilde{\beta}\overline{\Psi} h \Psi - i\tilde{\beta}\overline{\Psi}\gamma^5\varphi\Psi \end{aligned} \tag{G.12}$$

where $m = v\,\tilde{\beta}$ and $\tilde{\beta} = \frac{\lambda_e}{\sqrt{2}}$.

This model, albeit very simple, captures the most important non-decoupling heavy fermion effects in the trilinear gauge boson vertices in the Standard Model and its extensions. In the context of chiral anomalies it has been exploited in ref. [97]. With a light language deform it imitates the Standard Model with the difference that its Ward Identities for the currents corresponding to the gauge symmetry in eq. (G.6) are anomalous as we shall see below.

Appendix H: Three gauge boson vertex

In this Appendix we explicitly evaluate the three external gauge boson, fermionic one loop amplitude of Fig. 3.1. The loop function is calculated directly in four dimensions using standard methods studied in refs. [30, 120, 156–158]. Here, we review this calculation in detail for the toy model of Appendix G. At the end we generalise our results to the case of three different external (massive or massless) gauge bosons.

By naive power counting we observe that the two diagrams in Fig. 3.1 are linearly divergent. This means that their quantum amplitudes depend on the routing of the internal momenta circulating in the loop. In each of the two diagrams we shift the internal momenta with arbitrary four vectors a^μ and b^μ, respectively. By reading Feynman rules from eq. (G.7), the graphs in Fig. 3.1 become:

$$\begin{aligned}\Gamma^{\mu\nu\rho}(k_1,k_2;a,b) \;=\; (-1)\,e^3\times \mathrm{Tr}\Big\{\int\frac{d^4p}{(2\pi)^4}\times\\ \times\Big[\frac{\gamma^\mu(\alpha+\beta\gamma^5)(\not p-\not k_2+\not a+m)\gamma^\rho(\alpha+\beta\gamma^5)(\not p+\not a+m)\gamma^\nu(\alpha+\beta\gamma^5)(\not p+\not k_1+\not a+m)}{[(p-k_2+a)^2-m^2][(p+a)^2-m^2][(p+k_1+a)^2-m^2]}\\ +\frac{\gamma^\mu(\alpha+\beta\gamma^5)(\not p-\not k_1+\not b+m)\gamma^\nu(\alpha+\beta\gamma^5)(\not p+\not b+m)\gamma^\rho(\alpha+\beta\gamma^5)(\not p+\not k_2+\not b+m)}{[(p-k_1+b)^2-m^2][(p+b)^2-m^2][(p+k_2+b)^2-m^2]}\Big]\Big\},\end{aligned} \tag{H.1}$$

where m is the fermion mass and (-1) is a fermionic loop factor. The integral in the second line is the same as the first with the only difference that the upper two external legs in Fig.3.1 are interchanged, *i.e.*, $\{\nu,\rho\}\leftrightarrow\{\rho,\nu\}$ and $k_1\leftrightarrow k_2$. Dimensional regularization is a scheme not well suited in calculating (H.1) due to the problems in defining γ_5 and $\epsilon^{\mu\nu\rho\sigma}$ in $d>4$ spacetime dimensions. We here follow a method for calculating (H.1) first presented by Rosenberg in ref. [120] and later used by Adler in his classic paper on chiral anomaly [30]. Basically, this method relies on the fact that the abiguous part of the integral is stored in two form factors in $\Gamma^{\mu\nu\rho}$ expansion, A_1 and A_2, that multiply the external momenta k_2 and k_1, respectively. We then exploit physical arguments like for example conservation of charge, in order to determine the form factors A_1, A_2 - all others, $A_3...A_6$ are finite and can be calculated directly in 4-dimensions.

Our next step is to write down the WIs. This can be done in many ways, probably the most insightful is the use of functional methods (see for instance Chapter 9.6 in the textbook of ref. [34]). One finds the classical WIs of eq. (3.3), but not the last term on the r.h.s. We show below how to calculate this last term. We need first to calculate the divergence of the 1PI vertex: $q_\mu\Gamma^{\mu\nu\rho}=(k_1+k_2)_\mu\Gamma^{\mu\nu\rho}$. It is useful to employ the following algebraic identity:

$$\not q(\alpha+\beta\gamma^5)=-(\alpha-\beta\gamma^5)(\not p-\not k_2+\not a-m)+2\beta\gamma^5 m+(\not p+\not k_1+\not a-m)(\alpha+\beta\gamma^5), \tag{H.2}$$

in the first integral of (H.1) and a similar identity with $a\to b$ and $k_1\to k_2$ in the second one.

These identities split $q_\mu \Gamma^{\mu\nu\rho}$ into two parts,

$$q_\mu \Gamma^{\mu\nu\rho}(k_1,k_2;a,b) \;=\; -\frac{2m\beta e i}{\tilde{\beta}}\,\Gamma^{\nu\rho}(k_1,k_2;a,b) + \Pi^{\nu\rho}(k_1,k_2;a,b)\;, \tag{H.3}$$

a part that is proportional to the fermion mass m and a part which contains divergent two-point functions that *would had been zero if shifting of the momenta variable was allowed*. The latter integrals will be responsible for the failure of the axial vector WI's. Explicitly $\Gamma^{\rho\nu}$ and $\Pi^{\rho\nu}$ in eq. (H.3) read,

$$\begin{aligned}
&\Gamma^{\nu\rho}(k_1,k_2;a,b) = -i\,e^2\,\tilde{\beta}\,\times \\
&\times \mathbf{Tr}\Big\{ \int \frac{d^4p}{(2\pi)^4} \frac{\gamma^5(\not p - \not k_2 + \not a + m)\gamma^\rho(\alpha+\beta\gamma^5)(\not p + \not a + m)\gamma^\nu(\alpha+\beta\gamma^5)(\not p + \not k_1 + \not a + m)}{[(p-k_2+a)^2-m^2][(p+a)^2-m^2][(p+k_1+a)^2-m^2]} + \\
&\quad + \int \frac{d^4p}{(2\pi)^4} \frac{\gamma^5(\not p - \not k_1 + \not b + m)\gamma^\nu(\alpha+\beta\gamma^5)(\not p + \not b + m)\gamma^\rho(\alpha+\beta\gamma^5)(\not p + \not k_2 + \not b + m)}{[(p-k_1+b)^2-m^2][(p+b)^2-m^2][(p+k_2+b)^2-m^2]} \Big\} \\
&\quad = \frac{-i\,e^2\,m\,\tilde{\beta}}{2\pi^2}\varepsilon^{\lambda\nu\rho\sigma}\,k_{1\lambda}\,k_{2\sigma}\,I_0(k_1,k_2,m)\;,
\end{aligned} \tag{H.4}$$

where

$$I_0(k_1,k_2,m) = \int_0^1 \int_0^{1-x} \frac{(\alpha^2-\beta^2)+2(x+y)\beta^2}{x(x-1)k_2^2 + y(y-1)k_1^2 - 2xyk_1\cdot k_2 + m^2}\;. \tag{H.5}$$

Obviously, the integral of $\Gamma^{\nu\rho}$ in eq. (H.4) is obtained from $\Gamma^{\mu\nu\rho}$ in eq. (H.1) with the replacement $\gamma^\mu(\alpha+\beta\gamma^5) \to \gamma^5$, that is a replacement of a vector-axial vector coupling with a pseudoscalar. This validates the Partially Conserved Axial Current (PCAC) relation in eq. (H.3). Note that $\Gamma^{\nu\rho}$ is finite and independent on the arbitrary vectors a^μ and b^μ : $\Gamma^{\nu\rho}(k_1,k_2;a,b) = \Gamma^{\nu\rho}(k_1,k_2)$.

The divergent part $\Pi^{\nu\rho}$ in the WI of eq. (H.3) contains, among others, the anomalous term. It is written explicitly as,

$$\begin{aligned}
\Pi^{\nu\rho}(k_1,k_2;a,b) &= (-e^3)\,\mathbf{Tr}\int\frac{d^4p}{(2\pi)^4}\times \\
&\times\ \Big\{-\frac{(\alpha-\beta\gamma^5)(\alpha-\beta\gamma^5)\gamma^\rho(\not p+\not a+m)\gamma^\nu(\alpha+\beta\gamma^5)(\not p+\not k_1+\not a+m)}{[(p+a)^2-m^2][(p+k_1+a)^2-m^2]} \\
&+\ \frac{(\not p-\not k_2+\not a+m)\gamma^\rho(\alpha+\beta\gamma^5)(\not p+\not a+m)\gamma^\nu(\alpha+\beta\gamma^5)(\alpha+\beta\gamma^5)}{[(p+a)^2-m^2][(p-k_2+a)^2-m^2]} \\
&-\ \frac{(\alpha-\beta\gamma^5)(\alpha-\beta\gamma^5)\gamma^\nu(\not p+\not b+m)\gamma^\rho(\alpha+\beta\gamma^5)(\not p+\not k_2+\not b+m)}{[(p+b)^2-m^2][(p+k_2+b)^2-m^2]} \\
&+\ \frac{(\not p-\not k_1+\not b+m)\gamma^\nu(\alpha+\beta\gamma^5)(\not p+\not b+m)\gamma^\rho(\alpha+\beta\gamma^5)(\alpha+\beta\gamma^5)}{[(p+b)^2-m^2][(p-k_1+b)^2-m^2]}\Big\}\ .
\end{aligned} \tag{H.6}$$

This is an integral that is devided into two parts : a chiral expression *i.e.*, the one that contains γ^5 and a non-chiral expression that does not contain γ^5. Since the anomaly term is originated from the chiral part we start from there. Hence,

$$\begin{aligned}
&\Pi^{\nu\rho}_{\rm chiral}(k_1,k_2;a,b) = (\beta^3+3\alpha^2\beta)e^3\times \\
&\times\mathbf{Tr}\int\frac{d^4p}{(2\pi)^4}\Big\{\frac{(\not p+\not k_1+\not a)\gamma^\rho(\not p+\not a)\gamma^\nu\gamma^5}{[(p+k_1+a)^2-m^2][(p+a)^2-m^2]}-\frac{(\not p+\not a)\gamma^\nu(\not p-\not k_2+\not a)\gamma^\rho\gamma^5}{[(p+a)^2-m^2][(p-k_2+a)^2-m^2]} \\
&\qquad+\frac{(\not p+\not k_2+\not b)\gamma^\nu(\not p+\not b)\gamma^\rho\gamma^5}{[(p+k_2+b)^2-m^2][(p+b)^2-m^2]}-\frac{(\not p+\not b)\gamma^\rho(\not p-\not k_1+\not b)\gamma^\nu\gamma^5}{[(p+b)^2-m^2][(p-k_1+b)^2-m^2]}\Big\}.
\end{aligned} \tag{H.7}$$

Grouping together the first and the fourth as well as the third and the second terms in the integrand of eq. (H.7), we arrive at,

$$\begin{aligned}
&\Pi^{\nu\rho}_{\rm chiral}(k_1,k_2;a,b) = (\beta^3+3\alpha^2\beta)e^3\times \\
&\times\int\frac{d^4p}{(2\pi)^4}\Big\{\mathbf{Tr}(\gamma^\kappa\gamma^\rho\gamma^\lambda\gamma^\nu\gamma^5)\Big(\frac{(p+k_1+a)_\kappa(p+a)_\lambda}{[(p+k_1+a)^2-m^2][(p+a)^2-m^2]}- \\
&\qquad-\frac{(p+b)_\kappa(p-k_1+b)_\lambda}{[(p+b)^2-m^2][(p-k_1+b)^2-m^2]}\Big)+ \\
&\qquad+\mathbf{Tr}(\gamma^\kappa\gamma^\nu\gamma^\lambda\gamma^\rho\gamma^5)\Big(\frac{(p+k_2+b)_\kappa(p+b)_\lambda}{[(p+k_2+b)^2-m^2][(p+b)^2-m^2]}- \\
&\qquad-\frac{(p+a)_\kappa(p-k_2+a)_\lambda}{[(p+a)^2-m^2][(p-k_2+a)^2-m^2]}\Big)\Big\}.
\end{aligned} \tag{H.8}$$

Following the steps described in ref. [157], we first define a function and an integral,

$$f_{\kappa\lambda}(p;c,d) \ =\ \frac{(p+c)_\kappa(p+d)_\lambda}{[(p+c)^2-m^2][(p+d)^2-m^2]}\ , \tag{H.9}$$

and

$$I_{\kappa\lambda}(k;c,d) \;=\; \int \frac{d^4p}{(2\pi)^4}\Big[f_{\kappa\lambda}(p+k;c,d) - f_{\kappa\lambda}(p;c,d)\Big]\,, \tag{H.10}$$

where c, d are arbitrary four vectors. By exploiting the following "momentum shift" integral relation (see the lecture by R. Jackiw in ref. [156] and refs. [126, 127, 158])

$$\int \frac{d^4p}{(2\pi)^4}[f(p+a)-f(p)] = \frac{i}{(2\pi)^4}\Big[2\pi^2 a_\mu \lim_{p\to\infty} p^\mu p^2 f_o(p) + \pi^2 a_\mu a_\nu \lim_{p\to\infty} p^\mu p^2 \frac{\partial f_e(p)}{\partial p_\nu}\Big], \tag{H.11}$$

where only the first term on the r.h.s is relevant to linearly divergent diagrams, and,

$$f_o(p) = \frac{1}{2}[f(p)-f(-p)]\,, \qquad f_e(p) = \frac{1}{2}[f(p)+f(-p)]\,, \tag{H.12}$$

are the odd and even parts of $f(p)$ respectively, we obtain,[3]

$$I_{\kappa\lambda}(k;c,d) \;=\; \frac{i}{96\pi^2}\Big[2k_\lambda c_\kappa + 2k_\kappa d_\lambda - k_\lambda d_\kappa - k_\kappa c_\lambda - g_{\kappa\lambda}k\cdot(k+c+d) + k_\lambda k_\kappa\Big]. \tag{H.13}$$

Now we have all the necessary machinery to calculate $\Pi^{\nu\rho}$ in eq. (H.8) by applying to it eqs. (H.11) and (H.13). For the non-chiral part of $\Pi^{\nu\rho}$ the choice $b=-a$ results in $\Pi^{\nu\rho}_{\rm non-chiral}=0$ as we expect, since there should be *no* non-chiral anomalies. With this assignment for vector b we finally obtain for the chiral part:

$$\Pi^{\nu\rho}_{\rm chiral}(k_1,k_2;a,-a) = \frac{e^3(\beta^3+3\alpha^2\beta)}{4\pi^2}\varepsilon^{\kappa\nu\lambda\rho}a_\kappa(k_1+k_2)_\lambda. \tag{H.14}$$

Plugging in eqs. (H.4) and (H.14) into eq. (H.3), the WI associated to the leg $-\mu-$ becomes:

$$q_\mu\Gamma^{\mu\nu\rho}(k_1,k_2;a,-a) = -\frac{2me\beta i}{\tilde\beta}\,\Gamma^{\nu\rho}(k_1,k_2) + \frac{e^3(\beta^3+3\alpha^2\beta)}{4\pi^2}\,\varepsilon^{\kappa\nu\lambda\rho}\,a_\kappa\,(k_1+k_2)_\lambda. \tag{H.15}$$

Along the same lines we can build in the WIs for the other vertices. For example, the WI referring to the conservation of current in vertex $-\nu-$ (see Fig.3.1) reads:

$$-k_{1\nu}\widetilde\Gamma^{\nu\rho\mu}(k_1,k_2;a,-a) = -\frac{2m\beta ei}{\tilde\beta}\,\widetilde\Gamma^{\rho\mu}(k_1,k_2) - \frac{e^3(\beta^3+3\alpha^2\beta)}{4\pi^2}\varepsilon^{\kappa\rho\lambda\mu}\,(a-k_2)_\kappa\,k_{1\lambda}. \tag{H.16}$$

Vertices $\widetilde\Gamma^{\nu\rho\mu}(k_1,k_2;a,b)$ and $\widetilde\Gamma^{\rho\mu}(k_1,k_2)$ are obtained from $\Gamma^{\mu\nu\rho}(k_1,k_2;a,b)$ and $\Gamma^{\nu\rho}(k_1,k_2)$ in eqs. (H.1) and (H.4), respectively, after the following replacements

$$\begin{gathered}\mu\to\nu,\quad \nu\to\rho,\quad \rho\to\mu,\quad a\to a-k_2,\quad b\to b+k_2,\quad k_1\to k_2,\\ k_2\to -k_1-k_2,\qquad q=k_1+k_2\to k_2-k_1-k_2=-k_1\Rightarrow q\to -k_1\,.\end{gathered} \tag{H.17}$$

[3] There is a typographical error in the corresponding expression of a classic textbook written by S. Weinberg in ref. [157]. We thank Steve Martin and Howie Haber for communication related to this point.

It is straightforward to see from eq. (H.17) that the non-chiral part of $-k_{1\nu}\widetilde{\Gamma}^{\nu\rho\mu}(k_1,k_2;a,b)$ vanishes again for the choice $b=-a$. Similarly the WI for the current conservation in the $-\rho-$ vertex is:

$$-k_{2\rho}\widehat{\Gamma}^{\rho\mu\nu}(k_1,k_2;a,-a) = -\frac{2m\beta ei}{\tilde{\beta}}\,\widehat{\Gamma}^{\mu\nu}(k_1,k_2) - \frac{e^3(\beta^3+3\alpha^2\beta)}{4\pi^2}\,\varepsilon^{\kappa\mu\lambda\nu}\,(a+k_1)_\kappa\,k_{2\lambda}. \quad \text{(H.18)}$$

As previously, $\widehat{\Gamma}^{\rho\mu\nu}(k_1,k_2;a,b)$ and $\widehat{\Gamma}^{\mu\nu}(k_1,k_2)$ can be obtained from eqs. (H.1) and (H.4) by making the following replacements:

$$\mu\to\rho,\quad \nu\to\mu,\quad \rho\to\nu,\quad a\to a+k_1,\quad b\to b-k_1,\quad k_1\to -k_2-k_1,$$
$$k_2\to k_1,\quad q=k_1+k_2\to -k_2-k_1+k_1\Rightarrow q\to -k_2\,. \quad \text{(H.19)}$$

These replacements leave invariant the choice $b=-a$ so that finally, the non-chiral part of $-k_{2\rho}\widehat{\Gamma}^{\rho\mu\nu}(k_1,k_2;a,-a)$ vanishes identically everywhere. Furthermore, by direct calculation the vertices $\widetilde{\Gamma}^{\rho\mu}$ and $\widehat{\Gamma}^{\mu\nu}$ are found to be,

$$\widetilde{\Gamma}^{\rho\mu}(k_1,k_2) \;=\; \frac{ie^2m\tilde{\beta}}{2\pi^2}\,\varepsilon^{\lambda\mu\xi\rho}\,k_{1\lambda}\,k_{2\xi}\,I_1(k_1,k_2,m)\,, \quad \text{(H.20)}$$

and

$$\widehat{\Gamma}^{\mu\nu}(k_1,k_2) \;=\; \frac{ie^2m\tilde{\beta}}{2\pi^2}\,\varepsilon^{\lambda\mu\xi\nu}\,k_{1\lambda}\,k_{2\xi}\,I_2(k_1,k_2,m)\,, \quad \text{(H.21)}$$

respectively, where the corresponding integrals $I_{1,2}$ are written explicitly as,

$$I_1(k_1,k_2,m) \;=\; \int_0^1 dx\int_0^{1-x} dy\frac{-(\alpha^2+\beta^2)+2x\beta^2}{x(x-1)k_2^2+y(y-1)k_1^2-2xyk_1\cdot k_2+m^2}\,, \quad \text{(H.22)}$$

and

$$I_2(k_1,k_2,m) \;=\; \int_0^1 dx\int_0^{1-x} dy\frac{(\alpha^2+\beta^2)-2y\beta^2}{x(x-1)k_2^2+y(y-1)k_1^2-2xyk_1\cdot k_2+m^2}\,. \quad \text{(H.23)}$$

The three-point vertex obeys the following equality,

$$\Gamma^{\mu\nu\rho}=\widetilde{\Gamma}^{\nu\rho\mu}=\widehat{\Gamma}^{\rho\mu\nu}\,, \quad \text{(H.24)}$$

as the property of trace to remain invariant under cyclic permutations. It is instructive to write the arbitrary vector a^μ, appearing in the WIs, as a linear combination of the two independent momenta k_1 and k_2,

$$a^\mu \;=\; z\,k_1^\mu + w\,k_2^\mu\,, \quad \text{(H.25)}$$

with z, w arbitrary real numbers. Then the WIs in eqs. (H.15), (H.16) and (H.18) can be written explicitly in terms of the three integrals I_0, I_1, and I_2 and the real numbers

w and z as,

$$\begin{aligned} q_\mu \Gamma^{\mu\nu\rho}(k_1,k_2;w,z) &= -\frac{e^3\beta m^2}{\pi^2}\,\varepsilon^{\lambda\nu\rho\sigma}\,k_{1\lambda}\,k_{2\sigma}\,I_0(k_1,k_2;m) + \\ &+ \frac{e^3(\beta^3+3\alpha^2\beta)}{4\pi^2}\,\varepsilon^{\lambda\nu\rho\sigma}\;k_{1\lambda}\,k_{2\sigma}(w-z)\;, \end{aligned} \tag{H.26}$$

$$\begin{aligned} -k_{1\nu}\widetilde{\Gamma}^{\nu\rho\mu}(k_1,k_2;w) &= -\frac{e^3\beta m^2}{\pi^2}\,\varepsilon^{\lambda\mu\rho\sigma}\,k_{1\lambda}\,k_{2\sigma}\,I_1(k_1,k_2;m) + \\ &+ \frac{e^3(\beta^3+3\alpha^2\beta)}{4\pi^2}\varepsilon^{\lambda\mu\rho\sigma}\,(w-1)\,k_{1\lambda}k_{2\sigma}\;, \end{aligned} \tag{H.27}$$

$$\begin{aligned} -k_{2\rho}\widehat{\Gamma}^{\rho\mu\nu}(k_1,k_2;z) &= -\frac{e^3\beta m^2}{\pi^2}\,\varepsilon^{\lambda\mu\nu\sigma}\,k_{1\lambda}\,k_{2\sigma}\,I_2(k_1,k_2;m) + \\ &+ \frac{e^3(\beta^3+3\alpha^2\beta)}{4\pi^2}\,\varepsilon^{\lambda\mu\nu\sigma}\,(z+1)k_{1\lambda}k_{2\sigma}\;. \end{aligned} \tag{H.28}$$

Obviously, even if we choose $w=1$ and $z=-1$ so that the second and third anomalies vanish, it cannot be done so for the first one. The anomalous term, *i.e.*, the second term on the r.h.s of eq. (H.26), remains. It is quite interesting to note that in the limit where $k_1^2,\,k_2^2,\,k_1\cdot k_2 \ll m \to \infty$, there is a choice for $w=-z=1/3$ such that the right hand side of eqs. (H.26), (H.27) and (H.28) vanish identically. For this choice the fermions get decoupled completely.

Our goal is still to calculate the three gauge boson vertex $\Gamma^{\mu\nu\rho}(k_1,k_2;a,-a)$. The idea is to first write down the most general, Lorentz invariant vertex, as:[4]

$$\begin{aligned} \Gamma^{\mu\nu\rho}(k_1,k_2;a,-a) &= \Big[A_1(k_1,k_2;a,-a)\,\varepsilon^{\mu\nu\rho\sigma}\,k_{2\sigma} \;+\; A_2(k_1,k_2;a,-a)\,\varepsilon^{\mu\nu\rho\sigma}\,k_{1\sigma} \\ &+ A_3(k_1,k_2)\,\varepsilon^{\mu\rho\beta\delta}\,k_2^\nu\,k_{1\beta}\,k_{2\delta} + A_4(k_1,k_2)\,\varepsilon^{\mu\rho\beta\delta}\,k_1^\nu\,k_{1\beta}\,k_{2\delta} \\ &+ A_5(k_1,k_2)\,\varepsilon^{\mu\nu\beta\delta}\,k_2^\rho\,k_{1\beta}\,k_{2\delta} + A_6(k_1,k_2)\,\varepsilon^{\mu\nu\beta\delta}\,k_1^\rho\,k_{1\beta}\,k_{2\delta}\Big]. \end{aligned} \tag{H.32}$$

The form factors A_1 and A_2 are dimensionless and, by naive power counting, at most linearly divergent while all the rest, $A_3,..,A_6$ possess dimension of m^{-2} and are finite.

[4]There are two more terms allowed in the expansion,

$$A_7(k_1,k_2)\varepsilon^{\rho\nu\beta\delta}\,k_2^\mu\,k_{1\beta}\,k_{2\delta} + A_8(k_1,k_2)\varepsilon^{\rho\nu\beta\delta}\,k_1^\mu\,k_{1\beta}\,k_{2\delta}\;. \tag{H.29}$$

However, by exploiting the following, very useful, identities

$$\begin{aligned} k_1^\mu\varepsilon^{\rho\nu\beta\delta}k_{1\beta}k_{2\delta} &= -\varepsilon^{\mu\rho\beta\delta}k_1^\nu k_{1\beta}k_{2\delta} + \varepsilon^{\mu\nu\beta\delta}k_1^\rho k_{1\beta}k_{2\delta} \\ &+ \varepsilon^{\mu\nu\rho\alpha}[(k_1\cdot k_2)\,k_{1\alpha} - k_1^2\,k_{2\alpha}]\;, \end{aligned} \tag{H.30}$$

$$\begin{aligned} k_2^\mu\varepsilon^{\rho\nu\beta\delta}k_{1\beta}k_{2\delta} &= -\varepsilon^{\mu\rho\beta\delta}k_2^\nu k_{1\beta}k_{2\delta} + \varepsilon^{\mu\nu\beta\delta}k_2^\rho k_{1\beta}k_{2\delta} \\ &- \varepsilon^{\mu\nu\rho\alpha}[(k_1\cdot k_2)\,k_{2\alpha} - k_2^2\,k_{1\alpha}]\;, \end{aligned} \tag{H.31}$$

we arrive at the six form factors given in eq. (H.32).

The latter can be calculated directly in four dimensions from eq. (H.1). We find explicitly:

$$A_3(k_1,k_2) = -A_6(k_1,k_2) = -\frac{e^3(\beta^3+3\alpha^2\beta)}{\pi^2}\int_0^1 dx\int_0^{1-x} dy\frac{xy}{\Delta}\ , \tag{H.33}$$

$$A_4(k_1,k_2) = \frac{e^3(\beta^3+3\alpha^2\beta)}{\pi^2}\int_0^1 dx\int_0^{1-x} dy\frac{y(y-1)}{\Delta}\ , \tag{H.34}$$

$$A_5(k_1,k_2) = -\frac{e^3(\beta^3+3\alpha^2\beta)}{\pi^2}\int_0^1 dx\int_0^{1-x} dy\frac{x(x-1)}{\Delta}, \tag{H.35}$$

where the integrand denominator is common for all $A_3,...,A_6$ and reads:

$$\Delta \equiv x(x-1)k_2^2 + y(y-1)k_1^2 - 2xyk_1\cdot k_2 + m^2\ . \tag{H.36}$$

To estimate the two divergent integrals, A_1 and A_2, we apply the Ward Identities for the vertices ν and ρ, *i.e.,* eqs. (H.27) and (H.28) in the expansion (H.32) and obtain:

$$\begin{aligned} A_1(k_1,k_2;w) &= (k_1\cdot k_2)\,A_3(k_1,k_2) + k_1^2\,A_4(k_1,k_2) - \frac{m^2e^3\beta}{\pi^2}I_1(k_1,k_2,m) + \\ &+ \frac{e^3(\beta^3+3\alpha^2\beta)}{4\pi^2}(w-1)\ , \end{aligned} \tag{H.37}$$

$$\begin{aligned} A_2(k_1,k_2;z) &= (k_1\cdot k_2)\,A_6(k_1,k_2) + k_2^2\,A_5(k_1,k_2) - \frac{m^2e^3\beta}{\pi^2}I_2(k_1,k_2,m) + \\ &+ \frac{e^3(\beta^3+3\alpha^2\beta)}{4\pi^2}(z+1)\ . \end{aligned} \tag{H.38}$$

Equations (H.22-H.23, H.33-H.38) *complete* the evaluation of the vertex $\Gamma^{\mu\nu\rho}(k_1,k_2,w,z)$ in eq. (H.32). In Appendix J we present analytical expressions of the integrals $A_{3,..,6}$ and $I_{0,1,2}$ in various limits.

Even if the form factors $A_{i=1...6}$ had not been calculated explicitly there is much to say about their structure by exploiting possible Bose symmetries. Hence, referring to the notation of Fig. 3.1, Bose symmetry among j and k legs implies,

$$A_1(k_1,k_2) = -A_2(k_2,k_1)\ , \tag{H.39a}$$

$$A_3(k_1,k_2) = -A_6(k_2,k_1)\ , \tag{H.39b}$$

$$A_4(k_1,k_2) = -A_5(k_2,k_1)\ , \tag{H.39c}$$

while in i and j legs,

$$\begin{aligned} A_1(k_1,k_2) &= -A_1(-q,k_2) + A_2(-q,k_2) - (k_1\cdot k_2)\,[(A_3(-q,k_2) - A_4(-q,k_2)] + \\ &\quad + k_1^2 A_4(-q,k_2)\;, \end{aligned} \tag{H.40a}$$

$$\begin{aligned} A_2(k_1,k_2) &= A_2(-q,k_2) + k_2^2\,[A_3(-q,k_2) - A_4(-q,k_2)] - \\ &\quad - (k_1\cdot k_2)\,A_4(-q,k_2)\;, \end{aligned} \tag{H.40b}$$

$$A_3(k_1,k_2) = A_4(-q,k_2) - A_3(-q,k_2)\;, \tag{H.40c}$$

$$A_4(k_1,k_2) = A_4(-q,k_2)\;, \tag{H.40d}$$

$$A_5(k_1,k_2) = A_5(-q,k_2) - A_6(-q,k_2) + A_3(-q,k_2) - A_4(-q,k_2)\;, \tag{H.40e}$$

$$A_6(k_1,k_2) = -A_4(-q,k_2) - A_6(-q,k_2)\;, \tag{H.40f}$$

and, finally, in i and k legs we find,

$$\begin{aligned} A_1(k_1,k_2) &= A_1(k_1,-q) - k_1^2\,[(A_5(k_1,-q) - A_6(k_1,-q)] - \\ &\quad - (k_1\cdot k_2)A_5(k_1,-q)\;, \end{aligned} \tag{H.41a}$$

$$\begin{aligned} A_2(k_1,k_2) &= A_1(k_1,-q) - A_2(k_1,-q) + (k_1\cdot k_2)\,[A_5(k_1,-q) - A_6(k_1,-q)] + \\ &\quad + k_2^2 A_5(k_1,-q)\;, \end{aligned} \tag{H.41b}$$

$$A_3(k_1,k_2) = -A_3(k_1,-q) - A_5(k_1,-q)\;, \tag{H.41c}$$

$$A_4(k_1,k_2) = A_4(k_1,-q) - A_3(k_1,-q) - A_5(k_1,-q) + A_6(k_1,-q)\;, \tag{H.41d}$$

$$A_5(k_1,k_2) = A_5(k_1,-q)\;, \tag{H.41e}$$

$$A_6(k_1,k_2) = A_5(k_1,-q) - A_6(k_1,-q)\;. \tag{H.41f}$$

The above relations have been repeatedly used in section 3.4 when determining the anomaly parameters w and z. We should notice that in addition to relations due to Bose symmetry, there are few more relations originated solely from the fermionic triangle:

$$A_3(k_1,k_2) = A_3(k_2,k_1)\;, \quad A_6(k_1,k_2) = A_6(k_2,k_1)\;. \tag{H.42}$$

We can now exploit Bose symmetry to set constraints on the arbitrary parameters w and z. For example, if the gauge bosons associated with legs j and k in Fig. 3.1 are identical, then eq. (H.39) impose the following relation,

$$w + z = 0\;, \tag{H.43}$$

among the undefined (momentum route dependent) parameters. One last remark is that we can rediscover Bose symmetries by using one of the following equivalent representations (*i.e.*, they leave the double integral measure invariant) of the integrals

$A_3, ..., A_6$ by noting that

$$\Delta(k_1,k_2) \quad \xrightarrow{x\leftrightarrow y} \quad \Delta(k_2,k_1)\ , \tag{H.44}$$

$$\Delta(k_1,k_2) \quad \xrightarrow[x\to x]{y\to 1-x-y} \quad \Delta(k_1,-q)\ , \tag{H.45}$$

$$\Delta(k_1,k_2) \quad \xrightarrow[x\to 1-x-y]{y\to y} \quad \Delta(-q,k_2)\ , \tag{H.46}$$

where $\Delta(k_1,k_2)$ is a function defined in eq. (H.36). As a generalisation of eqs. (H.15), (H.16) and (H.18) we can proceed to the situation where there are three, in general different, external gauge bosons with different couplings to fermions. As in (H.1), we write the general three point vertex in Fig. 3.1 as:

$$\Gamma^{\mu\nu\rho}(k_1,k_2;a,b)=\tilde{\Gamma}^{\nu\rho\mu}(k_1,k_2;a,b)=\widehat{\Gamma}^{\rho\mu\nu}(k_1,k_2;a,b)=-e^3\int\frac{d^4p}{(2\pi)^4}\times$$

$$\times\Bigg\{\frac{\mathbf{Tr}\Big[\gamma^\mu(\alpha_i+\beta_i\gamma^5)(\not p-\not k_2+\not a+m)\gamma^\rho(\alpha_j+\beta_j\gamma^5)(\not p+\not a+m)\gamma^\nu(\alpha_k+\beta_k\gamma^5)(\not p+\not k_1+\not a+m)\Big]}{[(p-k_2+a)^2-m^2][(p+a)^2-m^2][(p+k_1+a)^2-m^2]}+$$

$$+\frac{\mathbf{Tr}\Big[\gamma^\mu(\alpha_i+\beta_i\gamma^5)(\not p-\not k_1+\not b+m)\gamma^\nu(\alpha_k+\beta_k\gamma^5)(\not p+\not b+m)\gamma^\rho(\alpha_j+\beta_j\gamma^5)(\not p+\not k_2+\not b+m)\Big]}{(p-k_1+b)^2-m^2][(p+b)^2-m^2][(p+k_2+b)^2-m^2]}\Bigg\}, \tag{H.47}$$

and the corresponding two point vertex functions as:

$$\begin{aligned}
\Gamma^{\nu\rho}(k_1,k_2) &= \frac{-ie^2m\tilde{\beta}}{2\pi^2}\varepsilon^{\lambda\nu\rho\sigma}k_{1\lambda}k_{2\sigma}\int_0^1dx\int_0^{1-x}dy\frac{(\alpha_j\alpha_k-\beta_j\beta_k)+2\beta_j\beta_k(x+y)}{\Delta}\ ,\\
\tilde{\Gamma}^{\rho\mu}(k_1,k_2) &= \frac{ie^2m\tilde{\beta}}{2\pi^2}\varepsilon^{\lambda\mu\xi\rho}k_{1\lambda}k_{2\xi}\int_0^1dx\int_0^{1-x}dy\frac{-(\alpha_i\alpha_k+\beta_i\beta_k)+2x\beta_i\beta_k}{\Delta}\ ,\\
\widehat{\Gamma}^{\mu\nu}(k_1,k_2) &= \frac{ie^2m\tilde{\beta}}{2\pi^2}\varepsilon^{\lambda\mu\xi\nu}k_{1\lambda}k_{2\xi}\int_0^1dx\int_0^{1-x}dy\frac{(\alpha_i\alpha_j+\beta_i\beta_j)-2y\beta_i\beta_j}{\Delta}\ ,
\end{aligned} \tag{H.48}$$

where as before $\Delta\equiv\Delta(k_1,k_2)$ is given by eq. (H.36). The complete $\Gamma^{\mu\nu\rho}(k_1,k_2,w,z)$ in this general case is presented in section 3.2.

Appendix I: Charged gauge boson vertex

In this Appendix we present the general three gauge boson vertex that contains charged gauge bosons (W^-, W^+) in the external legs. The calculation for $V^*W^-W^+$, $V = \gamma$, Z is slightly more complicated than the one for neutral triple gauge boson vertices for two reasons: first, the appearance in the loop of two, in general, different fermion masses and second, the appearance of different $Vf\overline{f}$ vertex for each particle contribution. Although the first complication leads to only technical difficulties, the latter one is more serious: it does not allow for an obvious exploitation of the master 4D "momentum shift" equation (H.11).

Our method for calculating this vertex follows exactly the same steps as described in detail in Appendix H and in section 3.2. The chiral part of the V^*WW vertex is still given by eq. (3.2).

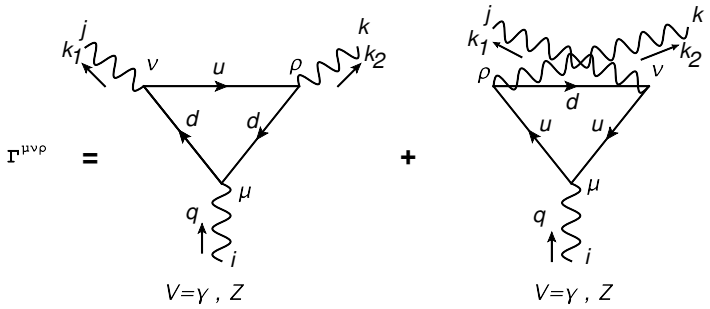

Figure I.1: *The one-loop effective triple gauge boson vertex,* $\Gamma^{\mu\nu\rho}_{VW^-W^+}$, $V = \gamma$, Z. *As in Fig. 3.1, indices* $\{i, j, k\}$ *denote distinct external gauge bosons in general.*

The finite form factors $A_3, ..., A_6$ for the first diagram in Fig. I.1 are exactly the half of the corresponding ones in eq.(3.8) but with the replacement of $\Delta(k_1, k_2)$ into:

$$\Delta(k_1,\, k_2;\, m^2_{f_u},\, m^2_{f_d}) \equiv x(x-1)k_2^2 + y(y-1)k_1^2 - 2xyk_1\cdot k_2 - (x+y)\,\Delta m^2 + m^2_{f_u}, \quad \text{(I.1)}$$

with the mass squared difference being $\Delta m^2 \equiv m^2_{f_u} - m^2_{f_d}$. Here, f_u and f_d denote each of the fermion pair (u, ν) and (d, e) for leptons and quarks, respectively. Obviously, the contribution of the crossed diagram *i.e.*, the second diagram in Fig. I.1, requires the replacement, $f_u \leftrightarrow f_d$. Our calculation here is quite general and is not confined only in to V^*WW vertex. For example, it could be used for the vertex VW_LW_R in an $SU(2)_L \times SU(2)_R \times U(1)$ gauge model.

As before, the "infinite" form factors, $A_{1,\,2}$ are fixed by the Ward Identities. The calculation of the first diagram of Fig. I.1 results in,

$$A_1(k_1,k_2) = (k_1\cdot k_2)A_3 + k_1^2 A_4 - \frac{\alpha_j(m_{f_u}-m_{f_d})}{4\pi^2}\, I_{11}(m_{f_u}^2, m_{f_d}^2) - \\ - \frac{\beta_j(m_{f_u}+m_{f_d})}{4\pi^2}\, I_{12}(m_{f_u}^2, m_{f_d}^2) + \frac{c}{8\pi^2}\,(w-1)\,, \tag{I.2a}$$

$$A_2(k_1,k_2) = (k_1\cdot k_2)A_6 + k_2^2 A_5 + \frac{\alpha_k(m_{f_u}-m_{f_d})}{4\pi^2}\, I_{21}(m_{f_u}^2, m_{f_d}^2) - \\ - \frac{\beta_k(m_{f_u}+m_{f_d})}{4\pi^2}\, I_{22}(m_{f_u}^2, m_{f_d}^2) + \frac{c}{8\pi^2}\,(z+1)\,, \tag{I.2b}$$

where $c \equiv (\alpha_i\alpha_j + \beta_i\beta_j)\beta_k + (\alpha_i\beta_j + \alpha_j\beta_i)\alpha_k$ is the usual anomaly factor. Again, the result depends upon two arbitrary four vectors, a^μ and b^μ, that parameterize the momentum routing in the loop. For chiral gauge anomalies to cancel after summing over all fermions, the arbitrary vectors a and b need to be set at $a=-b$. As before, we write a^μ as a linear combination of independent four vectors $a^\mu = z\,k_1^\mu + w\,k_2^\mu$, with z, w arbitrary real parameters. This includes γ, Z, W-self energy corrections. The latter depend on their own routing momenta arbitrary vectors that can be taken as such in order to eliminate their anomalous contributions. One then expects that this relation renders the non-chiral part independent of a as it does for the neutral vertices VVV, for $V=\gamma$, Z (see Appendix H). However, for VWW-vertices there are additional contributions to the non-chiral part of $\Gamma^{\mu\nu\rho}$ from Z,γ, W-self energy corrections that depend on routing momentum arbitrary vectors. When all these corrections are added, one expects the result to be independent on these arbitrary vectors.

Then the "non-decoupling" integrals, $I_{ij} \equiv I_{ij}(m_{f_u}^2, m_{f_d}^2)$ with $i,j=1,2$ appearing in eq. (I.2) are given by:

$$I_{11} = \int_0^1 dx \int_0^{1-x} dy\, \frac{1}{\Delta(k_1,k_2;m_{f_u}^2,m_{f_d}^2)}\Big[(\alpha_i\beta_k+\alpha_k\beta_i)\,m_{f_d}\,y \\ + (\alpha_i\beta_k+\alpha_k\beta_i)\,m_{f_u}\,(x+y-1) + (\alpha_i\beta_k-\alpha_k\beta_i)\,m_{f_d}\,x\Big]\,, \tag{I.3a}$$

$$I_{12} = \int_0^1 dx \int_0^{1-x} dy\, \frac{1}{\Delta(k_1,k_2;m_{f_u}^2,m_{f_d}^2)}\Big[-(\alpha_i\alpha_k+\beta_i\beta_k)\,m_{f_d}\,y \\ + (\alpha_i\alpha_k+\beta_i\beta_k)\,m_{f_u}\,(x+y-1) - (\alpha_i\alpha_k-\beta_i\beta_k)\,m_{f_d}\,x\Big]\,, \tag{I.3b}$$

$$I_{21} = \int_0^1 dx \int_0^{1-x} dy\, \frac{1}{\Delta(k_1,k_2;m_{f_u}^2,m_{f_d}^2)}\Big[(\alpha_i\beta_j-\alpha_j\beta_i)\,m_{f_d}\,y \\ + (\alpha_i\beta_j+\alpha_j\beta_i)\,m_{f_u}\,(x+y-1) + (\alpha_i\beta_j+\alpha_j\beta_i)\,m_{f_d}\,x\Big]\,, \tag{I.3c}$$

$$I_{22} = \int_0^1 dx \int_0^{1-x} dy\, \frac{1}{\Delta(k_1,k_2;m_{f_u}^2,m_{f_d}^2)}\Big[(\alpha_i\alpha_j-\beta_i\beta_j)\,m_{f_d}\,y \\ - (\alpha_i\alpha_j+\beta_i\beta_j)\,m_{f_u}\,(x+y-1) + (\alpha_i\alpha_j+\beta_i\beta_j)\,m_{f_d}\,x\Big]\,, \tag{I.3d}$$

where $\alpha_i \equiv \alpha_{f_d}$, $\beta_i \equiv \beta_{f_d}$,..etc, follow the first diagram of Fig. I.1. The corresponding expressions for the crossed diagram are easily obtained from those in eqs. (I.2) and (I.3) with the replacement $f_u \leftrightarrow f_d$. Note that CP-invariance is maintained since $A_1(k_1, k_2) = -A_2(k_2, k_1)$.

For reasons we explained at the beginning of this Appendix, finding the anomalous terms *i.e.*, the last terms in eq. (I.2), is not a straightforward task. The trick here is to add a Lorentz invariant but vanishing integral that generates exactly the anomaly integrals by momentum shift. It is then straightforward to use the 4-D expression (H.11).

To complete our analysis for the chiral fermionic triangle with general external charged and neutral gauge bosons, we append here the relevant WI's analogous to those presented in eq. (3.3) for neutral external gauge bosons:

$$q_\mu \, \Gamma^{\mu\nu\rho}(k_1, k_2) \;=\; -\frac{\beta_i}{2\pi^2} \, m_{f_d} \epsilon^{\nu\rho\lambda\sigma} \, k_{1\lambda} k_{2\sigma} \, I_{01}(m^2_{f_u}, m^2_{f_d}) + \frac{c}{8\pi^2} \, \epsilon^{\nu\rho\lambda\sigma} \, k_{1\lambda} k_{2\sigma} \, (w - z) \; , \tag{I.4a}$$

$$\begin{aligned} -k_{1\nu} \, \Gamma^{\mu\nu\rho}(k_1, k_2) \;=\; & -\frac{\alpha_j}{4\pi^2} \, (m_{f_u} - m_{f_d}) \, \epsilon^{\mu\rho\lambda\sigma} \, k_{1\lambda} k_{2\sigma} \, I_{11}(m^2_{f_u}, m^2_{f_d}) - \\ & - \frac{\beta_j}{4\pi^2} \, (m_{f_u} + m_{f_d}) \, \epsilon^{\mu\rho\lambda\sigma} \, k_{1\lambda} k_{2\sigma} \, I_{12}(m^2_{f_u}, m^2_{f_d}) + \\ & + \frac{c}{8\pi^2} \, \epsilon^{\mu\rho\lambda\sigma} \, k_{1\lambda} k_{2\sigma} \, (w - 1) \; , \end{aligned} \tag{I.4b}$$

$$\begin{aligned} -k_{2\rho} \, \Gamma^{\mu\nu\rho}(k_1, k_2) \;=\; & \frac{\alpha_k}{4\pi^2} \, (m_{f_u} - m_{f_d}) \, \epsilon^{\mu\nu\lambda\sigma} \, k_{1\lambda} k_{2\sigma} \, I_{21}(m^2_{f_u}, m^2_{f_d}) - \\ & - \frac{\beta_k}{4\pi^2} \, (m_{f_u} + m_{f_d}) \, \epsilon^{\mu\nu\lambda\sigma} \, k_{1\lambda} k_{2\sigma} \, I_{22}(m^2_{f_u}, m^2_{f_d}) + \\ & + \frac{c}{8\pi^2} \, \epsilon^{\mu\nu\lambda\sigma} \, k_{1\lambda} k_{2\sigma} \, (z + 1) \; . \end{aligned} \tag{I.4c}$$

Again, the corresponding expressions for the crossed diagram in Fig. I.1 are obtained from eq. (I.4) after the replacement $f_u \leftrightarrow f_d$. The integral $I_{01} \equiv I_{01}(m^2_{f_u}, m^2_{f_d})$ is given by:

$$\begin{aligned} I_{01} = \int_0^1 dx \int_0^{1-x} dy \frac{1}{\Delta(k_1, k_2; m^2_{f_u}, m^2_{f_d})} \Big[& (\alpha_j \alpha_k + \beta_j \beta_k) \, m_{f_d} \, y - \\ & - (\alpha_j \alpha_k - \beta_j \beta_k) \, m_{f_u} \, (x + y - 1) + (\alpha_j \alpha_k + \beta_j \beta_k) \, m_{f_d} \, x \Big] . \end{aligned} \tag{I.5}$$

As an extra check, note that in the limit of equal masses $m^2_{f_u} = m^2_{f_d}$, all the integral expressions in eq. (I.3) and eq. (I.5) reduce to the corresponding ones in eqs. (3.4), (3.5) and (3.8) for the neutral gauge boson vertex.

Appendix J: Useful integral expressions

In this Appendix we present analytical expressions for integrals related to $A_{3,..,6}$, and, $I_{1,2}$ in the limit $k_1^2,\, k_2^2 \to 0$ as well as their approximate expressions in various limits. We make an effort to write the latter in terms of standard functions *i.e.*, *not* dilogarithms, which are easy to handle both symbolically and numerically. We start out with integrals related to eq. (3.8),

$$\widetilde{A_3}(\xi) = \int_0^1 dx \int_0^{1-x} dy \frac{xy}{xy - \xi/4} = \frac{1}{2}[1 + \xi J(\xi)] \,, \tag{J.1}$$

where $\xi \equiv \frac{4m^2}{s}$, m is the loop fermion mass, and $s = (k_1 + k_2)^2$, while,

$$J(\xi) = -\arctan^2\left(\frac{1}{\sqrt{\xi - 1}}\right), \quad \xi \geq 1 \,, \tag{J.2a}$$

$$= \frac{1}{4}\left[\ln\left(\frac{1 - \sqrt{1-\xi}}{1 + \sqrt{1-\xi}}\right) - i\pi\right]^2, \quad \xi \leq 1 \,. \tag{J.2b}$$

This integral has also been calculated in ref. [138] and we find agreement. In the same limit the integral related to A_4 and A_5 is:

$$\widetilde{A_4}(\xi) = \widetilde{A_5}(\xi) = \int_0^1 dx \int_0^{1-x} dy \frac{x(x-1)}{xy - \xi/4} = \int_0^1 dx \int_0^{1-x} dy \frac{y(y-1)}{xy - \xi/4} \,, \tag{J.3}$$

with its exact answer written like

$$\widetilde{A_4}(\xi) = 1 - \sqrt{\xi - 1}\arctan\left(\frac{1}{\sqrt{\xi - 1}}\right), \quad \xi \geq 1 \,, \tag{J.4}$$

$$= 1 + \frac{\sqrt{1-\xi}}{2}\left[\ln\left(\frac{1 - \sqrt{1-\xi}}{1 + \sqrt{1-\xi}}\right) - i\pi\right], \quad \xi \leq 1. \tag{J.5}$$

Integrals that are related to I_1 and I_2 of eq. (3.5) are:

$$\widetilde{I_1}(\xi) = \int_0^1 dx \int_0^{1-x} dy \frac{1}{xy - \xi/4} \tag{J.6}$$

$$= -2\arctan^2\left(\frac{1}{\sqrt{\xi - 1}}\right), \quad \xi \geq 1 \tag{J.7}$$

$$= \frac{1}{2}\left[\ln\left(\frac{1 - \sqrt{1-\xi}}{1 + \sqrt{1-\xi}}\right) - i\pi\right]^2, \quad \xi \leq 1 \,, \tag{J.8}$$

and

$$\widetilde{I}_1'(\xi) = \int_0^1 dx \int_0^{1-x} dy \frac{x}{xy-\xi/4} = \int_0^1 dx \int_0^{1-x} dy \frac{y}{xy-\xi/4} \tag{J.9}$$

$$= 2\left[\sqrt{\xi-1}\,\arctan\left(\frac{1}{\sqrt{\xi-1}}\right) - 1\right], \quad \xi \geq 1 \tag{J.10}$$

$$= -2 - \sqrt{1-\xi}\left[\ln\left(\frac{1-\sqrt{1-\xi}}{1+\sqrt{1-\xi}}\right) - i\pi\right], \quad \xi \leq 1\,. \tag{J.11}$$

These integrals are related $A_3, .., A_6$, $I_{1,2}$, and in the limit $m_Z^2 \ll s < m^2$, become:

$$A_3(s;m^2) = -A_6(s;m^2) = \frac{c}{s}\widetilde{A_3}(\frac{4m^2}{s}) = -\frac{c}{m^2}\left[\frac{1}{24} + \frac{1}{180}\frac{s}{m^2} + \mathcal{O}(s^2/m^4)\right], \tag{J.12a}$$

$$A_4(s;m^2) = -A_5(s;m^2) = -\frac{c}{s}\widetilde{A_4}(\frac{4m^2}{s}) = -\frac{c}{m^2}\left[\frac{1}{12} + \frac{1}{120}\frac{s}{m^2} + \mathcal{O}(s^2/m^4)\right], \tag{J.12b}$$

$$I_1(s;m^2) = \frac{\alpha_i\alpha_k + \beta_i\beta_k}{s}\,\widetilde{I}_1(\frac{4m^2}{s}) - \frac{2\beta_i\beta_k}{s}\,\widetilde{I}_1'(\frac{4m^2}{s})$$
$$= -\frac{1}{m^2}\left[\frac{\beta_i\beta_k + 3\alpha_i\alpha_k}{6} + \frac{\beta_i\beta_k + 5\alpha_i\alpha_k}{120}\frac{s}{m^2} + \mathcal{O}(s^2/m^4)\right], \tag{J.12c}$$

$$I_2(s;m^2) = -\frac{\alpha_i\alpha_j + \beta_i\beta_j}{s}\,\widetilde{I}_1(\frac{4m^2}{s}) + \frac{2\beta_i\beta_j}{s}\,\widetilde{I}_1'(\frac{4m^2}{s})$$
$$= \frac{1}{m^2}\left[\frac{\beta_i\beta_j + 3\alpha_i\alpha_j}{6} + \frac{\beta_i\beta_j + 5\alpha_i\alpha_j}{120}\frac{s}{m^2} + \mathcal{O}(s^2/m^4)\right], \tag{J.12d}$$

where $c = \frac{e^3[(\alpha_i\alpha_j+\beta_i\beta_j)\beta_k+(\alpha_i\beta_j+\beta_i\alpha_j)\alpha_k]}{\pi^2}$ is the anomaly factor.

These expressions are in agreement with the corresponding ones presented in ref. [89]. In the high energy limit $m^2 \ll s$, we obtain:

$$A_3(s;m^2) = -A_6(s;m^2) \simeq c\left\{\frac{1}{2s} + \frac{m^2}{2s^2}\left[\ln^2\frac{s}{m^2} - \pi^2\right] + i\pi\frac{m^2}{s^2}\ln\frac{s}{m^2} + \mathcal{O}(m^4/s^3)\right\}, \tag{J.13a}$$

$$\begin{aligned} A_4(s;m^2) &= -A_5(s;m^2) \\ &\simeq c\left\{\frac{1}{s}\left[-1 + \frac{1}{2}\ln\frac{s}{m^2}\right] - \frac{m^2}{s^2}\left[\ln\frac{s}{m^2} + 1\right] + i\pi\left[\frac{1}{2s} - \frac{m^2}{s^2}\right] + \mathcal{O}(m^4/s^3)\right\}, \end{aligned} \tag{J.13b}$$

$$\begin{aligned} I_1(s;m^2) \simeq\ & \frac{(\alpha_i\alpha_k + \beta_i\beta_k)}{s}\left[\frac{1}{2}\left(\ln^2\frac{s}{m^2} - \pi^2\right) - 2\frac{m^2}{s}\ln\frac{s}{m^2}\right] - \\ & - \frac{2\beta_i\beta_k}{s}\left[\ln\frac{s}{m^2} - 2 - \frac{2m^2}{s}\left(\ln\frac{s}{m^2} + 1\right)\right] \\ & + i\pi\left\{\frac{(\alpha_i\alpha_k + \beta_i\beta_k)}{s}\left[\ln\frac{s}{m^2} - \frac{2m^2}{s}\right] - \frac{2\beta_i\beta_k}{s}\left[1 - \frac{2m^2}{s}\right]\right\} + \mathcal{O}(m^4/s^3), \end{aligned} \tag{J.13c}$$

$$\begin{aligned} I_2(s;m^2) \simeq & -\frac{(\alpha_i\alpha_j + \beta_i\beta_j)}{s}\left[\frac{1}{2}\left(\ln^2\frac{s}{m^2} - \pi^2\right) - 2\frac{m^2}{s}\ln\frac{s}{m^2}\right] + \\ & + \frac{2\beta_i\beta_j}{s}\left[\ln\frac{s}{m^2} - 2 - \frac{2m^2}{s}\left(\ln\frac{s}{m^2} + 1\right)\right] - \\ & - i\pi\left\{\frac{(\alpha_i\alpha_j + \beta_i\beta_j)}{s}\left[\ln\frac{s}{m^2} - \frac{2m^2}{s}\right] - \frac{2\beta_i\beta_j}{s}\left[1 - \frac{2m^2}{s}\right]\right\} + \mathcal{O}(m^4/s^3). \end{aligned} \tag{J.13d}$$

Only the real parts of these expressions have been presented in ref. [89] and we find agreement[5]. Other useful identities among A's that have been used in our numerical code for calculating the V^*ZZ-vertex are,

$$(A_3 - A_4)(k_1 = m_Z, k_2 = m_Z, s; m = 0) = \frac{s\, A_3(k_1 = m_Z, k_2 = m_Z, s; m = 0)}{2\, m_Z^2} - \frac{1}{4\, m_Z^2} \tag{J.14}$$

and for the $V^*\gamma Z$-vertex,

$$A_3(k_1 = 0, k_2 = m_Z, s; m = 0) = \frac{1}{2(s - m_Z^2)} - \frac{m_Z^2}{2(s - m_Z^2)^2}\ln\left(\frac{s}{m_Z^2}\right), \tag{J.15}$$

$$A_5(k_1 = 0, k_2 = m_Z, s; m = 0) = -\frac{1}{2(s - m_Z^2)}\ln\left(\frac{s}{m_Z^2}\right). \tag{J.16}$$

[5]For notational matter, our integrals are related to those in ref. [89] like $A_3 = -c_6$, $A_4 = \frac{1}{2}(c_4 - c_3 - 2\,c_6)$, where for example $A_3 \equiv A_3(k_1^2 = k_2^2 = m_W^2, s, m_{f_u}^2, m_{f_d}^2)$,...etc.

Finally, we derive full analytical expressions in the case $k_1^2 = 0$, where one of the external gauge bosons is massless e.g., the $V^*\gamma Z$-vertex. To this end it is useful to define an auxiliary function,

$$\mathscr{F}(m_Z, s, m) \equiv \int_0^1 dx \int_0^{1-x} dy \;\; \ln[x(x-1)m_Z^2 - xy(s - m_Z^2) + m^2] \,, \qquad \text{(J.17)}$$

out of which we read $A_3, .., A_6$, $I_{1,2}$ by simply taking appropriate derivatives w.r.t s, $k_2^2 = m_Z^2$ or m^2. Depending on the region of parameters s, m^2, m_Z^2 we have found the function $\mathscr{F}$ to be,

$$\begin{aligned}
\mathscr{F}(m_Z, s, m) &= -\frac{3}{2} + \frac{\ln(m^2)}{2} - \left(\frac{1}{m_Z^2 - s}\right)\left\{ s\sqrt{\frac{4m^2}{s} - 1}\, \arctan\left(\frac{1}{\sqrt{\frac{4m^2}{s} - 1}}\right)\right. \\
&+ 2m^2\left[\arctan^2\left(\frac{1}{\sqrt{\frac{4m^2}{s} - 1}}\right) - \arctan^2\left(\frac{1}{\sqrt{\frac{4m^2}{m_Z^2} - 1}}\right)\right] - \\
&- \left. m_Z^2\sqrt{\frac{4m^2}{m_Z^2} - 1}\, \arctan\left(\frac{1}{\sqrt{\frac{4m^2}{m_Z^2} - 1}}\right)\right\}, \quad \frac{4m^2}{s} > 1,\ \frac{4m^2}{m_Z^2} > 1,
\end{aligned} \qquad \text{(J.18)}$$

$$\begin{aligned}
\mathscr{F}(m_Z, s, m) &= -\frac{3}{2} + \frac{\ln(m^2)}{2} - \left(\frac{1}{m_Z^2 - s}\right)\left\{ s\sqrt{\frac{4m^2}{s} - 1}\, \arctan\left(\frac{1}{\sqrt{\frac{4m^2}{s} - 1}}\right) + \right. \\
&+ m^2\left[2\arctan^2\left(\frac{1}{\sqrt{\frac{4m^2}{s} - 1}}\right) + \frac{1}{2}\left(\ln(\frac{1 - \sqrt{1 - \frac{4m^2}{m_Z^2}}}{1 + \sqrt{1 - \frac{4m^2}{m_Z^2}}}) + i\pi\right)^2\right] + \\
&+ \left. m_Z^2\left[\frac{1}{2}\sqrt{1 - \frac{4m^2}{m_Z^2}}\, \left(\ln(\frac{1 - \sqrt{1 - \frac{4m^2}{m_Z^2}}}{1 + \sqrt{1 - \frac{4m^2}{m_Z^2}}}) - i\pi\right)\right]\right\}, \frac{4m^2}{s} > 1,\ \frac{4m^2}{m_Z^2} < 1 \,,
\end{aligned} \qquad \text{(J.19)}$$

$$\begin{aligned}
\mathscr{F}(m_Z, s, m) &= -\frac{3}{2} + \frac{\ln(m^2)}{2} + \\
&+ \left(\frac{1}{m_Z^2 - s}\right)\left\{ s\left[\frac{1}{2}\sqrt{1 - \frac{4m^2}{s}}\, \left(\ln(\frac{1 - \sqrt{1 - \frac{4m^2}{s}}}{1 + \sqrt{1 - \frac{4m^2}{s}}}) - i\pi\right)\right]\right. \\
&+ m^2\left[2\arctan^2\left(\frac{1}{\sqrt{\frac{4m^2}{m_Z^2} - 1}}\right) + \frac{1}{2}\left(\ln(\frac{1 - \sqrt{1 - \frac{4m^2}{s}}}{1 + \sqrt{1 - \frac{4m^2}{s}}}) - i\pi\right)^2\right] + \\
&+ \left. m_Z^2\left[\sqrt{\frac{4m^2}{m_Z^2} - 1}\;\; \arctan\left(\frac{1}{\sqrt{\frac{4m^2}{m_Z^2} - 1}}\right)\right]\right\}, \quad \frac{4m^2}{s} < 1,\ \frac{4m^2}{m_Z^2} > 1 \,,
\end{aligned} \qquad \text{(J.20)}$$

$$
\begin{aligned}
\mathscr{F}(m_Z,s,m) &= -\frac{3}{2}+\frac{\ln(m^2)}{2}+ \\
&+ \left(\frac{1}{m_Z^2-s}\right)\left\{s\left[\frac{1}{2}\sqrt{1-\frac{4m^2}{s}}\left(\ln(\frac{1-\sqrt{1-\frac{4m^2}{s}}}{1+\sqrt{1-\frac{4m^2}{s}}})-i\pi\right)\right]\right. \\
&+ m^2\left[\frac{1}{2}\left(\ln(\frac{1-\sqrt{1-\frac{4m^2}{s}}}{1+\sqrt{1-\frac{4m^2}{s}}})\pm i\pi\right)^2-\frac{1}{2}\left(\ln(\frac{1-\sqrt{1-\frac{4m^2}{m_Z^2}}}{1+\sqrt{1-\frac{4m^2}{m_Z^2}}})\pm i\pi\right)^2\right] \\
&- \left. m_Z^2\left[\frac{1}{2}\sqrt{1-\frac{4m^2}{m_Z^2}}\left(\ln(\frac{1-\sqrt{1-\frac{4m^2}{m_Z^2}}}{1+\sqrt{1-\frac{4m^2}{m_Z^2}}})-i\pi\right)\right]\right\},\ \frac{4m^2}{s}<1,\ \frac{4m^2}{m_Z^2}<1
\end{aligned}
\tag{J.21}
$$

In eq. (J.21), the plus sign corresponds to $s < m_Z^2$ while the minus sign to $s > m_Z^2$. As an example the full analytical expressions for A_3 and A_5 can be obtained by taking appropriate derivatives of function $\mathscr{F}$ like, $A_3 = c\,\frac{\partial \mathscr{F}}{\partial s}$ and $A_5 = -c\,(\frac{\partial \mathscr{F}}{\partial s}+\frac{\partial \mathscr{F}}{\partial m_Z^2})$, where, as above, c is a factor related to the couplings in the corresponding vertex. As a cross check, taking the limit $m \to 0$ in eq. (J.21) we arrive at,

$$
\mathscr{F}(m_Z,s,0) = -\frac{3}{2}-\frac{1}{2(m_Z^2-s)}\left[s\ln(s)-m_Z^2\ln(m_Z^2)\right]+\frac{i\pi}{2}. \tag{J.22}
$$

Differentiating w.r.t s and m_Z^2 we reproduce the expressions in eqs. (J.15) and (J.16).

Appendix K: Non-decoupling conditions

In this Appendix we present necessary conditions for anomaly cancellation and non-decoupling heavy fermion effects in a model with three different $U(1)$'s corresponding to three distinct, massive or massless gauge bosons X, Y and Z. For this model to be anomaly free, the following conditions among couplings must hold [see eq. (3.1)]:

$$\begin{aligned}
&\sum_{i=1}^{n}(\beta_X^3+3\alpha_X^2\beta_X)_i=\sum_{i=1}^{n}(\beta_Y^3+3\alpha_Y^2\beta_Y)_i=\sum_{i=1}^{n}(\beta_Z^3+3\alpha_Z^2\beta_Z)_i=0\ ,\\
&\sum_{i=1}^{n}(\beta_X^2\beta_Y+2\alpha_X\alpha_Y\beta_X+\alpha_X^2\beta_Y)_i=\sum_{i=1}^{n}(\beta_X^2\beta_Z+2\alpha_X\alpha_Z\beta_X+\alpha_X^2\beta_Z)_i=0\ ,\\
&\sum_{i=1}^{n}(\beta_Y^2\beta_X+2\alpha_X\alpha_Y\beta_Y+\alpha_Y^2\beta_X)_i=\sum_{i=1}^{n}(\beta_Y^2\beta_Z+2\alpha_Z\alpha_Y\beta_Y+\alpha_Y^2\beta_Z)_i=0\ ,\\
&\sum_{i=1}^{n}(\beta_Z^2\beta_X+2\alpha_X\alpha_Z\beta_Z+\alpha_Z^2\beta_X)_i=\sum_{i=1}^{n}(\beta_Z^2\beta_Y+2\alpha_Z\alpha_Y\beta_Z+\alpha_Z^2\beta_Y)_i=0\ ,\\
&\sum_{i=1}^{n}(\beta_X\beta_Y\beta_Z+\alpha_X\alpha_Z\beta_Y+\alpha_X\alpha_Y\beta_Z+\alpha_Z\alpha_Y\beta_X)_i=0\ .
\end{aligned}\tag{K.1}$$

Non-decoupling effects in XYZ-vertex are activated if, in addition to the requirements in eq. (K.1), at least one of the following expressions is non-zero:

$$\begin{aligned}
&\sum_{i=1}^{n}(\beta_X^2\beta_Y+3\ \alpha_X^2\beta_Y)_i\ ,\quad \sum_{i=1}^{n}(\beta_X^2\beta_Y+3\ \alpha_X\alpha_Y\beta_X)_i\ ,\quad \sum_{i=1}^{n}(\beta_X^2\beta_Z+3\ \alpha_X\alpha_Z\beta_X)_i\ ,\\
&\sum_{i=1}^{n}(\beta_X^2\beta_Z+3\ \alpha_X^2\beta_Z)_i\ ,\quad \sum_{i=1}^{n}(\beta_Y^2\beta_X+3\ \alpha_X\alpha_Y\beta_Y)_i\ ,\quad \sum_{i=1}^{n}(\beta_Y^2\beta_X+3\ \alpha_Y^2\beta_X)_i\ ,\\
&\sum_{i=1}^{n}(\beta_Y^2\beta_Z+3\ \alpha_Y^2\beta_Z)_i\ ,\quad \sum_{i=1}^{n}(\beta_Y^2\beta_Z+3\ \alpha_Y\alpha_Z\beta_Y)_i\ ,\quad \sum_{i=1}^{n}(\beta_Z^2\beta_X+3\ \alpha_X\alpha_Z\beta_Z)_i\ ,\\
&\sum_{i=1}^{n}(\beta_Z^2\beta_X+3\ \alpha_Z^2\beta_X)_i\ ,\quad \sum_{i=1}^{n}(\beta_Z^2\beta_Y+3\ \alpha_Y\alpha_Z\beta_Z)_i\ ,\quad \sum_{i=1}^{n}(\beta_Z^2\beta_Y+3\ \alpha_Z^2\beta_Y)_i\ ,\\
&\sum_{i=1}^{n}(\beta_X\beta_Y\beta_Z+3\ \alpha_X\alpha_Z\beta_Y)_i\ ,\quad \sum_{i=1}^{n}(\beta_X\beta_Y\beta_Z+3\ \alpha_X\alpha_Y\beta_Z)_i\ ,\\
&\sum_{i=1}^{n}(\beta_X\beta_Y\beta_Z+3\,\alpha_Y\alpha_Z\beta_X)_i\ .
\end{aligned}\tag{K.2}$$

Appendix L: Form factors for $H \to \gamma\gamma$

We append here the integrand expressions for the coefficients $\mathcal{A}_{ij}$ in eq. (4.3).

$$
\begin{aligned}
\mathcal{A}_{11} \quad &= \tfrac{1}{[(p+a)^2-m_W^2][(p+a-k_1)^2-m_W^2][(p+a-k_1-k_2)^2-m_W^2]} \times \\
\times\Big\{ & m_W^2 \Big[2\,(p+a)\cdot(p+a) - 3\,(p+a)\cdot k_1 - (p+a)\cdot k_2 - 2\,m_H^2 \Big] - \\
& - \Big[3\,[(p+a)\cdot(p+a)]^2 - 10\,[(p+a)\cdot k_1][(p+a)\cdot(p+a)] - \\
& \quad -2\,[(p+a)\cdot k_2][(p+a)\cdot(p+a)] + 8\,[(p+a)\cdot k_1]^2 + \\
& \quad +2\,m_H^2\,[(p+a)\cdot(p+a)] - 2\,m_H^2\,[(p+a)\cdot k_1] \Big] + \\
& + \tfrac{1}{m_W^2} \Big[[(p+a)\cdot(p+a)]^3 - 5\,[(p+a)\cdot k_1][(p+a)\cdot(p+a)]^2 + \\
& \quad +8\,[(p+a)\cdot k_1]^2[(p+a)\cdot(p+a)] - 4\,[(p+a)\cdot k_1]^3 - \\
& \quad -[(p+a)\cdot k_2] \Big([(p+a)\cdot(p+a)]^2 + 4\,[(p+a)\cdot k_1]^2 + \\
& \qquad -4\,[(p+a)\cdot k_1][(p+a)\cdot(p+a)]^2 \Big) \Big] \Big\} + \\
& + \tfrac{1}{[(p+b)^2-m_W^2][(p+b-k_2)^2-m_W^2][(p+b-k_1-k_2)^2-m_W^2]} \times \\
\times\Big\{ & m_W^2 \Big[2\,[(p+b)\cdot(p+b)] - 3\,(p+b)\cdot k_2 - (p+b)\cdot k_1 - 2\,m_H^2 \Big] - \\
& - \Big[3\,[(p+b)\cdot(p+b)]^2 - 10\,[(p+b)\cdot k_2][(p+b)\cdot(p+b)] - \\
& \quad -2\,[(p+b)\cdot k_1][(p+b)\cdot(p+b)] + 8\,[(p+b)\cdot k_2]^2 + \\
& \quad +2\,m_H^2[(p+b)\cdot(p+b)] - 2\,m_H^2\,[(p+b)\cdot k_2] \Big] + \\
& + \tfrac{1}{m_W^2} \Big[[(p+b)\cdot(p+b)]^3 - 5\,[(p+b)\cdot k_2][(p+b)\cdot(p+b)]^2 + \\
& \quad +8\,[(p+b)\cdot k_2]^2[(p+b)\cdot(p+b)] - 4\,[(p+b)\cdot k_2]^3 - \\
& \quad -[(p+b)\cdot k_1] \Big([(p+b)\cdot(p+b)]^2 + 4\,[(p+b)\cdot k_2]^2 \\
& \qquad -4\,[(p+b)\cdot k_2][(p+b)\cdot(p+b)]^2 \Big) \Big] \Big\} - \\
& - \tfrac{2}{[(p+c)^2-m_W^2][(p+c-k_1-k_2)^2-m_W^2]} \times \\
\times\Big\{ & m_W^2\,(d-1) - 2 \Big[[(p+c)\cdot(p+c)] - [(p+c)\cdot k_1] - [(p+c)\cdot k_2] + \tfrac{m_H^2}{2} \Big] + \\
& + \tfrac{1}{m_W^2} \Big[[(p+c)\cdot(p+c)]^2 - 2\,[(p+c)\cdot(p+c)]\,[(p+c)\cdot k_1] - \\
& -2\,[(p+c)\cdot k_2] \Big([(p+c)\cdot(p+c)] - [(p+c)\cdot k_1] \Big) + [(p+c)\cdot k_1]^2 + [(p+c)\cdot k_2]^2 \Big] \Big\}
\end{aligned}
\tag{L.1}
$$

$$\mathcal{A}_{21} = \frac{1}{[(p+a)^2 - m_W^2][(p+a-k_1)^2 - m_W^2][(p+a-k_1-k_2)^2 - m_W^2]} \times$$
$$\times \Bigg\{ (4\ d-6)\, m_W^2 + \Big[3\ (p+a)\cdot(p+a) - 5\ (p+a)\cdot k_1 - (p+a)\cdot k_2 + 2\ m_H^2 \Big] +$$
$$+ \frac{1}{m_W^2} \Big[-[(p+a)\cdot(p+a)]^2 + 3\ [(p+a)\cdot k_1][(p+a)\cdot(p+a)] - 2\ [(p+a)\cdot k_1]^2 -$$
$$-2\ [(p+a)\cdot k_1][(p+a)\cdot k_2] + [(p+a)\cdot(p+a)][(p+a)\cdot k_2] \Big] \Bigg\}\,, \qquad \text{(L.2)}$$

$$\mathcal{A}_{22} = \frac{1}{[(p+b)^2 - m_W^2][(p+b-k_2)^2 - m_W^2][(p+b-k_1-k_2)^2 - m_W^2]} \times$$
$$\times \Bigg\{ (4\ d-6)\, m_W^2 + \Big[3\ (p+b)\cdot(p+b) - 5\ (p+b)\cdot k_2 - (p+b)\cdot k_1 + 2\ m_H^2 \Big] +$$
$$+ \frac{1}{m_W^2} \Big[-[(p+b)\cdot(p+b)]^2 + 3\ [(p+b)\cdot k_2][(p+b)\cdot(p+b)] - 2\ [(p+b)\cdot k_2]^2 -$$
$$-2\ [(p+b)\cdot k_1][(p+a)\cdot k_2] + [(p+b)\cdot(p+b)][(p+b)\cdot k_1] \Big] \Bigg\}\,, \qquad \text{(L.3)}$$

$$\mathcal{A}_{23} = \frac{-1}{[(p+c)^2 - m_W^2][(p+c-k_1-k_2)^2 - m_W^2]} \times$$
$$\times \Bigg\{ 4 + \frac{2}{m_W^2} \Big[-[(p+c)\cdot(p+c)] + (p+c)\cdot k_1 + (p+c)\cdot k_2 \Big] \Bigg\}\,, \qquad \text{(L.4)}$$

$$\mathcal{A}_{31} = \frac{1}{[(p+a)^2 - m_W^2][(p+a-k_1)^2 - m_W^2][(p+a-k_1-k_2)^2 - m_W^2]} \times$$
$$\times \Bigg\{ (7-4\ d)\, m_W^2 - \Big[4\ (p+a)\cdot(p+a) - 7\ (p+a)\cdot k_1 + 3\ (p+a)\cdot k_2 \Big] +$$
$$+ \frac{1}{m_W^2} \Big[[(p+a)\cdot(p+a)]^2 - 3\ [(p+a)\cdot k_1][(p+a)\cdot(p+a)] + 2\ [(p+a)\cdot k_1]^2 +$$
$$+2\,[(p+a)\cdot k_1][(p+a)\cdot k_2] - [(p+a)\cdot(p+a)][(p+a)\cdot k_2] \Big] \Bigg\}\,, \qquad \text{(L.5)}$$

$$\mathcal{A}_{32} = \frac{-1}{[(p+b)^2 - m_W^2][(p+b-k_2)^2 - m_W^2][(p+b-k_1-k_2)^2 - m_W^2]} \times$$
$$\times \Bigg\{ m_W^2 + \Big[-(p+b)\cdot(p+b) + 6\ (p+b)\cdot k_2 \Big] \Bigg\}\,, \qquad \text{(L.6)}$$

$$\mathcal{A}_{33} = \frac{1}{[(p+c)^2 - m_W^2][(p+c-k_1-k_2)^2 - m_W^2]} \times \\ \times \left\{ 2 - \frac{1}{m_W^2} \left[(p+c)\cdot(p+c) - (p+c)\cdot k_1 - (p+c)\cdot k_2 \right] \right\} , \tag{L.7}$$

$$\mathcal{A}_{41} = \frac{-1}{[(p+a)^2 - m_W^2][(p+a-k_1)^2 - m_W^2][(p+a-k_1-k_2)^2 - m_W^2]} \times \\ \times \left\{ m_W^2 + \left[-(p+a)\cdot(p+a) + 6\ (p+a)\cdot k_1 \right] \right\} , \tag{L.8}$$

$$\mathcal{A}_{42} = \frac{1}{[(p+b)^2 - m_W^2][(p+b-k_2)^2 - m_W^2][(p+b-k_1-k_2)^2 - m_W^2]} \times \\ \times \left\{ (7-4\,d)\, m_W^2 - \left[4\,(p+b)\cdot(p+b) - 7\ (p+b)\cdot k_2 + 3\ (p+b)\cdot k_1 \right] + \right. \\ + \frac{1}{m_W^2} \left[[(p+b)\cdot(p+b)]^2 - 3\ [(p+b)\cdot k_2][(p+b)\cdot(p+b)] + 2\ [(p+b)\cdot k_2]^2 + \right. \\ \left. \left. + 2\ [(p+b)\cdot k_1][(p+b)\cdot k_2] - [(p+b)\cdot(p+b)][(p+b)\cdot k_1] \right] \right\} , \tag{L.9}$$

$$\mathcal{A}_{43} \ = \ \mathcal{A}_{33} \ , \tag{L.10}$$

$$\mathcal{A}_{51} = \frac{1}{[(p+a)^2 - m_W^2][(p+a-k_1)^2 - m_W^2][(p+a-k_1-k_2)^2 - m_W^2]} \times \\ \times \left\{ 5\, m_W^2 + \left[3\ (p+a)\cdot(p+a) - 2\ (p+a)\cdot k_1 \right] \right\} + \\ + \frac{1}{[(p+b)^2 - m_W^2][(p+b-k_2)^2 - m_W^2][(p+b-k_1-k_2)^2 - m_W^2]} \times \\ \times \left\{ 5\, m_W^2 + \left[3\ (p+b)\cdot(p+b) - 2\ (p+b)\cdot k_2 \right] \right\} - \\ - \frac{2}{[(p+c)^2 - m_W^2][(p+c-k_1-k_2)^2 - m_W^2]} \ . \tag{L.11}$$

Note that the number of dimensions d has been kept arbitrary throughout and on-shell conditions for the external particles have been imposed. It is straightforward, but long and tedious, to show that after implementing the condition (4.7) to coefficients in eqs.(L.2-L.10), we arrive at eq. (4.8) which is *at the most logarithmically divergent.*

For complementarity reasons, it is useful in deriving eq. (4.24) to present the expression for the coefficient $\mathcal{A}_{11}$ after the imposition of the arbitrary vector relation eq. (4.7).

$$\begin{aligned}
\mathcal{A}_{11} \;=\; & \frac{1}{[(p+a)^2-m_W^2][(p+a-k_1)^2-m_W^2][(p+a-k_1-k_2)^2-m_W^2]}\times \\
& \times\Bigg\{\Big((p+a-k_1)^2-m_W^2\Big)\,(1-d)\,m_W^2 + \\
& \qquad +4\,[(p+a)\cdot k_1][(p+a)\cdot k_2]-[3m_W^2+(p+a)^2]\,m_H^2\Bigg\}+ \\
& +\frac{1}{[(p+a)^2-m_W^2][(p+a-k_2)^2-m_W^2][(p+a-k_1-k_2)^2-m_W^2]}\times \\
& \times\Bigg\{\Big((p+a-k_2)^2-m_W^2\Big)\,(1-d)\,m_W^2 \;+ \\
& \qquad +4\,[(p+a)\cdot k_1][(p+a)\cdot k_2]-[3m_W^2+(p+a)^2]\,m_H^2\Bigg\}\,. \qquad \text{(L.12)}
\end{aligned}$$

This integrand expression, under $\int d^4p$, is obviously *at the most logarithmically divergent.*

Appendix M: 4-dimensional surface integral

In this Appendix we would like to examine the surface terms arising in $d = 4$ when calculating the integral on the l.h.s of eq. (4.12). This integral after Wick rotation into Euclidean space, reads:

$$i \int d^{2\omega}\ell \, \frac{\ell^2 \, g_{\mu\nu} - 4\,\ell_\mu\,\ell_\nu}{(\ell^2+\Delta)^3} \, , \tag{M.1}$$

where $\ell \equiv \ell_E$, and drop for clarity the subscript E from now on. We follow very closely 't Hooft and Veltman's seminal paper in ref. [33]. In our calculation for a physical process we should notice first that ℓ_μ, ℓ_ν are strictly 4-vectors since they are contracted with physical external momenta $k^\mu_{1,\,2}$ or $k^\nu_{1,\,2}$. On the other hand, the loop momentum ℓ in ℓ^2 has components in all, $d = 2\,\omega$, dimensions. We write ℓ as a sum of a vector $\ell_\parallel$ which has non-zero components in dimensions $0, 1, 2, 3$ and a vector $\ell_\perp$ which has nonzero components in $(2\,\omega - 4)$-dimensions,

$$\ell \;=\; \ell_\parallel + \ell_\perp \, . \tag{M.2}$$

With this definition, the integral (M.1) reduces to

$$i \int d^{2\omega}\ell \, \frac{\ell^2_\perp \, g_{\mu\nu}}{(\ell^2+\Delta)^3} \, , \tag{M.3}$$

where the $\ell_\parallel$ components in the numerator of (M.1) vanish thanks to symmetric integration formula, $\ell^\mu_\parallel \ell^\nu_\parallel \to \frac{1}{4}\ell^2_\parallel g^{\mu\nu}$. In order not to carry the $g_{\mu\nu}$ in all formulae below we just concentrate on the integral

$$\mathcal{I} \;\equiv\; i \int d^{2\omega}\ell \, \frac{\ell^2_\perp}{(\ell^2+\Delta)^3} = i \int d^4\ell_\parallel \int d^{2\omega-4}\ell_\perp \, \frac{\ell^2_\perp}{(\ell^2_\parallel + \ell^2_\perp + \Delta)^3} \, . \tag{M.4}$$

Integrating over the extra dimensional solid angle $d\Omega_{2\omega-4}$ we arrive at:

$$\mathcal{I} = \frac{2\,i\,\pi^{\omega-2}}{\Gamma(\omega-2)} \int d^4\ell_\parallel \int_0^\infty dL \, \frac{L^{2\omega-3}}{(\ell^2_\parallel + L^2 + \Delta)^3} \, , \tag{M.5}$$

where $\Gamma(x)$ is the Euler Γ-function and L is the length of the $\ell_\perp$ vector. This integral is UV divergent for $\omega \geq 2$ and IR divergent for $\omega \leq 1$. Therefore, the region of convergence, $1 < \omega < 2$, is finite but it does not yet include the point $\omega = 2$. In order to enlarge the region of convergence to include $\omega = 2$, one has to analytically continue $\mathcal{I}$ by inserting the identity,

$$1 \;=\; \frac{1}{5}\left(\frac{\partial \ell_{\parallel\,\mu}}{\partial \ell_{\parallel\,\mu}} \;+\; \frac{\partial L}{\partial L}\right) , \tag{M.6}$$

in (M.5). After integrating by parts in the region of convergence, rewriting the r.h.s in terms of $\mathcal{I}$ from eq. (M.5) and keeping only, potentially, non-vanishing surface terms, we arrive at:

$$\mathcal{I} = \frac{i\,\pi^{\omega-2}\,\Gamma(4-\omega)}{4} \oint d^3 S^\mu \, \frac{\ell_{\parallel\,\mu}}{(\ell^2_\parallel+\Delta)^{4-\omega}} \;-\; \frac{6\,i\,\pi^{\omega-2}\Delta}{\Gamma(\omega-1)} \int d^4\ell_\parallel \int_0^\infty dL \, \frac{L^{2\omega-3}}{(\ell^2_\parallel + L^2 + \Delta)^4} \, , \tag{M.7}$$

where the first integral is over the Euclidean spatial components of a 4-vector on a three-sphere. The surface integral converges in $1 < \omega < 2$, while the other in $1 < \omega < 3$. By taking the surface integral on a three-sphere with radius R and eventually taking the limit $R \to \infty$ we find:

$$\oint d^3 S^\mu \, \frac{\ell_{\parallel\,\mu}}{(\ell_\parallel^2 + \Delta)^{4-\omega}} \;=\; 2\pi^2 \lim_{R\to\infty} R^{2\omega-4} \,, \tag{M.8}$$

which now converges in the region $\omega \leq 2$, that is, it includes the point $\omega = 2$. For $\omega < 2$ this surface term vanishes, while for $\omega = 2$ there is a finite piece, $2\pi^2$, remaining. This is exactly the term that spoils gauge invariance and the equivalence theorem. In DR this term is axiomatically absent - the shifting of integral momenta is among DR's main properties.

Turning into the second integral of eq. (M.7) we note first that the region of convergence includes now $\omega = 2$. It gives,

$$\int d^4\ell_\parallel \int_0^\infty dL \, \frac{L^{2\omega-3}}{(\ell_\parallel^2 + L^2 + \Delta)^4} \;=\; \frac{\pi^2}{12} \, \frac{\Gamma(\omega-1)\Gamma(3-\omega)}{\Delta^{3-\omega}} \,. \tag{M.9}$$

By placing eqs. (M.8) and (M.9) into eq. (M.7) we finally arrive at eq. (4.12).

Appendix N: Generalised Gordon identities

In this last Appendix, we present a set of generalised Gordon identities that are helpful in simplifying matrix element calculations. For fermions with four-momenta p' and p and masses m_1 and m_2 respectively, the equation of motion is:

$$\overline{u}(p')\not{p}' = m_1\overline{u}(p'),\ \overline{u}(p)\not{p} = m_2\overline{u}(p),\ \not{p}'u(p') = m_1u(p'),\ \not{p}\,u(p) = m_2u(p). \tag{N.1}$$

Let write the expression $\overline{u}(p')\gamma^\mu u(p)$ in the following form:

$$\overline{u}(p')\gamma^\mu u(p) = \overline{u}(p')\Big[A\,p'^\mu + B\,p^\mu + i\,C\,\sigma^{\mu\nu}p'_\nu + i\,D\,\sigma^{\mu\nu}p_\nu\Big]u(p), \tag{N.2}$$

where A, B, C, D are coefficients to be determined later and $\sigma^{\mu\nu} = \frac{i}{2}\big(\gamma^\mu\gamma^\nu - \gamma^\nu\gamma^\mu\big)$. For the term $\overline{u}(p')\sigma^{\mu\nu}\,p'_\nu u(p)$ we find:

$$\begin{aligned}\overline{u}(p')\sigma^{\mu\nu}\,p'_\nu u(p) &= \frac{i}{2}\overline{u}(p')\big(\gamma^\mu\gamma^\nu - \gamma^\nu\gamma^\mu\big)\,p'_\nu u(p) = \frac{i}{2}\overline{u}(p')\big(2g^{\mu\nu} - 2\gamma^\nu\gamma^\mu\big)\,p'_\nu u(p) = \\ &= \frac{i}{2}\overline{u}(p')\big(2p'^\mu - 2\not{p}'\gamma^\mu\big)\,u(p) = i\overline{u}(p')p'^\mu u(p) - i\,m_1\overline{u}(p')\gamma^\mu u(p),\end{aligned} \tag{N.3}$$

where we used the fact that $\{\gamma^\mu, \gamma^\nu\} = 2\,g^{\mu\nu}$, and the equations of motion from eq. (N.1). In a similar way we find:

$$\overline{u}(p')\sigma^{\mu\nu}\,p_\nu u(p) = -i\overline{u}(p')p^\mu u(p) + i\,m_2\overline{u}(p')\gamma^\mu u(p). \tag{N.4}$$

Making use of eqs. (N.2), (N.3) and (N.4) we obtain:

$$\overline{u}(p')\gamma^\mu u(p) = \overline{u}(p')\Big[(A-C)\,p'^\mu + (B+D)\,p^\mu + (C\,m_1 - D\,m_2)\gamma^\mu\Big]u(p) \tag{N.5}$$

In order the equation above be satisfied, it must be $A - C = 0$, $B + D = 0$ and $C\,m_1 - D\,m_2 = 1$. There are four unknown parameters and three equations, therefore there is an infinity of solutions of the system above. If we choose $C = -D$, then $A = B = C = -D = \frac{-1}{m_1+m_2}$. However if we choose $C = D$, then $A = -B = C = D = \frac{1}{m_1-m_2}$. In the last case it must be $m_1 \neq m_2$. With the choices above we obtain the following vectorial Gordon identities:

$$\overline{u}(p')\gamma^\mu u(p) = \overline{u}(p')\left[\frac{p'^\mu + p^\mu}{m_1+m_2} + \frac{i\,\sigma^{\mu\nu}(p'-p)_\nu}{m_1+m_2}\right]u(p),$$

or

$$\overline{u}(p')\gamma^\mu u(p) = \overline{u}(p')\left[\frac{p'^\mu - p^\mu}{m_1-m_2} + \frac{i\,\sigma^{\mu\nu}(p'+p)_\nu}{m_1-m_2}\right]u(p), \tag{N.6}$$

respectively with $m_1 \neq m_2$ in the last expression.

We can use the same procedure to obtain the axial Gordon identities. Let write now the expression $\overline{u}(p')\gamma^\mu\gamma^5 u(p)$ in the following form:

$$\overline{u}(p')\gamma^\mu\gamma^5 u(p) = \overline{u}(p')\Big[A\,p'^\mu\gamma^5 + B\,p^\mu\gamma^5 + i\,C\sigma^{\mu\nu}\,\gamma^5\,p'_\nu + i\,D\,\sigma^{\mu\nu}\,\gamma^5\,p_\nu\Big]u(p). \quad \text{(N.7)}$$

Analyzing the third and fourth term of the expression above we find the two following expressions:

$$\begin{aligned}
\overline{u}(p')\,\sigma^{\mu\nu}\,\gamma^5\,p'_\nu u(p) &= i\,\overline{u}(p')p'^\mu\,\gamma^5\,u(p) - i\,m_1\,\overline{u}(p')\gamma^\mu\gamma^5 u(p), \\
\overline{u}(p')\,\sigma^{\mu\nu}\,\gamma^5\,p_\nu u(p) &= -i\,\overline{u}(p')p^\mu\,\gamma^5\,u(p) - i\,m_2\,\overline{u}(p')\gamma^\mu\gamma^5 u(p),
\end{aligned} \quad \text{(N.8)}$$

where as previously we used the equations of motion and the fact that $\{\gamma^\mu,\gamma^\nu\} = 2\,g^{\mu\nu}$ and $\{\gamma^\mu,\gamma^5\} = 0$. After substituting these expressions in eq. (N.7), this takes the form:

$$\overline{u}(p')\gamma^\mu\gamma^5 u(p) = \overline{u}(p')\Big[(A-C)\,p'^\mu\gamma^5 + (B+D)\,p^\mu\gamma^5 + (C\,m_1 + D\,m_2)\gamma^\mu\gamma^5\Big]u(p). \quad \text{(N.9)}$$

As in the previous case we obtain the following system $A - C = 0$, $B + D = 0$ and $C\,m_1 + D\,m_2 = 1$. There is an infinity of solutions for this system. If we choose $C = D$, then $A = -B = C = D = \frac{1}{m_1+m_2}$, however if we choose $C = -D$, then $A = B = C = -D = \frac{1}{m_1-m_2}$. As previously in the last case $m_1 \neq m_2$. Finally, for these two cases the axial Gordon identities are written as:

$$\overline{u}(p')\gamma^\mu\,\gamma^5 u(p) = \overline{u}(p')\left[\frac{p'^\mu - p^\mu}{m_1+m_2} + \frac{i\,\sigma^{\mu\nu}(p'+p)_\nu}{m_1+m_2}\right]\gamma^5 u(p),$$

or

$$\overline{u}(p')\gamma^\mu\,\gamma^5 u(p) = \overline{u}(p')\left[\frac{p'^\mu + p^\mu}{m_1-m_2} + \frac{i\,\sigma^{\mu\nu}(p'-p)_\nu}{m_1-m_2}\right]\gamma^5 u(p). \quad \text{(N.10)}$$

Bibliography

[1] S. Glashow, *Nucl.Phys.* **22**, 579 (1961).

[2] S. Weinberg, *Phys.Rev.Lett.* **19**, 1264 (1967).

[3] A. Salam, in *"Proceedings of the Eighth Nobel Symposium"*, edited by N. Svartholm (Wiley, New York, 1968)

[4] **ATLAS** Collaboration, G. Aad *et al.*, *Phys.Lett.* **B** (2012), `arXiv:1207.7214 [hep-ex]`.

[5] **CMS** Collaboration, S. Chatrchyan *et al.*, *Phys.Lett.* **B** (2012), `arXiv:1207.7235 [hep-ex]`.

[6] F. Englert, R. Brout (1964). *Phys.Rev.Lett.* **13** (9).

[7] P.W. Higgs (1964). *Phys.Rev.Lett.* **13** (16).

[8] G.S. Guralnik, C.R. Hagen, T.W.B. Kibble (1964). *Phys.Rev.Lett.* **13** (20).

[9] G.S. Guralnik (2009). International Journal of Modern Physics **A24** (14).

[10] F.Zwicky, *Helv. Phys. Acta* **6**, (1933).

[11] F. Zwicky, *Astrophys. J.* **86** (1937).

[12] V. C. Rubin, Kent W. Ford, *Astrophys. J.*, **159**.

[13] V. C. Rubin, Ford, Thonnard, N. ; *Astrophys. J.*, Part 1, **238**, 1980.

[14] Hinshaw, G.; *et al.* (2009). *Astrophys. J. Supplement* **180**, `arXiv:astro-ph/0803.0732`.

[15] P. A. R. Ade, N. Aghanim, C. Armitage-Caplan *et al.* (Planck Collaboration) `arXiv:1303.5062 [astro-ph.CO]`.

[16] O. Adriani *et al.*, *Nature*, 2009, `arXiv:0810.4995 [astro-ph]`.

[17] O. Adriani *et al.*, *Phys.Rev.Lett.*, 2009, `arXiv:0810.4994 [astro-ph]`.

[18] S.W. Barwick *et al*, *Astrophys. J.* **482** (1997) l191; `arXiv:astro-ph/9703192`.

[19] J.J. Beatty *et al*, *Phys.Rev.Lett.* **93** (2004) 241102; arXiv:astro-ph/0412230.

[20] A. A. Abdo *et al.* [The Fermi LAT Collaboration], *Phys.Rev.Lett.*, 2009, arXiv:0905.0025 [astro-ph].

[21] F. Aharonian *et al.* [H.E.S.S. Collaboration], *Phys.Rev.Lett.* **101** (2008) arXiv:0811.3894 [astro-ph]; H. E. S. Aharonian, *Astron. Astrophys.* **508**, 2009 arXiv:0905.0105 [astro-ph].

[22] J. Chang, *et al*, [ATIC Collaboration], *Nature* (2008).

[23] J. Yoo [CDMS Collaboration], arXiv: 0810.3527 [hep-ex].

[24] J. Angle *et al.* [XENON Collaboration], *Phys.Rev.Lett.* **100** (2008) arXiv:0706.0039 [astro-ph].

[25] R. Bernabei *et al.* [DAMA Collaboration], *Eur.Phys.J.* **C56**, 333 (2008) arXiv:0804.2741 [astro-ph].

[26] G. Steigman and M.S. Turner, *Nucl.Phys.* **B253**, 375 (1985).

[27] L. E. Strigari *et al.*, *Nature* 454, 1096 (2008).

[28] M. G. Walker *et al.*, *ApJ* **704**, 1274 (2009).

[29] J. Wolf *et al.*, *MNRAS* **406**, 1220 (2010).

[30] S. L. Adler, *Phys. Rev.* **177**, 2426 (1969).

[31] W. A. Bardeen, *Phys.Rev.* **184**, 1848 (1969).

[32] J. Goldstone, *Nuov.Cim.* **19** (1961) 154.

[33] G.'t Hooft, Veltman, M. (1972), *Nucl.Phys.* **B44** (1)

[34] M. E. Peskin and D. V. Schroeder, Reading, USA: Addison-Wesley (1995)

[35] A. Dedes, I. Giomataris, K. Suxho, J.D. Vergados. Jul 2009. *Nucl.Phys.* **B826** (2010) arXiv:0907.0758 [hep-ph].

[36] M. Aguilar *et al.* [AMS-01 Collaboration], *Phys.Lett.* **B646** (2007) 145 arXiv:astro-ph/0703154.

[37] M. Cirelli, M. Kadastik, M. Raidal and A. Strumia, *Nucl.Phys.* **B813**, 1 (2009) arXiv:0809.2409 [hep-ph].

[38] P. Meade, M. Papucci, A. Strumia and T. Volansky, *Nucl.Phys.* **B831**, 2009. arXiv:0905.0480 [hep-ph].

[39] D. P. Finkbeiner *et al*, *Astrophys. J.* **684** (2004) 186; arXiv:astro-ph/0312547.

[40] D. Hooper, D. P. Finkbeiner and G. Dobler , *Phys.Rev.* **D76** (2007) arXiv:0705.3655.

[41] A.W. Strong *et al*, *Astron. Astrophys.* **444** (2005) 405; arXiv:astro-ph/0509092.

[42] B. Holdom, *Phys.Lett.* **B166**, 196 (1986); *ibid.* **B259** 329 (1991).

[43] M. Pospelov, A. Ritz and M. B. Voloshin, *Phys.Lett.* **B662**, 53 (2008) arXiv:0711.4866 [hep-ph].

[44] D. P. Finkbeiner and N. Weiner, *Phys.Rev.* **D76**, 083519 (2007) arXiv:astro-ph/0702587].

[45] S. Abrahamyan *et al.*, *Phys.Rev.Lett.* 107, 191804 (2011).

[46] N. Arkani-Hamed, D. P. Finkbeiner, T. R. Slatyer and N. Weiner, *Phys.Rev.* **D79** (2009) 015014 arXiv:0810.0713 [hep-ph];

[47] N. Arkani-Hamed, N. Weiner, *JHEP* **0812** (2008) 104 arXiv:0810.0714 [hep-ph];

[48] M. Pospelov and A. Ritz, *Phys.Lett.* **B671** 391, 2009. arXiv:0810.1502 [hep-ph].

[49] A. Sommerfeld, *Ann.Phys.* **11** 257 (1931); Relevant to the abelian models considered here is the article, M. Cirelli, A. Strumia, M. Tamburini, *Nucl.Phys.* **B787** (2007) arXiv:0706.4071 [hep-ph].

[50] C. Boehm and P. Fayet, *Nucl.Phys.* **B683** (2004) 219 arXiv:hep-ph/0305261; C. Boehm, P. Fayet and J. Silk, *Phys.Rev.* **D69**, 101302 (2004) arXiv:hep-ph/0311143].

[51] E. C. G. Stueckelberg, *Helv.Phys.Acta* **11**, 225 (1938).

[52] D. Feldman, Z. Liu and P. Nath, *Phys.Rev.* **D79** 063509, 2009. arXiv:0810.5762 [hep-ph].

[53] P. J. Fox and E. Poppitz, *Phys.Rev.* **D79** 083528, 2009 arXiv:0811.0399 [hep-ph].

[54] S. Baek and P. Ko, *JCAP* **0910**, 2009. arXiv:0811.1646 [hep-ph].

[55] R. Harnik, G. D. Kribs, *Phys.Rev.* **D79** 095007, 2009 arXiv:0810.5557 [hep-ph].

[56] C. R. Chen, F. Takahashi and T. T. Yanagida, *Phys.Lett.* **673:255**, 2009 arXiv:0811.0477 [hep-ph].

[57] A. Ibarra, A. Ringwald, D. Tran and C. Weniger, *JCAP* **0908** (2009) 017 arXiv:0903.3625 [hep-ph].

[58] R. Bernabei *et al.*, *Phys.Rev.* **D77**, 023506 (2008) arXiv:0712.0562 [astro-ph]. In the case of inelastic dark matter and DAMA prospects see, Y. Cui, D. E. Morrissey, D. Poland and L. Randall, *JHEP* **0905**, 076 (2009) arXiv:0901.0557 [hep-ph].

[59] P. Q. Hung and J. J. Sakurai, *Nucl.Phys.* **B143** (1978) 81 [Erratum-ibid. **B148** (1979) 538].

[60] M. Baumgart, C. Cheung, J. T. Ruderman, L. T. Wang and I. Yavin, *JHEP* **0904**, 2009 arXiv:0901.0283 [hep-ph].

[61] For a review see, F. Jegerlehner and A. Nyffeler, arXiv:0902.3360 [hep-ph].

[62] M. Pospelov, *Phys.Rev.* **D80**, 095002, 2009 arXiv:0811.1030 [hep-ph].

[63] D. E. Morrissey, D. Poland and K. M. Zurek, *JHEP* 0907, 2009 arXiv:0904.2567 [hep-ph].

[64] J. D. Bjorken, R. Essig, P. Schuster and N. Toro, *Phys.Rev.* **D80**, 2009 arXiv:0906.0580 [hep-ph].

[65] B. Batell, M. Pospelov and A. Ritz, arXiv:0906.5614 [hep-ph].

[66] B. Kors and P. Nath, *Phys.Lett.* **B586** (2004) 366 arXiv:hep-ph/0402047; D. Feldman, Z. Liu and P. Nath, *Phys.Rev.* **D75** (2007) 115001 arXiv:hep-ph/0702123.

[67] P. Fayet "U-boson production in $e^+ e^-$ annihilations, ψ and Υ decays, and Light Dark Matter." *Phys.Rev.* **D75**, (2007) 115017.

[68] J. D. Vergados, *J.Phys.* **G30**, 1127 (2004) arXiv:hep-ph/0406134.

[69] N.Tetradis, J.D. Vergados and A. Faessler, *Phys.Rev.* **D75**, 023504 (2007)

[70] See for example, Hans A. Bethe, "Intermediate Quantum Mechanics," *Lecture notes and supplements in physics*. Notes by R. W. Jackiw.

L. Schiff, "Quantum Mechanics," *McGraw-Hill Education (1968) 584p.*

[71] J. I Collar, I. Giomataris, *Nucl.Instrum.Meth.* A 471:254-259, 2000.

[72] I. Giomataris, J, D. Vergados, *Nucl.Instrum. Meth.* A 530:330-358, 2004.

[73] Chris Hagmann, Adam Bernstein, IEEE Trans. *Nucl. Sci.* 51:2151-2155, 2004.

[74] Henry T. Wong, *Mod. Phys. Lett.* **A23**:1431-1442, 2008.

[75] Y. Giomataris, P. Rebourgeard, J. P. Robert and G. Charpak, *Nucl.Instrum. Meth.* **A376** (1996) 29.

[76] P. Gorodetzky *et al.*, *Nucl. Instrum. Meth.* **A433**, 554 (1999).

[77] P. Buzhan *et al.*, *Nucl. Instrum. Meth.* **A504**, 48 (2003).

[78] P. Abbon *et al.*, *New J.Phys.* **9** (2007) 170 arXiv:physics/0702190.

[79] I. Giomataris *et al.*, *JINST* **3**, P09007 (2008) arXiv:0807.2802.

[80] R. Adhikari, J. Erler and E. Ma, *Phys.Lett.* **B672** (2009) 136 arXiv:0810.5547 [hep-ph].

[81] Q. H. Cao, E. Ma and G. Shaughnessy, *Phys.Lett.* **B673** arXiv:0901.1334 [hep-ph].

[82] D. Suematsu, T. Toma and T. Yoshida, *Phys.Rev.* **D79**, arXiv:0903.0287 [hep-ph].

[83] E. Ma, arXiv:0810.5574 [hep-ph].

[84] A.Dedes, unpublished work.

[85] J. Kopp, V. Niro, T. Schwetz, and J. Zupan, *Phys.Rev.* **D80**, 083502 (2009), arXiv:0907.3159.

[86] M. Williams, C. Burgess, A. Maharana, and F. Quevedo, (2011), arXiv:1103.4556.

[87] A. Dedes and K. Suxho, *Phys.Rev.* **D85** (2012), arXiv:1202.4940 [hep-ph].

[88] T. Appelquist and J. Carazzone, *Phys.Rev.* **D11**, 2856 (1975).

[89] C.-r. Ahn, M. E. Peskin, B. W. Lynn, and S. B. Selipsky, *Nucl.Phys.* **B309**, 221 (1988).

[90] D. Kennedy, *Phys.Lett.* **B268**, 86 (1991).

[91] J. Bell and R. Jackiw, *Nuovo Cim.* **A60**, 47 (1969).

[92] K. Fujikawa, *Phys.Rev.* **D21**, 2848 (1980).

[93] J. A. Harvey, (2005), arXiv:hep-th/0509097.

[94] C. T. Hill, (2006), arXiv:hep-th/0601155.

[95] A. Bilal, (2008), arXiv:0802.0634.

[96] C. Bouchiat, J. Iliopoulos, and P. Meyer, *Phys.Lett.* **B38**, 519 (1972).

[97] D. J. Gross and R. Jackiw, *Phys.Rev.* **D6**, 477 (1972).

[98] E. D'Hoker and E. Farhi, *Nucl.Phys.* **B248**, 77 (1984).

[99] E. D'Hoker and E. Farhi, *Nucl.Phys.* **B248**, 59 (1984).

[100] J. Wess and B. Zumino, *Phys.Lett.* **B37**, 95 (1971).

[101] E. Witten, *Nucl. Phys.* **B223**, 422 (1983).

[102] O. Kaymakcalan, S. Rajeev, and J. Schechter, *Phys. Rev.* **D30**, 594 (1984).

[103] J. A. Harvey, C. T. Hill, and R. J. Hill, *Phys.Rev.* **D77**, 085017 (2008), arXiv:0712.1230.

[104] J. A. Harvey, C. T. Hill, and R. J. Hill, *Phys.Rev.Lett.* **99**, 261601 (2007), arXiv:0708.1281.

[105] J. L. Diaz-Cruz, *Phys.Rev.* **D56**, 523 (1997), arXiv:hep-ph/9705476.

[106] E. D'Hoker, *Phys. Rev. Lett.* **69**, 1316 (1992).

[107] G.-L. Lin, H. Steger, and Y.-P. Yao, *Phys.Rev.* **D44**, 2139 (1991).

[108] F. Feruglio, A. Masiero, and L. Maiani, *Nucl.Phys.* **B387**, 523 (1992).

[109] R. Jackiw, *Int.J.Mod.Phys.* **B14**, 2011 (2000), arXiv:hep-th/9903044, Rajaramanfest, New Delhi, March 1999.

[110] I. Antoniadis, A. Boyarsky, S. Espahbodi, O. Ruchayskiy, and J. D. Wells, *Nucl.Phys.* **B824**, 296 (2010), arXiv:0901.0639.

[111] E. Dudas, Y. Mambrini, S. Pokorski, and A. Romagnoni, *JHEP* **08**, 014 (2009), arXiv:0904.1745.

[112] J. Preskill, *Ann. Phys.* **210**, 323 (1991).

[113] P. Anastasopoulos, M. Bianchi, E. Dudas, and E. Kiritsis, *JHEP* **11**, 057 (2006), arXiv:hep-th/0605225.

[114] J. Kumar, A. Rajaraman, and J. D. Wells, *Phys.Rev.* **D77**, 066011 (2008), arXiv:0707.3488.

[115] C. Coriano, N. Irges, and S. Morelli, *JHEP* **0707**, 008 (2007), arXiv:hep-ph/0701010.

[116] N. Irges, C. Coriano, and S. Morelli, *Nucl.Phys.* **B789**, 133 (2008), arXiv:hep-ph/0703127.

[117] R. Armillis, C. Coriano, and M. Guzzi, *JHEP* **0805**, 015 (2008), arXiv:0711.3424.

[118] K. Hagiwara, R. Peccei, D. Zeppenfeld, and K. Hikasa, *Nucl.Phys.* **B282**, 253 (1987).

[119] K. Gaemers and G. Gounaris, *Z.Phys.* **C1**, 259 (1979).

[120] L. Rosenberg, *Phys.Rev.* **129**, 2786 (1963).

[121] A. Barroso, F. Boudjema, J. Cole, and N. Dombey, *Z.Phys.* **C28**, 149 (1985).

[122] U. Baur and E. L. Berger, *Phys.Rev.* **D47**, 4889 (1993).

[123] G. Gounaris, J. Layssac, and F. Renard, *Phys.Rev.* **D61**, 073013 (2000), arXiv:hep-ph/9910395.

[124] G. Gounaris, J. Layssac, and F. Renard, *Phys.Rev.* **D62**, 073013 (2000), arXiv:hep-ph/0003143.

[125] G. Gounaris, J. Layssac, and F. Renard, *Phys.Rev.* **D62**, 073012 (2000), arXiv:hep-ph/0005269.

[126] J. Jauch and F. Rohrlich, *"The Theory of Photons and Electrons,"* Springer-Verlag, New York, 1976.

[127] R. Pugh, *Can.J.Phys.* **47**, 1263 (1969).

[128] V. Elias, G. McKeon, and R. B. Mann, *Phys.Rev.* **D28**, 1978 (1983).

[129] J. M. Cornwall, D. N. Levin, and G. Tiktopoulos, *Phys.Rev.* **D10**, 1145 (1974), [*Erratum-ibid.D11:972,1975.*]

[130] C. E. Vayonakis, *Nuovo Cim. Lett.* **17**, 383 (1976).

[131] B. W. Lee, C. Quigg, and H. B. Thacker, *Phys.Rev.* **D16**, 1519 (1977).

[132] DELPHI, J. Abdallah *et al.*, *Eur.Phys.J.* **C51**, 525 (2007), arXiv:0706.2741.

[133] D0, V. M. Abazov *et al.*, *Phys.Lett.* **B671**, 349 (2009), arXiv:0806.0611.

[134] CDF, T. Aaltonen *et al.*, (2011), arXiv:1103.2990.

[135] L. D. Landau, *Dokl. Akad. Nauk Ser. Fiz.* **60**, 207 (1948).

[136] C.-N. Yang, *Phys.Rev.* **77**, 242 (1950).

[137] S. Aminneborg, L. Bergstrom, and B. A. Lindholm, *Phys.Rev.* **D43**, 2527 (1991).

[138] S. Rudaz, *Phys.Rev.* **D39**, 3549 (1989).

[139] The DELPHI Collaboration, J. Abdallah *et al.*, *Eur.Phys.J.* **C66**, 35 (2010), arXiv:1002.0752.

[140] The D0 Collaboration, V. M. Abazov *et al.*, *Phys.Rev.Lett.* **107**, 241803 (2011), arXiv:1109.4432.

[141] P.-F. Giraud, (2012), arXiv:1201.4868.

[142] A. Martelli, arXiv:1201.4596.

[143] M. E. Peskin and T. Takeuchi, *Phys.Rev.* **D46**, 381 (1992).

[144] M. Baak *et al.*, (2011), arXiv:1107.0975.

[145] The CDF, T. Aaltonen *et al.*, *Phys.Rev.Lett.* **106**, 141803 (2011), arXiv:1101.5728.

[146] M. E. Peskin, (2011), arXiv:1110.3805.

[147] A. Wingerter, (2011), arXiv:1109.5140.

[148] CMS Collaboration, *JHEP* **05** (2012) 123, arXiv:1204.1088

[149] CMS collaboration, CMS-PAS-EXO-11-054.

[150] P. Langacker, *Rev.Mod.Phys.* **81**, 1199 (2009), arXiv:0801.1345.

[151] T. Appelquist, B. A. Dobrescu, and A. R. Hopper, *Phys.Rev.* **D68**, 035012 (2003), arXiv:hep-ph/0212073.

[152] E. Salvioni, G. Villadoro, and F. Zwirner, *JHEP* **11**, 068 (2009), arXiv:0909.1320.

[153] E. Salvioni, A. Strumia, G. Villadoro, and F. Zwirner, *JHEP* **03**, 010 (2010), arXiv:0911.1450.

[154] N. Deshpande and J. Trampetic, *Phys.Lett.* **B206**, 665 (1988).

[155] W.-Y. Keung, I. Low, and J. Shu, *Phys.Rev.Lett.* **101**, 091802 (2008), arXiv:0806.2864.

[156] S. B. Treiman, E. Witten, R. Jackiw, and B. Zumino, *"Current Algebra And Anomalies,"* Singapore: World Scientific (1985) 537p.

[157] S. Weinberg, *"The Quantum Theory of Fields, Volume 2: Modern Applications"* Cambridge, UK: Univ. Pr. (1996) 489 p.

[158] H. K. Dreiner, H. E. Haber, and S. P. Martin, *Phys. Rept.* **494**, 1 (2010), arXiv:0812.1594.

[159] J. F. Gunion, H. E. Haber, G. L. Kane, and S. Dawson, *Front.Phys.* **80** (2000).

[160] A. Djouadi, *Phys.Rept.* **457** (2008) , arXiv:hep-ph/0503172 [hep-ph].

[161] J. R. Ellis, M. K. Gaillard, and D. V. Nanopoulos, *Nucl.Phys.* **B106** (1976).

[162] B. Ioffe and V. A. Khoze, *Sov.J.Part.Nucl.* **9** (1978).

[163] M. A. Shifman, A. Vainshtein, M. Voloshin, and V. I. Zakharov, *Sov.J.Nucl.Phys.* **30** (1979).

[164] M. Gavela, G. Girardi, C. Malleville, and P. Sorba, *Nucl.Phys.* **B193** (1981).

[165] D. Huang, Y. Tang, and Y.-L. Wu, *Commun.Theor.Phys.* **57** (2012) , arXiv:1109.4846 [hep-ph].

[166] H.-S. Shao, Y.-J. Zhang, and K.-T. Chao, *JHEP* **1201** (2012), arXiv:1110.6925 [hep-ph].

[167] F. Bursa, A. Cherman, T. C. Hammant, R. R. Horgan, and M. Wingate, arXiv:1112.2135 [hep-ph].

[168] F. Piccinini, A. Pilloni, and A. Polosa, arXiv:1112.4764 [hep-ph].

[169] W. J. Marciano, C. Zhang, and S. Willenbrock, *Phys.Rev.* **D85** (2012), arXiv:1109.5304 [hep-ph].

[170] S. Weinberg, *Phys.Rev.* **D7** (1973).

[171] J. C. Collins, "Renormalization," *Cambridge, University Press, 380p* (1984) .

[172] R. Pittau, arXiv:1208.5457 [hep-ph].

[173] A. Dedes and K. Suxho, arXiv:1210.0141 [hep-ph], (to be published in Advances in High Energy Physics).

[174] R. Gastmans, S. L. Wu, and T. T. Wu, arXiv:1108.5322 [hep-ph].

[175] R. Gastmans, S. L. Wu, and T. T. Wu, arXiv:1108.5872 [hep-ph].

[176] J. Bagger and C. Schmidt, *Phys.Rev.* **D41** (1990).

[177] M. Shifman, A. Vainshtein, M. Voloshin, and V. Zakharov, *Phys.Rev.* **D85** (2012) 013015, arXiv:1109.1785 [hep-ph].

[178] F. Jegerlehner, arXiv:1110.0869 [hep-ph].

[179] J. M. Cornwall, D. N. Levin, and G. Tiktopoulos, *Phys.Rev.Lett.* **30** (1973).

[180] M. S. Chanowitz and M. K. Gaillard, *Nucl.Phys.* **B261** (1985).

[181] G. Gounaris, R. Kogerler, and H. Neufeld, *Phys.Rev.* **D34** (1986) 3257.

[182] S. Dawson and S. Willenbrock, *Phys.Rev.* **D40** (1989) 2880.

[183] A. Vainshtein, V. I. Zakharov, and M. A. Shifman, *Sov.Phys.Usp.* **23** (1980) .

[184] B. A. Kniehl and M. Spira, *Z.Phys.* **C69** (1995), arXiv:[hep-ph]/9505225.

[185] A. Pilaftsis, *Phys.Lett.* **B422** (1998), arXiv:hep-ph/9711420 [hep-ph].

[186] J. Callan, Curtis G., S. R. Coleman, and R. Jackiw, *Annals Phys.* **59** (1970).

[187] J. Horejsi and M. Stohr, *Phys.Lett.* **B379** (1996), arXiv:[hep-ph]/9603320.

[188] S. L. Adler, J. C. Collins, and A. Duncan, *Phys.Rev.* **D15** (1977) 1712.

[189] M. Klute, R. Lafaye, T. Plehn, M. Rauch, and D. Zerwas, `arXiv:1205.2699 [hep-ph]`.

[190] P. P. Giardino, K. Kannike, M. Raidal, and A. Strumia, `arXiv:1207.1347 [hep-ph]`.